D51660/84

230

D51660/84

SAHROM, B.H.

230

POLYMER TECH.
POLY. OF NORTH LONDON.

Energy changes on deformation of a pneumatic tyre

A thesis submitted to the
Council for National Academic Awards
in partial fulfilment of the requirements
for the Degree of
Doctor of Philosophy

by

Sahrom bin Hasshim
B.Sc. (Eng), A.N.C.R.T., Grad. PRI.

London School of Polymer Technology
The Polytechnic of North London
Holloway Road
London N7 8DB.

December 1983

DECLARATION BY THE CANDIDATE

I declare that while registered as a candidate for the degree of Doctor of Philosophy I have not been a registered candidate for another award of the CNAA, or of a University.

ABSTRACT

The major part of this work is concerned with the development of the apparatus and the techniques involved in the measurements of the load-deflection characteristics of a pneumatic tyre and its associated changes in the pressure and volume of the air contained in it. A satisfactory results were obtained from this arrangement.

From the measurements of the changes in volume and pressure of the air in the tyre, relationship was derived whereby the volume of the tyre at a particular inflation pressure was determined. The volume obtained by this method agree favourably with the value obtained by the conventional method of filling the tyre with water, and also it has the advantage over the conventional method due to its ease of operation.

The most important aspect of this work is to determine qualitatively the amount of work required to deform the tyre structure. This is determined from the relationship that the work done on the structure is the difference between the total work done and the work done on air. An isothermal process was assumed.

It was found that the work done on the structure accounts for only 10-20% of the total external work done on the tyre and is independent of the inflation pressure.

A simplified quantitative treatment of the result based on the Gent and Thomas theory of air spring was developed and it agrees satisfactorily with the experimental results.

ACKNOWLEDGEMENTS

I am deeply indebted to Dr. E. Southern for his supervision, continuous encouragement and interest during the course of this work. Appreciation is also expressed to Prof. A. G. Thomas for his comments and suggestions of this research.

My special gratitude to the Rubber Research Institute of Malaysia and the Government of Malaysia for granting the study leave and for providing financial support for the completion of this work.

I would like to express my sincere appreciation to all my colleagues, especially to Dr. A.D. Harman for their comments and moral support during this work.

Lastly, I am indebted to my wife to her patience, understanding and encouragement during the course of the work.

CONTENTS

APPENDICES	CALCULATION, ANALYSIS OF EXPERIMENTAL ERRORS OF CALCULATED VALUES AND COMPUTER PROGRAMS
Appendix I	Determination of the coefficient of friction of pulley bearing
Appendix II	Determination of the centre of gravity of the beam assembly
Appendix III	Determination of the coefficient of friction of the pivot bearing
Appendix IV	Determination of load acting on the tyre
Appendix V	Determination of the volume of the tyre
Appendix VI	Determination of work done on/by air
Appendix VII	Determination of corrected readings of barometer and manometer
Appendix VIII	Computer program for the calculation work done on tyre
Appendix IX	Computer programe for the analysis of load-deflection behaviour of tyre at various inflation pressures
Appendix X	Computer program for the analysis of load-deflection behaviour of tyre using the Gent and Thomas theory of air-spring

CHAPTER 1

INTRODUCTION

1.1 History.

The pneumatic tyre was first patented in England by Robert Thompson in 1845. It was made up of pneumatic tubes made of several layers of canvas saturated in a rubber solution, cemented together and vulcanised. However, it was not until 1888, when John Boyd Dunlop applied the basically same type of tyre to the wheels of his son's bicycle to make it more comfortable to ride, that the use of pneumatic tyre really become well-known (1).

Pneumatic tyres has undergone numerous constructional developments since then with separate plies of cotton cord being introduced in about 1916, introduction of modern radial tyres in the lates 1940's and the development of the modern tubeless tyre in the early 1950's (2).

1.2 General structure of a tyre.

The modern pneumatic tyre is a highly complex load carrying structure because it is made of a composite of rubber, cords and steel wire. The composite nature of the tyre gives rise to a body which is neither homogeneous nor isotropic. Fig. 1.1. shows the structural regions and

and components of a bias-ply or cross-ply truck tyre and it illustrares the principal features of any form of pneumatic tyre.

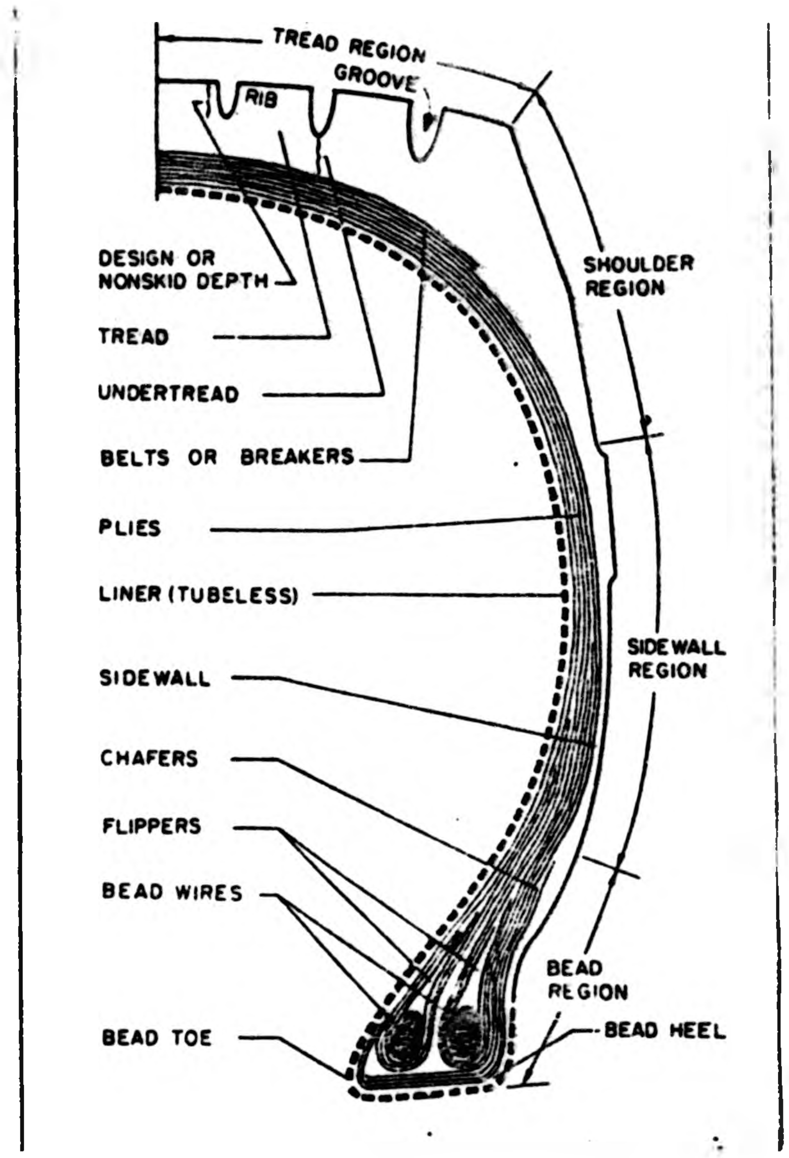

Fig. 1.1. Structural components (3)

Basically the components of the pneumatic tyre may be divided into its primary and secondary components. The primary components constitute the carcass plies, beads, belt and tread. They are responsible for the fundamental tyre characteristics, geometric shape and the stress-strain capacity. The secondary components such as chafers, flippers or ply turn-up, and breakers, reinforce or protect the primary components from high stress concentration by distributing forces over greater areas or through materials capable of withstanding particular stress conditions. They are used to modify the tyre's mechanical properties to obtain special characteristics.

1.3 Construction of tyres.

Basically the construction of the tyre can be classified into three types, namely a) bias or cross-ply tyre, b) bias-belted tyre and, c) radial-ply tyre. These three constructions are shown in Figs. 1.2, 1.3, and 1.4 respectively.

The difference between these three types of tyre lies in the construction of the casing and the presence of the belt around the outer circumference of the casing.

In a cross-ply tyre, the casing consists of two or more plies of rubberised cord fabric. The cords on each ply crossed the cords on the adjacent ply at approximately equal angle with the meridian. The crown angle, i.e, the angle at which the cords cross the centre circumferential line determine the stiffness of the casing and hence the comfort and stability of the ride. A low crown angle will give good stability and steering performance, but a harsh

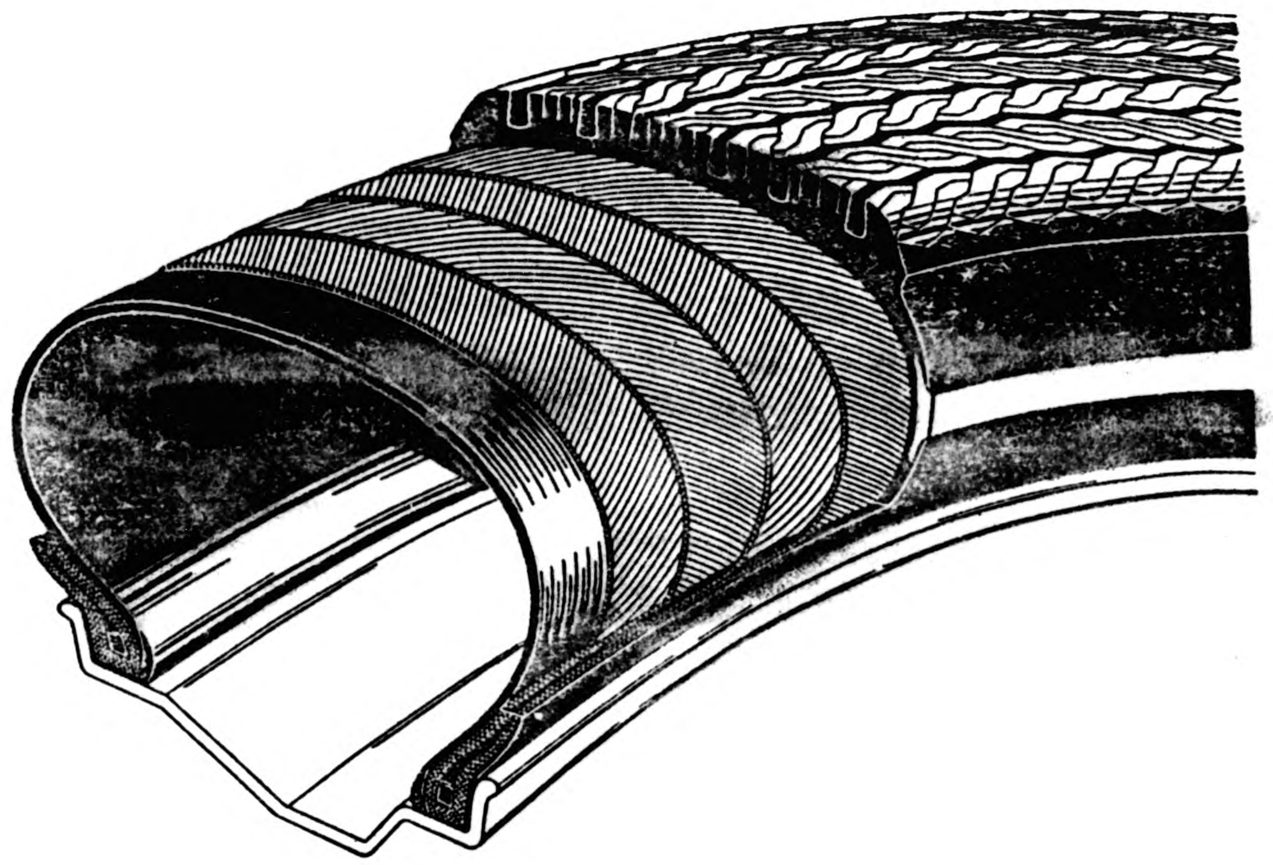

Fig. 1.2. Cross-ply construction (4)

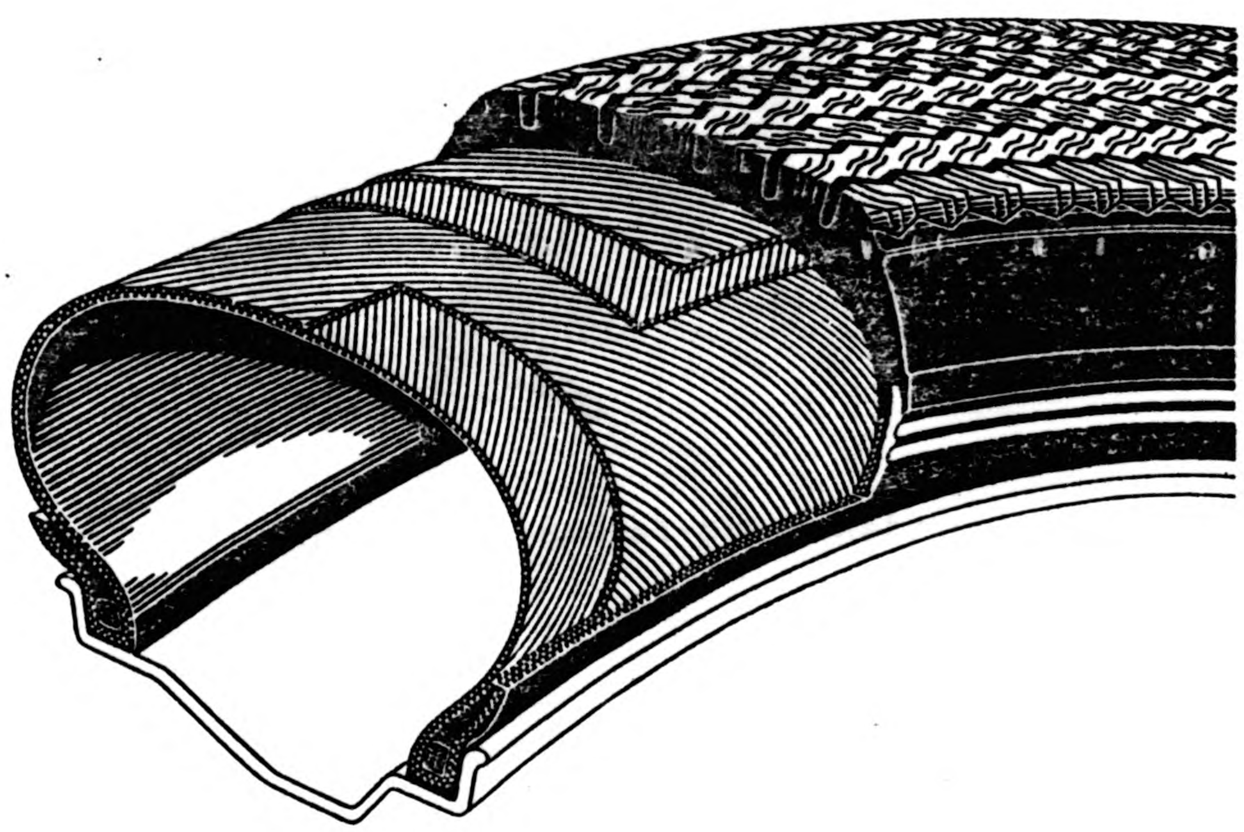

Fig. 1.3. Belted-bias construction (4)

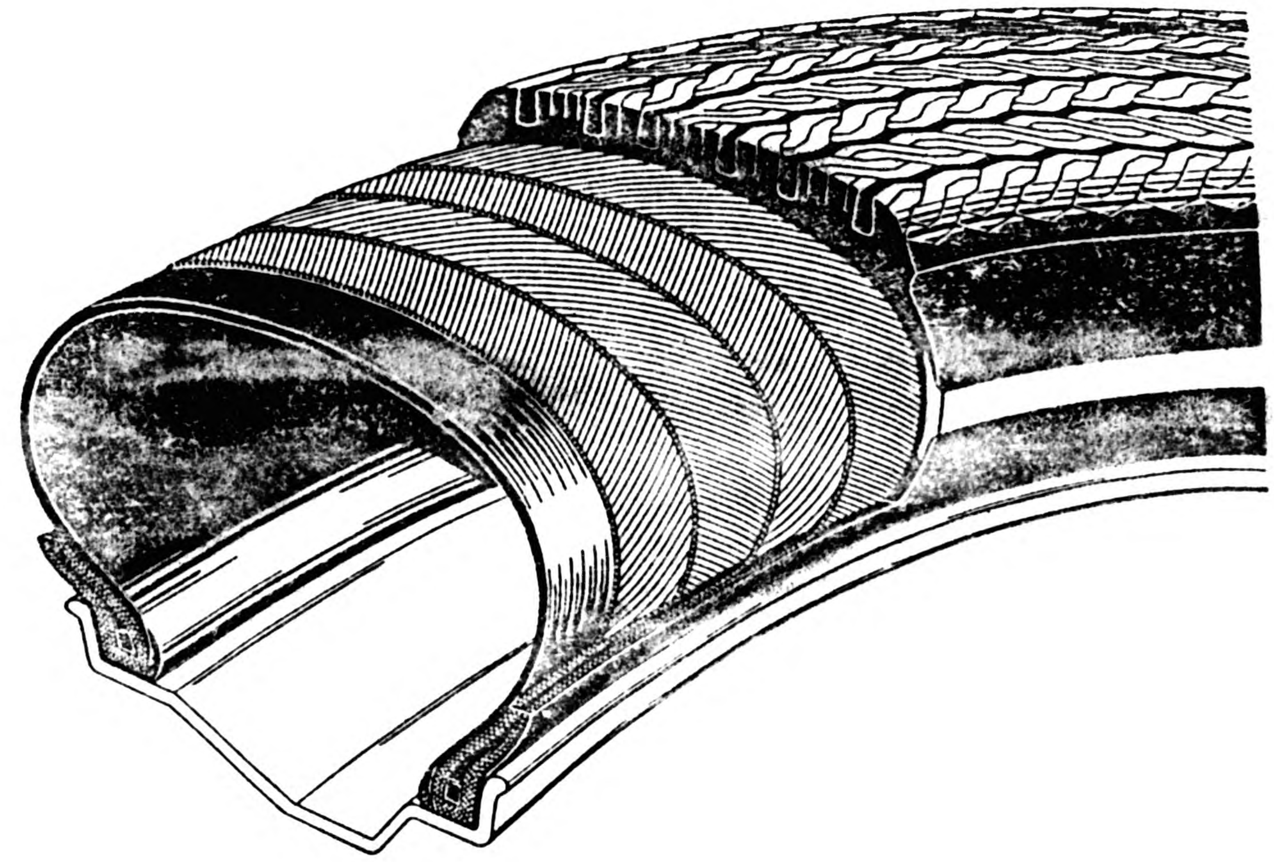

Fig. 1.2. Cross-ply construction (4)

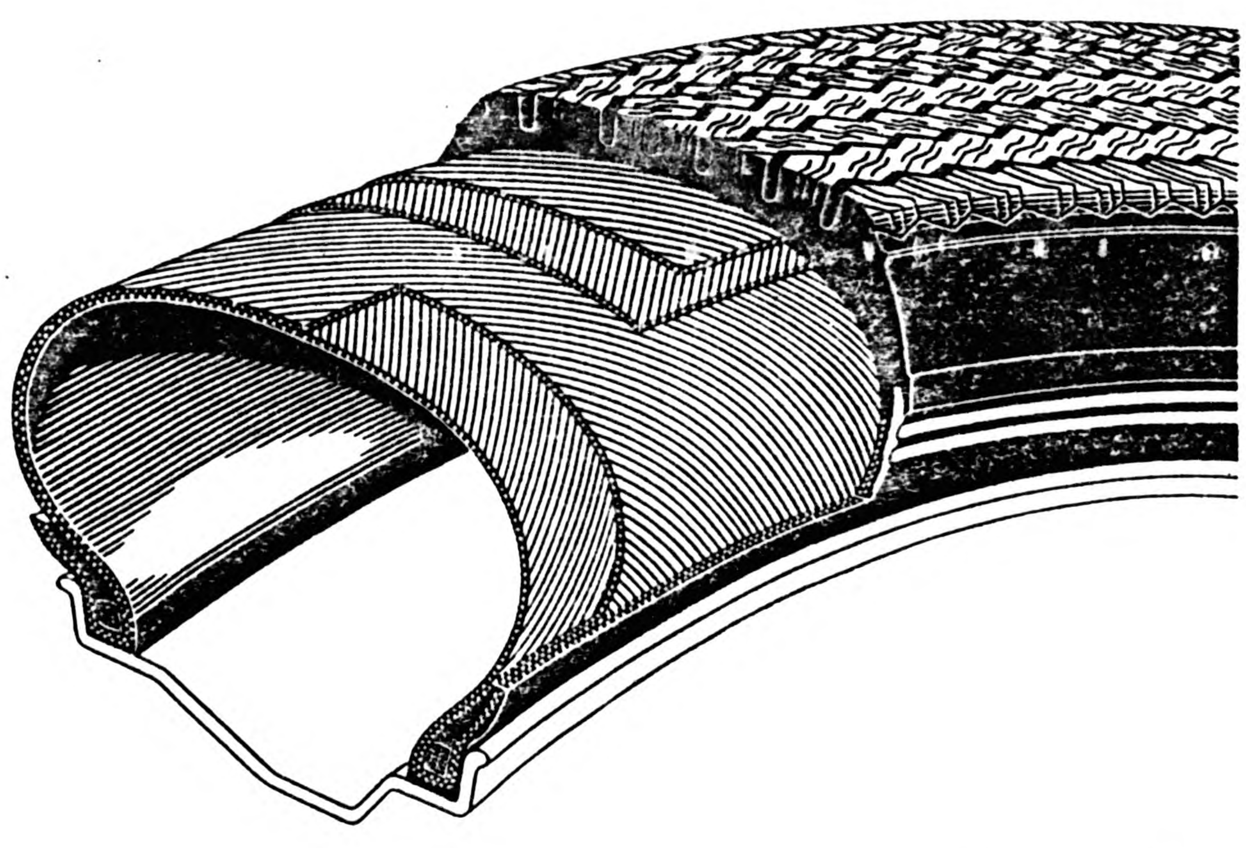

Fig. 1.3. Belted-bias construction (4)

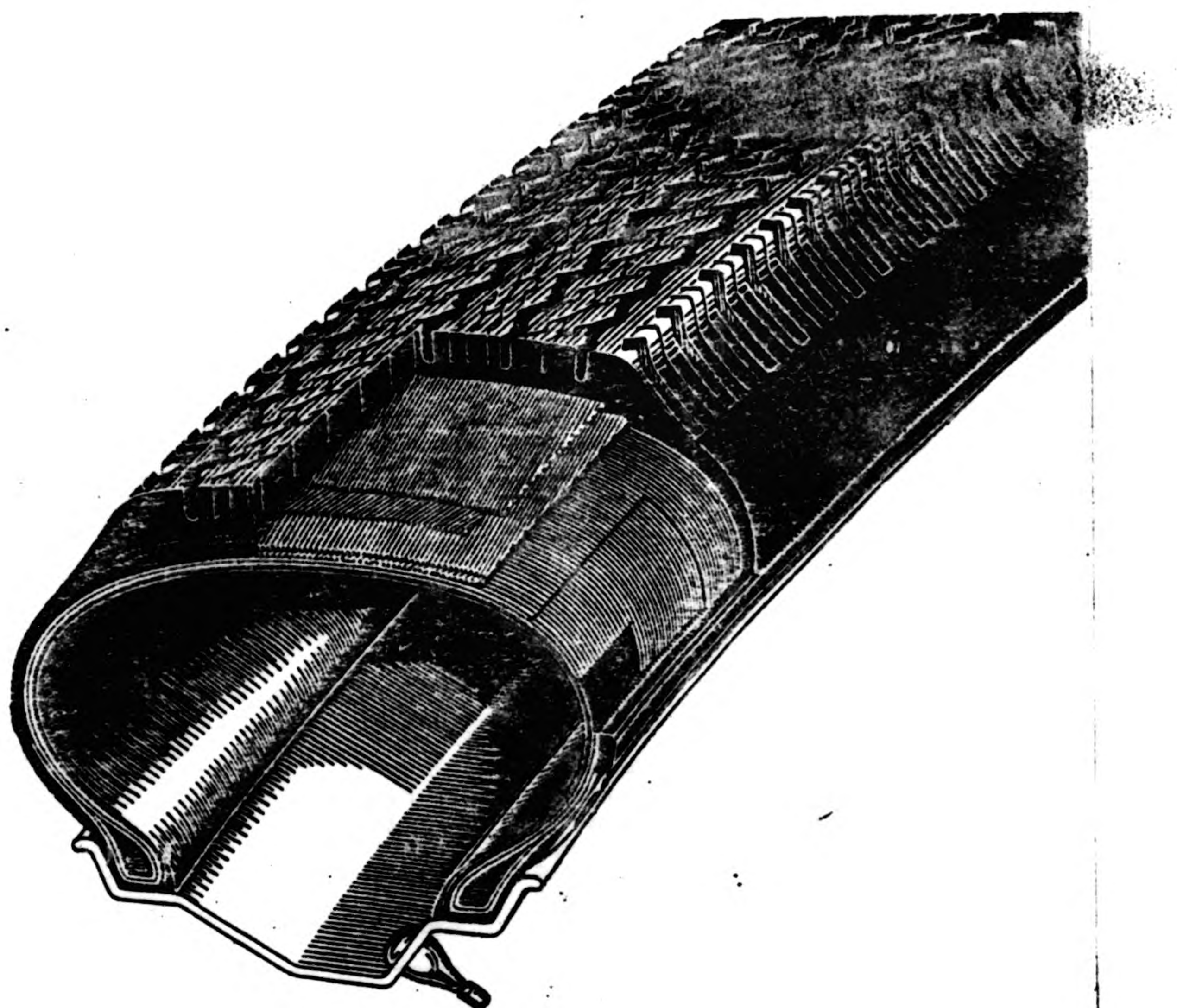

Fig. 1.4. Radial-ply construction (4)

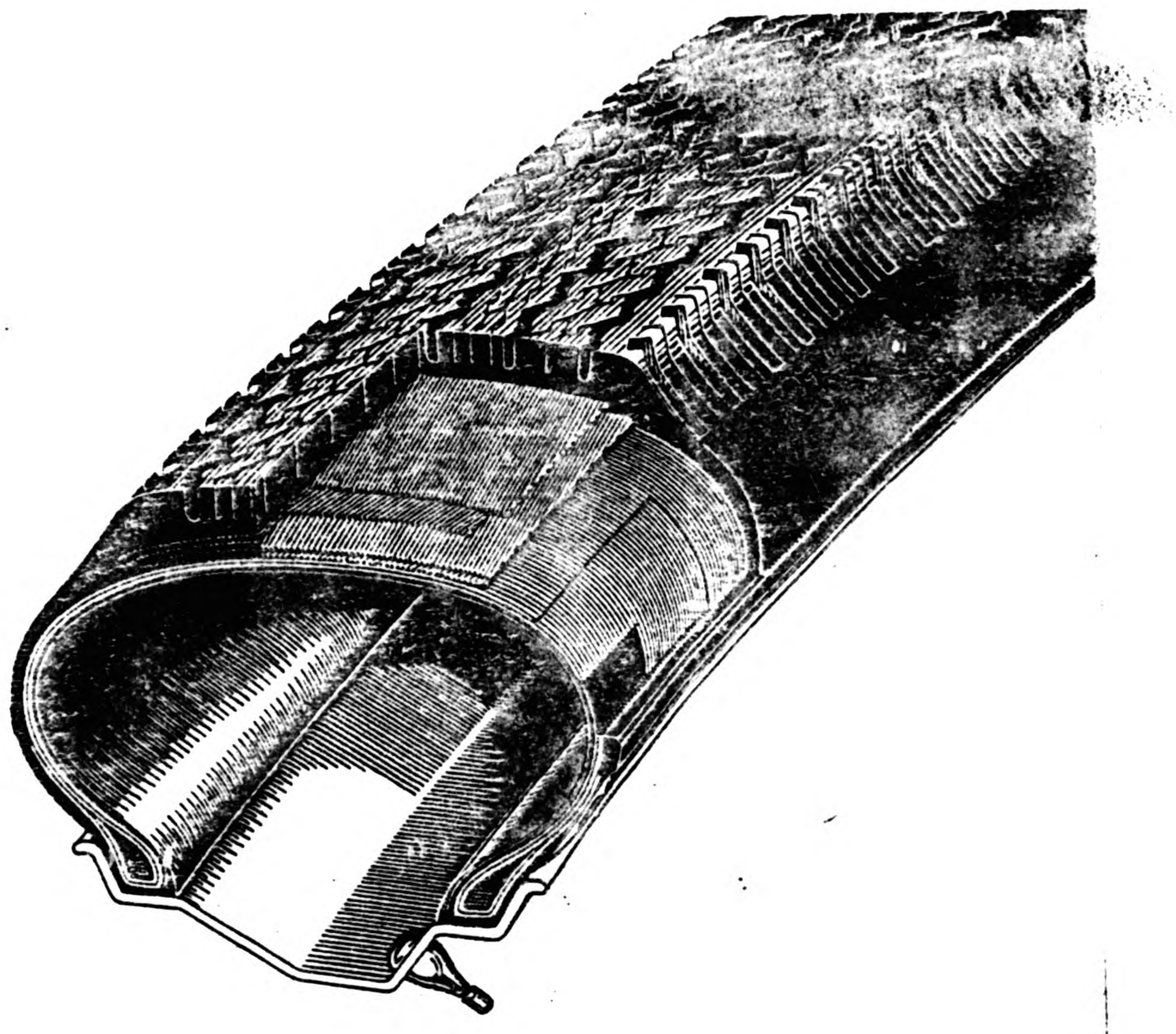

Fig. 1.4. Radial-ply construction (4)

fibres in the manufacture of tyres has been reported by Young(5) and Gardner(6).

Typical composition of a tread formulation is shown in Table 1.1. The choice of materials used is an important factor in a bid to get the desired optimum properties. A compromise has to be made in many instances since some requirements are mutually exclusive. For example compounds which have lower hysteresis and hence a lower rolling resistance coefficient are deficient in other properties such as wear and resistance to skidding.

Table 1.1. Tread composition of typical passenger car tyre(7)

Ingredient	Percentage (wt.)	Function	Raw Material
Styrene/Butadiene Rubber	23-28	Rubber	Refined Petroleum (light)
Polybutadiene Rubber	15-18	Rubber	Refined Petroleum (light)
Zinc Oxide	1-2	Vulcanization Activator	Zinc Metal
Stearic Acid	0.5-1	Vulcanization Activator	Refined Animal Fat
Process Oil	18-22	Processing Aid	Refined Petroleum (heavy)
Carbon Black	30-35	Reinforcing Material	Petroleum By-Product
Antioxidant/Antiozonant	0.5-1	Protective Material	Refined Petroleum (light)
Sulfur	0.5-1	Crosslinking Agent	Refined Sulfur
Accelerator	0.3-0.8	Vulcanization Catalyst	Refined Petroleum (light)

The fabric/cords used in the manufacture of a tyre has changed considerably during the years. The selection of the specific cord construction and material depends on the intended service requirements, the inflation stress level and from the economic point of view, on the cost of the materials.

ride , and as speed and inflation pressure increase, the cross-sectional shape of the tyre will show a considerable distortion. Increasing the angle will give a softer ride with an inadvertable loss of stability. Most cross-ply tyres have crown angle in the range of 36-41 degrees.

In the case of radial-ply tyre, the crown angle is 90 degrees. This gives maximum flexibility but minimum directional stability. A belt of two or more layers of fabric or steel rubberised cords is fitted around the outer circumference of the casing to provide the necessary directional stability needed. The cord angle of the belt are usually in the region of 18-21 degrees with the centre line along the circumference depending on the material used.

The bias-belted tyre is a combination of the cross-ply and the radial ply in its construction. It is claimed to combine the advantage of both. It has bias type of casing and a belt around the casing. It has not proved to be a commercial success and the market is being increasingly dominated by the radial construction.

1.4 Materials used in a tyre.

Basically a tyre is made up of cords impregnated with rubber, a tread made of a suitably compounded rubber and wire bead. A review of the development of cords and fibres in the manufacture of tyres has been reported by Young(5) and Gardner(6).

Typical composition of a tread formulation is shown in Table 1.1. The choice of materials used is an important factor in a bid to get the desired optimum properties. A compromise has to be made in many instances since some requirements are mutually exclusive. For example compounds which have lower hysteresis and hence a lower rolling resistance coefficient are deficient in other properties such as wear and resistance to skidding.

Table 1.1. Tread composition of typical passenger car tyre(7)

Ingredient	Percentage (wt.)	Function	Raw Material
Styrene/Butadiene Rubber	23-28	Rubber	Refined Petroleum (light)
Polybutadiene Rubber	15-18	Rubber	Refined Petroleum (light)
Zinc Oxide	1-2	Vulcanization Activator	Zinc Metal
Stearic Acid	0.5-1	Vulcanization Activator	Refined Animal Fat
Process Oil	18-22	Processing Aid	Refined Petroleum (heavy)
Carbon Black	30-35*	Reinforcing Material	Petroleum By-Product
Antioxidant/Antiozonant	0.5-1	Protective Material	Refined Petroleum (light)
Sulfur	0.5-1	Crosslinking Agent	Refined Sulfur
Accelerator	0.3-0.6	Vulcanization Catalyst	Refined Petroleum (light)

The fabric/cords used in the manufacture of a tyre has changed considerably during the years. The selection of the specific cord construction and material depends on the intended service requirements, the inflation stress level and from the economic point of view, on the cost of the materials.

Currently cords are made from a variety of materials such as rayon, nylon, polyester, glass fibre and steel wire. Each of these cord materials has qualities desirable for specific structural design and applications. Some of the relative properties of cord materials currently used are shown in Table 1.2.

Table 1.2. Cord material properties(3)

Property	Rayon, [illegible] in. dia	Nylon, [illegible] in. dia	Polyester, 0.[illegible]30 in. dia	Fiberglass, 0.02[illegible] in. dia	Wire, 0.014 in. dia
Tenacity (GPD)	4.0	7.5	7.5	8.[illegible]	3.5
Strength, lb					
Slow speed	[illegible]	[illegible]	67.0	75.0	54.0
Impact	71.0	71.0	78.0	95.0	69.0
Elongation at break, %	13.0	19.0	17.0	4.0	3.0
Modulus rating	100.0	60.0	100.0	1000.0	1000.0
Dimensional stability					
Shrinkage, %	3.9	6.0	3.0	0.1	0.1
Growth, %	2.0	8.0	3.0	0.1	0.1
Moisture, %	11.0	3.5	0.3	0.1	0.1
Heat resistance rating	100.0	150.0	210.0	1000.0	1000.0
Wet strength, %	60.0	90.0	99.0	99.0	99.0
Flatspotting rating	100.0	25.0	100.0	300.0	300.0
Specific gravity	1.52	1.14	1.38	2.52	7.8

Rayon, which replaced cotton as the principal tyre cord fibre has itself under the threat of being replaced by the newer cord fibre such as polyester and nylon in the carcass construction and by steel wire, glass fibre and aramid in belt construction.

1.5 Energy consumed by a tyre.

When a tyre is externally loaded, a portion of the tyre in contact with the road will be flattened. As well as the tyre being flattened, there are also extensive changes in the geometry of the tyre within the vicinity of the contact region(8).

These distortions are created as a result of the following factors, namely:

1. The creation of the bending strains in the tread and the belt/breaker of the tyre due to bending.

2. The formation of the compression strains in the tread as it is being compressed against the surface.

3. A tyre, being a doubly curved surface structure, when flattened there exists a region around the contact area where it extends. The sidewall bulge is the result of this extension.

4. The cords in the tyre suffers both the effect of extensions and compressions. Owing to their rigidity they do not stretch much, but

rather undergo substantial local changes to accomodate the extensions and compressions. This effect is generally known as 'squirming'. As a result of this shear strains are developed in the rubber. This effect is more pronounced in the cross-ply tyre than in the radial tyre.

All these distortions combine to form a complex distortion pattern.

Thus, as a tyre rolls each of its components will undergo the process of stretching, bending, shearing and relaxing. These components, being hysteretic in nature, tend to retain part of the energy and dissipate it as heat. Thus energy is being consumed by the tyre.

It has been stated on energy losses in tyres(9) that 90-95 percent of the energy loss is due to the hysteresis of the rubber and the cords, 5-10 percent to the friction between the tyre and road due to slip, and 1.5-3 percent to friction of tyre with air. While there is general agreement regarding the percentage loss due to hyteresis, there are differences in opinion on the ratio of distribution of the losses attributable to each of the two major components, namely, tyre cords and tyre compounds (10,11,12,13). At the moment, it is generally accepted that the cords contribute to about 20-40 percent of total energy losses and that the rubber compounds contribute the most of it. Hence improvement or change in the nature and amount of the rubber compounds used in the tyre will bring about the greatest improvement in the rolling losses of tyre. This has long been realised by the number of new inventions being patented (14,15,16) to mention a few. Fig. 1.5. shows the contributions of the various components to the rolling losses of tyre.

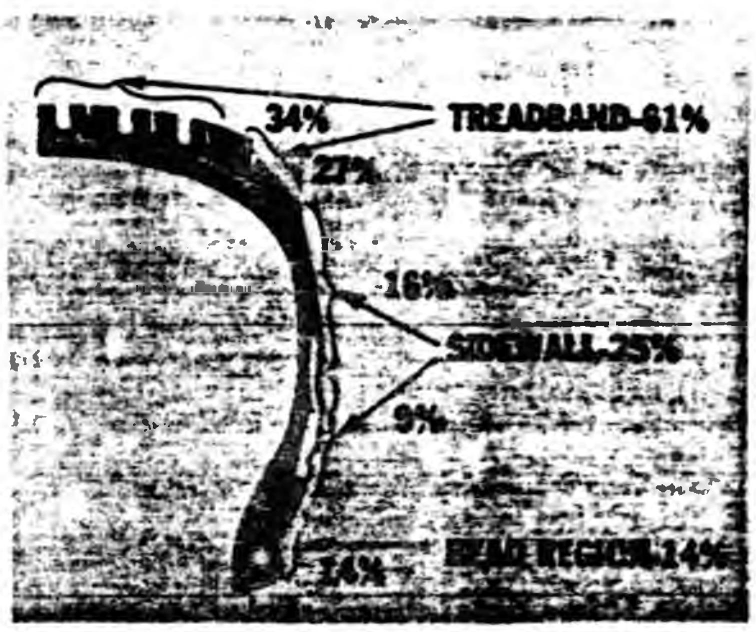

Fig. 1.5. Distribution of the rolling losses in the tyre components(17)

Reduction in the rolling losses of the tyre can also be brought about by the changes in the construction and design of the tyre. Studies(18) have shown that, depending on operating conditions, a 20-30 percent difference in rolling loss exists between the cross-ply and radial ply tyres especially in radial tyres having belt made up of steel cords. This difference is particularly due to the smaller deformation of the tread band and larger deformation of the sidewalls of the radial tyres. Low profile tyres also has a significant effect on the rolling losses of the tyre. Owing to their greater longitudinal tension and the lesser transversal tension of the belt, this will give rise to smaller deformations of the tyre tread band and consequently to a lower rolling resistance.

The effect of operating variables such as load, deflection and inflation pressure on the rolling losses of tyre has been extensively studied and is being comprehensively reviewed by Clark(19), Schuring(20) and recently by Chang and Shackleton(17). A lattice plot showing the effect of the operating variables on the rolling losses of tyre is shown in Fig. 1.6. Amongst other things, it indicates that at constant deflection the rolling losses increases with increase in load and inflation pressure. If on the other hand, the load is held constant then the influence of deflection is more dominant than inflation pressure on the rolling losses of tyre(21,22).

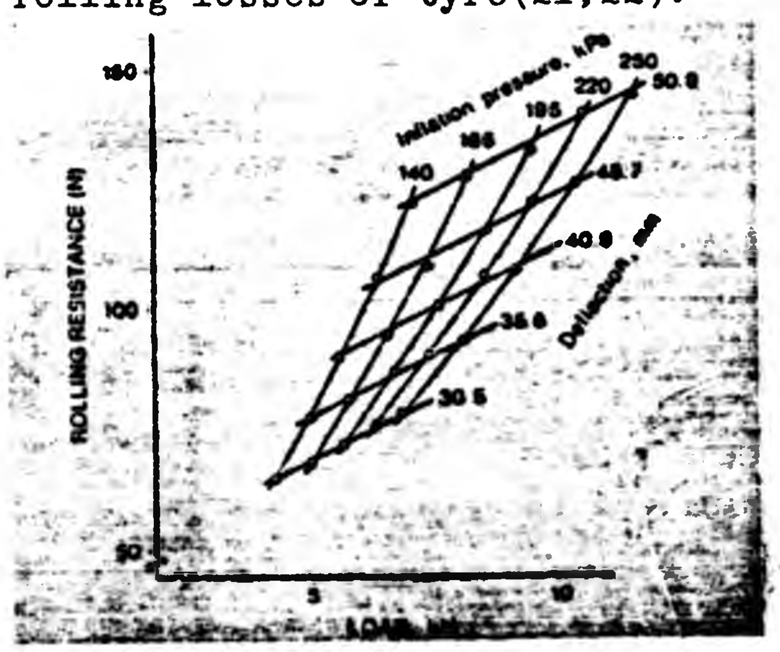

Fig. 1.6. Lattice plot of rolling losses as a function of load, inflation pressure and deflection (20).

1.6. Objectives of the project.

The main objective of this project is to study the energy storage characteristics of a statically loaded tyre of different constructions under a range of radial loads and inflation pressures. Apparatus to accurately measure the changes in tyre pressure, volume and deflection under load will be constructed and, therefore some time will be spent in detailing the design, construction and calibration of this equipment.

The requirements of the apparatus that will be needed to determine the energy storage in this project may conveniently be divided into two parts, namely;

1. Load application and deflection measuring assembly.

2. Equipment to measure the changes in the pressure and volume of the air under investigation.

The work to be carried out is therefore a fundamental investigation into the energy changes that occurs when an inflated tyre is loaded. It is perhaps surprising in view of the very widespread use of tyres that more work has not been published in this area. In the early days of tyre development progress in tyre design and construction was made by empirical trial and error and fundamental scientific work was bypassed. In this case, however, it is still a useful area for investigation because fundamental studies can provide a better understanding of the importance of the air and carcass contribution to load carrying performance of tyres and also as indication whether or not development of non-pneumatic tyres are feasible.

This thesis has been arranged into eight chapters. The present chapter has been concerned with a general introduction to the structure and components of the tyre and its influence to the rolling losses, together with the objectives of this investigation. Chapter 2 deals with the survey of literature pertaining to this work. Chapter 3 is concerned with the fundamental theory of the Equation of state of the air and the First Law of thermodynamics. Chapter 4 describes the experimental apparatus developed and the theory of determining the volume of the tyre based on the measurement of the changes in the volume and pressure of the air contained in the tyre. It also describes the application of the Equation of state and the thermodynamics Laws for the calculation of work done on air during the compression and and expansion process. Chapter 5 describes the experimental procedures; this include the determination of the parameters characterising the performance of the loading process and the calibration of the system. Chapter 6 presents and discuss the results which have been obtained for the effect of the investigated variables upon the energy changes in the tyre. Chapter 7 is concerned with the application of a simplified theory based on Gent and Thomas theory of air-spring in predicting the load-deflection behaviour of tyres. Chapter 8 gives a summary of the main conclusions which have emerged from this work, together with the suggestions for further work.

Following the main body of this thesis, appendices give the mathematical formulae for the analysis of the experimental errors of the data, and the computer programs to perform the calculation and analysis

CHAPTER 2

SURVEY OF LITERATURE.

As mentioned in the preceeding chapter, a pneumatic tyre is a toroidal shell made up of superimposed layers of rubberised cords. The cords may be of several different natural or synthetic fibres, or metal and the matric in which they are imbedded may be of natural or synthetic rubbers. As a result of this combination of materials of different rigidity, a high degree of anisotropy existed in the rubber-cord structure. Although the problem of stress analysing a pneumatic tyre under radial load has attracted the effort of many researchers, due to the complexity of the tyre structure, it is still not fully understood. The earliest known publication in this field was the work of Schippel (1).

The first step in an attempt to analyse stresses in a pneumatic tyre is the determination of an equation for the equilibrium shape of the tyre.

2.1. Shapes of pneumatic tyres.

An extensive review of th e theory of the equilibrium shapes of pneumatic tyre is presented by Frank and Hofferberth (2) and later by Yoshimura (3) Generally the equilibrium shape of thepneumatic tyre could be approximated by the use of the following theories.

(a) Network theory
(b) Membrane theory
(c) Shell theory

The network theory which is widely accepted as a basis for the calculation of the bias tyre is a result of the work of Hofferberth (4) which was published in the 1956. Purdy had carried out some work in this field in 1928, however, his work was not published until 1963 (5). This theory assumes that the entire inflation load is being carried by the cords in the carcass. These cords are assumed to behave as a trellis with the effect of rubber being neglected. The equation governing the shape of the inflated tyre in terms of its dimensions and its cords path is expressed in the form of hyperelliptical integral for which there is no known direct solution. Biderman(6) overcome this problem through the use of numerous nomograms based on graphical and numerical procedures (7). Bukhin (8) later extended the work of Biderman by taking into consideration the effect of the elongation of the cords.

With the advent of modern computers, Lauterbach and Ames (9) and Frank and Ellis (10) incorporated a digital computer to solve the complicated equation and obtained estimates of cords stresses. An extension of the theory whereby the cord path is taken into account has been performed by Ames and Walston (11).

The presence of the belt in radial tyres possed a different problem in the calculation of its equilibrium shapes because of the non-suitability of the network models. A laminar model which is based on the membrane and network theory was proposed by Robecchi et. al.(12). This theory which takes into account the strength of the orthotropic structure of the cord plies seems to satisfy the condition imposed by the radial tyres. Later shell theory which incorporates the flexural rigidity of the tyre belt was used to predict the shape of radial tyres. This theory is best exemplified by the work of Brewer (13).

An alternative approach which is based on the principle of energy minimisation was developed by Clark et. al (14). This approach has the benefit of overcoming the tedious problem encounterd by Brewer in dealing with orthotropic toroid inflation problem. Koutny(15) on the other hand applied this method to the energy of the air contained in the tyre to predict its equilibrium shape.

The use of Finite Element Method (FEM) in the field of structural engineering is well-known but not so in the tyre industry. One of the pioneers to introduce the FEM in tyre is Zorowski(16). He used it to model the shape of a rotating tyre. Nowadays, with the deeper understanding of the nature of the orthotropic laminates and the availability of more powerful computers, the use of FEM in the rubber industry has become widespread.

2.2. Effect of internal pressure on profile shape.

When the tyre is pressurised, at first the volume of the tyre changed substantially but on subsequent increase in pressure produced no significant increase in the volume of the tyre. This behaviour was observed by Biderman et. al.(17) in their work on a 9.00-20 cross-ply truck tyre. They proposed that at low pressure the shape of the tyre was determined by forces acting on the rubber only whereas at higher inflation pressures the shape changes depend on elongation of the cords which is very difficult in view of their rigidity. Clark et. al.(14), amongst others, have carried out some work on the effect of cord angles and cord stiffness upon the shape of an inflated truck tyre. They found that the inflated shape of a tyre made from rayon cords to be substantially different from the shape of a tyre made from nylon cords. This is shown in Figs. 2.1a and 2.1b.

In the case of radial tyre, Robecchi(12) have carried out calculations for the 165SR13 tyre. Amongst

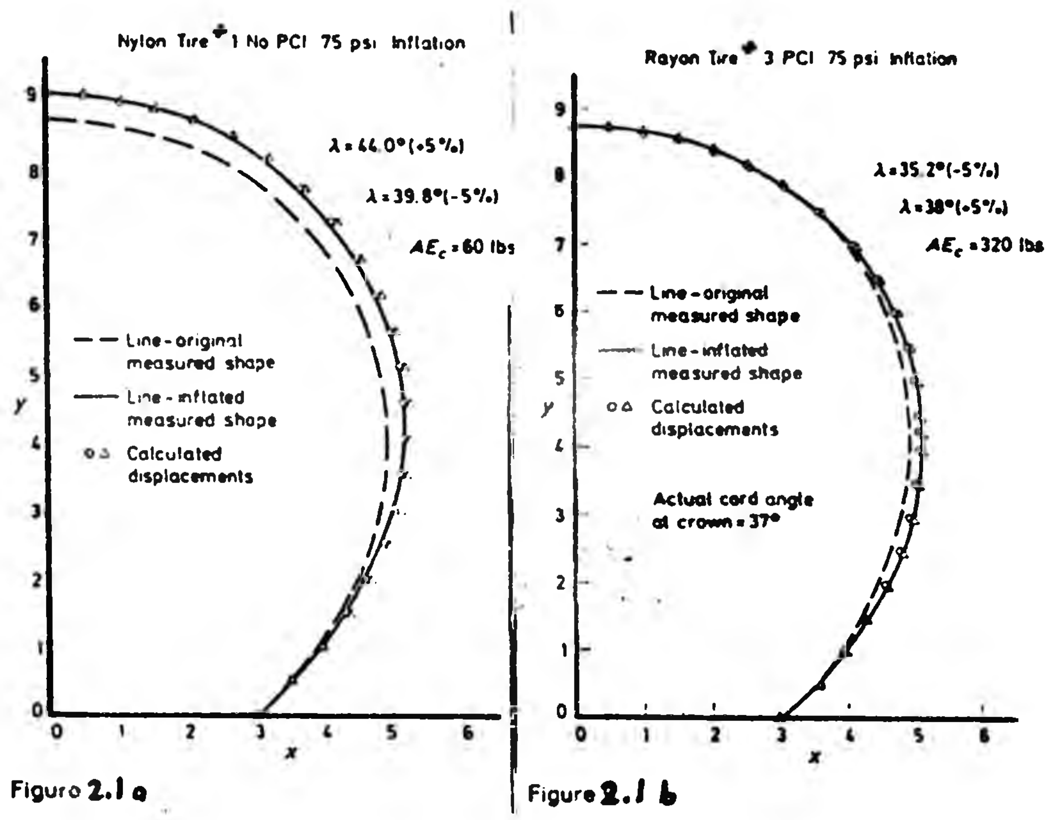

Fig. 2.1. Comparison of an inflated and initial shape of truck tyre at 75 psi. (14)
(a) Nylon cord (b) Rayon cord

other things they found that there is not very much change in shape from the uninflated to the inflated state, Fig. 2.2.

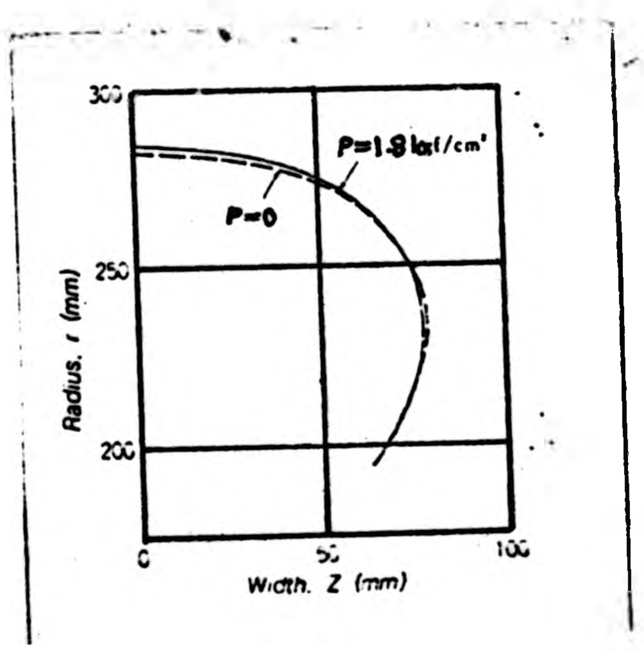

Fig. 2.2. Comparison between the shapes of an uninflated and inflated 165 SR13 tyre (12)

2.3. Effect of shape of tyre on the load carrying capacity of tyre.

W.L. Jackson (18) claimed that the load carrying capacity of a tyre could be increased by changing the curvature of the sidewall i.e., by straigtening the walls of the tyre. The straigtening of the walls will enhance the pneumatic stiffness of the tyre and thus increased its load carrying capacity. The relationship between the pneumatic stiffness and the shape factor is derived.

Monzini (19) used the same equation to relate pneumatic stiffness to sidewall curvature but he extrapolates in a different direction to arrive at a tyre having a radically different shape which again offers improved load carrying capacity.

Markow (20) has taken a different approach to bring about an increase in the load-carrying capacity of the tyre. Instead of the conventional breaker construction, he uses sheets of steel thereby producing a tyre having a different cross-sectional shape which is capable of carrying a standard load at a greatly reduced inflation pressure.

G.V. Nadezdin (21) on the other hand have carried out an experimental study of the effect rim width on the deformation of tyre by varying the ratio of rim width to width of tyre. He concluded that increasing the ratio of rim width to width of tyre increases the tyre loading capacity and also that the tyre-loading capacity depends upon the change in the air-volume with radial deformation.

Slyudikov (22) experimental with model tyres having different aspect ratios. He found that a reduction in the aspect ratio brings about a decrease in the tension of the carcass due to inflation pressure and as a consequence of this an increase in the radial stiffness of the tyre.

Another theoretical approach based on the principles of calculus of variations and laws of thermo-dynamics was developed by Koutny (15) Using this approach the volume of the model tyre under radial deformation can be estimated and hence the change in volume. He claimed that the predicted change volume of the tyre under deformation were in close agreement with the results obtained experimentally.

2.4. Mechanism of load transmission.

The mechanism of load transmission from a contact surface to the rim has been postulated by Gough (23). He postulates that there are two mechanisms involved and that these take place simultaneously.

The first mechanism is between the tread band and the wheel whereby the tyre behaves as a structure. This is analogous to that of a cycle wheel where the hub hangs by the steel wire spokes from the top of the rim.

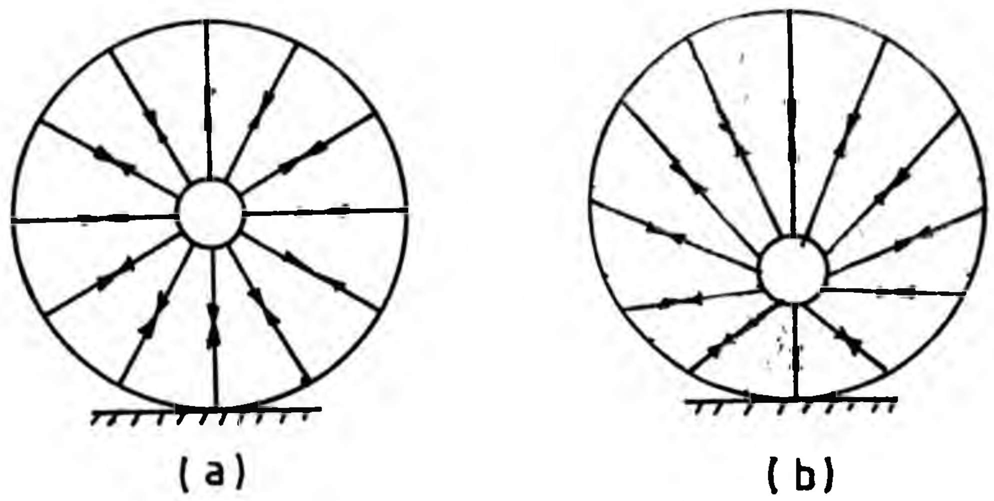

Fig. 2.3. Schematic diagram of the tensions in the spokes (a) Unloaded (b) Loaded.

If the weight of the hub is assumed to be negligible, then the initial tension in all the spokes will be the same and the nett outward forces will be zero. When a plate is pressed against the lower sector of the rim, part of the spokes in this sector will experience a reduction in the tension whereas the spokes in the upper sector will experience an increase in their tension. As a result of this imbalance of tension there will be a nett upwards force.

In the case of a tyre this upwards force will pull the bead coil above the contact region upwards against the base of the wheel rim and hence transmitting the contact force to the wheel.

The second mechanism of load transmission can be explained in terms of a tyre behaving as an inflated membrane. On inflation tension is introduced into the cords and this is resisted by the tension developed in the bead coil. The initial radial component of bead coil reaction is shown in the diagram as f_o and

$$f_o = t_o \cos \theta_o = Pr_o \cos \theta_o \qquad (2.1)$$

where t_o is the reaction at the bead coil, P is the inflation pressure and r_o is the radius of curvature.

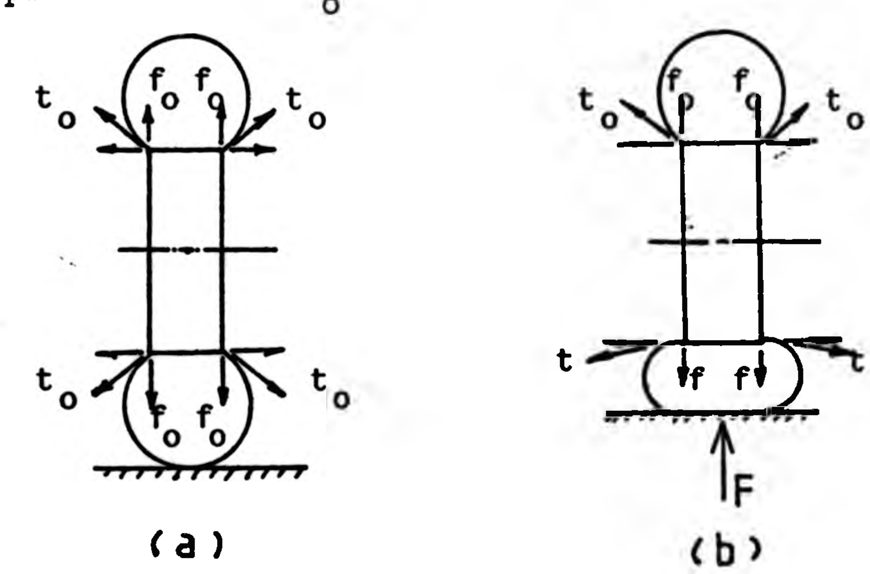

Fig. 2.4. Schematic diagram of the reaction at the bead coil. (a) Inflation (b) Inflation and loaded.

When a load is applied onto the tyre, this causes the sidewall near the contact patch to deflect and hence there is an increase in the curvature of the wall. As a consequence of this there is a reduction in the tension of the cords and hence a reduction in the radial component of the reaction at the bead coil to f where

$$f = Pr\cos\theta \tag{2.2}$$

This unbalances the forces round the bead with the nett result the bead coil in the lower section being pulled upwards against the base wheel rim.

A secondary form of support mechanism is provided by bending moments. Applied through the lower sidewall to the bead, as shown in Fig. 2.5.

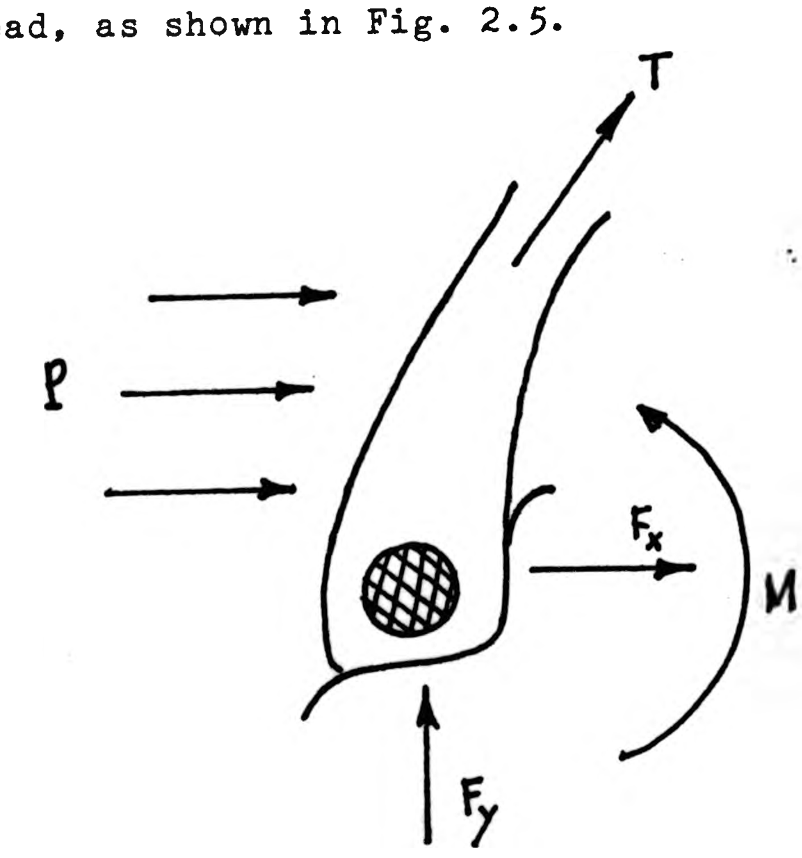

Fig. 2.5. Bending moments exerted by the lower region of the sidewalls.

Thus from these mechanisms of support it is evident that the wheel is not supported within the tyre by air pressure but rather by the air pressure stiffened tyre structure.

2.5. Contact between a tyre and road.

When a tyre is deformed by a vertical load, there will exist a balance in the contact region between the applied load and the integral of the pressure over the whole of the contact area.

In the case of a tyre having an infinitely thin wall, the pressure will be equal to the inflation pressure and its distribution over the contact area will be equal. In an actual tyre, the contact pressure will not be equal to the inflation pressure and it will be unequally distributed over the contact area. This is due to the inherent stiffness of the tyre tread, sidewall and carcass. Fig. 2.6 shows the distribution of the pressure of a radial tyre. It is evident that the pressure is high at the edges and low at the centre of the contact area.

See overleaf.

Fig. 2.6. Pressure distribution

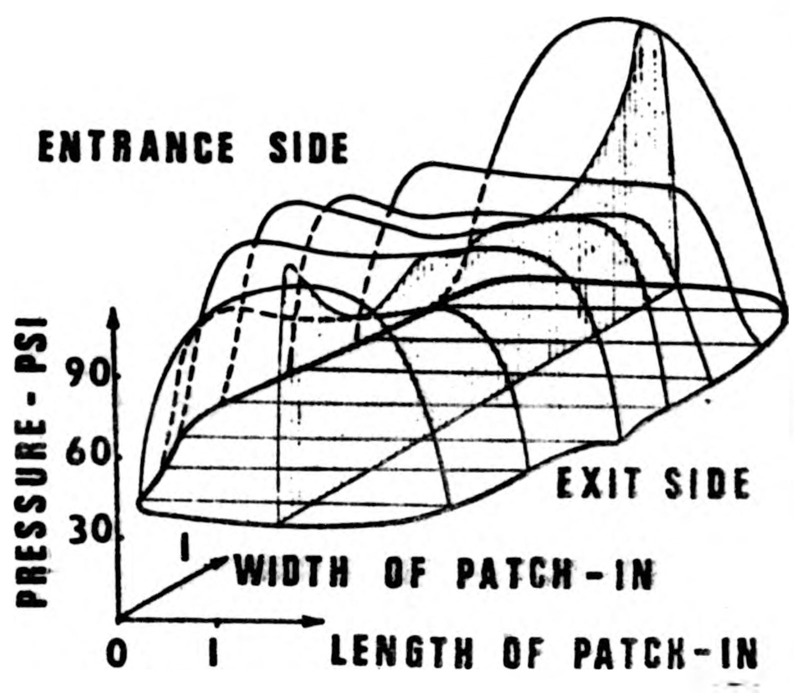

Fig. 2.6. Pressure distribution of a radial-ply automobile tyre (32)

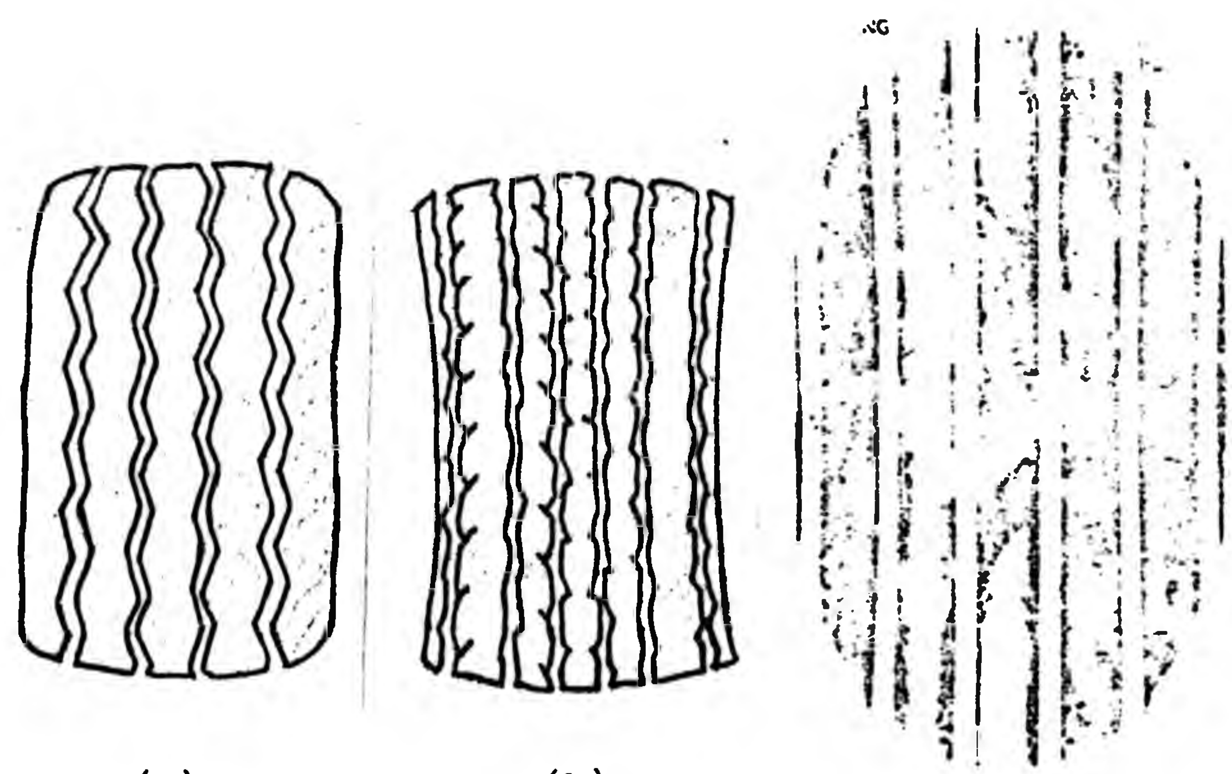

(a) (b) (c)

Fig. 2.7a. Contact patch of automobile and aeroplane tyre.

(a) radial-ply tyre and (b) cross-ply tyre autonobile tyres(33)

(c) aeroplane tyres (34)

2.5.1 Contact Area

The shape of the contact area depends on the cross-sectional shape and structure of the tyre. For an aeroplane tyre, it has a shape more or less of an ellipse, Fig. 2.7. Automobile tyres, on the other hand due to the stiffness of its structure especially at its shoulder, exhibit a contact area which is almost rectangular in shape.

Simplified theory for the calculation of the area of contact between a tyre a flat surface, is based on an equation relating to the geometry of intersection of a toroidal envelope of revolution by a plane, Fig. 2.8. In deriving this equation, it is assumed that the deformed tyre undergoes no distortion in the contact region. From Fig. 2.8, an equation relating the contact length and the diameter and deflection of the tyre is given as,

$$a = D_t \sqrt{\frac{z_c}{D_t} - \left(\frac{z_c}{D_t}\right)^2} \quad \ldots\ldots\ldots\ldots\ (2.3)$$

and the width of the contact is given by the expression,

$$b = \sqrt{wz_c - z_c^2} \quad \ldots\ldots\ldots\ldots\ldots\ldots\ (2.4)$$

Since the contact area is elliptical in shape, its value is given by

$$A = \pi \frac{a}{2} \cdot \frac{b}{2}$$

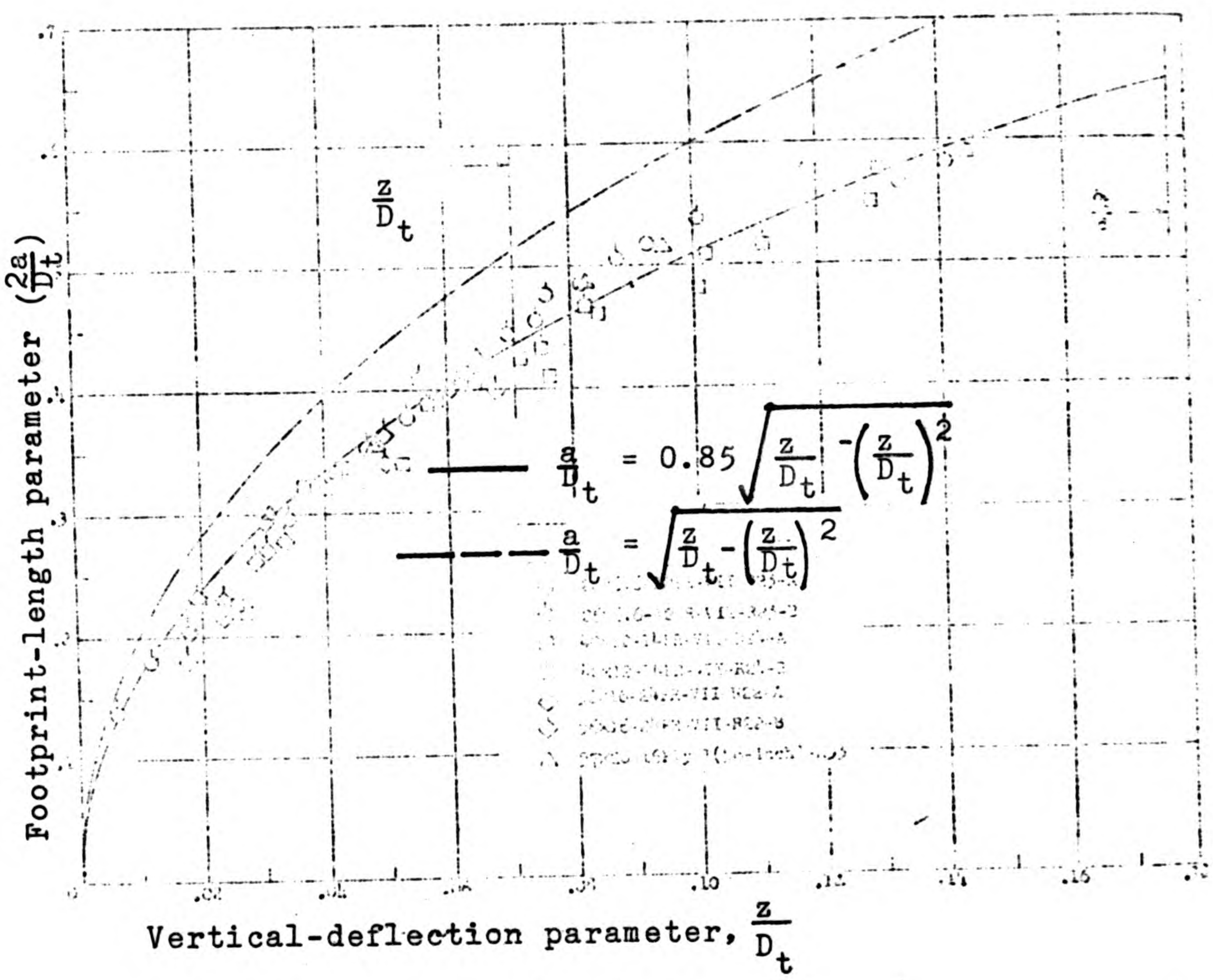

Fig. 2.7b. Variation of contact length against vertical deflection (27).

$$= \pi z_c \sqrt{(w - z_c)(D_t - z_c)} \qquad (2.5)$$

$$\simeq \pi z \sqrt{D_t w}$$

Regarding the contact length when the flexural rigidity of the tyre in the circumferential direction is taken into consideration, the actual contact length will be smaller than that calculated from equation (2.3). Rotta (24) proposes the relationship

$$a^{-} = a - 0.08R_t \qquad \ldots\ldots\ldots\ldots (2.6)$$

where a^{-} is the actual contact length.

Experimental works carried out by Rekiter (25) on truck tyres, Dunlop Rubber Co. Ltd. as reported by Hadekel (26) and Smiley and Horne (27) on aeroplane tyres suggest that the actual contact length is related to the choid length according to the relationship,

$$a^{-} = k\,a \qquad (2.7)$$

where $k = 0.7 \sim 0.8$ for automobile tyre

$\simeq 0.85$ for aeroplane tyres

Fig. 2.7 shows the variation of the contact length against vertical deflection for various aeroplane tyres.

2.6. Relationship between pressure rise and volume change.

When an inflated pneumatic tyre is deflected by a vertical load there will be a decrease in the volume of the air in the tyre and as a consequence of this there will be a corresponding rise in the pressure of the air. The relationship between the volume change and pressure rise may be approximated according to the equation[27]

$$(P_{i,a} + \Delta P)(V_o + \Delta V)^n = P_{i,a} V_o^n$$

or

$$1 + \frac{P}{P_{i,a}} \quad 1 + \frac{\Delta V}{V_o}^{\,n} = 1 \qquad (2.8)$$

where $P_{i,a}$ = the initial absolute inflation pressure

ΔP = pressure rise

V_o = initial air volume

ΔV = change in volume

n = polytropic exponent

For small pressure and volume changes, equation (2.8) can by means of binomial series expansion of the factor $(1 + \frac{\Delta V}{V_o})^n$ and neglect small higher order terms, be put in the simple form.

$$1 = (1 + \frac{\Delta P}{P_{i,a}})\,(1 + n\frac{\Delta V}{V_o} + \ldots\ldots\ldots)$$

$$= 1 + \frac{\Delta P}{P_{i,a}} + n\frac{\Delta V}{V_o} + \ldots\ldots\ldots\ldots$$

or, approximately

$$\frac{\Delta P}{P_{i,a}} = -n \frac{\Delta V}{V_o} \qquad (2.9)$$

If the compression process takes place very slowly, the process can then be regarded as isothermal and hence n = 1 and equation (2.9) can be written as

$$\frac{\Delta P}{P_{i,a}} = - \frac{\Delta V}{V_o} \qquad (2.10)$$

2.7. Effect of change in volume and pressure rise in tyre upon deflection.

Although much work has been done in the study of the equilibrium shapes of pneumatic tyres, little information is available on the theoretical study of the change in volume of the tyre under radial deflection. This is because of the difficulties in ascertaining the change in the configuration of the tyre under deformation. Early work by Hadekel(26) in the determination of the change in volume of tyre upon deflection was based on the assumption that the deflection was small and the area of contact was an ellipse. He approximated the change in volume, ΔV, to be proportional to the volume of elliptical segment with the semi-axes a and b and the deflection of the carcass, z_c,

$$\Delta V \propto \tfrac{1}{2} \pi ab z_c \qquad (2.11)$$

or, approximately

$$\frac{\Delta P}{P_{i,a}} = - n \frac{\Delta V}{V_o} \qquad (2.9)$$

If the compression process takes place very slowly, the process can then be regarded as isothermal and hence n = 1 and equation (2. 9) can be written as

$$\frac{\Delta P}{P_{i,a}} = - \frac{\Delta V}{V_o} \qquad (2.10)$$

2.7. Effect of change in volume and pressure rise in tyre upon deflection.

Although much work has been done in the study of the equilibrium shapes of pneumatic tyres, little information is available on the theoretical study of the change in volume of the tyre under radial deflection. This is because of the difficulties in ascertaining the change in the configuration of the tyre under deformation. Early work by Hadekel(26) in the determination of the change in volume of tyre upon deflection was based on the assumption that the deflection was small and the area of contact was an ellipse. He approximated the change in volume, ΔV, to be proportional to the volume of elliptical segment with the semi-axes a and b and the deflection of the carcass, z_c,

$$\Delta V \propto \tfrac{1}{2} \pi \, ab \, z_c \qquad (2.11)$$

But a and b are related to the external diameter of the tyre, D_t, and the radius of curvature of the carcass, R, (See Fig. 2.8) according to the relationship

$$a = \sqrt{D_t z_c} \quad \text{and} \quad b = \sqrt{2Rz_c} \qquad (2.12)$$

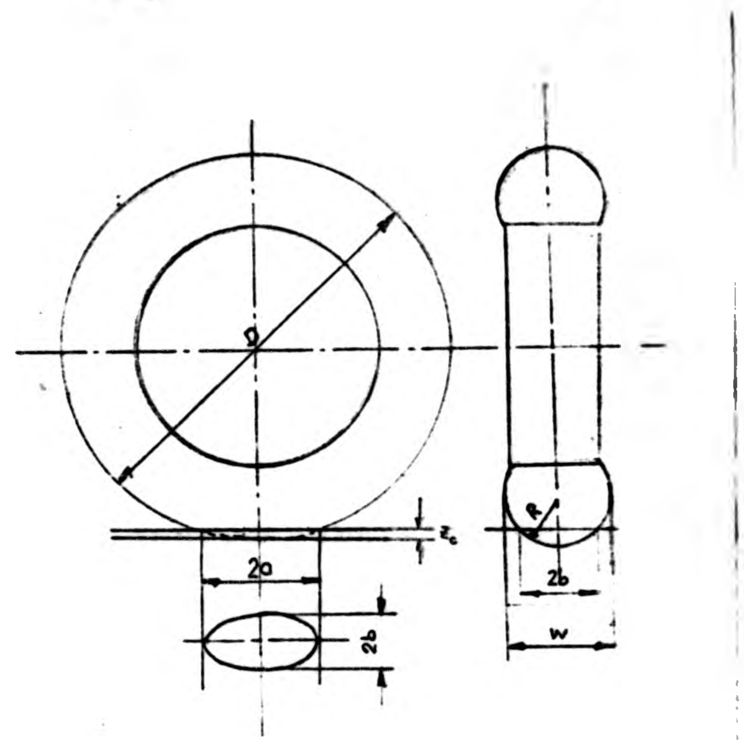

Fig. 2.8. Cross-sectional view of a deformed tyre.

substituting the values of a and b into the equation (211) and introducing a constant of proportionality k_1 gives

$$\Delta V = k_1^{\frac{1}{2}} z_c^2 \sqrt{2D_t R}$$

$$\text{or,} \qquad \Delta V = k_2 \; z_c^2 \sqrt{D_t W} \qquad (213)$$

where W is the width of the tyre.

The effect of rise in pressure of the air in the tyre upon deflection can be estimated by using equation (2.10) and (2.13). Micheal (30) has carried out measurements of the rise in pressure for aeroplane tyres of various proportions, and suggested the expression

$$\frac{\Delta P}{P_{i,a}} = x\left(\frac{z_c}{W}\right)^2 \qquad (2.14)$$

where x is a constant depending on the ratio $\frac{W}{D}$.

2.8. Load-deflection characteristics of tyre.

The deflection characteristics of a vertically loaded tyre depends on the relative change in the stress in the carcass cords as the load is applied, and on the numbers of cords experiencing this change. The mechanisms of load transmission have been fully described in the preceeding section.

An equation based on the assumption that the work of compression is an isobaric process was proposed by Biderman (6) for relating the deflection and the load of a standard construction (bias) type tyre,

$$z = \frac{C_2F}{2P} + \sqrt{\left(\frac{C_2F}{2P}\right)^2 + C_1F} \qquad (2.15)$$

where z = deflection of tyre, cm

C_1 & C_2 = constant coefficients for a given tyre

F = load, kgf

P = inflation pressure, kgf/cm^2

The values of C_1 and C_2 can also be found graphically from static tests of tyres[28].

The disadvantage about Biderman's semi-empirical formula is that the deflection becomes infinite at zero pressure. Thus, there is an unspecified set of conditions of pressure below which it does not apply.

The principle of regarding the tyre behaving as a structure and as an inflated membrane has been long known. Cooper(29) applied this principle in modelling the tyre as consisting of two springs in parallel, one of these being the air contained in the tyre and the other being the tyre structure. From his analysis, whereby the effect of rise in pressure is being ignored, he derived an equation relating the total load done onto the tyre to the load done to deform the structure and air in the form,

$$F = zk_s + Pk_p\left\{ z - z_o \left(1 - e^{z/z_o}\right)\right\} \quad (2.16)$$

where z = radial deflection

k_s = structural stiffness

P = inflation pressure

k_p = pneumatic stiffness

z_o = the intercept on the z-axis of a straight line represented by the equation $\frac{dF}{dP} = k_p(z - z_o)$

$\frac{dF}{dP}$ = equivalent contact area

The first term in the equation (2.16) corresponds to the load required to deform the structure while the second term corresponds to the load required to deform the air contained in the tyre.

Micheal (30) having ascertained that the contact area varies linearly with deflection attributes the non-linearity of the load-deflection curve purely to rise in pressure and therefore writes

$$F = A\ (P + P_c + \Delta p) \qquad (2.17)$$

where
A = area of contact
P = inflation pressure
P_c = ground pressure due to cover only
Δp = rise in pressure

Tiemann (31) found great similarity between reduced load-deflection curves for a great variety of passenger and truck tyres. The dimensionless load versus dimensionless deflection can be reasonably represented by a single curve

$$\frac{F}{W\ P\sqrt{2rH}} = f\left(\frac{z}{H}\right) \qquad (2.18)$$

where W = section width of the tyre

H = section height of the tyre

r = radius of the rim

f = function

z = radial deflection

In the above equation, howver, distinction has to be made between the bias-ly and radial-ply tyres.

A similar equation was proposed by Smiley and Horne (27) for aeroplane tyres. In their proposed equation which takes into account the rigidity of the tyre structure, P is replaced by $P + 0.08\ P_r$ where P_r is the rated inflation pressure.

2.9. Use of models for predicting the load-deflection behaviour of tyres.

The study of the behaviour of the load-deflection characteristics of a pneumatic tyre through the use of idealised models such as an inflated tube between parallel plates[35] and an inflated ring between parallel plates[36] have been proposed and analysed by several workers. The use of an inflated tube between parallel plates as a model, however, neglects the effect of the bending rigidity of the tread and the carcass components of the tyre which was found experimentally to contribute about 10-20 percent of the vertical load. The inflated ring model has an advantage over the inflated tube model because it takes into account the bending rigidity of the tread band. It has been generally accepted that the load imposed on a tyre is being carried by the structural and the pneumatic components of the tyre. Nicholson(37) used the inflated ring model in his analysis of the structural and the pneumatic contributions to the tyre behaviour under vertical load. Recently Yamagishi(38) and Yamagishi and Jenkins(39) used the ring model to determine the contact pressures of the truck tyres. The linear differential equations of the model are solved by using the singular perturbation technique.

CHAPTER 3

EQUATION OF STATE AND THERMODYNAMICS

3.1. Equation of State

One of the simplest form of the equation of state of a gas is the equation of state of an Ideal gas. An Ideal gas is defined as one which satsifies the following two equations (1)

$$PV = nR_uT = \frac{m}{M} R_uT \quad \text{................} \quad (3.1)$$

and

$$u = f(T) \quad \text{............................} \quad (3.2)$$

where P = pressure of the gas (absolute)
V = volume of the gas
T = absolute temperature of gas
m = mass of the gas
M = molecular weight of the gas
n = number of moles of the gas
R_u = universal gas constant
U = internal energy of one mole of the gas.

Equation (3.1) is a combination of the Boyle's and Charle's laws and since these laws are not exact, the Ideal Gas

Law holds only approximately for real gases, describing their behaviour under moderate pressure and well above the critical temperature. Some deviations from the Ideal Gas Law do exist when measurements were made at higher pressure or even when very accurate measurements were made at ordinary pressures, as shown in Figs. 3.1 and 3.2 respectively.

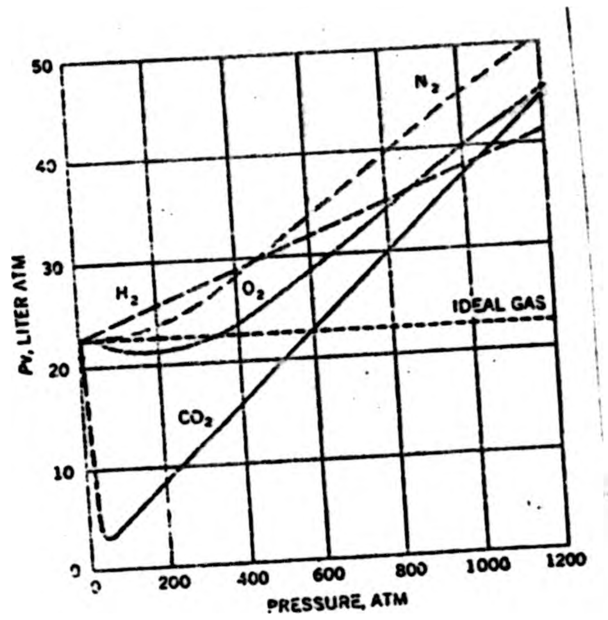

Fig. 3.1. Behaviour of gases at high pressure (2)

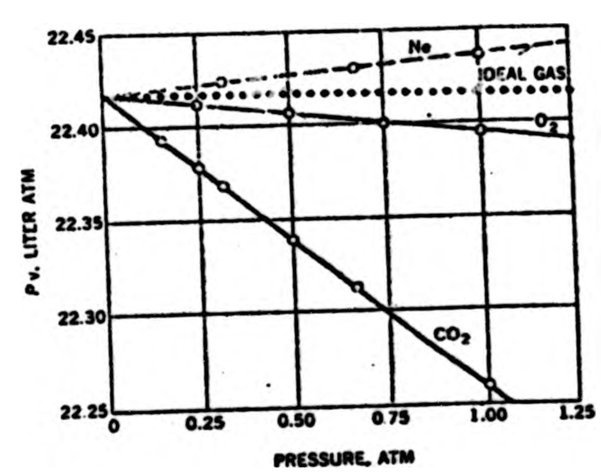

Fig. 3.2. Deviations of the Pressure-volume measurements of gases or ordinary pressure (2)

Many equation of state have been suggested (3) to represent the actual behaviour of real gases at critical temperatures and pressures, amongst others Van der Waals equation, Dieterici equation and the Virial equation to mention the few.

3.2. Partial pressure of a gas in a mixture of Ideal Gases.

Suppose a gas of different chemical composition, and each constituents behaves as an ideal gas, then the mixture would behave as an Ideal Gas in accordance with the Ideal Gas equation,

$$P_i V = \frac{m_i}{M_j} RT = n_i RT \quad \ldots\ldots\ldots\ldots\ldots (3.3)$$

where m_i = mass of the gas i in a container volume V

M_i = molecular weight of the gas i

n_i = number of moles of the gas i

P_i = pressure exerted by the gas i

According to the Dalton's law of partial pressures, which states that the total pressure exerted by the mixture of ideal gases is equal to the sum of its individual pressures exerted by each gas if it alone occupied the total volume, i.e.,

$$P = \sum_{j=1}^{i} P_j \quad \ldots\ldots\ldots\ldots\ldots\ldots\ldots\ldots\ldots (3.4)$$

and

$$n = \sum_{j=1}^{i} n_j \quad \ldots\ldots\ldots\ldots\ldots\ldots\ldots\ldots (3.5)$$

where p = total pressure of the mixture

n = total number of moles

Hence, in accordance with the Dalton's law of partial pressure, the mixture of ideal gases would also behave as an Ideal Gas. This relationship can also be extended to moist air.

$$P = P_a + P_w \quad \ldots\ldots\ldots\ldots\ldots\ldots\ldots\ldots (3.6)$$

where P = pressure of the moist air

P_a = partial pressure of the dry air in the mixture

P_w = partial pressure of the water vapour in the mixture

and on assuming that the constituents of the moist air behaves as an Ideal Gas,

$$P_w V = \frac{M_w}{M_w} RT \quad \ldots\ldots\ldots\ldots\ldots\ldots\ldots\ldots (3.7)$$

and

$$P_a V = \frac{M_a}{M_a} RT \quad \ldots\ldots\ldots\ldots\ldots\ldots\ldots\ldots (3.8)$$

3.2.1. Saturation mixing ratio over water on Ideal Gas basis.

When a mixture consisting of dry air and water vapour is in equilibrium with a plane surface of liquid water at a given pressure, P, and temperature, T, such that the moist air is saturated with respect to the water, there exist a definite mixing ratio, r_w between the dry air and the water vapour. The mixing ratio or more commonly known as the specific humidity is defined as the ratio of the mass of the water vapour in a sample of moist air to the mass of dry air with which the water vapour is associated. Hence,

$$r_w = \frac{M_w}{M_a} \qquad \text{(3.9)}$$

From Equation (3.7) and (3.8) and substituting into Equation (3.9) gives,

$$r_w = \frac{M_w}{M_a} = \frac{M_w}{M_a}\,\frac{P_w}{P - P_w} \qquad \text{(3.10)}$$

Calculated on the basis	Dry clean atmospheric air	Water Vapour
O = 16	28.966	18.0160
C = 12	28.9645	18.0153

Table 3.1. Molecular weight (4)

From Table 3.1.

$$\frac{M_w}{M_a} = \frac{18.016}{28.966} = 0.62198 \approx 0.622$$

substituting this value in Equation (3.10),

$$r_w = 0.622 \frac{P_w}{P - P_w} \qquad \text{..........} \quad (3.11)$$

Values of saturation vapour pressure over water, P_w, as a function of temperature is given in Table 3.2.

Table 3.2. Values of saturation vapour pressure over water as a function of temperature (4).

Temperature ^oC	P_w m_b
10	12.273
20	23.373
30	42.430

3.3. Thermodynamics.

Thermodynamics is the study of transformation of different forms of energy, the natural limitations of these transformations, and their practical consequences. One of the most important laws of thermodynamics is the First law of thermodynamics.

3.3.1. First law of thermodynamics.

The first law of thermodynamic states that the total energy of an isolated system, measured with respect to any given frame of reference remains constant. Hence, in an isolated system even though the kinetic, potential and internal energies may change individually the total sums of the energies remains constant. In the case of a non-isolated system, the system energy can change due to interactions with the surroundings. In a general process ΔE represents the change in energy content of the system as a result of any change in the interal energy, temperature, composition, potential and kinetic energy. There are two different methods whereby this can take place, i.e., work and heat. The generally adopted convention is that energy transfer as heat from the surroundings is positive and that energy exchange as work from the system to the surroundings is positive, Fig. 3.3.

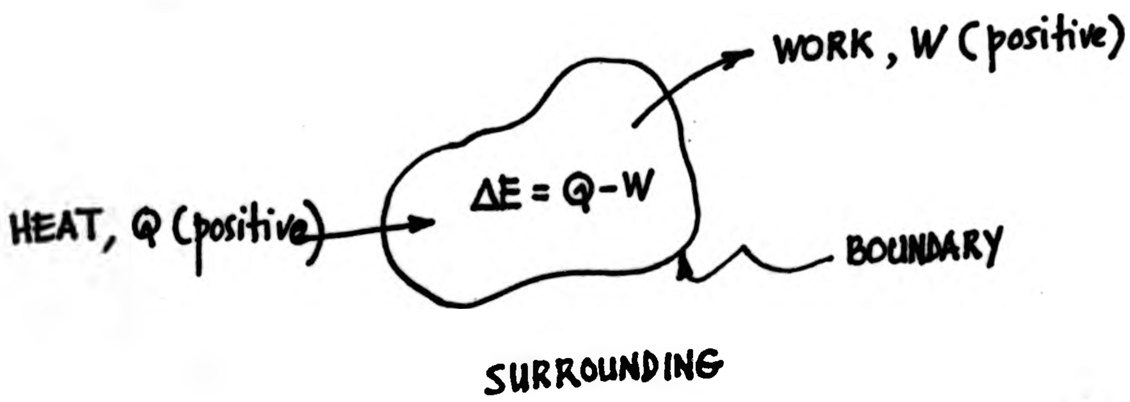

Fig. 3.3. Sign convention for energy exchanges.

The general energy equation may be written, designating input items by the subscript 1 and the output items by subscript 2, as (5).

$$\sum m_1u_1 + \sum m_1p_1V_1 + \sum \frac{m_1\bar{u}_1^2}{2g_s} + \sum m_1z_1\frac{g_1}{g_s} + \sum m_1E_{\sigma_1} + Q =$$

$$\sum m_2u_2 + \sum m_2p_2V_2 + \sum \frac{m_2\bar{u}_2^2}{2g_s} + \sum m_2z_2\frac{g_1}{g_s} + \sum m_2E_{\sigma_1} + W + \Delta E \; .... \qquad .... (3.19)$$

where (i) $\sum mu$ = the total internal energy designated by the symbol u per unit mass or mU for mass M.

(ii) $\sum mpV$ is the total energy added in forcing a stream of materials into the system under the restraint of pressure. P is the pressure of the system and V is the volume per unit mass.

(iii) $\sum mz\,\frac{g_1}{g_s}$ is the total external potential energies of all materials entering or leaving the system relative to an arbitrary selected datum plane. z is the height of the centre of gravity of the mass of material above the datum plane. g_1 and g_s are the local and standard acceleration to gravity respectively.

(iv) $\frac{\sum mu^2}{2g_s}$ is the total kinetic energies, $\bar{u}$ is the average velocities.

(v) $\sum mE_{\sigma}$ is the surface energies of all materials entering and leaving the system.

(vi) Q is the net energy added to the system as heat

(vii) W is the net energy removed as work done by the system.

(viii) ΔE is the net change in the energy content within the system during the course of the process.

Simplification of this general equation result in most specific cases. In steady-flow process, without fluctuations in temperature, composition, internal energy, the term ΔE becomes zero. For a non-flow process where the surface energy is negligible the equation can be further reduce to

$$Q = W + \Delta E \quad \text{..........................(3.20)}$$

where ΔE will be the net total sum of the internal potential and kinetic energies.

In a differential form, the above equation may be written as,

$$\delta Q = \delta W + dE \quad \text{..........................(3.21)}$$

where δQ and δW are small energy transfers as heat and work respectively while dE is a differential change in the total energy. In the above equation Q and W are path functions i.e., they depend upon the path followed by a certain process in changing from state to state, and hence they are not properties whereas E is a point-function, depends only on the state, is a property.

In many instances, changes in kinetic and potential energies are negligible compared to the change in internal energy. If this is the case, then Equation (3.21) can be written as,

$$\delta Q = \delta W + dU \qquad \text{.....................(3.22)}$$

where dU is the internal energy of the system.

3.4. Work Done on or by the system.

The state of a system initially in equilibrium may be changed infinitely due to the application of a generalised force, F. This generalised force may be a pressure, an electrical or some other property. As a result of the application of this generalised force there follows a change in another system property such as volume, polarisation or a magnetic moment. This change may be termed as generalised displacement, dX. For a quasi-static process, the total work done during the process can be calculated from the relationship,

$$W = \int_1^2 F.\ dX \quad \ldots\ldots\ldots\ldots\ldots\ldots\ldots\ldots (3.23)$$

The limits 1 and 2 of the integral correspond to the initial and final states of the system respectively. Fig. 3.4 shows a representation of the integral. A major consequence of a quasi-static process is that the work done is maximum.

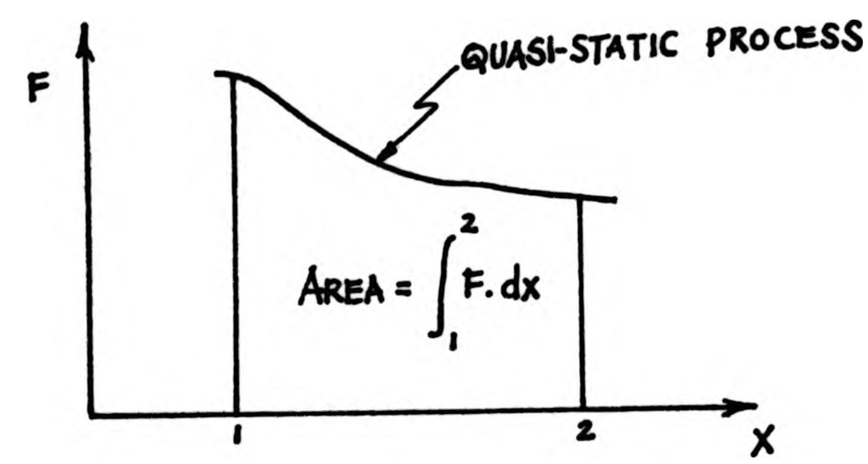

Fig. 3.4. Area representation of work for quasi-static process.

3.4.1. Expansion and compression work for gas system.

When the system is a gas, then the work done on/by the system can be calculated with the help of the equation of state of the gas. For an example consider a gas enclosed in frictionless piston-cylinder assembly as shown in Fig. 3.5, where the force exerted on the piston by the gas within the cylinder is resisted by an external force, F, just maintaining mechanical equilibrium. The cross-sectional area of the piston is A, and the

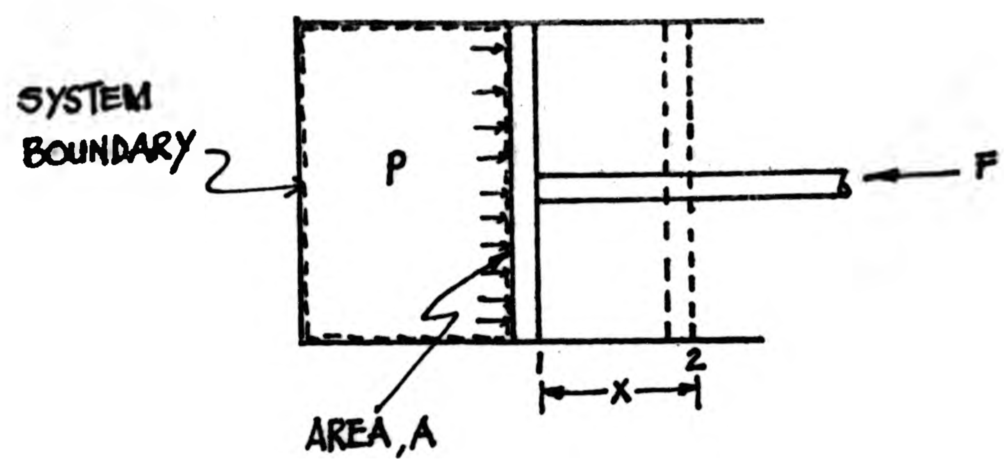

Fig. 3.5. Work done by expanding gas

pressure at the initial equilibrium state is P. If the piston moves outwards an elemental distance dx, the mechanical work done by the system on the surroundings will be,

$$\delta W = + F.dx = p.A.dx = p.dV$$

Therefore the total work done by the gas during a finite change in volume is the sum of the P.dV terms for each differential change in volume. Substituting these values in Equation (3.23) gives,

$$W_{boundary} = \int_{V_i}^{V_f} P.dV \quad \ldots\ldots\ldots\ldots\ldots\ldots \quad (3.24)$$

where V_i and V_f are the initial and final volumes of the gas.

The integration of the equation for the boundary work requires a knowledge of the functional relationship between P and V and the process whereby the change of states took place.

For an Ideal Gas, the calculation of work in certain processes is exhibited below.

(a) <u>A constant pressure process.</u>

A constant pressure(isobaric) process is approximated by a system consisting of a vertical cylinder fitted with a frictionless piston, on top of which rests a mass as shown in Fig. 3.5. A gas is enclosed in the space below the piston. The pressure of the gas is maintained constant, due to the combined weight of the mass and the piston. When the cylinder is heated, the gas within expands at constant pressure, the volume changing from V_1 to V_2. The work done by the gas on expanding is,

$$W = \int_{V_1}^{V_2} p.\, dV$$

$$= p(V_2 - V_1) \qquad \text{....................(3.25)}$$

(b) <u>Constant volume process.</u>

In this process, the change in volume is zero so that $dV = 0$.

$$W = \int p.\,dV = 0$$

(c) Constant temperature process.

Since in this process pressure and volume of the gas both change, an equation of state is used for the evaluation of the integral $\int p.dV$.

For an Ideal Gas, the relationship between pressure and volume is given by Equation (3.1). Substituting this equation into into Equation (3.24) gives,

$$W = nR_uT \int_{V_1}^{V_2} \frac{dV}{V}$$

$$= nR_uT \ \ell n \frac{V_2}{V_1} \qquad \text{.......................(3.26)}$$

(d) Adiabatic process.

By definition an adiabatic change of state is carried out so that the system exchanges no heat with the surroundings i.e., dQ=0 . Any work by or on the gas will therefore change the internal energy of the system.

$$dU = -\delta W = -p.dV \qquad \text{.................(3.27)}$$

If the energy content is considered a function of temperature and volume only i.e., U = f(T,V), its total differential is,

$$dU = \left(\frac{\partial U}{\partial T}\right)_V dT + \left(\frac{\partial U}{\partial T}\right)_V dV \quad \ldots\ldots\ldots\ldots\ldots(3.28)$$

For an Ideal gas, the specific heat of the gas at constant volume is $C_v = \left(\frac{\partial U}{\partial T}\right)_v$. Thus the following relationship is obtained,

$$dU = C_v \, dT \quad \ldots\ldots\ldots\ldots\ldots\ldots\ldots\ldots\ldots\ldots(3.29)$$

Therefore for n moles of Ideal Gas, the work done by the gas between temperatures T_1 and T_2 can be expressed as

$$W = -\int_{T_1}^{T_2} nC_v \, dT$$

$$= nC_v(T_1 - T_2). \quad \ldots\ldots\ldots\ldots\ldots\ldots(3.30)$$

Several alternative forms of Equation (3.38) can be derived from the relationship $C_v - C_R = R$, and the equation of state of the gas, for example,

$$W = \frac{1}{\chi - 1}(P_1V_1 - P_2V_2) \quad \ldots\ldots\ldots\ldots\ldots(3.31)$$

where χ is $\frac{C_p}{C_v}$ and C_p is the specific heat of the gas at constant pressure.

CHAPTER 4

EXPERIMENTAL METHODS AND THEORY

4.1 Methods for the determination of the volume of a tyre.

There are numerous methods in which the volume of a tyre can be determined. Basically the methods of determination can be divided into two categories,

(a) Direct method

(b) Indirect method

(a) Direct method.

This method can further be divided into two types, namely, the dimensional metrology and the filling the tyre with liquid of known density and weighing.

Although the method of dimensional metrology is in principle capable of very high accuracy, precise determination could not be made in this case because of its irregular shape and also the changes in its dimensions during inflation makes this method rather unattractive.

The method of filling the tyre with liquid of known density and weighing has been adopted by several workers, not only in the determination of the volume of tyre(1) but also of the volume of vessels of irregular shapes(2). The liquid used is usually deareated water. This is due to the fact that its density is accurately known as a function of temperature and also the overall uncertainty caused by small variations in temperature is relatively small. While it is a rather simple procedure to carry out this method for many volumetric shapes there are certain problems when applied to tyres. Since the position of the valve is not situated at its uppermost position, there is always the possibility of air pocket being formed during the filling process. A possible way of overcoming this problem is to apply a vacuum to the tyre initially and then water is pumped into the tyre.

(b) <u>Indirect method.</u>

The most common method for volumetric determination of irregular shaped vessels is by the method of gas expansion based on the principle of Gas laws. It has been reported (2) that this method has been adopted successfully by several workers in the determination of volume ratios of several vacuum vessels. The sensitivity of this method is governed by the precision with which the pressure can be measured and the precision of the calibrated volumes.

Another method of volume calibration is developed by Rutherford[3]. He used a volumetric calibration technique based on the quantitative transfer of Xenon gas from a vessel of unknown volume to a weighing bottle.

One of the main advantage of the expansion method over the method of filling the tyre with liquid and weighing is the ease of operation and also that the apparatus does not has to be dismantled once it has been set-up. It was, therefore, felt that the expansion method would be the best choice for this type of experiment.

4.2. Description of pressure and volume measurement system.

The set-up of the apparatus is shown schematically in Fig. 4.1. Essentially is it consisted of a test-tyre(1), whose characteristics is to be determined, fitted with a tyre valve adaptor. One one end of the adaptor is coupled by a rubber pressure tubing to a reference tyre(4) via a water-differential manometer(3) fitted with a screw-clip(2) and other end is connected to a needle valve(13), a filter unit(12) and a T-piece connecting to a mercury U-tube manometer(6) and an expansion/compression column(7). The expansion/compression column which is made up of glass tubing tightly enclosed by a clear pvc tubing along its length and is connected at its lower end to a lower outlet of a glass volume vessel(9) by a pvc tubing and suitable fittings and connectors. The reason for enclosing the expansion/compression column is to minimise the influence of the ambient temperature to the air in the column and also for safety reasons. The volume vessel which is half-filled with liquid e.g., dibutyl phthalate, is sealed at its upper outlet by a rubber bung carrying one end of a pvc tubing. The other end of the pvc tubing is coupled with a T-piece and two needle-valves, (10) and (11), air inlet and outlet valves respectively.

For safety reason and also to minimise the influence of ambient conditions on the system, the glass volume vessel (9) is enclosed in a metal container (8) with packing between the glass volume vessel and the metal container.

Paper scales are attached along the arms of the water-differential manometer, mercury U-tube manometer and the expansion/compression column.

The connection between the expansion/compression column to the T-piece and also the float-valve system (5) is shown in schematically in Fig. 4.2.

The working of the float-valve system is based on the principle of difference in pressure in the liquid

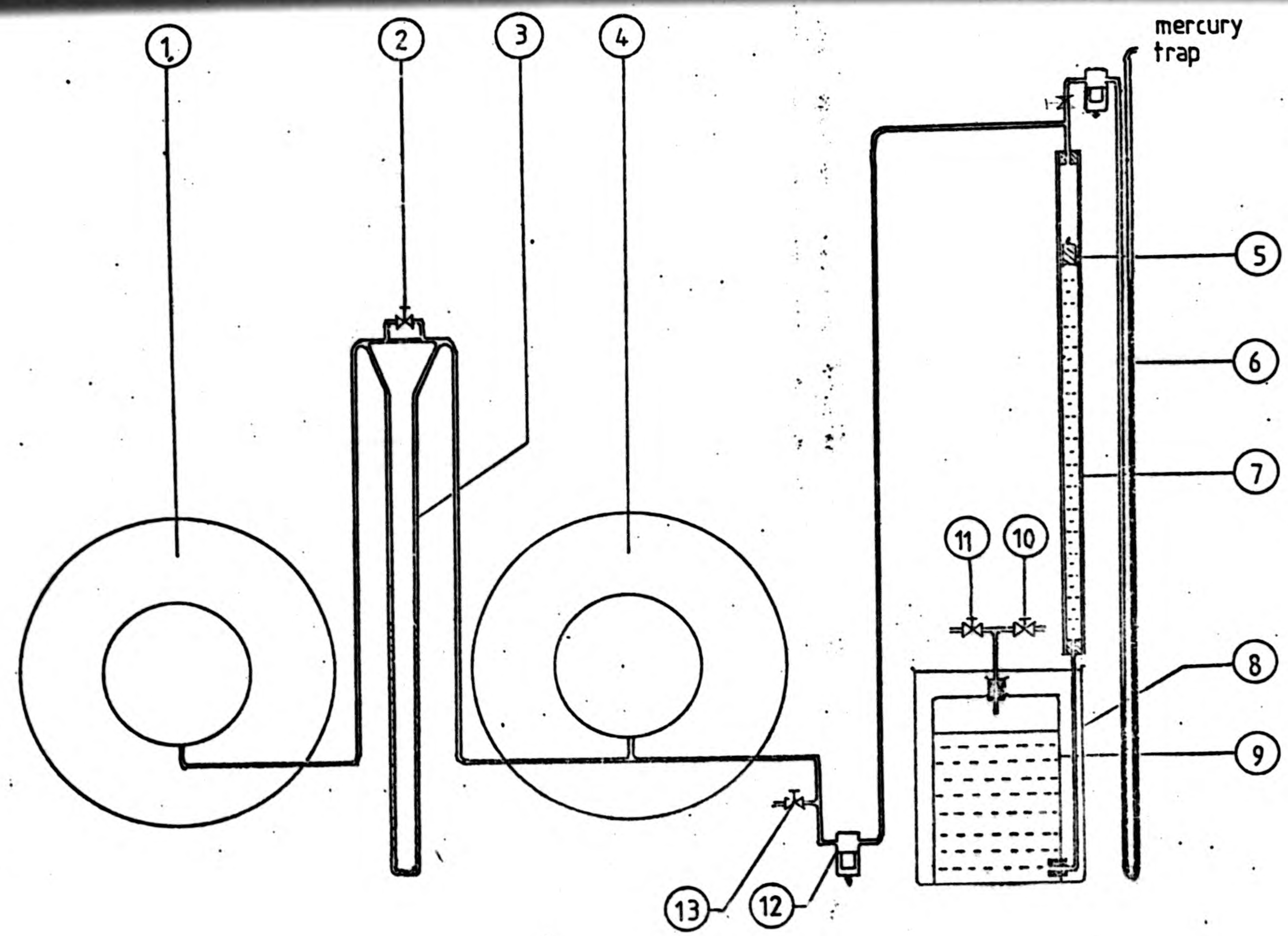

FIG 4.1. SCHEMATIC DIAGRAM OF PRESSURE AND VOLUME MEASUREMENT SYSTEM

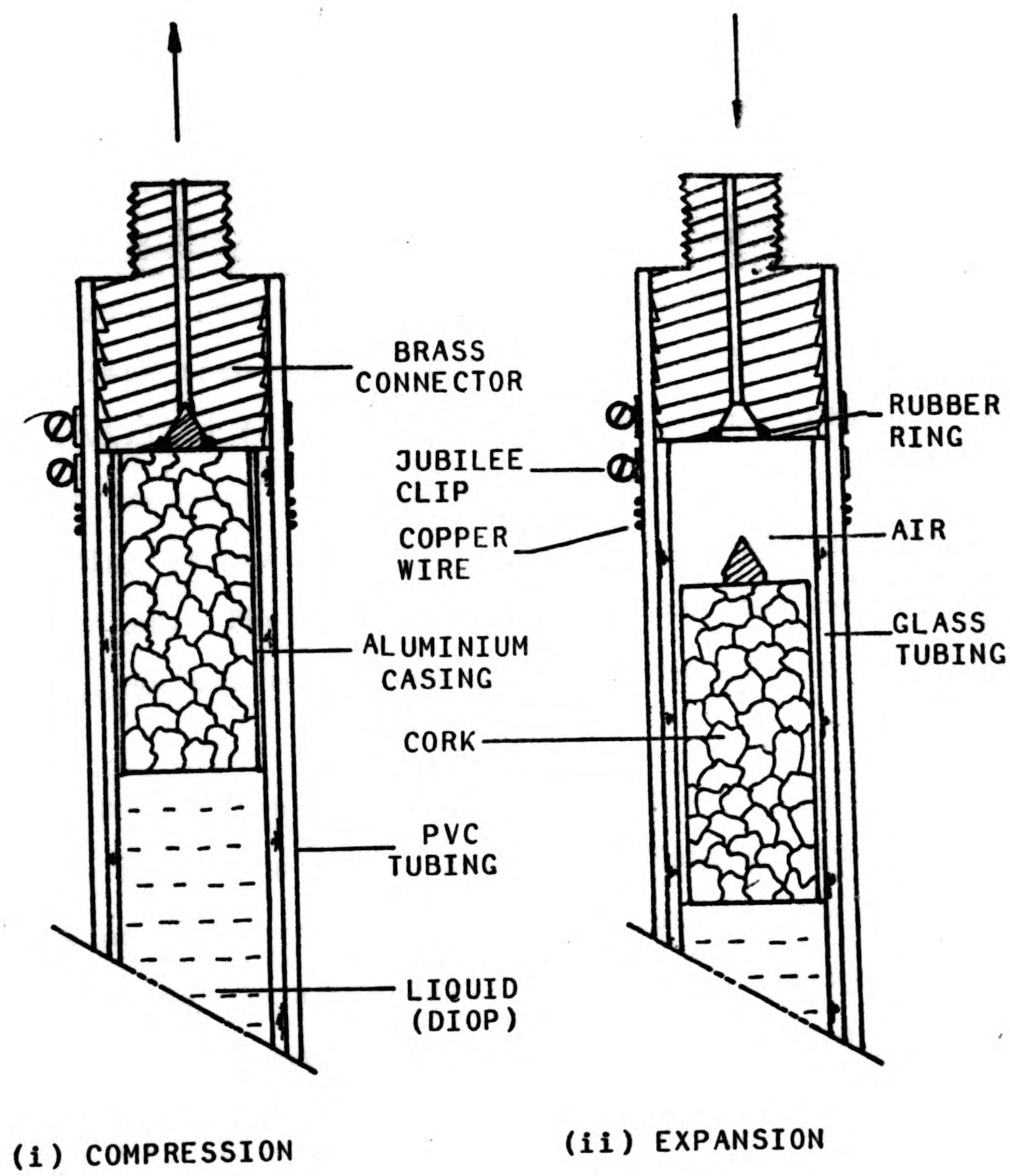

Fig. 4.2. Schematic diagram of the float valve system.

column and that of the air. In the initial stage, the pressure in the liquid column is made to be higher than that of the air in the system. As a result of this, the float will be forced up along the column by the liquid until it is stopped at the top by the 'brass connector'. The 'brass connector' is designed primarily to prevent the liquid from entering the air system. The reading of the scale corresponding to the bottom position of the float is noted as 'zero' position. When the pressure in the liquid column is less than the pressure of the air in the system, the float will be forced down along the column until a balance of pressure is attained. The reading of the scale corresponding to the position of the bottom of the float is again noted. The difference between the two readings will be equivalent to the change in volume of air.

One of the main features of this design is the use of the reference tyre. Here the reference tyre is used as a compensator for the fluctuations in the ambient temperature and the atmospheric pressure. Ideally, the choice of the reference tyre would be a tyre which has identical characteristics to the tyre whose characters is to be determined.

4.3. <u>Theory for the determination of the volume of tyre by method of gas expansion.</u>

The arrangement of the apparatus used for this determination is shown schematically in Fig. 4.1. Initially the pressure and temperature in both tyres are the same,

$$P_{T_i} = P_{R_i} = \rho_m g h_m + \rho_m g h_b = \rho_m g(h+h_b) \qquad (4.1)$$

where ρ_m = density of the mercury

h_m = difference in height of mercury levels in the mercury differential manometer.

h_b = height of mercury level in the barometer

and $T_{T_i} = T_{R_i} = T$. The initial volume of the reference tyre and test tyre are V_{R_i} and V_{T_i} respectively.

The screw-clip of the water-differential manometer was then closed and the volume of the air in the test tyre was then expanded by lowering the height of the water column in the expansion/compression column. Assuming that the tyres both experience temperature and pressure changes as a result of the volume expansion and that the air obeys the gas laws, the initial and the final properties of the air in both tyres can be written as below.

For the reference tyre.

$$\frac{P_{R_i} V_{R_i}}{T_{R_i}} = \frac{P_{R_f} V_{R_f}}{T_{R_f}} \qquad (4.2)$$

where $T_{R_f} = T_{R_i} + \Delta T_R$ and $V_{R_f} = V_{R_i} + \Delta V_R$. Substituting

these values into equation (4.2) and rearranging,

$$P_{R_f} = P_{R_i} \left[\frac{1}{1 + \frac{\Delta V_R}{V_{R_i}}} \right] \left[1 + \frac{\Delta T_R}{T_{R_i}} \right] \qquad (4.3)$$

Similarly the final pressure of the test tyre can be written

as

$$P_{T_f} = P_{T_i} \left[\frac{1}{1 + \frac{\Delta V_T}{V_{T_i}}} \right] \left[1 + \frac{\Delta T_T}{T_{T_i}} \right] \qquad (4.4)$$

The difference in pressure between the two tyres is denoted by the difference in height of the water levels in the water differential manometer where

$$\rho_w gh = P_{R_f} - P_{T_f} \qquad (4.5)$$

Substituting (4.3) and (4.4) into (4.5) and recalling that

$P_{T_i} = P_{R_i} = \rho_m g(h_m + h_b)$ and $T_{R_i} = T_{T_i} = T$ gives

$$\rho_w gh = \rho_m g(h_m + h_b)\left(1 + \frac{\Delta T}{T}\right) \left[\frac{1}{1 + \frac{\Delta V_R}{V_{R_i}}} - \frac{1}{1 + \frac{\Delta V_T}{V_{T_i}}} \right]$$

$$h = \frac{\rho_m}{\rho_w} \cdot (h_m + h_b)\left(1 + \frac{\Delta T}{T}\right)\left[\frac{1}{1 + \frac{\Delta V_R}{V_{R_i}}} - \frac{1}{1 + \frac{\Delta V_T}{V_{T_i}}}\right] \quad (4.6)$$

Assuming that in equation (4.6), $\frac{\Delta V_R}{V_{R_i}} << 1$ and $\frac{\Delta V_T}{V_{T_i}} << 1$,

therefore, $\frac{1}{1 + \frac{\Delta V_R}{V_{R_i}}} \simeq 1 - \frac{\Delta V_R}{V_{R_i}}$

and $\frac{1}{1 + \frac{\Delta V_T}{V_{T_i}}} \simeq 1 - \frac{\Delta V_T}{V_{T_i}}$

and $\frac{\Delta T}{T} << 1$ so that $1 + \frac{\Delta T}{T} \simeq 1$, equation (4.6) can be

written as

$$h = \frac{\rho_m}{\rho_w} (h_m + h_b)\left[\frac{\Delta V_T}{V_{T_i}} - \frac{\Delta V_R}{V_{R_i}}\right] \quad (4.7)$$

Let assume that the change in volume due to water movement in the water differential manometer is significant.

According to this assumption $\Delta V_R \simeq ah/2$ and $\Delta V_T \simeq A_c H - ah/2$

where a = cross-sectional area of the water-differential manometer tube.

A_c = cross-sectional area of the expansion/compression column.

H = difference between the initial and the final position of the float valve in the expansion/ compression column.

Substituting these values into the equation (4.7) gives,

$$h = \frac{\rho_m (h_m + h_b)}{\rho_w} \left[\frac{A_c H - ah/2}{V_{T_i}} - \frac{ah/2}{V_{R_i}} \right] \qquad (4.8)$$

if $V_{T_i} = V_{R_i}$, then equation (4.8) can be written as

$$h = \frac{\rho_m (h_m + h_b)}{\rho_w \quad V_{T_i}} (A_c H - ah/2 - ah/2)$$

$$h = \frac{\rho_m (h_m + h_b)}{\rho_w \quad V_{T_i}} (A_c H - ah)$$

therefore,

$$h = \frac{1}{\left[\dfrac{V_{T_i}}{\dfrac{\rho_m (h_m + h_b) A_c}{\rho_w}} + \dfrac{a}{A_c} \right]} H \qquad (4.9)$$

If on the other hand the change in the volume due to water movement in the water-differential manometer is insignificant then rearranging equation (4.9) and assuming that $A_c H >> ah$ gives

$$h = \frac{\rho_m (h_m + h_b) A_c H}{\rho_w \quad V_{T_i}} \qquad (4.10)$$

Having known the values of ρ_m, ρ_w, h_m, h_b, A_c and a the volume of the tyre can be calculated from the slope of the graph of h against H.

4.4 Experimental methods of determination of the work done on the tyre structure.

There are two methods whereby the work done on the tyre structure can be determined i.e., the direct and indirect method. The direct method is based on the assumption that the work done on the tyre structure is a function of the deflection only and is independent of the inflation pressure. If this assumption is true, then the work done on the tyre structure at zero inflation pressure can be calculated from the load-deflection curve. This has been done by Martin as reported by Hadekel[4].

The indirect method is based on the assumption that the total work done on the tyre is equal to the work done to deform the tyre structure and the work done on the air contained in the tyre. Thus if the total work done on the tyre and the work done on the air are known, then the work done on the structure can be obtained from the difference of the two quantities.

The work done on the air in the tyre can be determined from the measurement of the changes in the pressure or volume of the air contained upon deflection.

4.4.1. Measurement of the changes in the internal pressure upon deflection.

Most of the workers, amongst others, Koutny[1] reported the use of mercury U-tube manometer to measure the change in the air pressure in the tyre upon deflection. However, little information is being reported regarding the actual set-up of the apparatus.

4.4.2. Measurement of the changes in the volume upon deflection.

Little information is available concerning the experimental method of determination of the work done on air by measurement of the change in the volume of the tyre as a result of radial deformation. An attempt to measure this change in volume was made by Biderman[5]. He used an apparatus which is shown schematically in Fig. 4.3. Instead of air, water was used as a medium of pressurising the tyre and its auxiliary system. A brief description of the apparatus and procedure is as follows:-

The water in the tyre (1) and the reservoir (2) attached to it is maintained by constant air pressure in the tank (3). When load, F, is applied on the tyre, the tyre deformed and as a consequence of it there is a change in the internal volume of the tyre accompanied by a rise in pressure. The change in volume is determined by the measurement of the change in height of the water level in the water measuring tube (4).

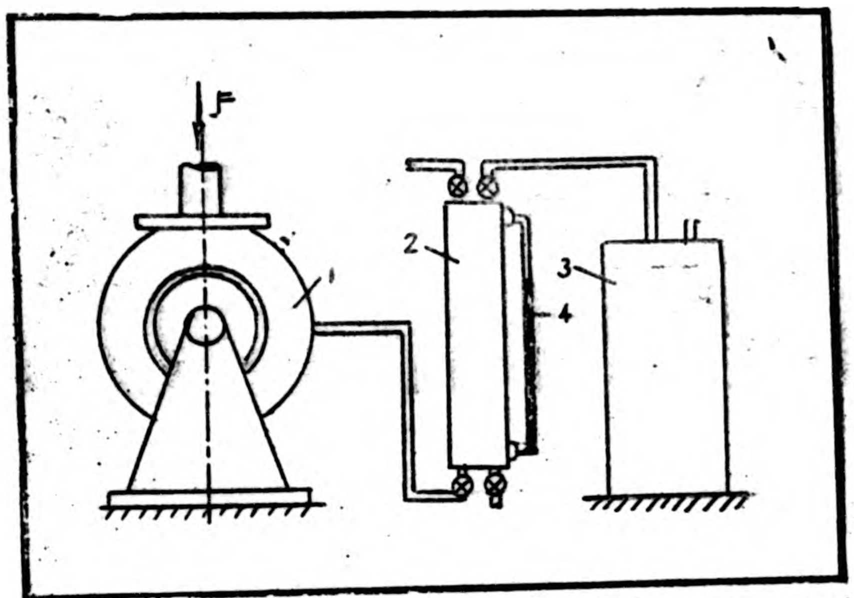

Fig. 4.3. Schematic diagram of the apparatus used for the determination of change in volume of tyre upon deformation[5]

Though this set-up can offer a reasonably accurate measurement of the change in the volume of the tyre upon deflection, it does not represent the actual working of a pneumatic tyre.

However, there does not appear to be any published information concerning the experimental set-up for the measurement of the change in volume of air contained in the tyre.

4.5. Application of thermodynamics and Gas Laws for the calculations of the work done on air.

According to Hadekel[4] the total work done on a tyre which is deformed by a static load can be represented by the relationship,

$$W_T = W_s + W_p \tag{4.11}$$

where

W_T = total work done on the tyre

W_s = work done on the tyre structure

W_p = work done on the contained air

The theory for the calculation of the work done on the air adopted here is similar to that given in Ref. (1) and elsewhere and is based on the principle of thermodynamics and Ideal Gas laws.

If a static load, F, is exerted on the tyre, the corresponding displacement, z, of the point of the load application, an equation for the work, W_T, of the force, F, over the distance, z, can be determined from the relationship

$$W_T = \int_0^z F.dz \tag{4.12}$$

and for the quasi static deflection, the work done on the contained air,

$$W_p = \int_{V_o}^{V_z} P.dv$$

where V_z in the equation (4.13) is the volume of the tyre as a result of deformation, z, and P is the pressure of the air corresponding to the volume V.

For an isothermal process and applying the Ideal Gas Law, the pressure of the tyre at deformation z is,

$$P = (P_i + P_a)\frac{V_o}{V} - P_a \tag{4.14}$$

where

P_i = inflation pressure

P_a = atmospheric pressure

V_o = initial volume of the tyre

Combining equations (4.13) and (4.14), the following equation is obtained.

$$W_p = -\int_{V_o}^{V_z} P.dV$$

$$= -\int_{V_o}^{V_z}\left\{(P_i + P_a)\frac{V_o}{V} - P_a\right\}. dV$$

$$= -(P_i + P_a)\, V_o \int_{V_o}^{V_z}\frac{dV}{V} + P_a\int_{V_o}^{V_z} dV$$

$$W_p = (P_i + P_a)\, V_o \ln.\frac{V_o}{V_z} + P_a\,(V_z - V_o) \tag{4.15}$$

Equation (4.15) can also be written as a function of pressure and initial volume only. From equation (4.14), let the final pressure p be denoted as P_f.

Therefore,

$$V_z = \left[\frac{P_i + P_a}{P_f + P_a}\right] V_o$$

substituting the above expression into equation (4.15)

$$W_p = (P_i + P_a)V_o \ln.\left[\frac{P_f + P_a}{P_i + P_a}\right] + P_a V_o \left[\frac{P_i + P_a}{P_f + P_a} - 1\right] \qquad (4.16)$$

With the tyre in its deformed state, the contained air is expanded until its pressure return to its initial value, P_i. The work done by the air on expanding can be calculated from the relationship given in equation (4.14) and the relationship,

$$V_c = V_o - V_z \qquad (4.17)$$

where V_c is the volume of air expanded.

Substituting equations (4.14) and (4.17) into the equation,

$$W_p = \int_{V_z}^{V_o} P.dV$$

and intergrating gives

$$W_p = (P_i + P_a)V_o \ln.\left[\frac{V_o}{V_o - V_c}\right] - P_a V_c$$

$$W_p = (P_i + P_a)V_o \ln. \left[\frac{1}{1 - \frac{V_c}{V_o}}\right] - P_a V_c \quad (4.18)$$

Assuming that if $\frac{V_c}{V_o} << 1$ then $\frac{1}{1 - \frac{V_c}{V_o}} \simeq 1 + \frac{V_c}{V_o}$

and $\ln \left(1 + \frac{V_c}{V_o}\right) \simeq \frac{V_c}{V_o}$, equation (4.18) can be written as

$$W_p \simeq (P_i + P_a)V_o \frac{V_c}{V_o} - P_a V_c$$

$$W_p \simeq P_i V_c \quad (4.19)$$

Equations (4.16), (4.18) and (4.19) will be used for the calculation of work done on air and the work done by the air.

4.6. <u>Description of the apparatus for deforming the tyre.</u>

The set-up of the equipment is shown schematically in Fig. 4.4. Attached to the movable beam assembly (10), made up of 'Dexion Channel bars' joined by bolts and nuts, is a weight hanger (11). A compression plate (7) made of steel is fixed to the movable beam assembly at a fixed distance from the pivot bearing assembly (5) which can be moved vertically by means of turning the bolts (6). A schematic diagram of the pivot bearing assembly is shown in Fig. 4.5.

When weights (12) are placed on the weight hanger, the beam assembly turns and consequently the compression plate depresses the test-tyre (9), which is held in a vertical position by means of a face plate (2) fixed to the tyre stand (1). The tyre stand is held rigidly to the immovable base frame.

The movable beam assembly which is no longer in a horizontal position as a result of the application of the weight is brought back to a horizontal position again by turning the bolts (6) of the pivot bearing assembly. A spirit level (8) positioned on the centre of the compression plate at a fixed distance from the pivot bearing centre serves as an indicator of the position of the beam assembly.

The load applied on the tyre is calculated from the principle of moments and the radial deflection of the tyre is measured by 'mercer' dial guages (4), which are fixed to swivel bases (4). The swivel bases themselves are fixed to the tyre stand.

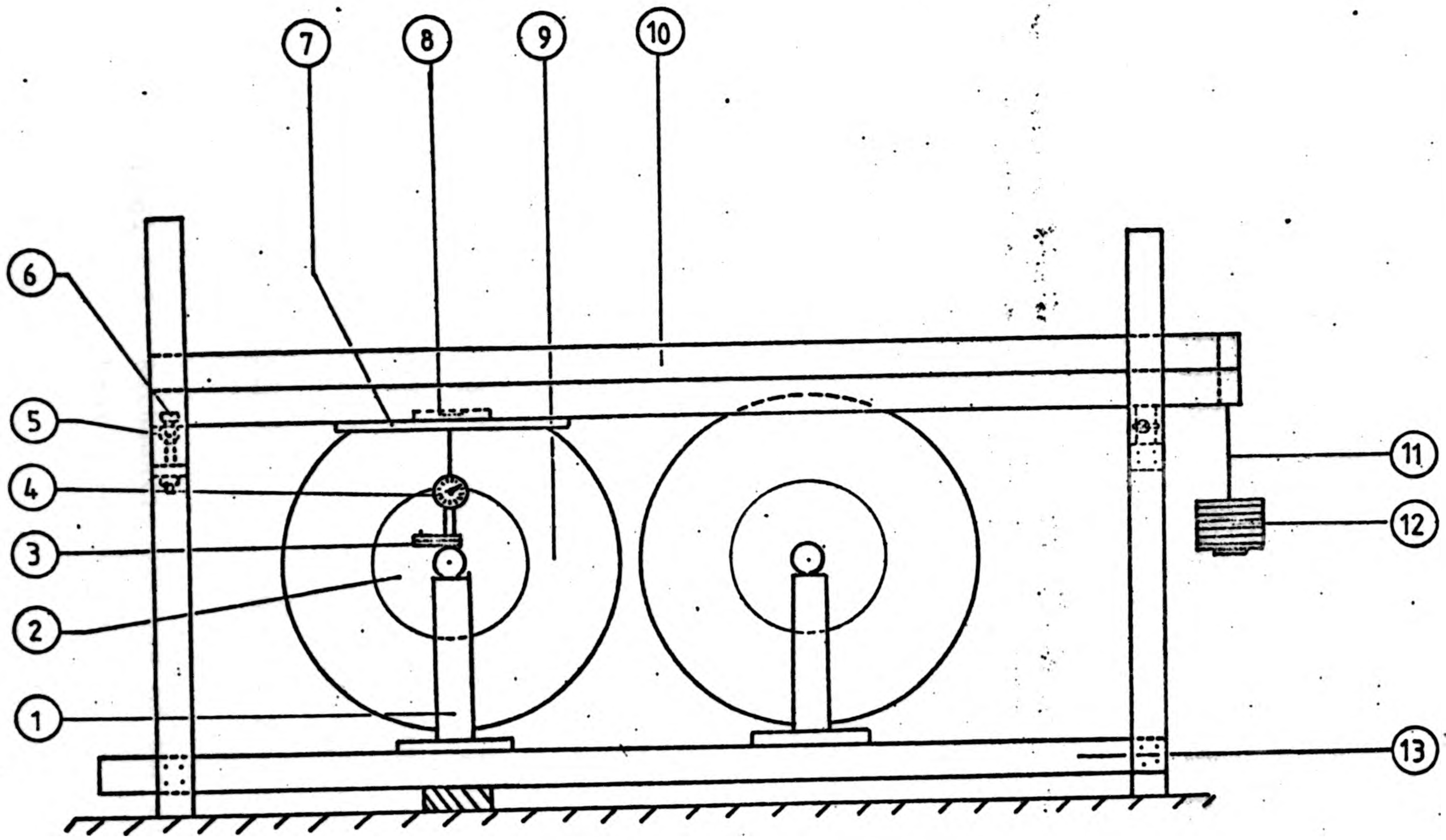

FIG 4.4. SCHEMATIC DIAGRAM OF LOAD AND DEFLECTION MEASUREMENT SYSTEM

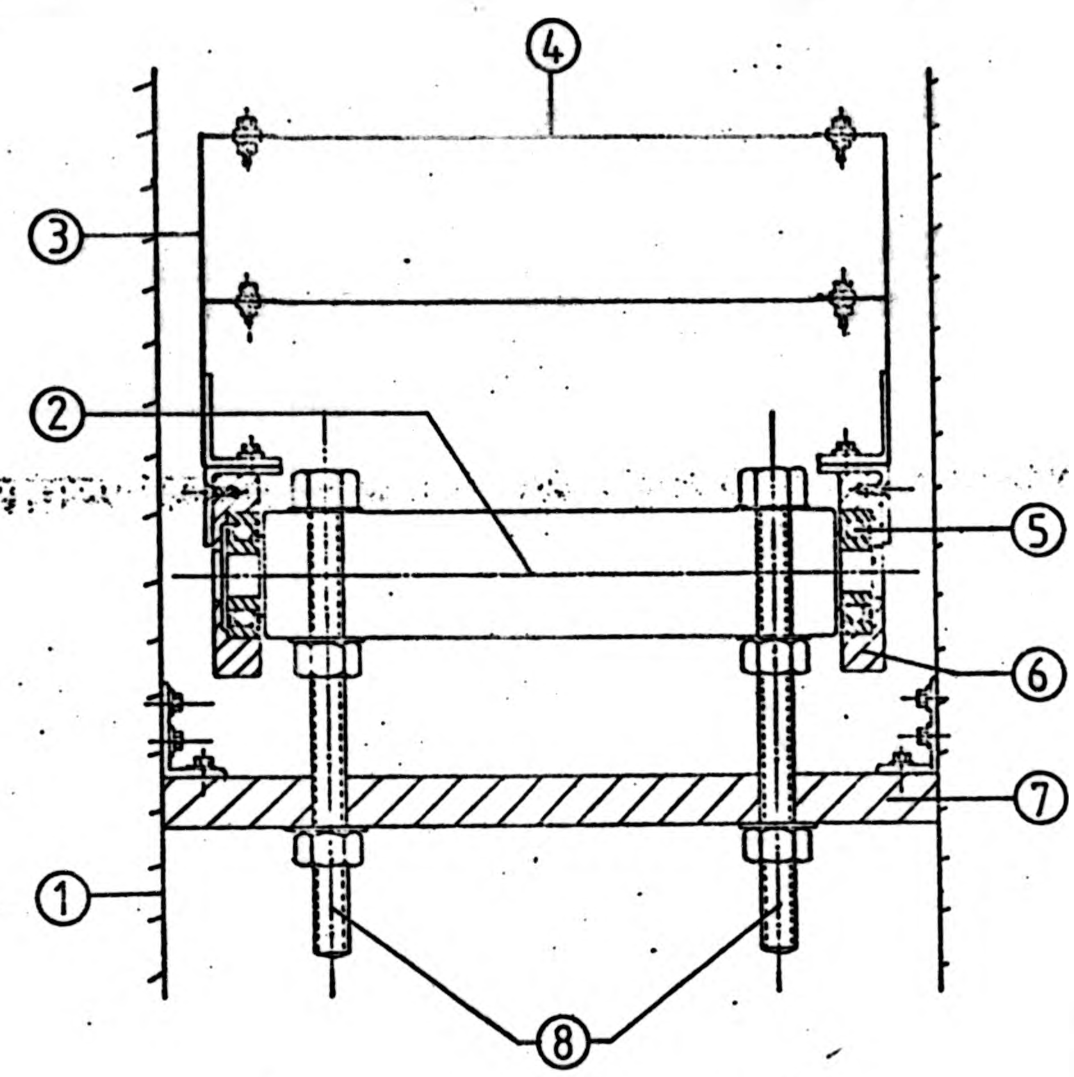

(1) UPRIGHT STAND	(5) BALL RACE
(2) SHAFT	(6) BEARING HOUSING
(3) BEAM	(7) SUPPORTING BAR
(4) CROSSBAR	(8) BOLTS & NUTS

Fig. 4.5. Aschematic diagram of the pivot bearing assembly.

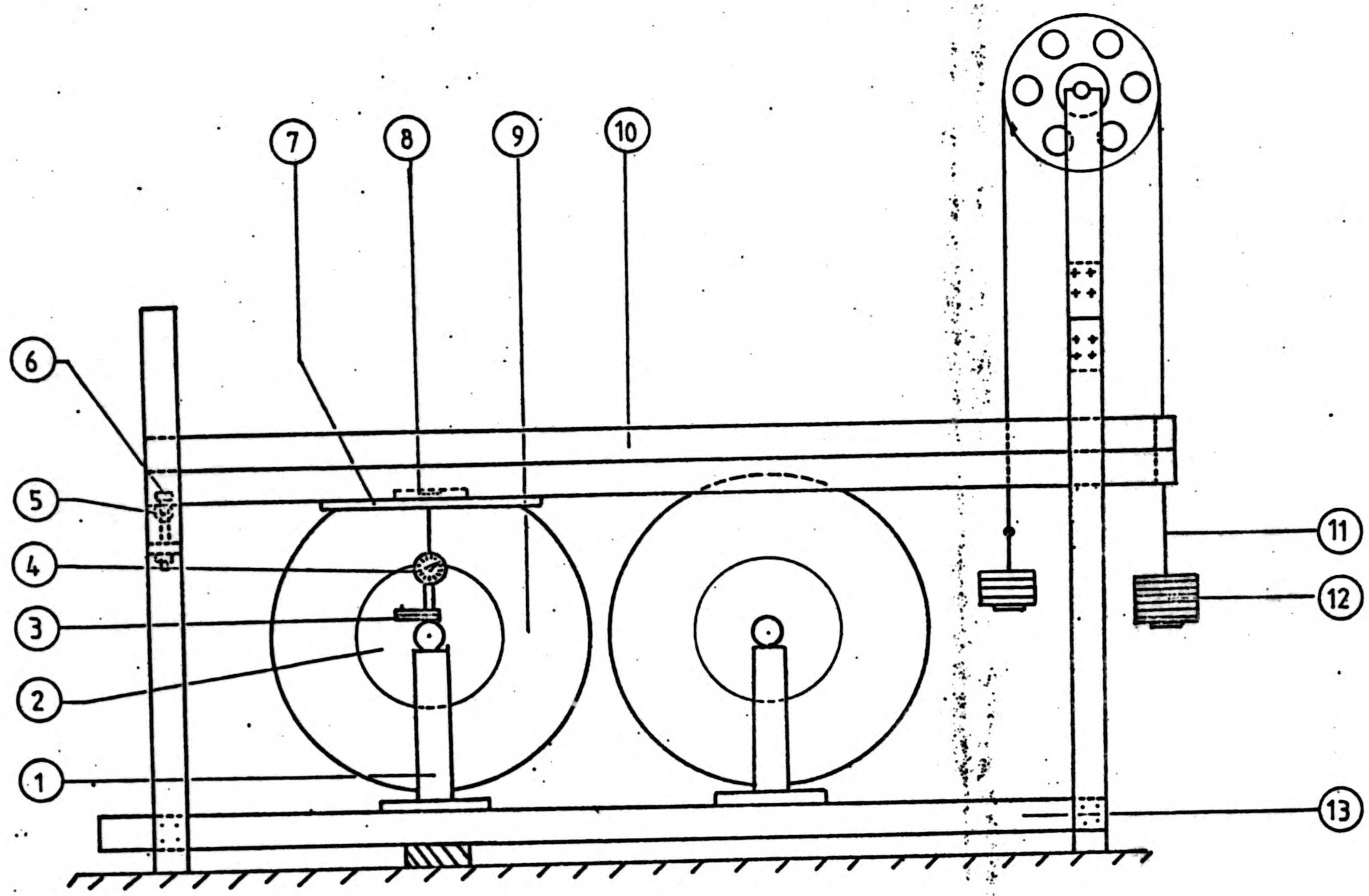

FIG 4.6 SCHEMATIC DIAGRAM OF LOAD AND DEFLECTION MEASUREMENT SYSTEM

CHAPTER 5

MATERIALS AND EXPERIMENTAL PROCEDURE.

5.1 Materials.

The tyres used for the experiment were:-

(1) Dunlop SP 68 (Worn)
165 SR 13
2 plies rayon breakers
2 plies rayon casing

(2) Dunlop SP 4 (New)
165 SR 13
2 plies steel breakers
2 plies rayon casing

(3) Dunlop D 75 (Retread)
6.40/6.50 S 13
4 plies nylon casing

5.1.1 Instruments Used

The following instruments were used.

(1) Fortin Barometer
(2) Mercury U-tube manometer
(3) Water U-tube manometer
(4) Cathetometer

(5) 'Mercer' Dial gauges

(6) Mercury thermometer

(7) Spirit level

(8) Expansion/compression column

(9) 'M.A. Webb' weighing scale

5.2 Experimental Procedure

5.2.1 Procedure for cleaning the glass surfaces of Mercury manometer.

The following steps were taken for cleaning the glass surfaces of the Mercury U-tube manometer.

(i) the U-tube was filled with chromic acid and was then left to stand for more than twenty-four hours.

(ii) the chromic acid was poured away and the tube was then rinsed with running tap water.

(iii) some detergent was then poured into the U-tube and the entire internal surface of the U-tube was then cleaned with a brush fitted with a long stiff wire.

(iv) The U-tube was thoroughly clean with running tap water to remove any particles that were present. When it was evident that no more particles were visible, the

U-tube was cleaned and rinsed with distilled water.

(v) the U-tube was then cleaned with acetone then dried by passing dry nitrogen through it.

5.2.2 Procedure of leak detection.

The system was filled with compressed air to a desired inflation. When equilibrium has been reached, the screw-clip of the water-differential manometer was closed. The levels of the water in the arms of the water-differential manometer were noted. The system was then left to stand.

Observations of the pressure difference with time were made. If the change in pressure difference was only one-sided and continuous, detergent solution was used to located the possible position of the leak, and the fault rectified.

5.2.3 Procedure to study the effect of ambient temperature upon pressure.

The tyres were inflated to a desired pressure, and were then left to stand to equilibrate. Then the valve connecting the system to the mercury U-tube manometer and the screw-clip of the water-differential manometer were closed. The readings of the ambient pressure, ambient temperature and the height of the water-levels in the arms of the water-differential manometer were made.

Observations of the change in the water-levels in the water-differential manometer, ambient temperature and pressure with time were made.

5.2.4 Procedure for determination of loading parameters.

In order to facilitate the calculation of the load applied on the tyre, the following parameters have to be determined.

(i) the coefficient of friction of the pulley bearing,

(ii) the weight of the beam assembly,

(iii) the centre of gravity of the beam assembly,

(iv) the coefficient of friction of the pivot bearings.

(i) The coefficient of friction of the pulley bearing. μ_p

A pulley of known weight, w_p, is supported by a low friction bearing on a fixed shaft. A wire cable is attached at one of its end a weight hanger (1) and passes over the pulley to support a weight hanger (2) at its other end as shown in Fig. 5.1

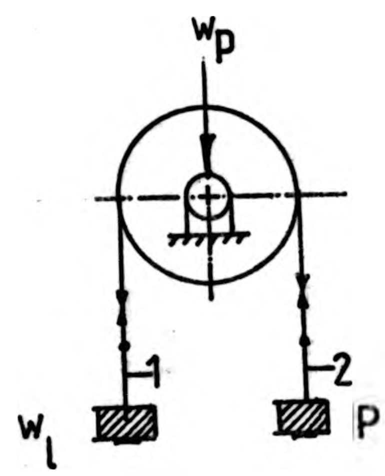

Fig. 5.1 Schematic diagram of the pulley assembly.

A known load, W_1 was placed on the weight hanger (1) and weights, P, were added to the other hanger until the pulley just start to move. The value of W_1 and P were recorded.

The procedure were repeated with different known loads.

(ii) <u>The weight of the beam assembly, w_b</u>

The weight of the beam assembly was obtained by "Wm.A.Webb" weighing scale which has an accuracy of ± 0.46N (± 2 oz.). The weight of the beam assembly was obtained again when pivot bearings and spirit level were included.

(iii) <u>The centre of gravity of the beam assembly, x_b</u>

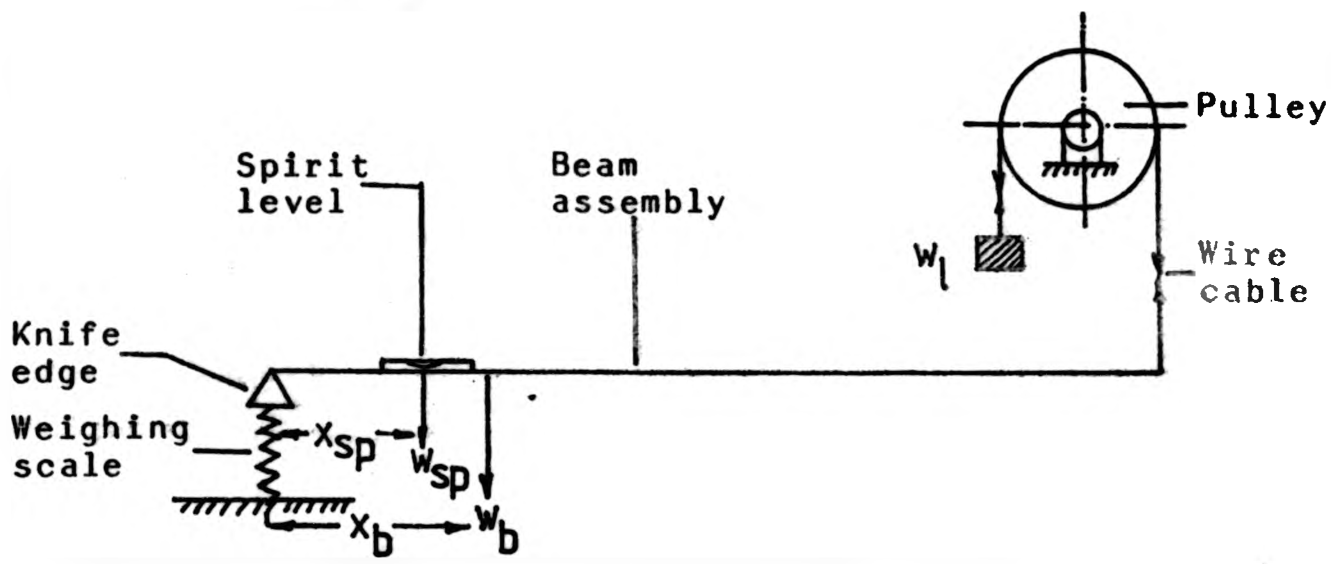

Fig. 5.2. Schematic diagram of the beam and pulley assembly.

The apparatus was set up as shown schematically in Fig. 5.2. A beam assembly of known weight, w_b, is pivoted at one end of its edges on a knife edge, and the knife edge itself is supported on a weighing scale, and is supported in a horizontal position by a wire cable which is attached at one end to the middle point of the opposite edge of the beam assembly. The wire cable passes vertically upwards from that point over a fixed pulley of known weight and coefficient of friction and carries a hanging weight, w_l, at the other end. The horizontality of the beam assembly is indicated by the spirit level positioned on the compression plate and at a distance of x_{sp} from the knife edge.

The least weight, w_l, required to maintain the beam assembly in a horizontal position is recorded.

(iv) <u>The coefficient of friction of the pivot bearing, μ_{pb}.</u>

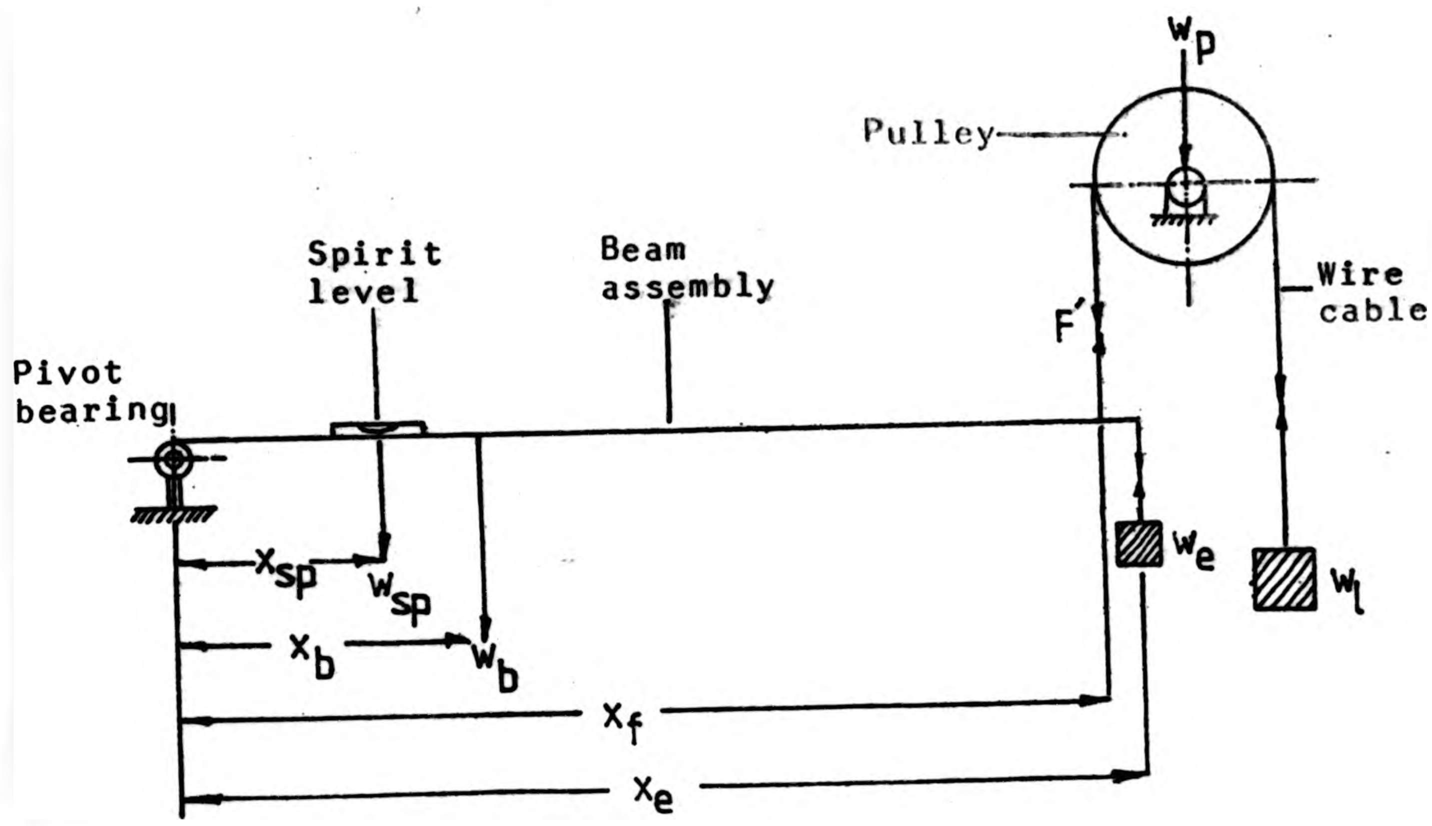

Fig. 5.3. Schematic diagram of the beam, pulley and pivot bearing assembly.

The apparatus is set up as shown schematically in Fig. 5.3. The beam assembly of known weight, w_b, and whose centre of gravity from the pivot centre is x_b, is free to turn about one of its edges, i.e., at the pivot, and is supported in a horizontal position by a wire cable which is attached at one end to the middle point of the opposite edge of the beam assembly, passes vertically upwards from that point over a fixed pulley of known weight, w_p, and coefficient of friction, μ_p, and carries a hanging weight, w_1, at the other end. The horizontality of the beam assembly is indicated by the spirit level of known weight, w_{sp}, and is positioned on the compression plate at a distance x_{sp} from the pivot centre.

Small weights were removed from the w_1 until the beam assembly started to turn. The least weight of w_1 remained to cause the beam assembly to turn was recorded.

With the present set up, a weight hanger and a known weight was attached at one end of the beam assembly as shown in the diagram. The beam assembly was brought to a horizontal position by adding weights to w_1. Once the beam assembly has attained an equilibrium position, weights were removed from w_1 until the beam assembly just start to turn. The weight, w_e, and the least weight to cause the beam assembly to turn, w_1, were recorded.

5.2.5 <u>Experimental determination of the volume of the tyre using the pressure-volume measuring apparatus.</u>

The apparatus was set up as shown in Fig. 4.1. With the valves (10), (11) closed and valve (13) and screw clip (2) opened, compressed air was introduced into the system via valve (13) to a desired inflation pressure as indicated by the mercury U-tube manometer (6). Valve

(13) was then closed. With valve (10) opened, air was forced into the glass volume vessel as a result of which caused the liquid level and the float valve (5) to rise along the expansion/compression column (7). When the float valve has reached the top of the column, valve (10) was closed. The system was then left to stand for a few hours for it to reach equilibrium.

When the system has reached equilibrium, the height of the levels of the mercury in the mercury U-tube was noted. The atmospheric pressure was read from the 'Fortin' barometer and the ambient temperature from the 'mercury-in-glass' thermometer. The screw-clip was then closed slowly. The position of the water levels in the water differential manometer (3) was noted. The system was now ready for the expansion/compression experiment.

Air in the volume vessel (9) was allowed to leak slowly by opening valve (11). As a result of this, the liquid level and the float-valve in the expansion/compression column started descending. There was also a corresponding change in the levels of the water in the arms of the water-differential manometer. When the float valve has reached a predetermined mark, the valve (11) was closed. The system was then allowed to stand for ten minutes for it to attain equilibrium. When equilibrium of the pressure has been reached, the volume of the air expanded as indicated by the distance travelled by the float valve, H, and the corresponding levels of the water in the water-differential manometer were noted. The difference in the levels of the water in the water-differential manometer was noted as h.

The process was repeated until a series of valves of H and h were obtained.

When the float valve has reached the maximum position, i.e., the bottom of the expansion/compression column the process was reversed. This was done by opening the valve (10) and forcing air through it. As a result of this the float valve started to rise. When the float valve has reached a predetermined mark the valve (10) was closed and the system was left to stand for a few minutes. The values of H and h were again noted.

The process were repeated until the float valve has reached the top of the expansion/compression column.

5.2.6 <u>Determination of the volume of the tyre by method of inflating the tyre with water and weighing.</u>

The valve of the tyre was connected to a connector, fitted with needle valves A and B. The connector is shown schematically in the Fig. 5.4.

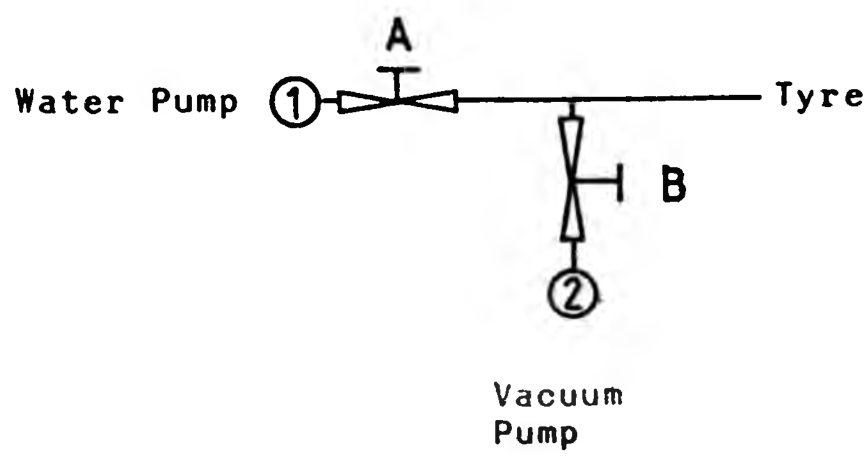

Fig. 5.4. Schematic diagram of the connector.

The tyre was placed upright on a stand and the whole assembly was then placed on a weighing scale. With valve A closed and valve B opened, (2) was connected to the vacuum pump by rubber tubing and air was vacuumed out of the tyre. Valve B was then closed and the rubber tubing disconnected from (2). The weight of the assembly was noted. With (1) connected to the water pump, fitted with a pressure gauge, valve A was opened and water was pumped into the tyre to a predetermined pressure. Valve A was then closed and (1) disconnected from the water pump. The new weight of the assembly was noted. The process of pressurising the tyre in stages and noting its corresponding weights was repeated until the inflation pressure reach 275 kPa (≈ 40 psi).

5.2.7 **Experimental procedure for the determination of the work done on the tyre.**

The determination of the relationship between the total work of the deforming the tyre and the portion of this work expanded on air compression was carried out by using the apparatus shown in Fig. 4.1 and 4.4.

With the valves (10) and (11) closed and valves (13) and screw-clip opened, compressed air was introduced into the system to a desired inflation pressure as indicated by the levels of the mercury in the mercury U-tube manometer (6). Valve (13) was then closed. Then valve (10) was opened and air was introduced into the volume vessel (9) and as a result of this, the liquid in the volume vessel was forced up along the expansion/ compression column (7). When the float valve (5) reached the top of the column, valve (10) was closed and the system was left to stand for it to stabilise.

When equilibrium has been attained, the levels of the mercury were recorded. At the same time the atmospheric pressure was reach from the 'Fortin' barameter and the ambient temperature was read from the mercury-in-glass thermometer. The screw-clip (2) was then clsoed and the levels of the water in the arms of the water-differential manometer were noted.

The beam assembly was then lowered by adjusting the screw-jack at one end and by turning the bolts of the pivot bearing assembly at the other end until the compression plate just touched the highest point of the test-tyre. A spirit level which was positioned on the compression plate was used as a guide for adjusting the beam assembly to a horizontal position when it just touched the tyre. This initial position of the compression plate was recorded by means of 'Mercer' dial gauges. Then the screw-jack was lowered slowly until the weight of the beam assembly acted on the tyre and the screw-jack was then removed. The position of the beam assembly was then made horizontal by adjusting the bolts of the pivot assembly.

As a result of load applied on the test-tyre, there was a pressure difference between the test-tyre and the reference tyre. The system was then left to stand for 10 minutes. When the ten minutes has elapsed, the height of water levels in the water-differential manometers, the height of mercury levels in the mercury manometer, the atmospheric pressure, the ambient temperature and the deflection of the tyre were all recorded.

Valve (11) was opened slightly and air from the volume vessel was allowed to leak slowly. As the pressure inside the volume vessel decreases, the float-valve and the water level in the expansion/compression column descends. They were allowed to descend until there were no more pressure difference between the two tyres. The system was then allowed to stand a few minutes after which the height of the level of float-valve was recorded. Readings of the ambient temperature, atmospheric pressure and the dial gauges were also recorded.

Valve (10) was opened and air was forced slowly into the volume vessel until the float-valve has reached the top of the expansion/compression column. The system was then allowed to stand for a few minutes after which the readings of the levels of the water in the water-differential manometer, levels of the mercury, the ambient pressure, the ambient temperature and the dial gauges readings were all recorded.

Then the beam assembly was raised horizontally with the aid of a screw-jack at one end turning the bolts of the pivot assembly at the other until the compression plate just touched the top of the test-tyre. The system was then left to stand for a few minutes after which the dial gauges readings, the water levels in the water-differential manometer, the mercury levels, the atmospheric pressure and the ambient temperature were all recorded.

The procedure were repeated by hanging a load of known weight at the end of the beam assembly.

CHAPTER 6

RESULTS AND DISCUSSIONS

Basic measurements of the performance of the load deflection system and the pressure-volume system were carried out and subsequent modifications and improvements of the apparatus were made during the preliminary experiments.

6.1. External load applied on the tyre.

The following parameters were calculated according to the relationship given in the Appendix I.

(i) the coefficient of friction of pulley
(ii) the weight of the beam assembly
(iii) the centre of gravity of the beam assembly.
(iv) the coefficient of friction of the pivot assembly.

The calculated values of (i), (ii), (iii) and (iv) are given in the Table (6.1) overleaf.

The external load applied on the tyre were found

Table 6.1. Summary Of Results Of Load Parameters.

Weight of beam assembly, W_p :81.911 $\pm$ 0.028 kg.

Weights of spirit level, W_{sp}:1.479 $\pm$ 0.001 kg.

Weight of pulley, W_p :2.186 $\pm$ 0.028 kg.

Weight of pivot bearings, W_{pb}:1.189 $\pm$ 0.001 kg.

Distance from beam assembly c.g to centre of pivot bearing : 77.70 $\pm$ 0.15 cm.

Distance from spirit level c.g to centre of pivot bearing : 58.10 $\pm$ 0.01 cm.

Distance from the end load to the centre of pivot bearing : 222.∅ $\pm$ 0.1 cm.

External diameter of pulley, D_p : 35.56 $\pm$ 0.10 cm.

Bore of pulley, d_p : 2.46 $\pm$ 0.01 cm.

Diameter of pivot bearing shaft, d_{pb}:1.59 $\pm$ 0.01 cm.

Coefficient of friction of pulley bearing, μp: 0.0236 $\pm$ 0.001

Coefficient of friction of pivot bearing, μ_{pb}: 0.224 $\pm$ 0.020

to be related to the end load, W_e (kg), by the relationship given in the Appendix IV.

$$F_t = (112.919 + 3.812\ W_e)\ g_1$$

where F_t is in N and g_1 is the acceleration due to gravity in ms^{-2}.

A graph of F_t against end load, W_e, was plotted as shown in Fig. 6.1. From the graph it can be seen that the calculated values of F_t are in good agreement when calibrated against the experimental values obtained by the use of 'W^m.A.Webb' weighing scale. The uncertainty in F_t was calculated in the region of 1%.

However, it was later discovered that at low inflation pressure, the amount of deflection caused by the smallest applied load (1.414 kN) was too high to enable the calculation of work done on the tyre at low deflection. In order to obtain further data in the lower region of the load-deflection curves, it was decided to make some modifications to the apparatus. This was done by the use of counter weight at the end of the beam assembly. The modified version of the apparatus set-up is shown in Fig. 4.6. The minimum counterweight required to hold the beam assembly in equilibrium was 30.02 ± 0.02 kg. The load applied on the tyre was then calculated according to the relationship

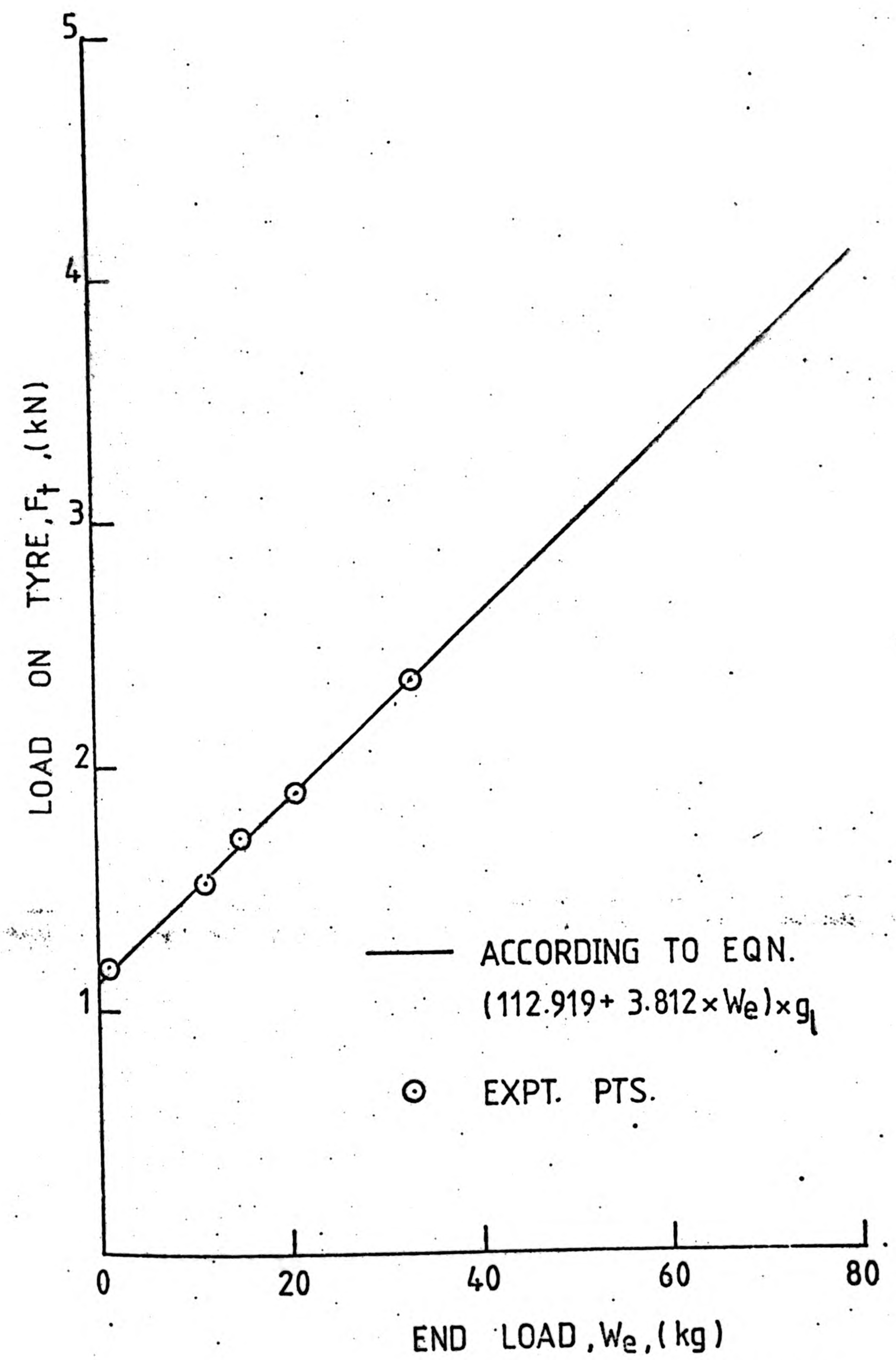

Fig. 6.1 A graph of load, F_t, against end load, W_e.

$$F_t = (3.777\ W_e - 0.346)\ g_1$$

where F_t is in N . The least force required to move the beam assembly was calculated to be equal to ≈ 7.9 N.

6.2. Effect of time upon radial deflection.

The deflection of the tyre under a load is a time dependent because of the viscoelastic nature of the rubber and the cords. This is evident from the curves shown in Fig. 6.2. The change in deflection was significant in the early stages of loading up to a period of 5 minutes, after which no appreciable change in the deflection were observed.

It was, therefore, decided that all subsequent measurements of the deflection of the tyre were to be taken after a lapse of 15 minutes of loading.

6.3. Effect of ambient temperature upon pressure difference between tyres.

The influence of ambient temperature upon the pressure difference between the two tyres can be readily seen in Fig. 6.3. Initially an increase in the ambient temperature caused a decrease in the test pressure with respect to the reference tyre, or in other words the

$$F_t = (3.777\ W_e - 0.346)\ g_1$$

where F_t is in N . The least force required to move the beam assembly was calculated to be equal to = 7.9 N.

6.2. Effect of time upon radial deflection.

The deflection of the tyre under a load is a time dependent because of the viscoelastic nature of the rubber and the cords. This is evident from the curves shown in Fig. 6.2. The change in deflection was significant in the early stages of loading up to a period of 5 minutes, after which no appreciable change in the deflection were observed.

It was, therefore, decided that all subsequent measurements of the deflection of the tyre were to be taken after a lapse of 15 minutes of loading.

6.3. Effect of ambient temperature upon pressure difference between tyres.

The influence of ambient temperature upon the pressure difference between the two tyres can be readily seen in Fig. 6.3. Initially an increase in the ambient temperature caused a decrease in the test pressure with respect to the reference tyre, or in other words the

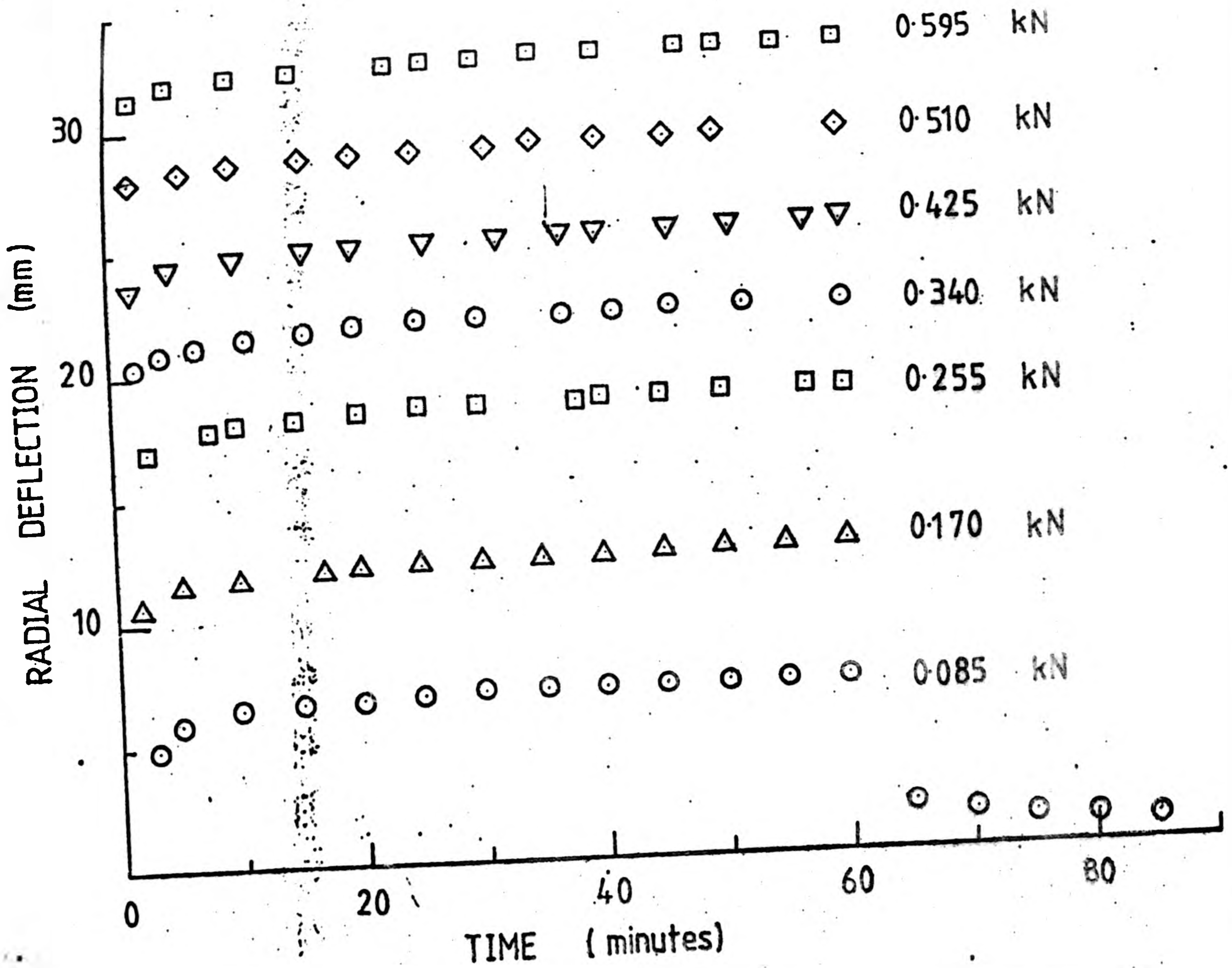

Fig.6.2. Graphs of the effect of time upon radial deflection of tyres at various loading of a rayon-belted radial tyre.

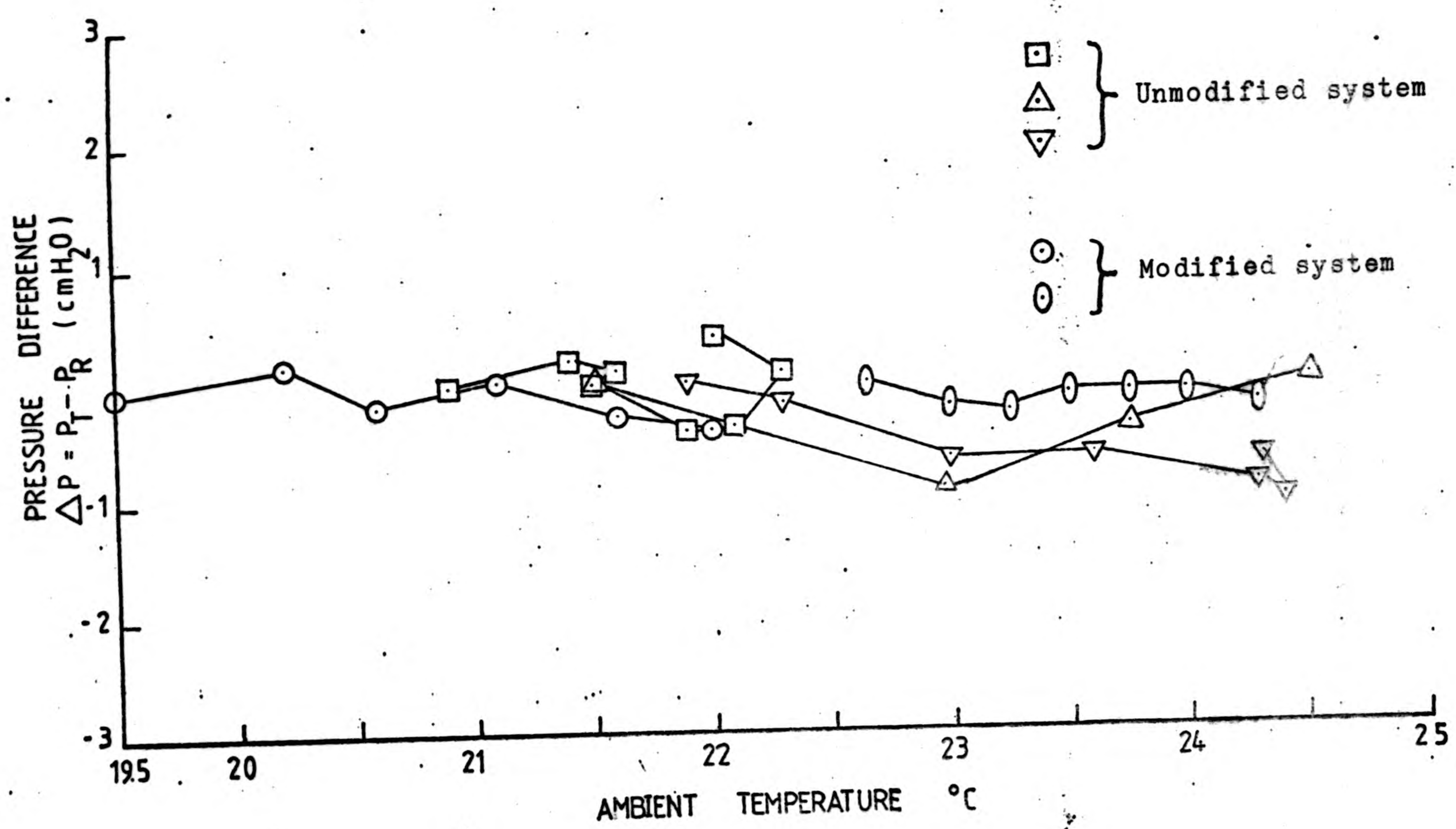

Fig. 6.3. Graphs of the effect of ambient temperature upon pressure difference between the tyres.

relative increase in pressure in the reference tyre is greater than that of the test tyre. However, as can be seen in the Fig. 6.3., the pressure in the two tyres came to equilibrium again with each other in the later stages.

A plausible explanation for this behaviour may be attributed to the following factors:-

(i) The reference tyre section is situated relatively nearer to the heating system as compared to the test tyre section. As a consequence of this, the reference tyre section may be exposed to a relatively higher temperature gradient, thereby causing the pressure in the section to rise at a slightly higher rate than the test tyre section. The reverse will occur when it is suddenly cooled. With time, however, as the temperature in the room becomes more uniform, the pressure in the two sections will come to equilibrium with each other again.

(ii) There is a difference in the volume between the test tyre and the reference tyre. Probably as a consequence of this there is a time lag for the tyres to achieve the equilibrium condition.

(iii) The change in the saturated vapour pressure of the water in the water-differential manometer.

It was then decided that to reduce the effect of (i) and (ii), the reference tyre was moved to a position as close as possible to the test tyre. Some improvement was observed as a result of this alteration of position.

6.3.1 Analysis of the effect of increase in temperature upon the difference of pressures between the two tyres.

The increase in the internal pressures of the tyres as a result of an increase in the internal temperature can be determined by the relationship:

$$P = \frac{P_i}{T_i} T$$

where P_i, T_i is the initial pressure and temperature respectively.

Hence, according to the above relationship, the difference in pressure between the test and reference tyres is,

$$P_t - P_r = \frac{P_i}{T_i} (T_t - T_r)$$

where the subscript t and r denotes the test and reference tyre respectively.

Substituting $P_t - P_r = \rho_w g_1 h_w$ and $P_i = \rho_m g_1 (h_m + h_b)$ into Equation (6.2) and rearranging, gives

$$h_w = \frac{\rho_m}{\rho_w} (h_m + h_b) \left[\frac{T_t - T_r}{T_i} \right] \qquad \text{.........(6.3)}$$

From Equation (6.3) it can be readily seen that the difference in pressure between the two tyres, as measured by the difference in height of the water columns in the water-differential manometer,is a function of the initial temperature and pressure, and the difference in the temperature increase between them.

A measure of the sensitivity of the water-differential manometer with respect to change in temperature between the two tyres is illustrated in the example below.

Ambient pressure, h_b	= 760	mmHg
Initial pressure, h_m	= 760	mmHg
Initial temperature, T_i	= 20	C
Specific gravity of mercury $\frac{\rho_m}{\rho_w}$	= 13.57	

If the temperature difference between the two tyres is 0.1 C, then

$$h_w = 13.57\ (760 + 760)\ \frac{0.1}{(273 + 20)}$$

$$= 7.04 \quad mmH_2O$$

From the above calculation, it can be seen that the difference in temperature between the two tyres can greatly influence the measurement of the pressure changes. It is therefore essential to allow sufficient time to elapse before the readings are taken.

6.4. Volume of the tyre.

The volume of the is determined by the expansion/ compression method according to the relationship given in Equation (4.9) and (4.10), and by the method of completely filling the tyre with distilled water and weighing. Fig. 6.4. shows a typical relationship between the pressure difference, h, and volume of air expanded/compressed. H. From the graph, it can be seen that the relationship is linear and there is a slight difference in slopes between the compression and the expansion process. The slope of the line is calculated by regression method and the error in the slope is taken at 95 percent confidence limit. The volume of the dead space was estimated to be 313.5 $\pm$ 2 cm^3.

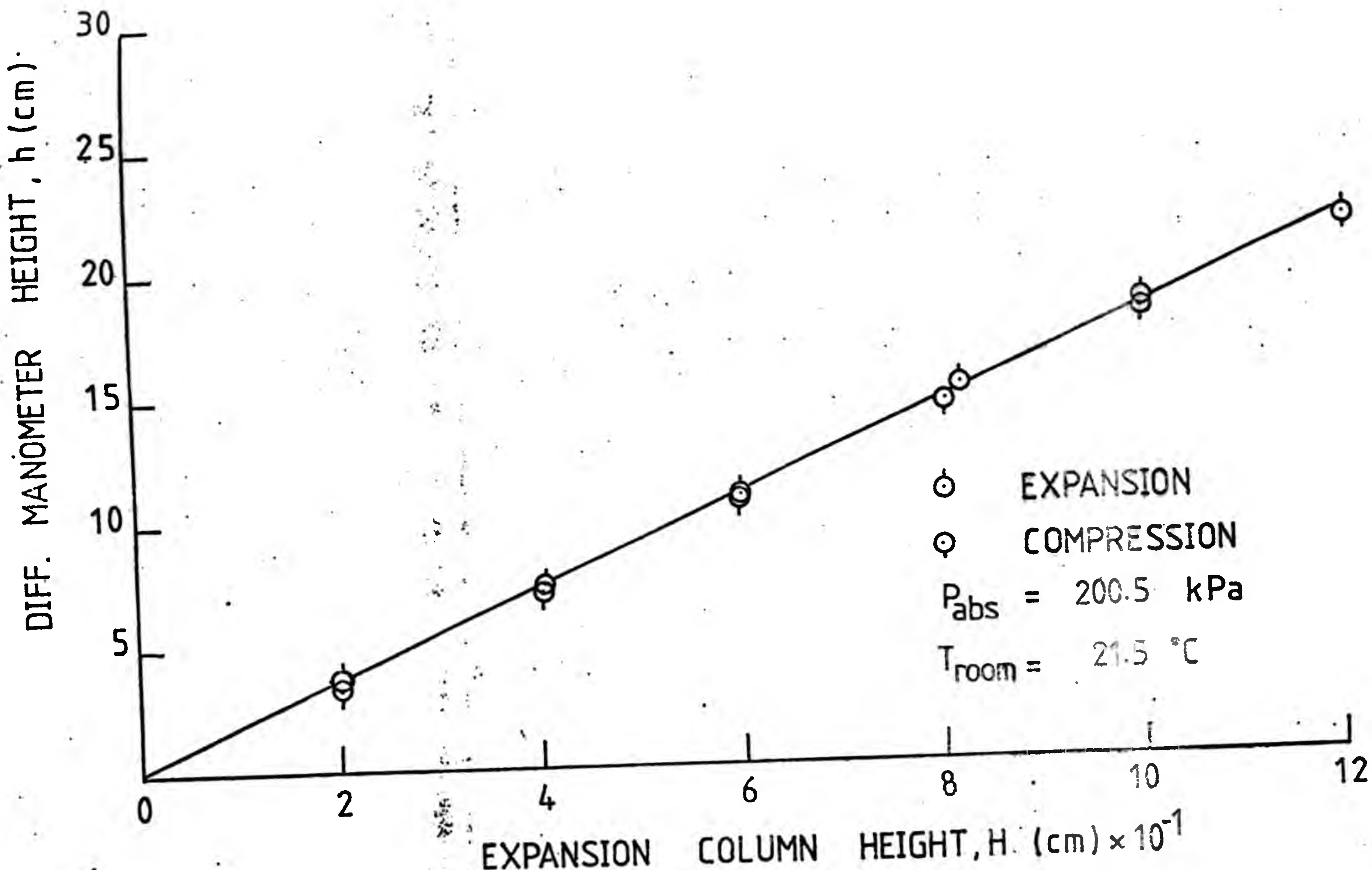

Fig. 6.4. Typical graph of the relationship between pressure difference, h, and volume, H.

6.4.1 Effect of inflation pressure upon internal volume of the tyre.

The volume of the tyre obtained by method of filling with distilled water is shown in Fig. 6.5. It can be seen that for both tyres, the test tyre and the reference tyre, the internal volume increases non-linearly up to a pressure of ≈55 kPa, above it the relationship is linear. It can also be seen that the volume of the test tyre is significantly higher than the volume of the reference tyre. The volume of the test tyre is calculated to be 1.05 times greater than the greater than the volume of the reference tyre.

The differences between the volume of the test tyre obtained by the two methods is depicted in Fig. 6.6. The volume of the test tyre calculated from Equation (4.9) when compared against the value obtained from the method of filling the tyre with water and weighing was found to be not significant at 5 percent level of significance.

The slight difference in values between the two methods may be due to several factors. One of the factors is the presence of some air bubbles being generated during the pumping of water into the tyre and as a result of this air pocket is being formed at the uppermost section of the tyre. As a result of this, the calculated value will be

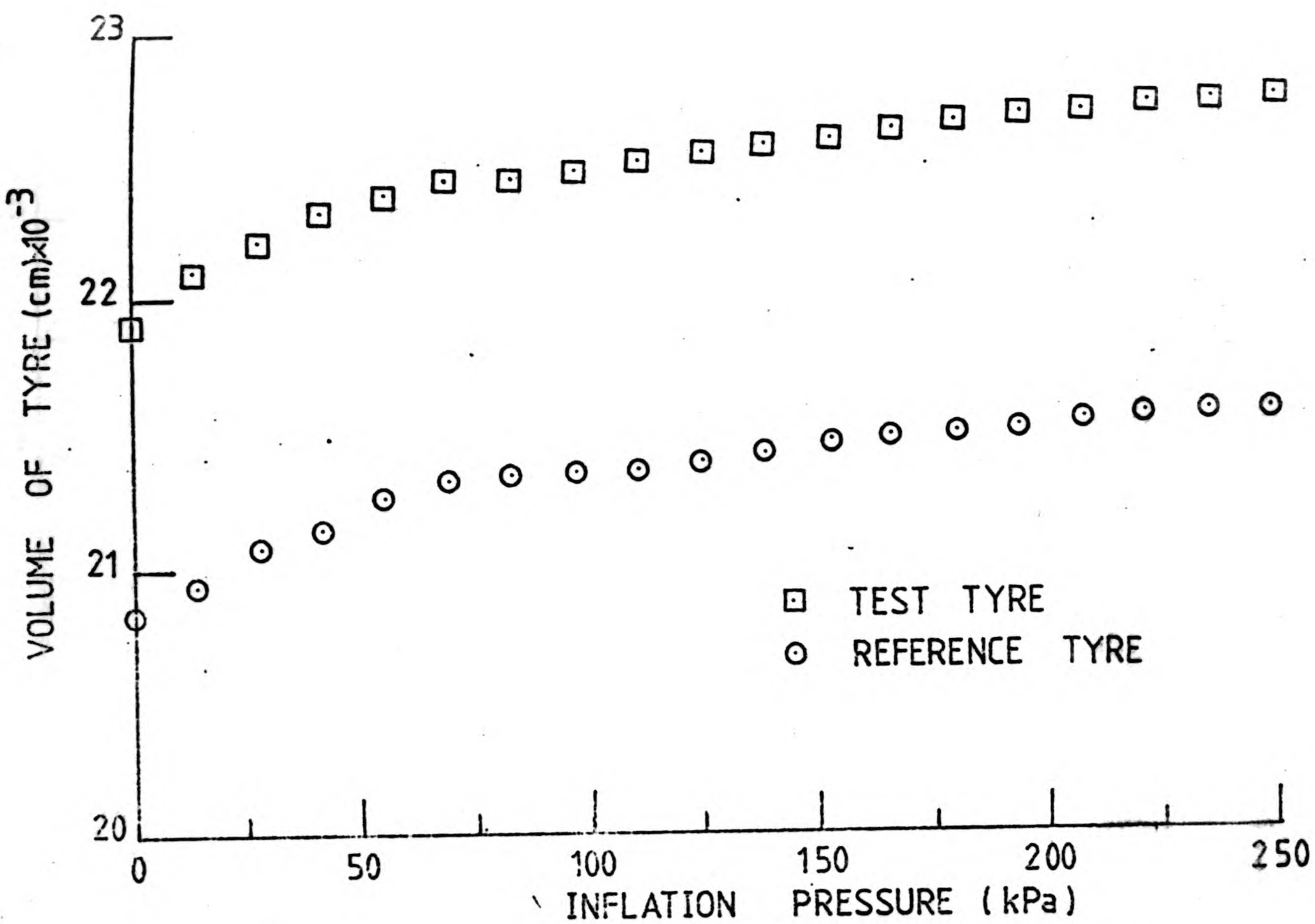

Fig.6.5. Plot of the variation of the internal volume of the 165-SR-13 Rayon-belted tyre against inflation pressure.

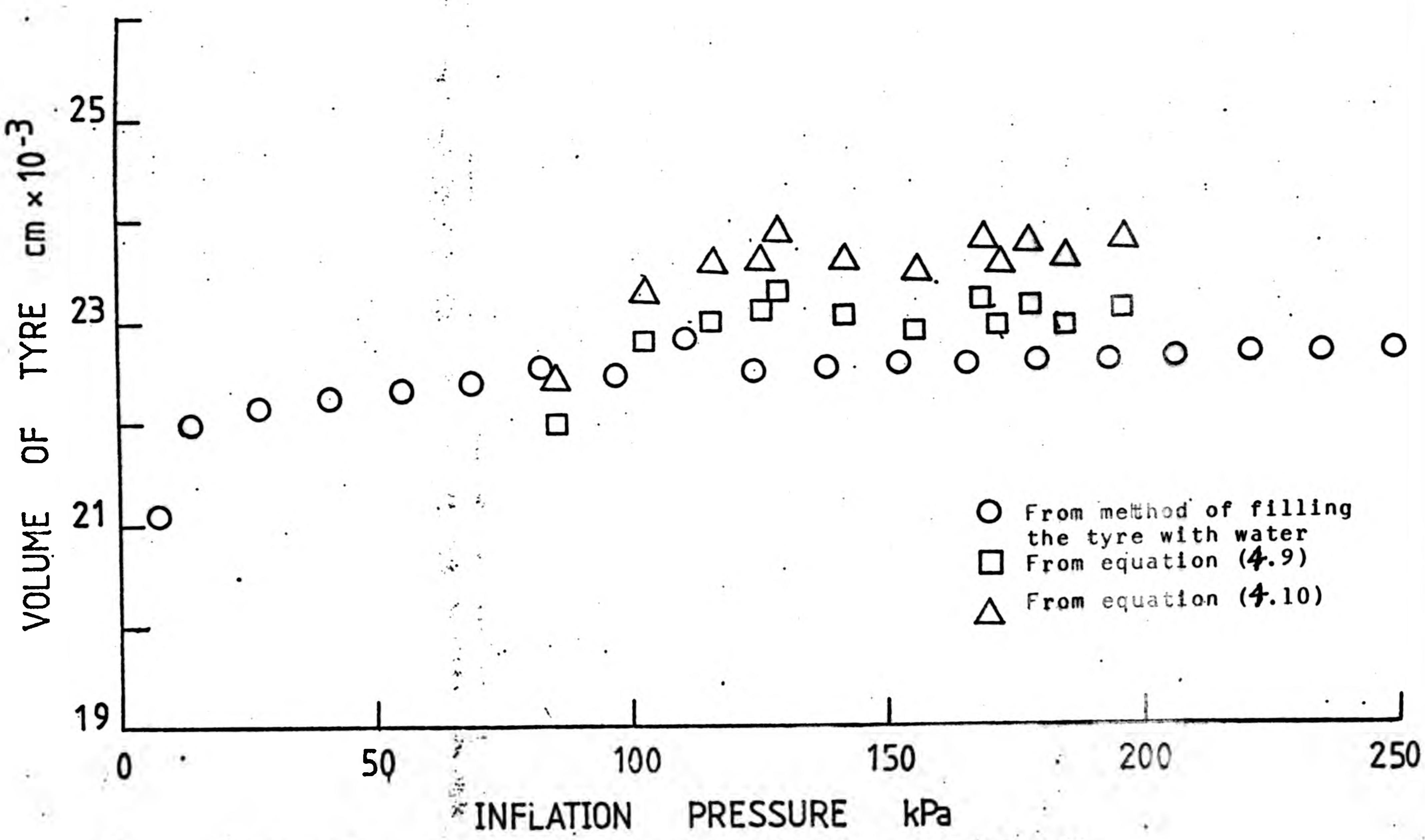

Fig. 6.6. Plot of the effect of inflation pressure upon volume of test tyre. (165-SR-13 Rayon-belted tyre)

slightly lower than the actual value. On the other hand, in the case of the expansion/compression method, the effect of temperature changes during the process and also the effect of difference in the volume of the test tyre and the reference tyre were not taken into consideration. The temperature changes during the process is evident from the graph of h against H in Fig. 6.4. for the expansion and compression process. The compression process exhibit a higher slope compared to the expansion process. Since the volume of the tyre calculated from Equation (4.10) is inversely proportional to the slope of the line, the value obtained for the expansion process tends to be on the high side and the reverse with the compression process. This however, can be minimised by taking the mean of the two. The volume of the test tyre obtained by this method is reduced by 0.2 percent when the difference between the test and reference tyres is taken into consideration.

6.5. Load-deflection relationship.

A series of load-deflection curves at varying inflation pressures for cross-ply tyre, rayon-belted and steel-belted radial tyres are constructed in the form of lattice plot as shown in Figs. 6.7a, 6.7b and 6.7c respectively. The lattice plot is formed by initially plotting load as a function of radial deflection at the maximum inflation pressure used for the particular tyre.

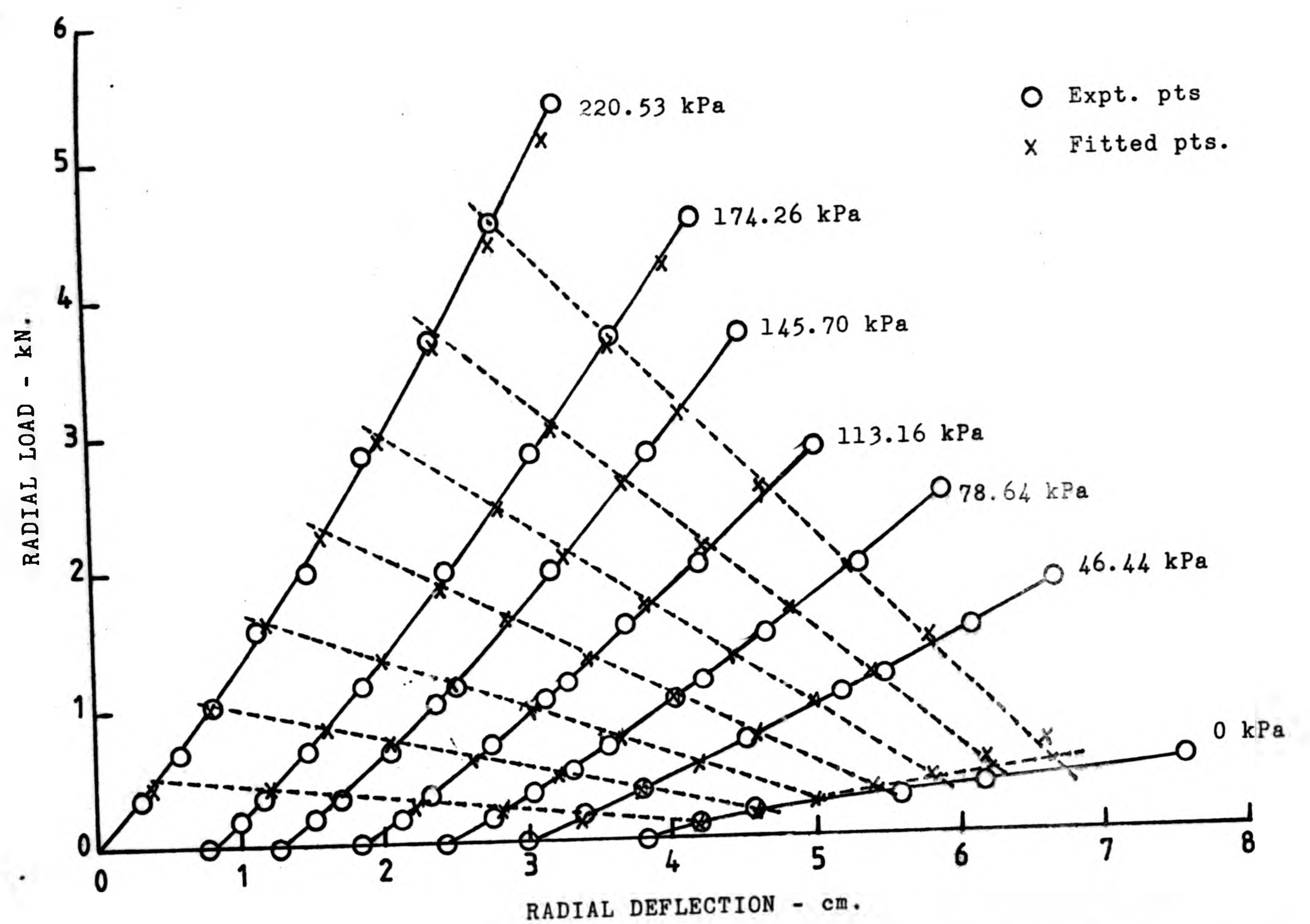

Fig. 6.7c. Load-deflection characteristics at various inflation pressure of a steel-belted radial tyre.

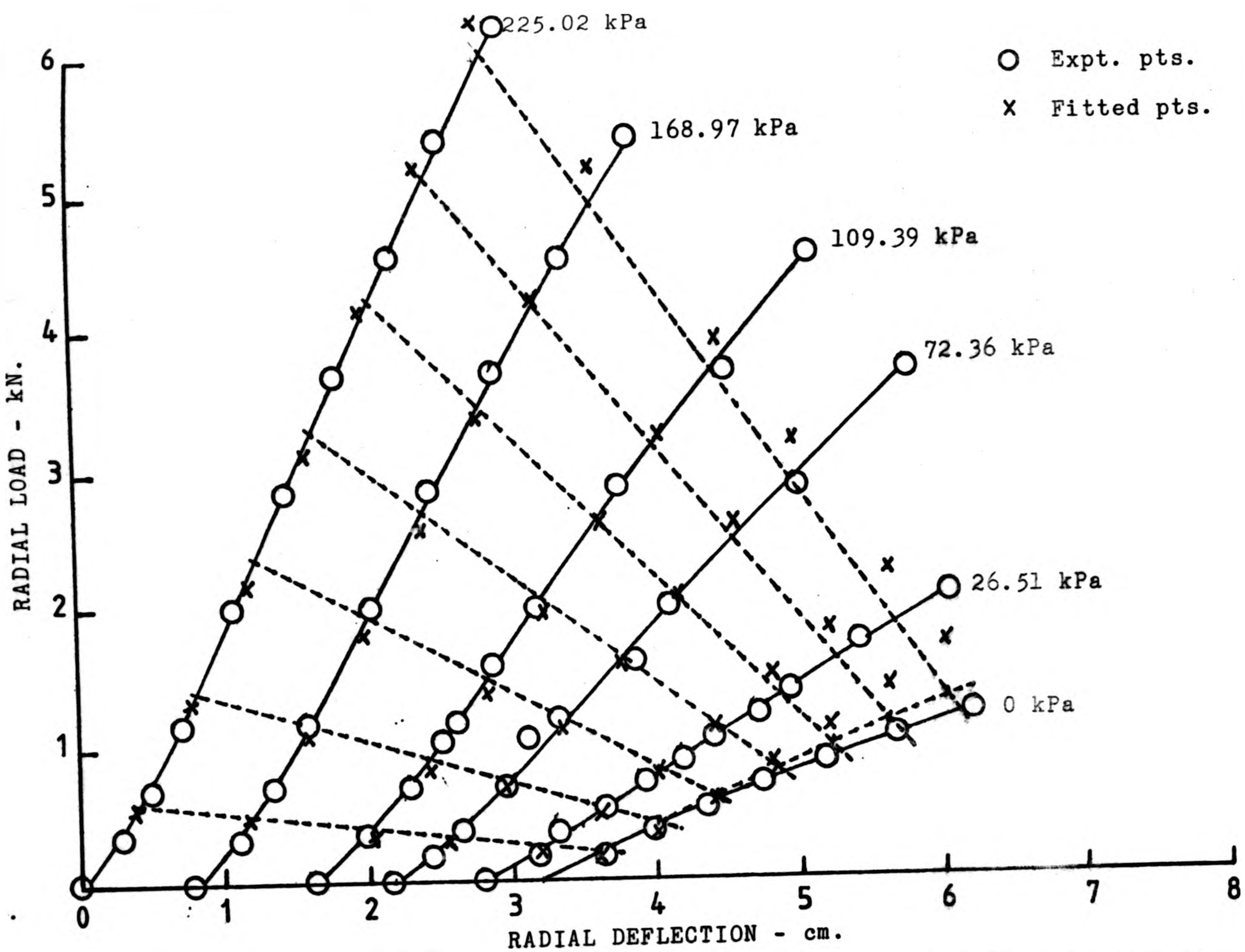

Fig. 6.7a. Load-deflection characteristics at various inflation pressure of a cross-ply tyre.

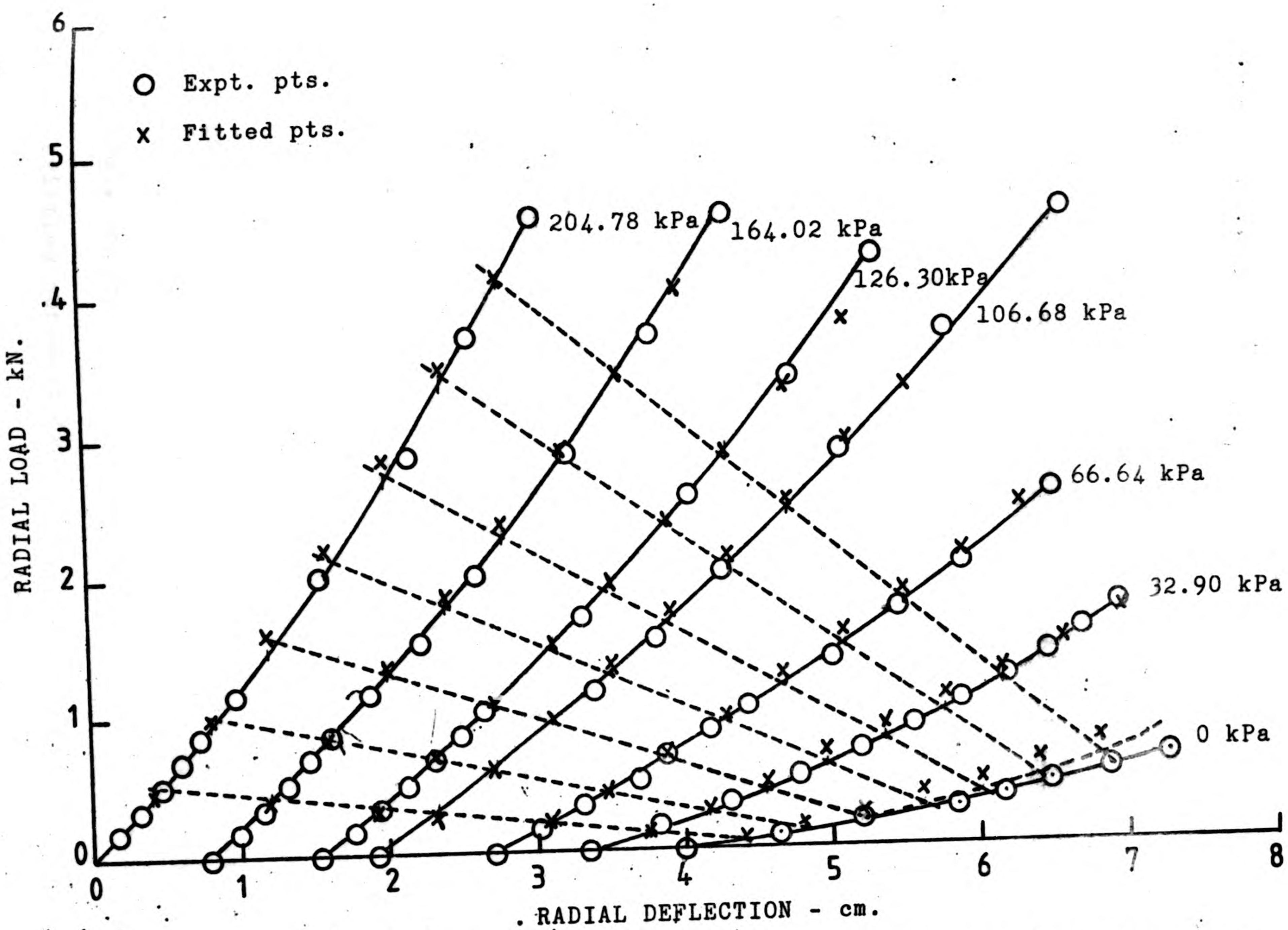

Fig. 6.7b. Load-deflection characteristics at various inflation pressure of a rayon-belted radial tyre.

Results at subsequent inflation pressures are plotted with their origins displaced along the deflection axis by an increment proportional to the change in the inflation pressures. From the graphs it can be seen that inflation pressure is a predominant factor in the load-deflection characteristics of the tyre. The radial stiffness of the tyre increases with increase in the inflation pressure. The increase in the radial stiffness of a cross-ply tyre is faster when compared to the radial tyres. This is evident from the shape of the curves. The curve for the cross-ply tyre has a point of inflection which is not evident for the radial-ply tyres.

6.5.1. The effect of rise in pressure upon deflection.

The rise of the air pressure in the tyre upon radial deflection for the cross-ply tyre, rayon-belted and steel-belted radial tyres are shown in Figs. 6.8a, 6.8b, and 6.8c respectively. From the graphs it can be seen that at a constant deflection, the rise in pressure is greater in tyres with higher inflation pressure. The graphs of the ratio of pressure rise, Δp, to absolute inflation pressure, P_{abs}, against radial deflection for the cross-ply tyre, rayon-belted and steel-belted radial tyres are shown in Figs. 6.9a, 6.9b and 6.9c respectively. It can be seen that, in the case of the cross-ply tyre, the ratio $\Delta p/P_{abs}$ deviaties somewhat from the other data at very low inflation

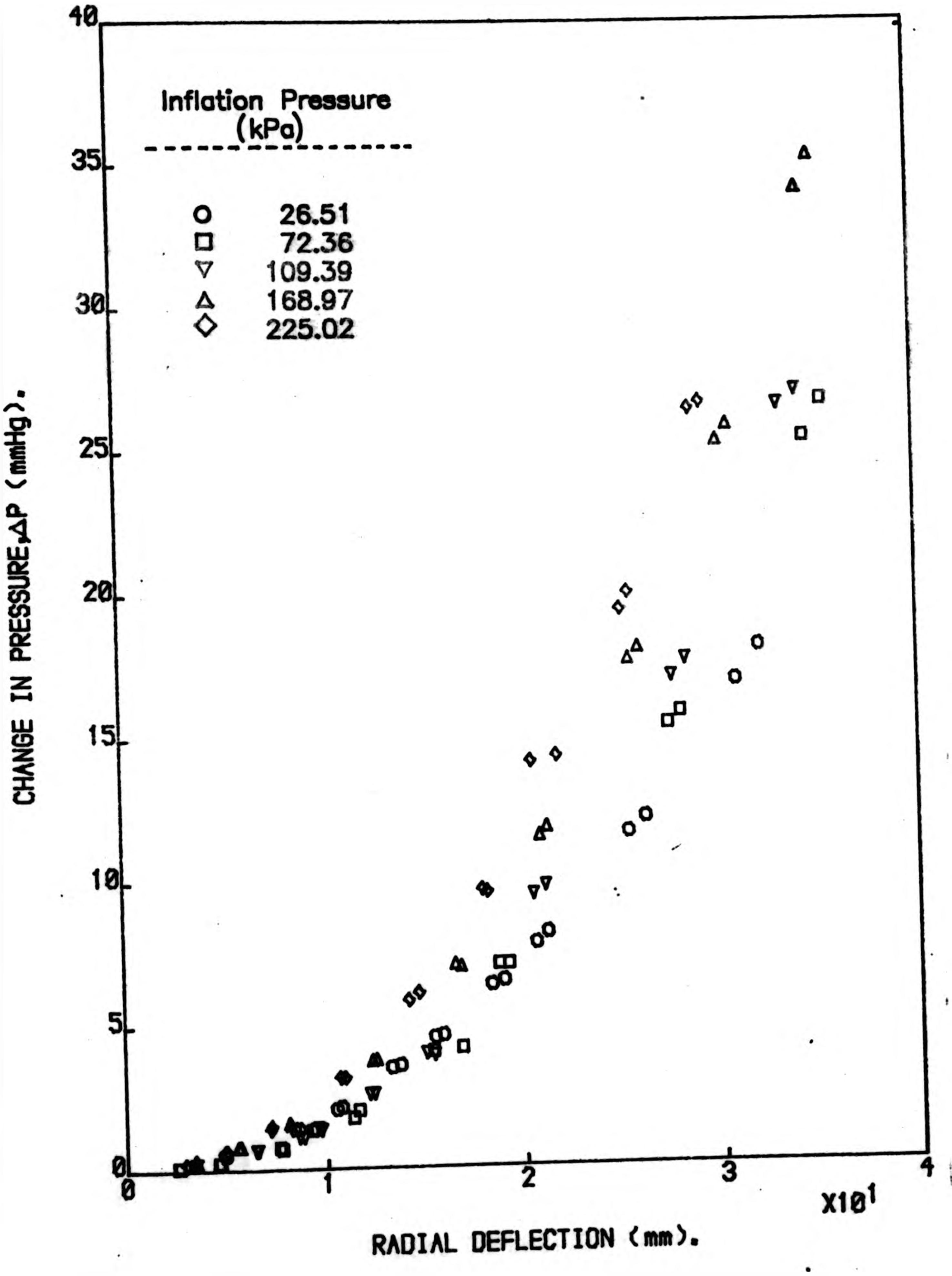

Fig. 6.8a. Plot of rise in air pressure of a cross-ply tyre against radial deflection at various inflation pressure.

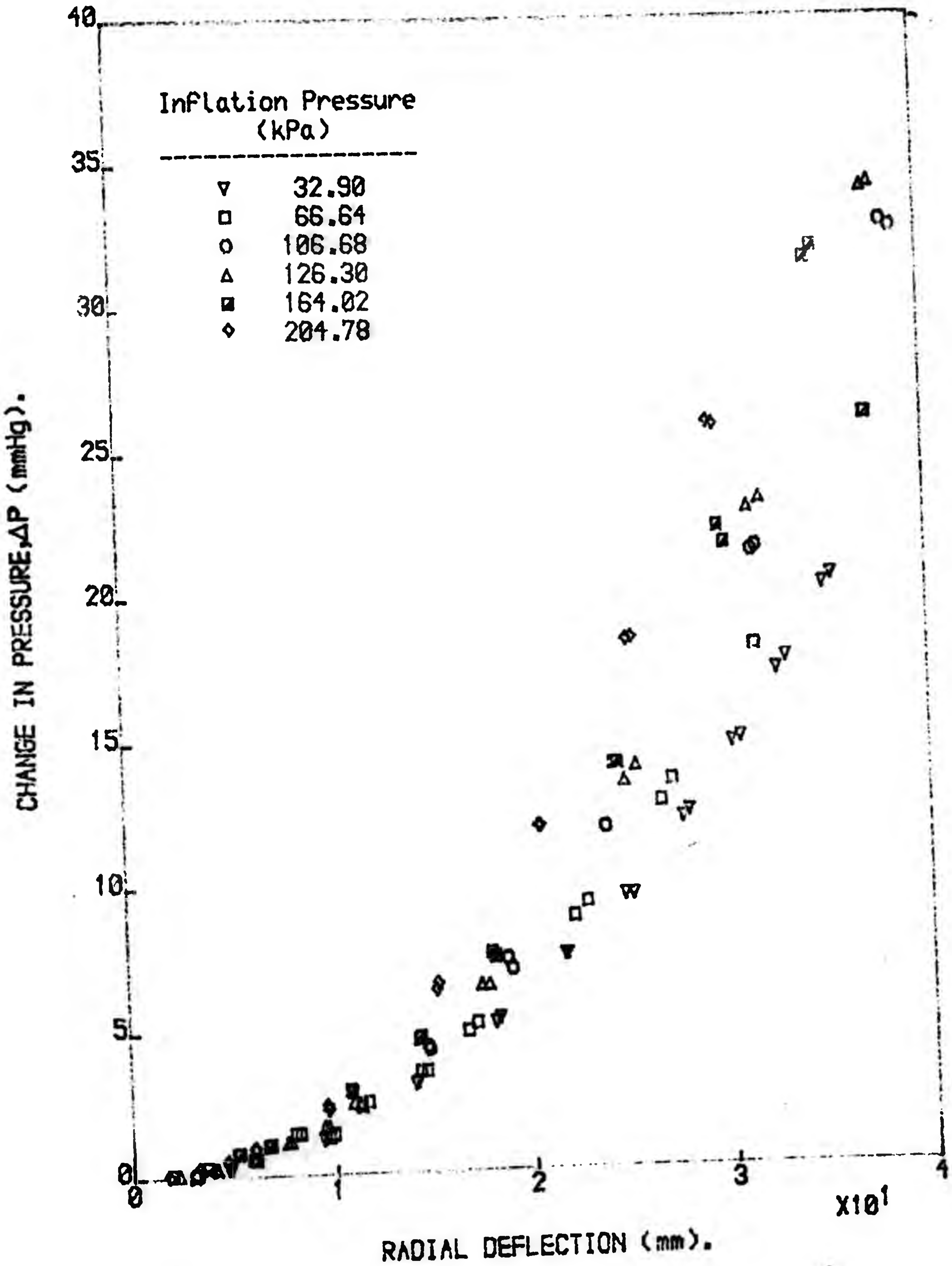

Fig. 6.8b. Plot of rise in air pressure of rayon-belted radial tyre against radial deflection at various inflation pressure.

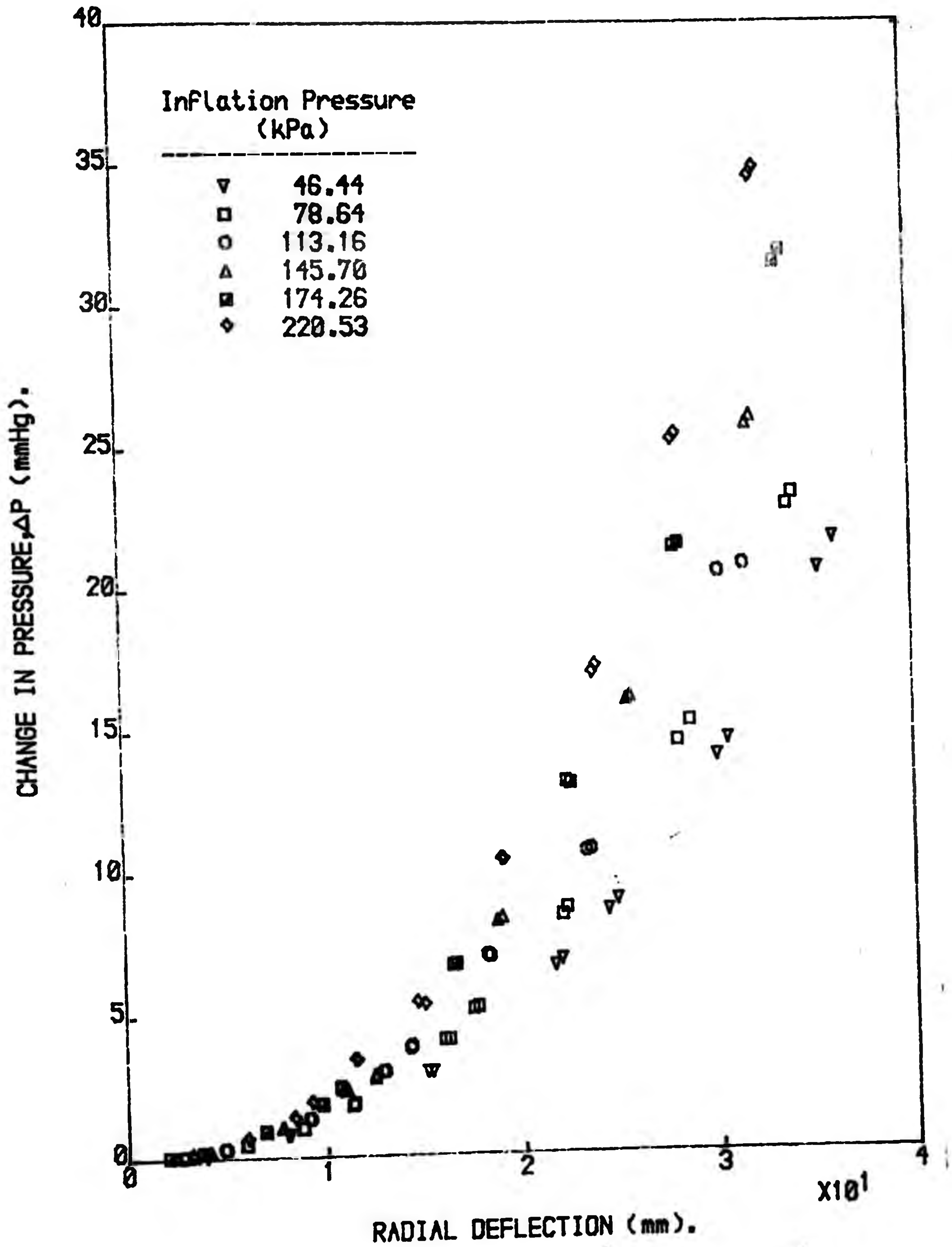

Fig. 6.8c. Plot of rise in air pressure of a steel-belted radial tyre against radial deflection at various inflation pressure.

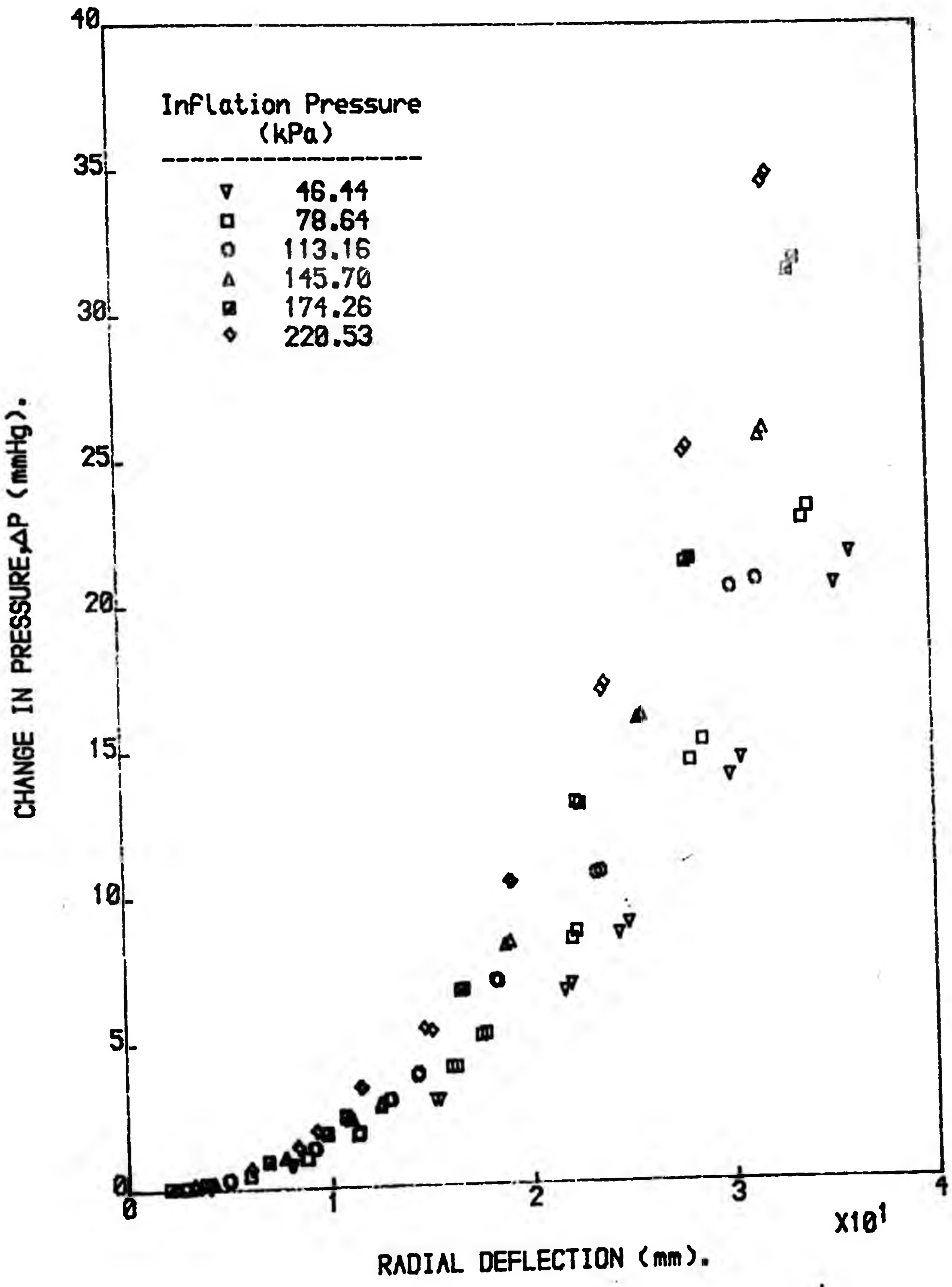

Fig. 6.8c. Plot of rise in air pressure of a steel-belted radial tyre against radial deflection at various inflation pressure.

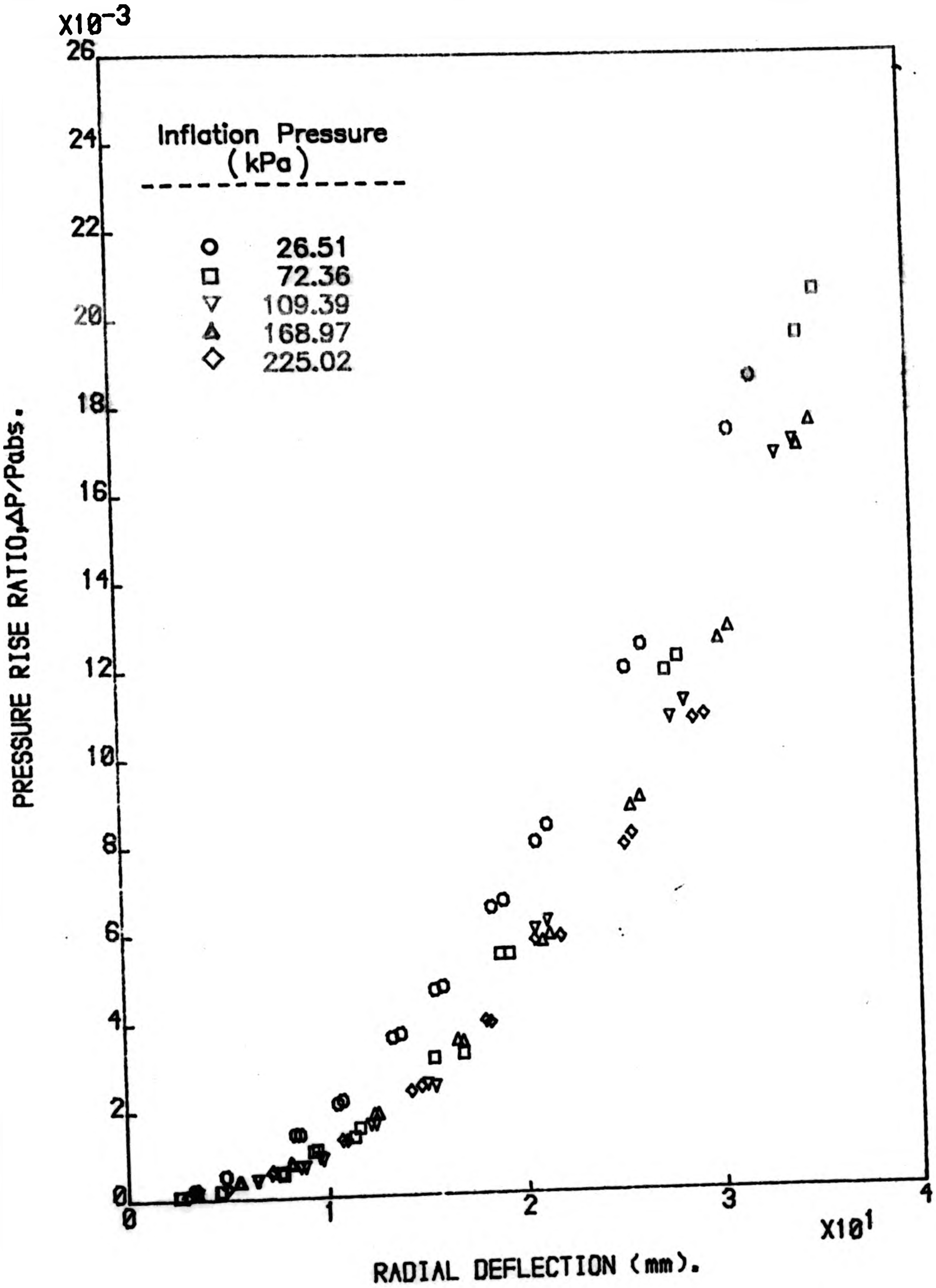

Fig. 6.9a. Plot of pressure rise ratio against radial deflection at various inflation pressures for cross-ply tyre.

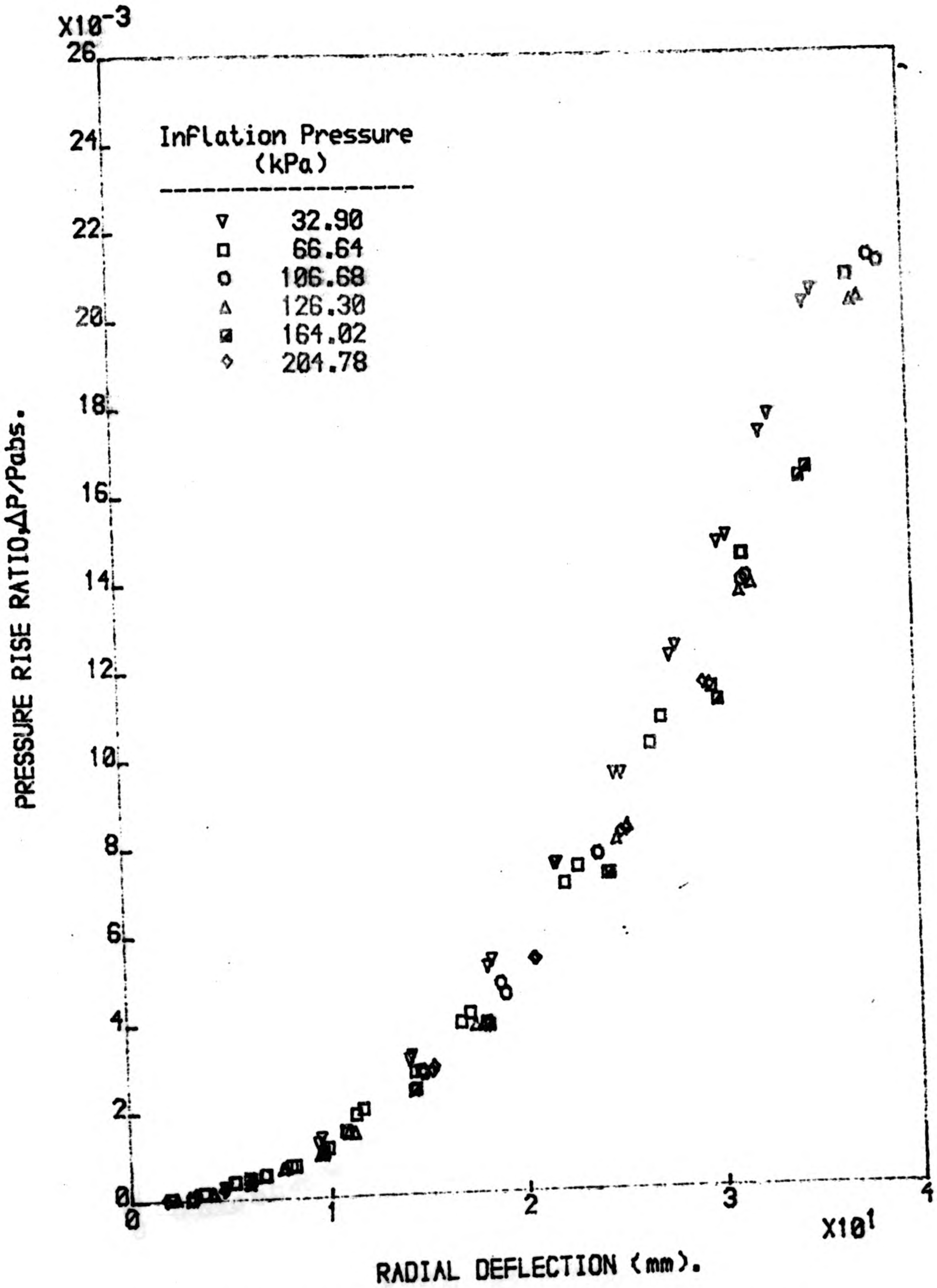

Fig. 6.9 b. Plot of pressure rise ratio against radial deflection at various inflation pressures for rayon-belted.

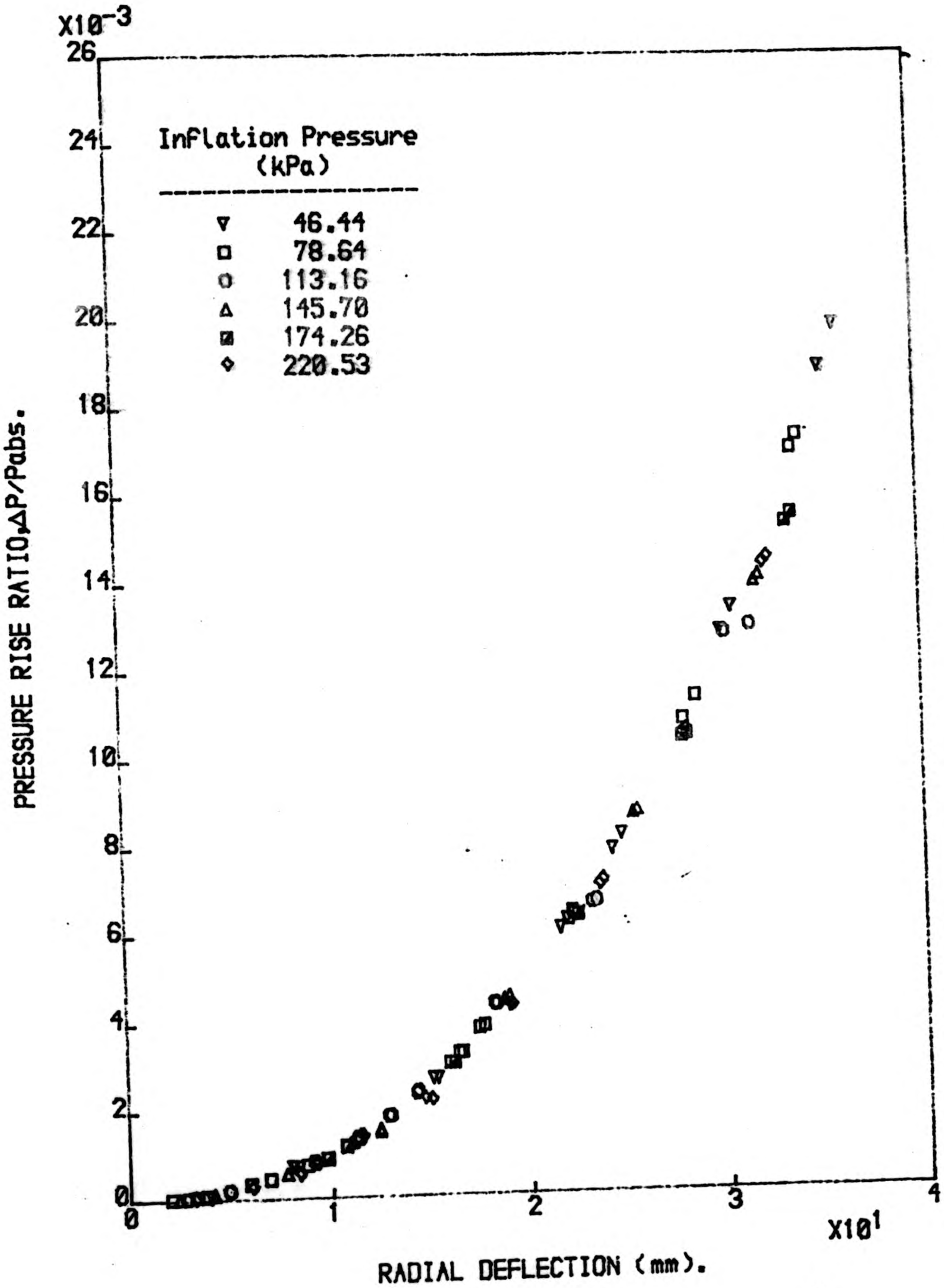

Fig. 6.9 c. Plot of pressure rise ratio against radial deflection at various inflation pressures for steel-belted.

pressure whereas at higher pressure in the tyre the values of $\Delta p/P_{abs}$ are almost coincident in one single curve. Hence, it is admissible to represent the relationship of $\Delta p/P_{abs}$ with respect to radial deflection by a simple exponential function. The test data for both radial tyres show a similar type of relationship.

The percentage rise in the pressure of the tyres at 3 cm deflection was calculated to be not more than 2 percent.

6.5.2. Effect of change in volume upon deflection.

The change in the volume of the tyre upon radial deflection for the cross-ply tyre, rayon-belted and steel-belted radial tyres is shown in Figs. 6.10a, 6.10b and 6.10c respectively. From the graphs it can be seen that with exception of the data obtained at a very low inflation pressure, almost all the test points seem to lie within the proximity of a single curve. From this it can be inferred that the relationship between change in the volume of the tyre and the radial deflection is independent of the initial inflation pressure and that there is a negligible change in the internal volume of the tyre as a result of increase in pressure due to loading.

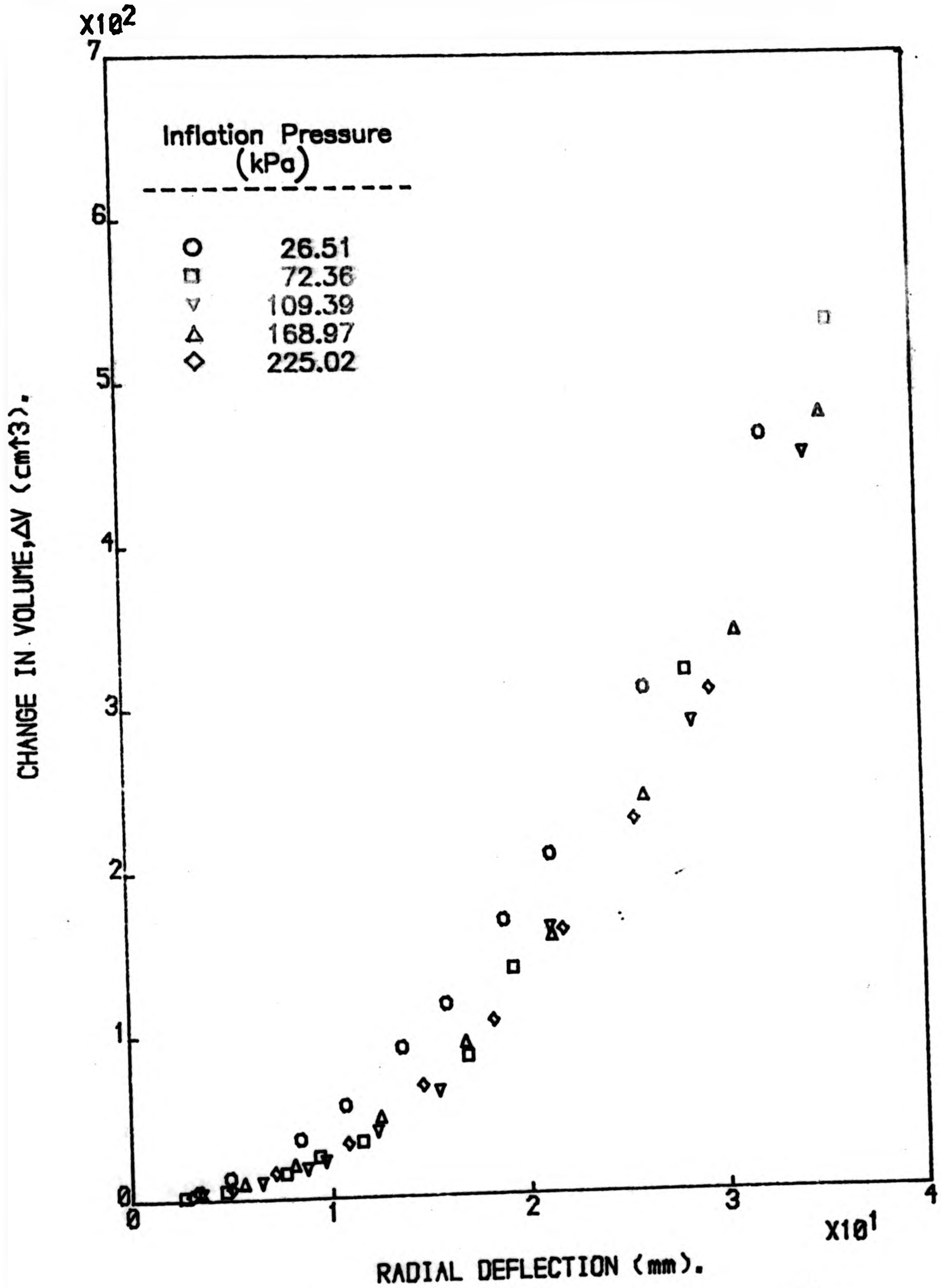

Fig. 6.10a. Plot of change in volume against radial deflection at various inflation pressures for cross-ply tyre.

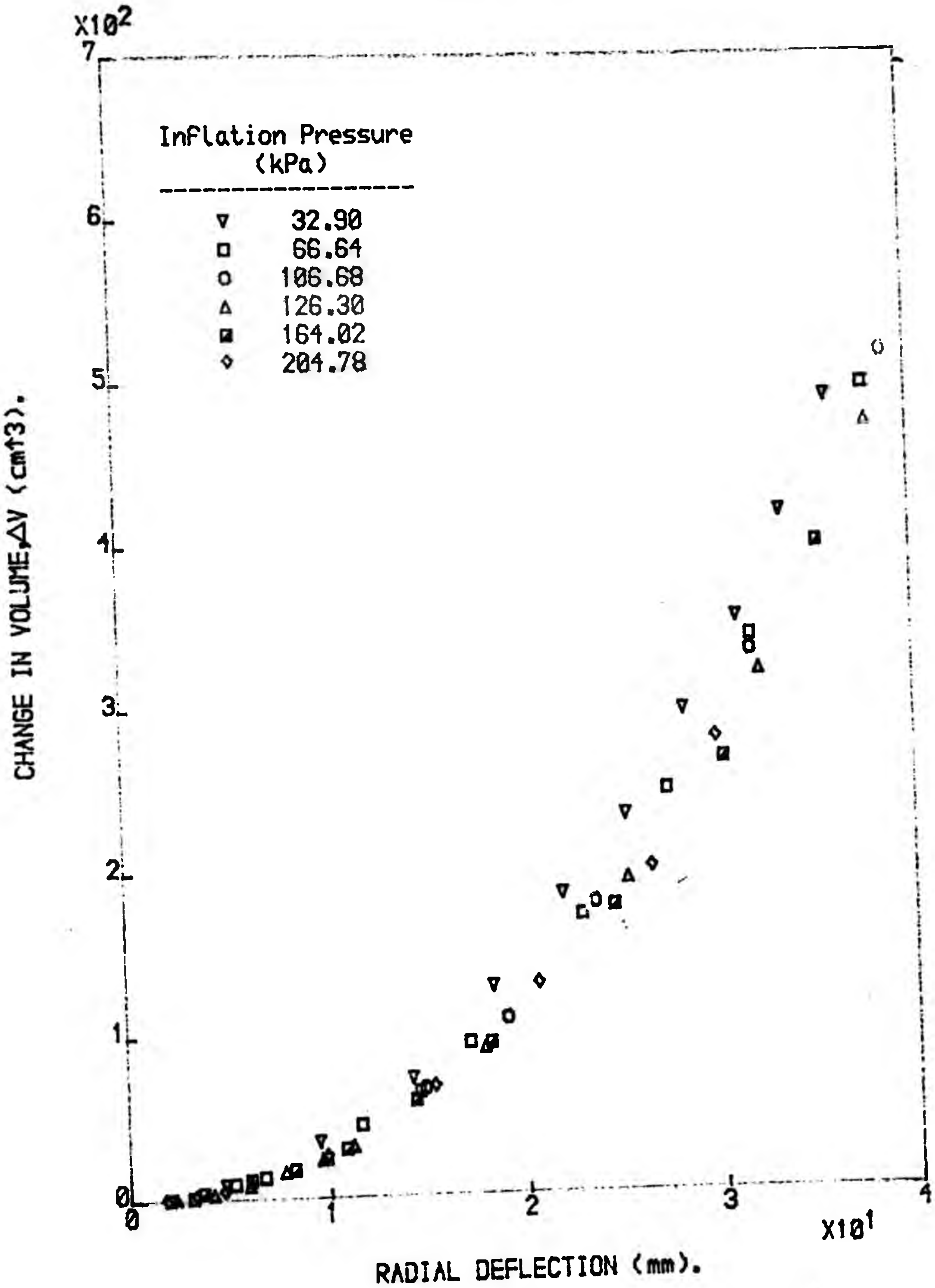

Fig. 6.10b. Plot of change in volume against radial deflection at various inflation pressures for rayon-belted tyre.

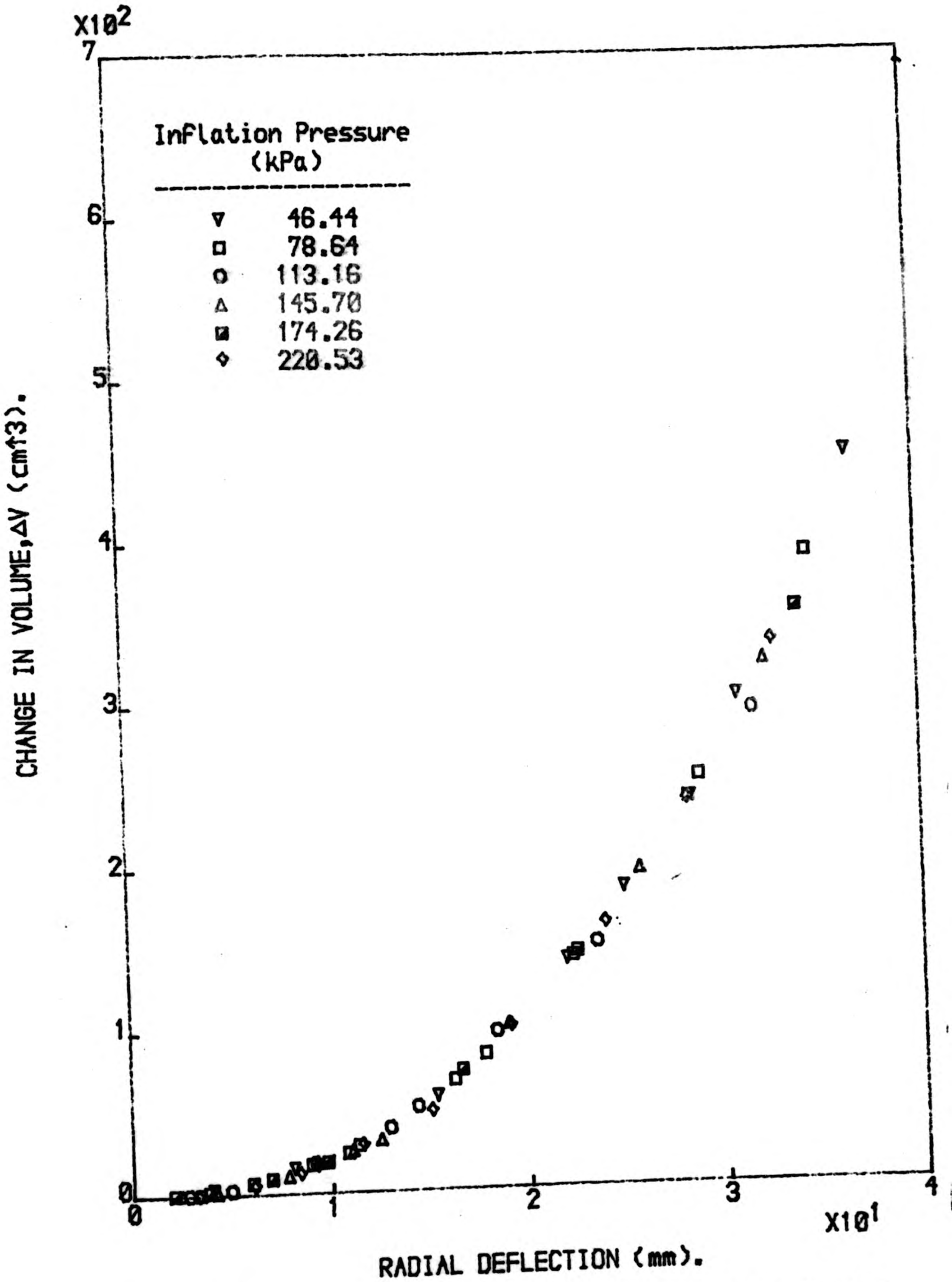

Fig. 6.10c. Plot of change in volume against radial deflection at various inflation pressures for steel-belted tyre.

6.5.3. Relationship between change in volume and pressure rise ratio.

The relationship between the change in volume and the pressure rise ratio for the cross-ply tyre, rayon-belted and steel-belted tyres are shown in Figs. 6.11a, 6.11b and 6.11c respectively. In the case of the radial tyres, within the limit of experimental error, all the points seem to lie along a straight line irrespective of the initial inflation pressures. Thus it can be inferred that the loading process took place isothermally and the air contained in the tyre obeys the Ideal Gas Law. Hence the use of Equation (2.3) for the calculation of the internal volume of the tyre and the dead space is applicable here. It can also be inferred that there is a negligible increase in the volume of the tyre with increase in the inflation pressure. In the case of the cross-ply tyre, however, there is some indication of a slight increase in the volume of the tyre by the slight variation in the slopes of the curves with increase in inflation pressure as shown in Fig. 6.11a. Whereas in the case of the radial tyres, the slopes of the lines in Figs. 6.11b and 6.11c are almost identical. This tend to suggest that the cross-ply tyre experience more interlaminar movement with increase in pressure when compared to radial tyres due to its bias construction. The variations of the volumes of the tyres with inflation pressures as calculated by

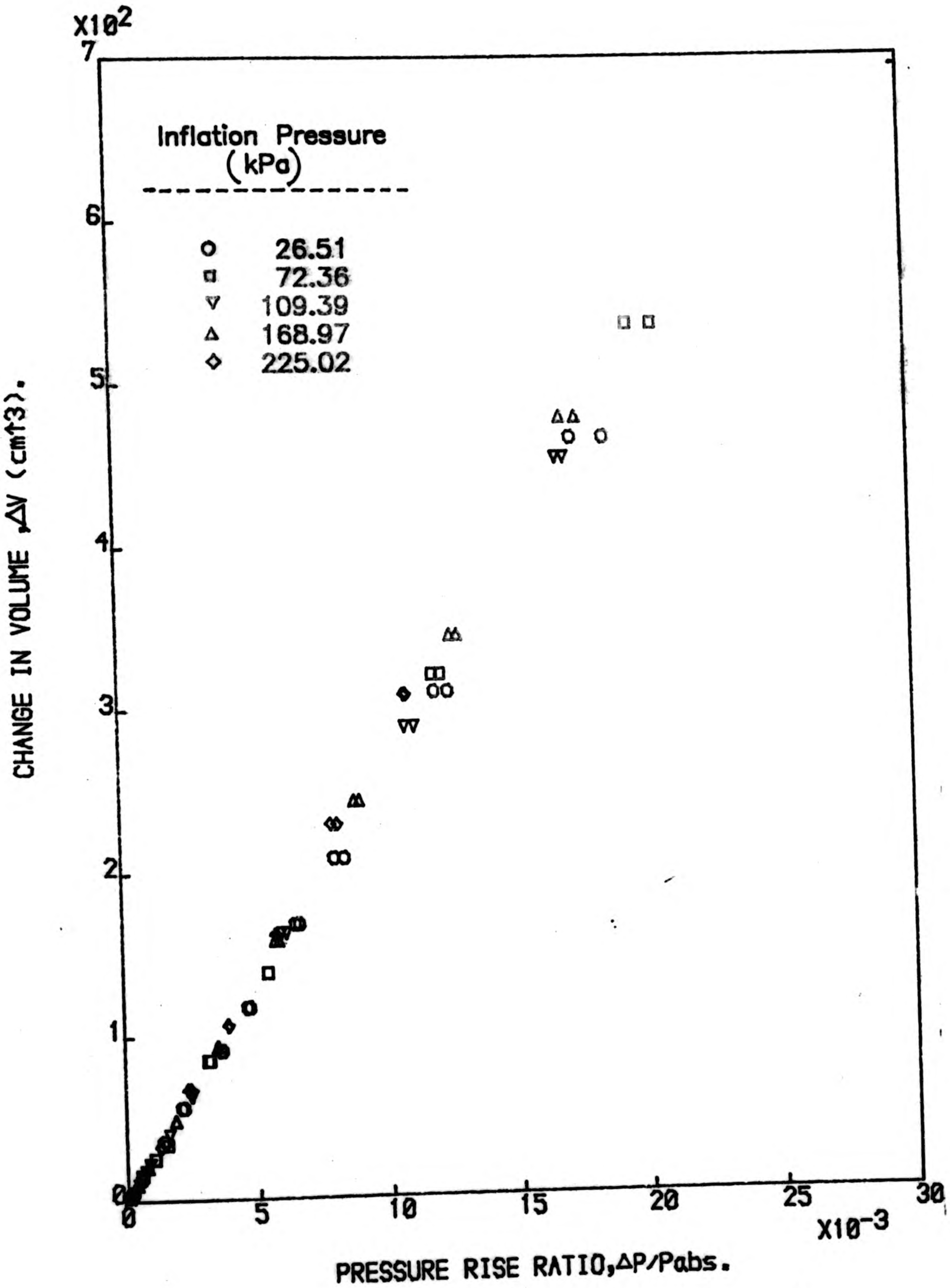

Fig. 6.11a. Plot of change in volume against pressure rise ratio for cross-ply tyre.

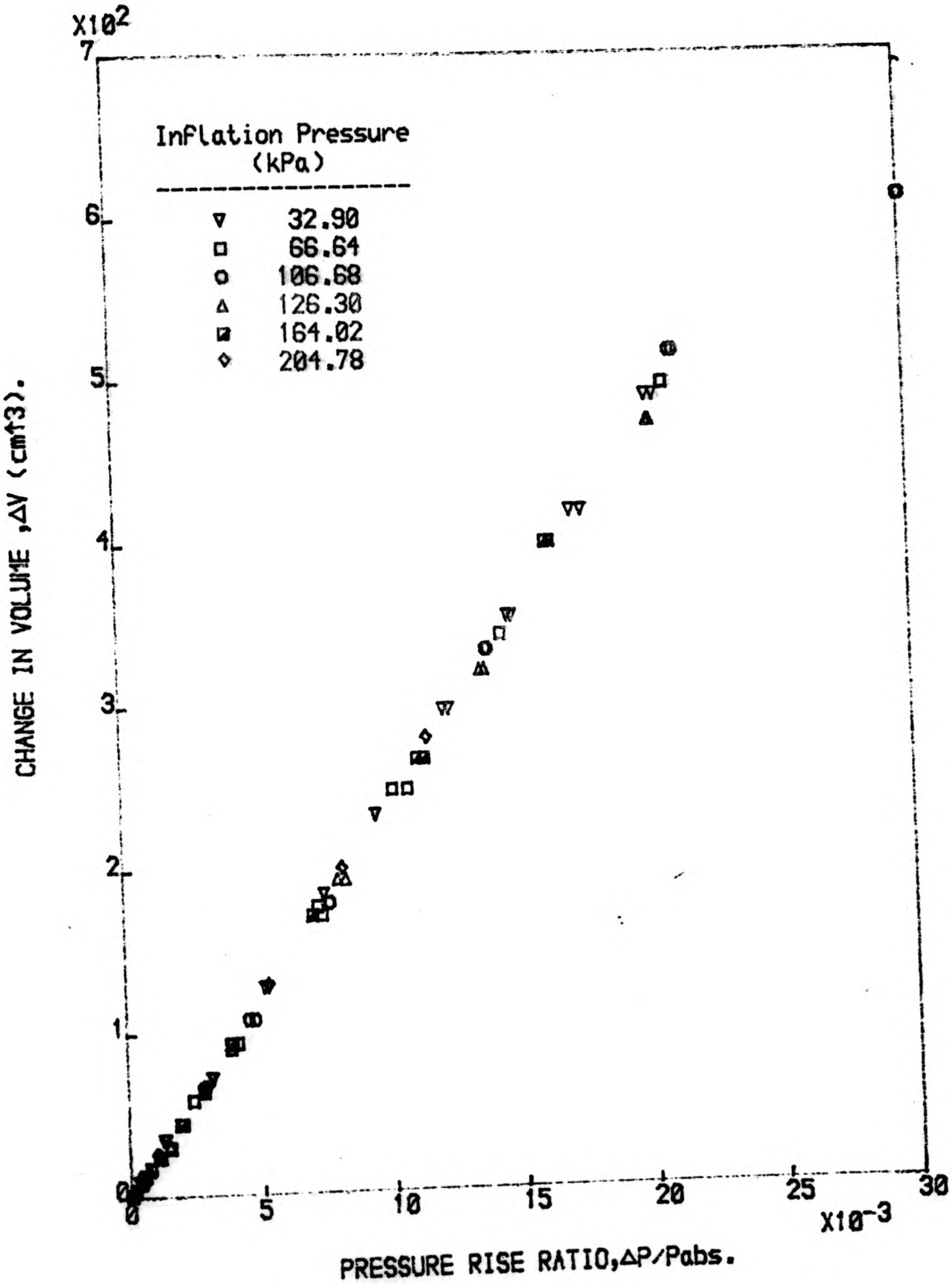

Fig. 6.11b. Plot of change in volume against pressure rise ratio for rayon-belted tyre.

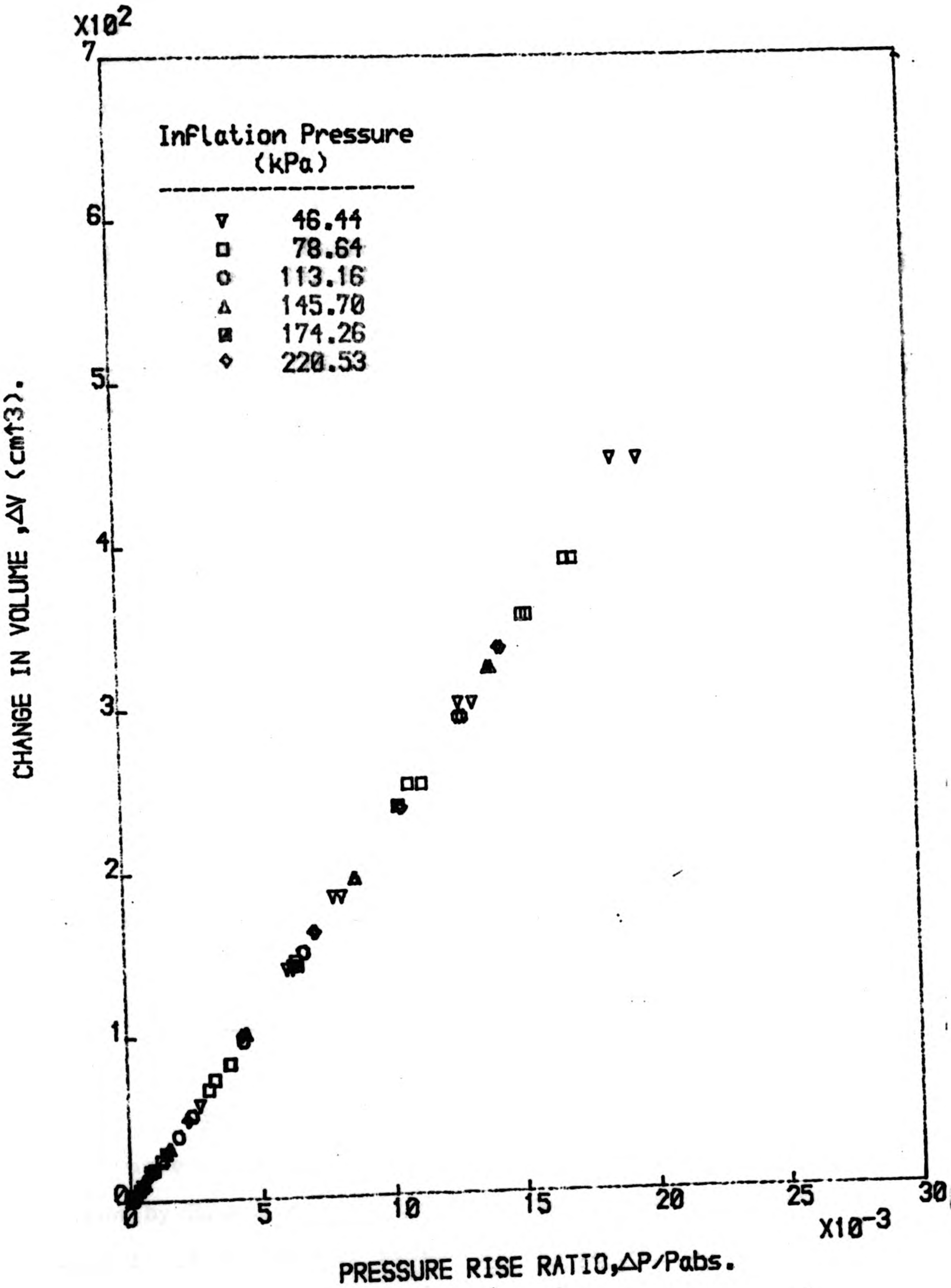

Fig. 6.11c. Plot of change in volume against pressure rise ratio for steel-belted tyre.

regressing ΔV against $\Delta p/P_{abs}$ is shown in Fig. 6.12. This confirms the earlier suggestion that the cross-ply tyre internal volume increases with increase in inflation pressure and also that the difference between the volumes of rayon-belted and steel-belted radial tyres is of the order of 2 to 3 percent.

6.6. Work done

6.6.1. External work done on the tyre.

The external work done on the tyre by the load is calculated from the area enclosed between the load-deflection curve and the deflection axis. The area is calculated using the trapezoidal method. The graph of the external work done on the tyre against radial deflection at various inflation pressures for the cross-ply tyre, rayon-belted and steel-belted radial tyres are plotted as depicted in Figs. 6.13a, 6.13b and 6.13c respectively.

6.6.2. Work done on/by the air.

The work done on the air in the tyre when it is compressed, Wp, is evaluated according to the relationship given by Equation (4.16) and the work done by the air, Wv, when it is allowed to expand to its initial pressure is calculated from Equation (4.19). The calculated values of

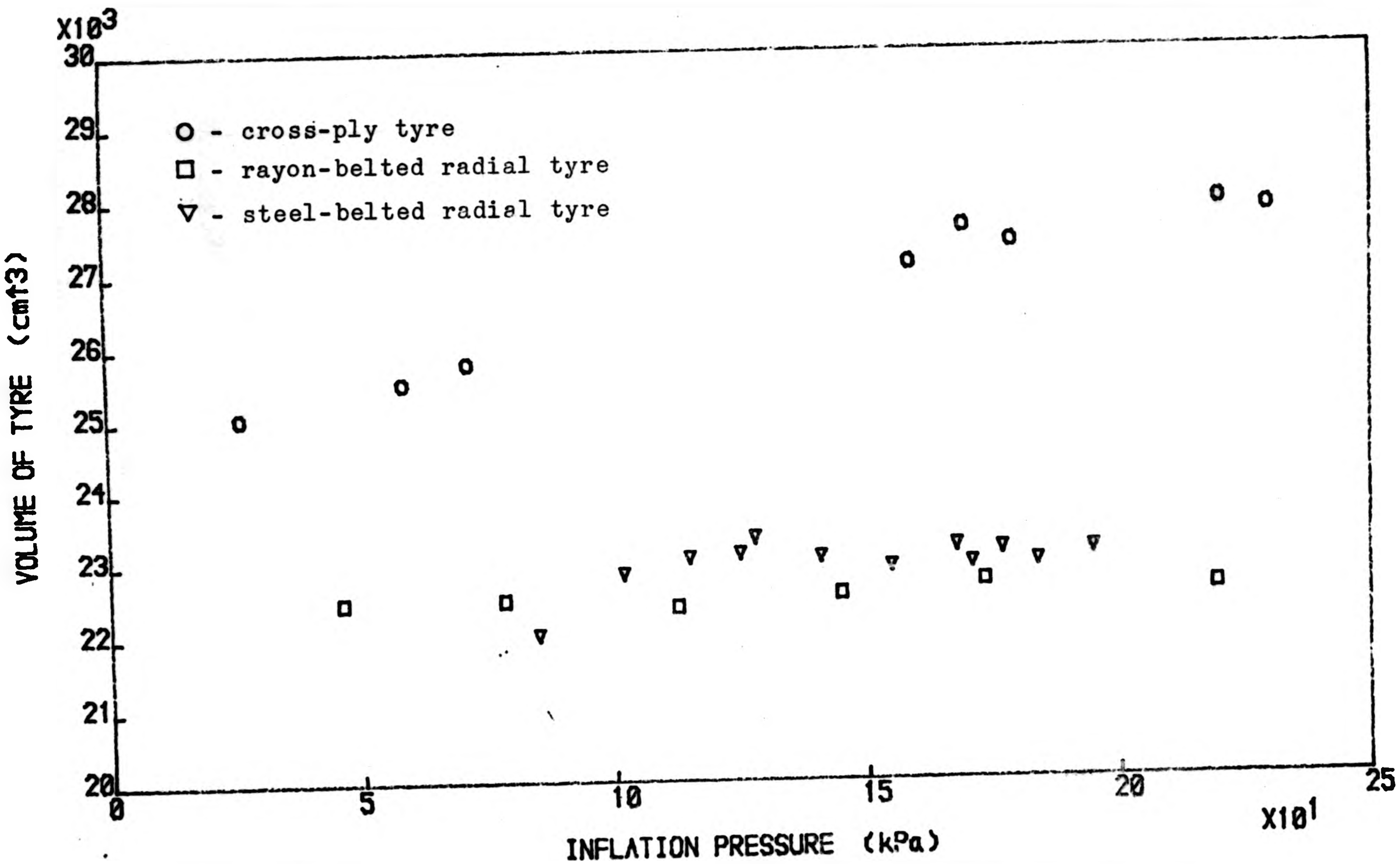

Fig. 6.12. Variation of the volume of the tyre with inflation pressure.

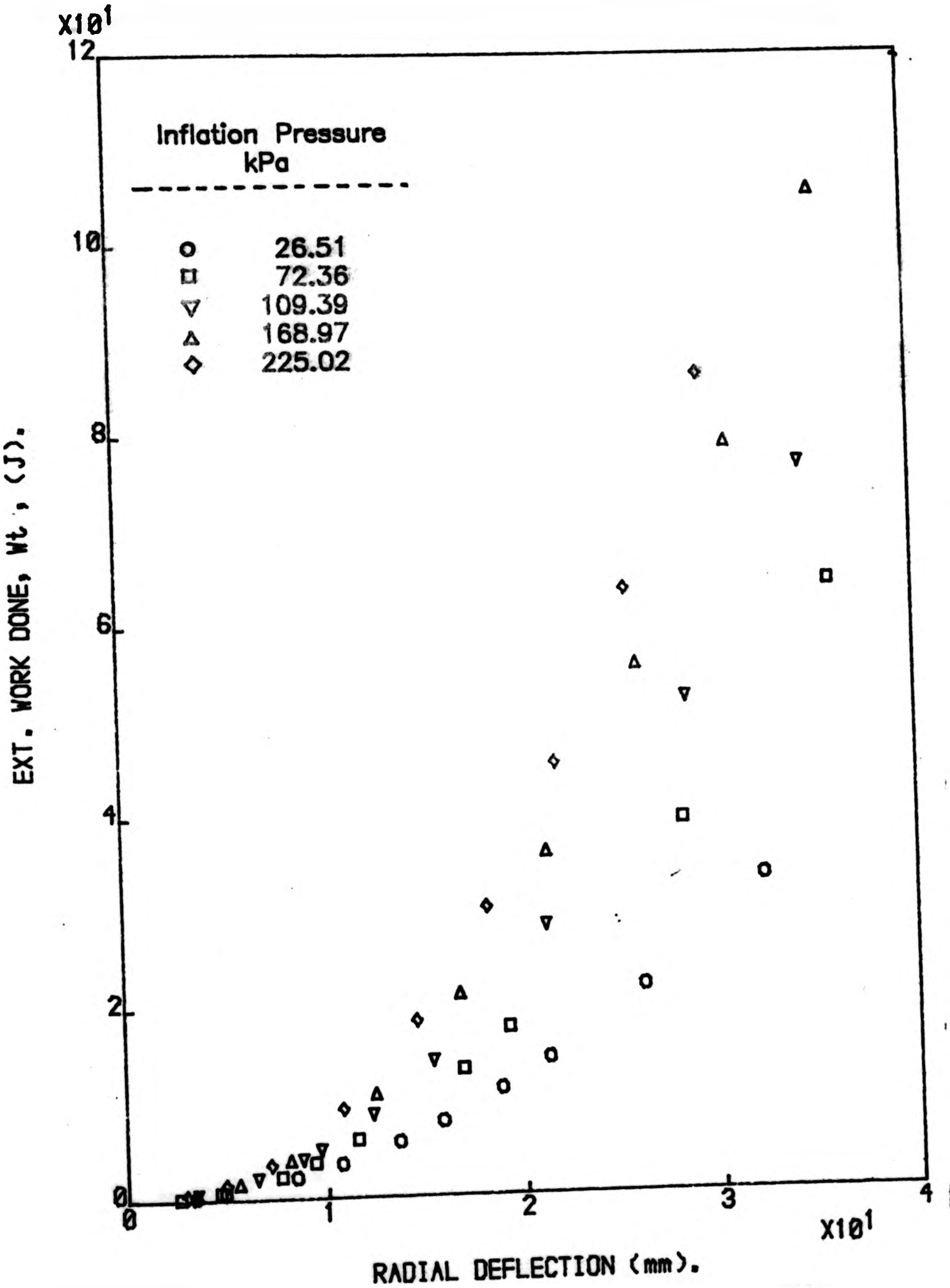

Fig. 6.13a. Plot of the external work done against radial deflection for cross-ply tyre.

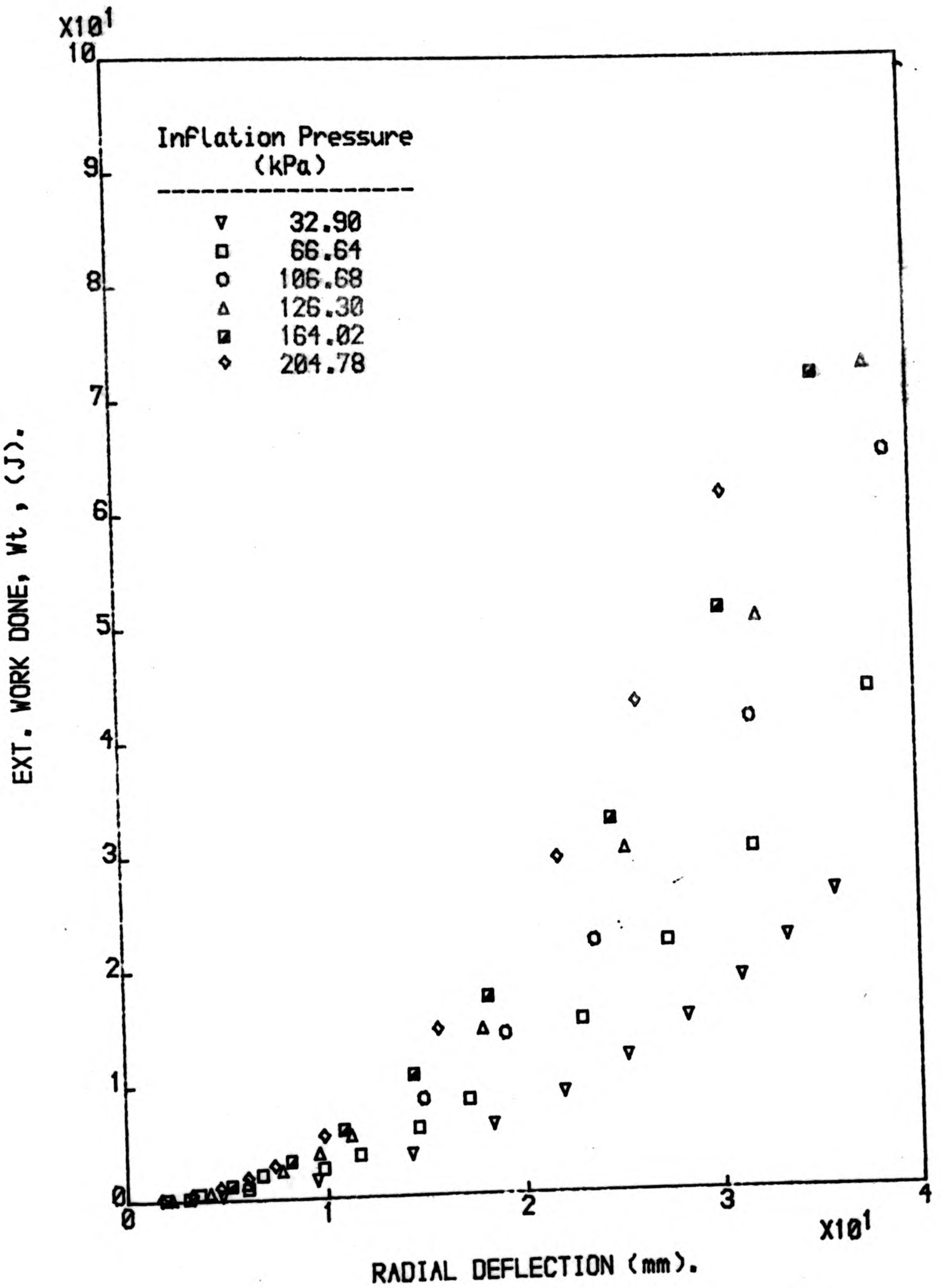

Fig. 6.13b. Plot of the external work done against radial deflection for rayon-belted tyre.

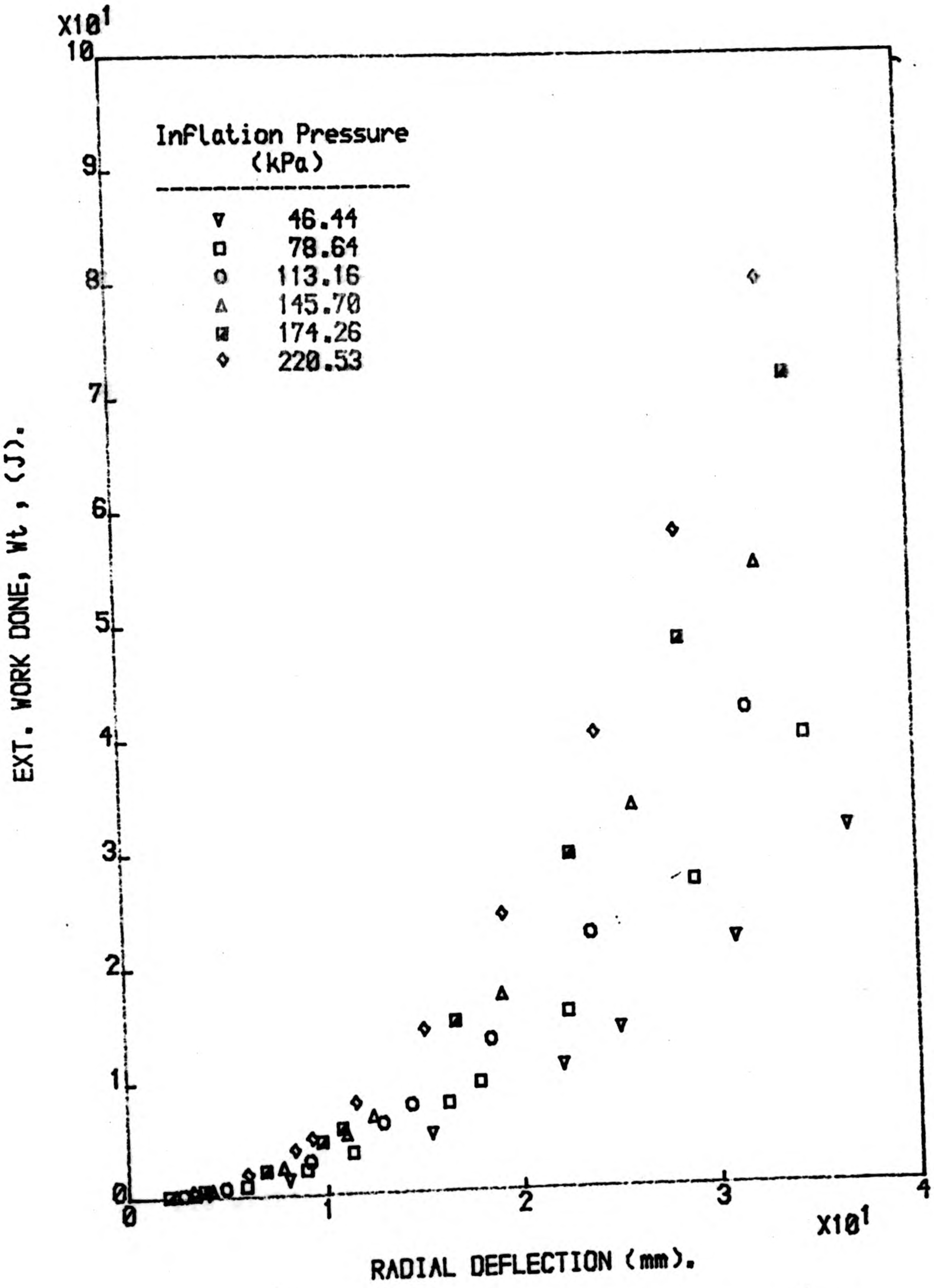

Fig. 6.13c. Plot of the external work done against radial deflection for steel-belted tyre.

Wp and Wv are plotted against radial deflection for cross-ply tyre (Figs. 6.14 - 6.15), rayon-belted radial tyre (Figs. 6.17 - 6.18) and steel-belted radial tyre (Figs. 6.20 - 6.21). The relationship between Wp and Wv for the cross-ply tyre, rayon-belted radial tyre and the steel-belted radial tyre are shown in Figs. 6.16, 6.19 and 6.22 respectively. It can be seen that for the three tyres the relationship between Wp and Wv is linear. This indicates that the process of compression and expansion took place reversibly.

6.6.3. Work done on the tyre structure.

The work required to deform the structure of the tyre is calculated from the different between the total external work done on the tyre and the work done on/by the air contained. The relationship between the work done on the tyre structure against radial deflection is shown in Figs. 6.23a, 6.23b and 6.23c for the cross-ply tyre, rayon-belted and steel-belted radial tyres respectively. Within the limits of experimental errors it can be safely said that the work done on the tyre structure is independent of the inflation pressure. This is highlighted by the fact that the experimental points corresponding to zero inflation pressure lie within the cluster of the points corresponding to various inflation pressures. From the graphs it is evident that the work done on the cross-ply tyre structure is almost twice that required to deform the radial tyres.

This is mainly due to the heavy shoulder of cross-ply tyre. Another contributory factor is its stiffer sidewalls.

The percentage ratio of work done on tyre structure to external work done against radial deflection for the cross-ply tyre, rayon-belted and steel-belted tyres are shown in Figs. 6.24a, 6.24b and 6.24c respectively. From the graphs it can be seen that the proportion of work required to deform the tyre structure decreases with increase in inflation pressure. Also, at constant inflation pressure there seem to be no significant increase in the proportion of the work done on the structure at deflection more than 1 cm. At deflection less than 1 cm. a difference in behaviour of the tyres are observed. This suggest that the tyres undergo two stages of deformations. In the early stage, bending and compression of the tread band dominates and in later stages the bending of sidewalls dominates. In the case of the cross-ply tyre and the rayon-belted radial tyre, the tyre structure release part of its stored energy whereas in the case of the steel-belted radial tyre positive work is being done on the tyre structure. In the later stages, the order of proportion of work done on the tyre structure is ,

cross-ply > rayon-belted > steel-belted

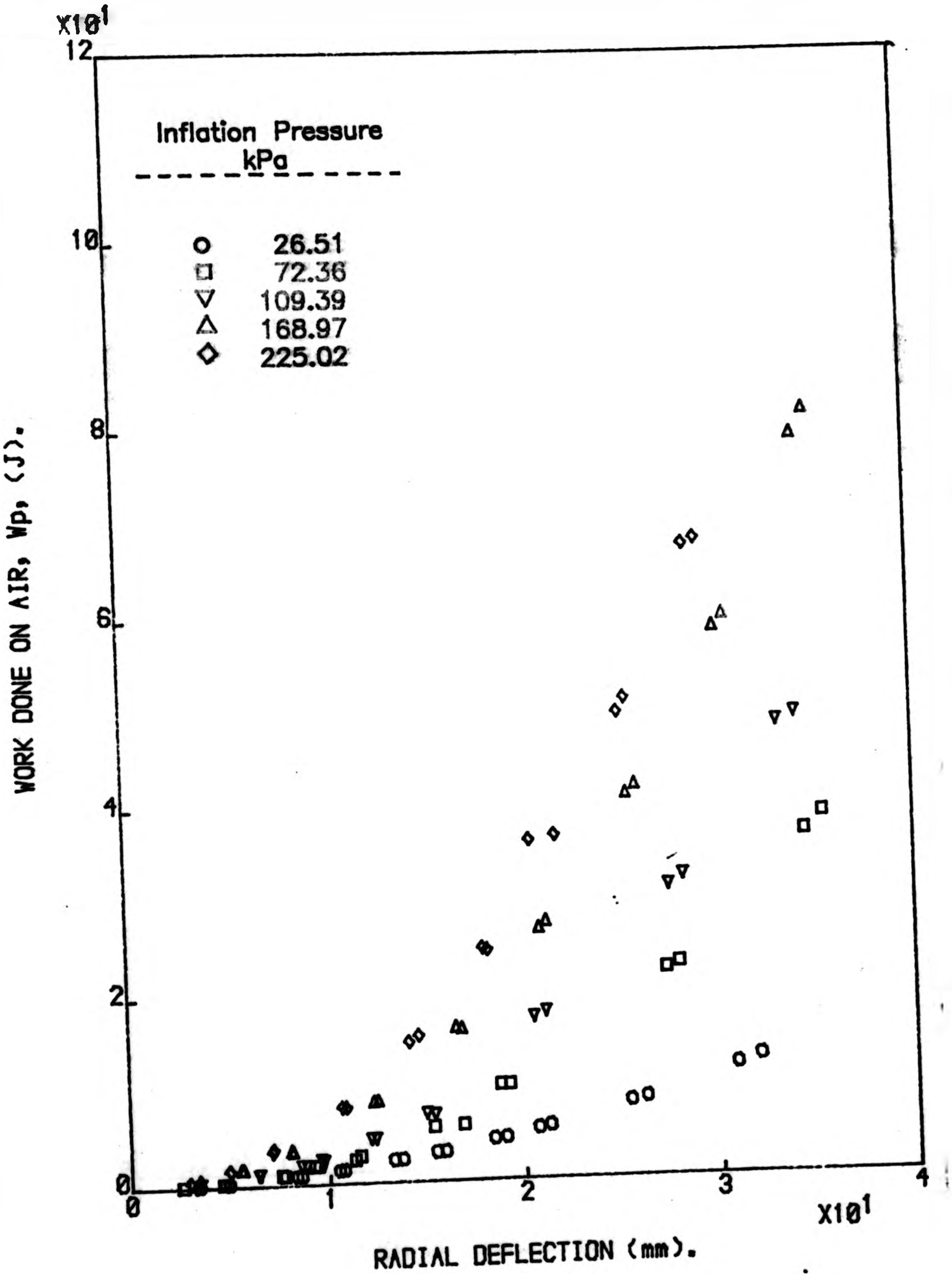

Fig. 6.14. Plot of work done on air against radial deflection for cross-ply tyre.

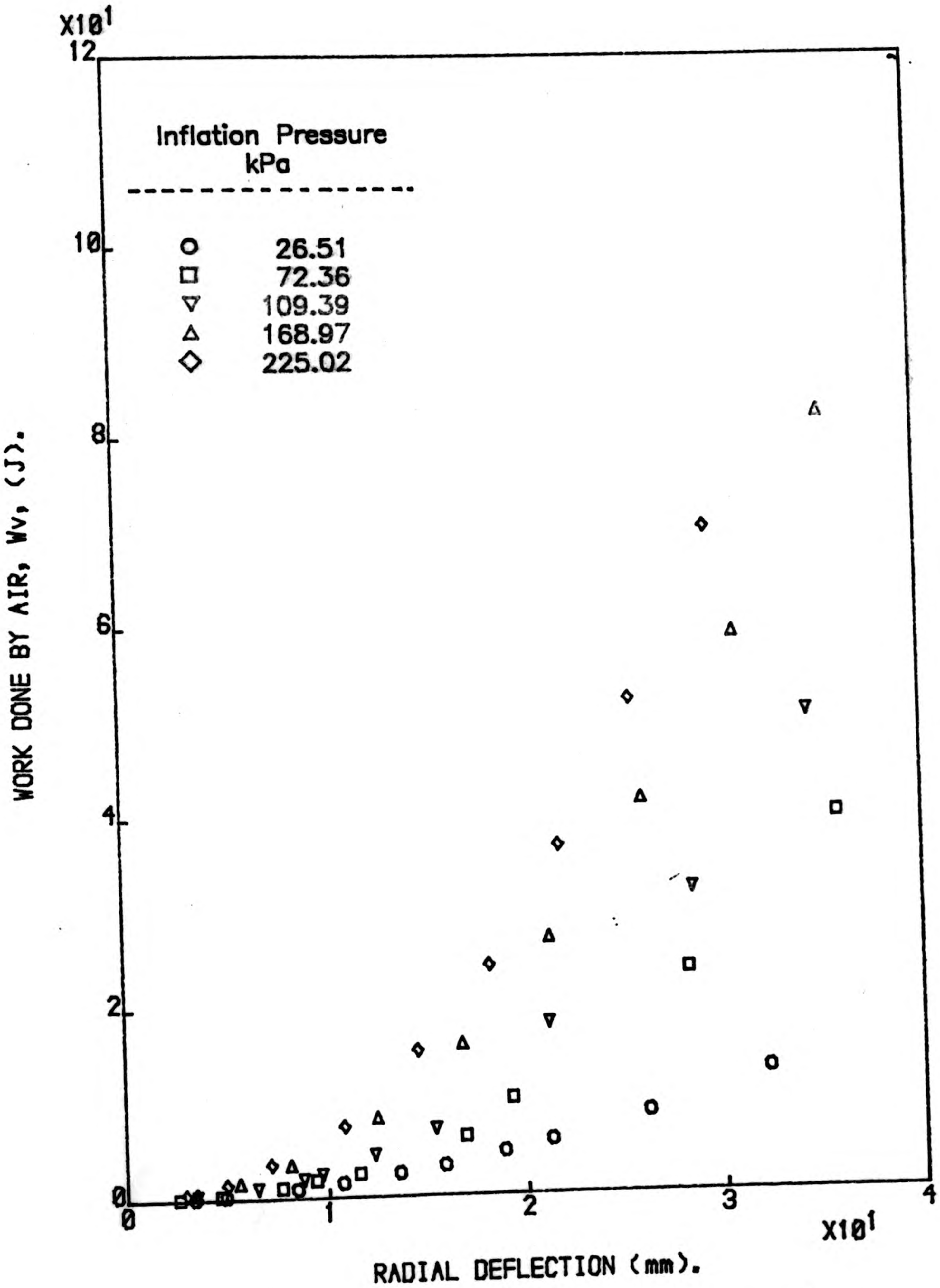

Fig. 6.15. Plot of work done by air against radial deflection for cross-ply tyre.

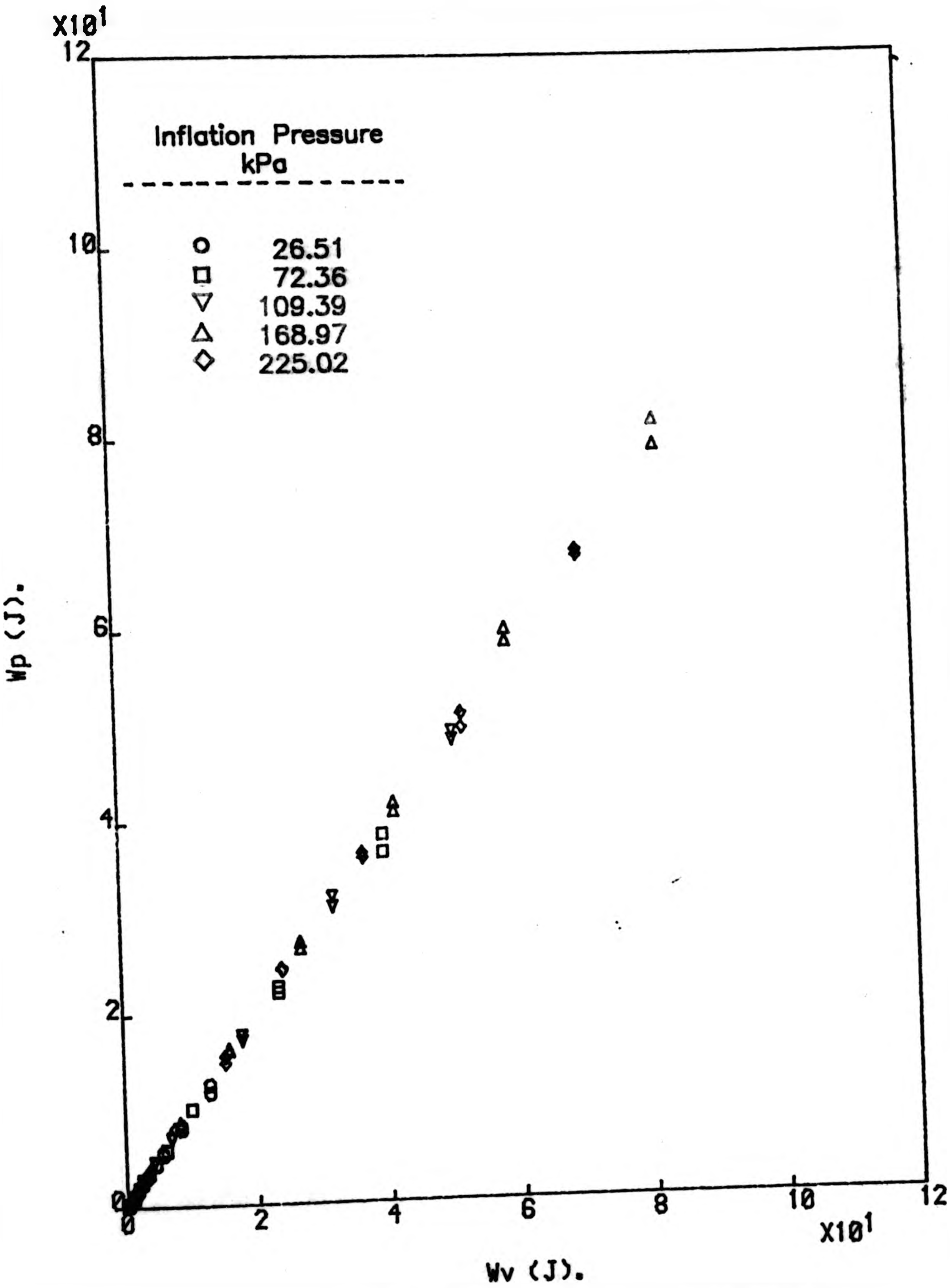

Fig. 6.16. Plot of work done on air against work done by air of a cross-ply tyre.

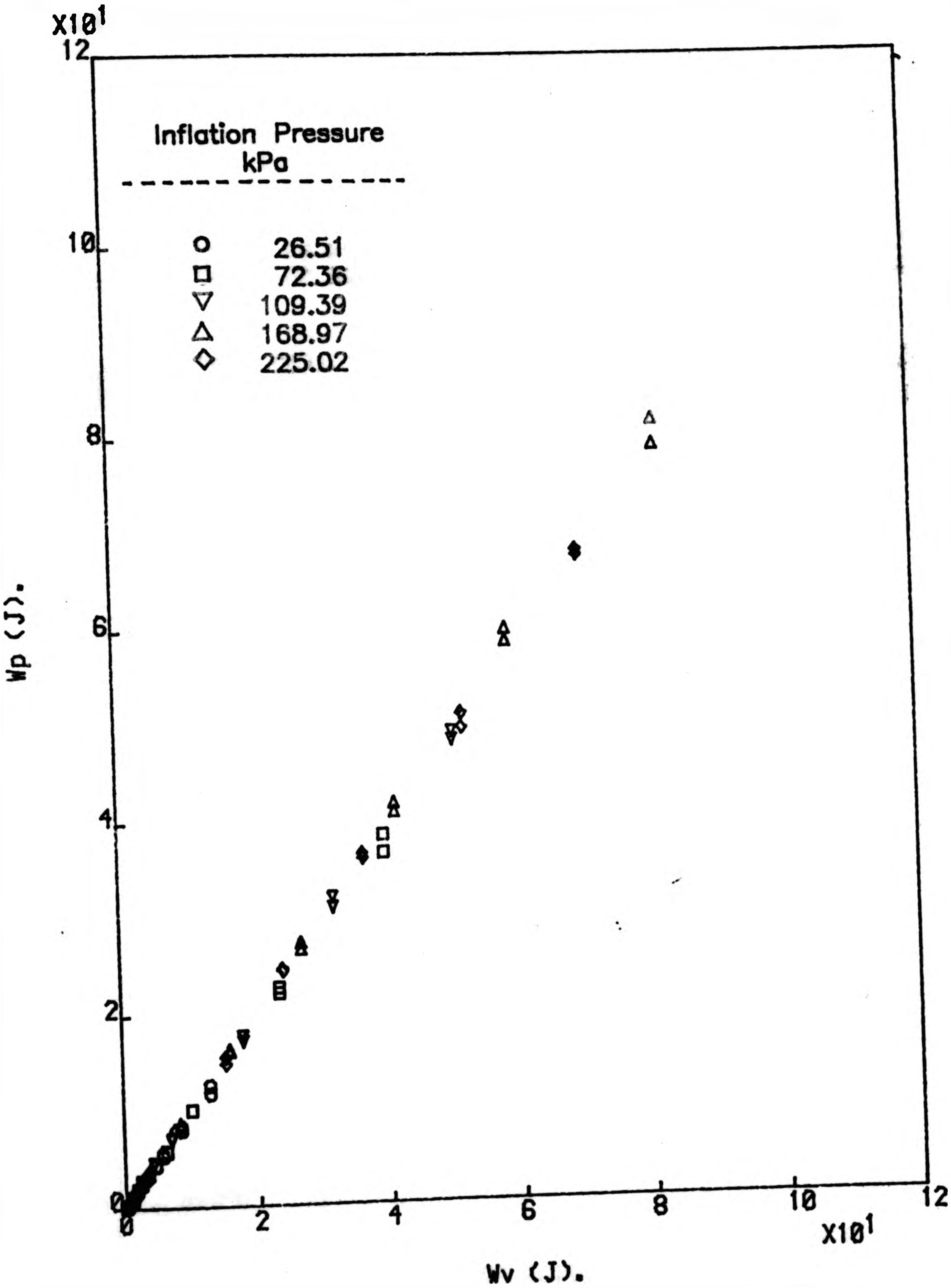

Fig. 6.16. Plot of work done on air against work done by air of a cross-ply tyre.

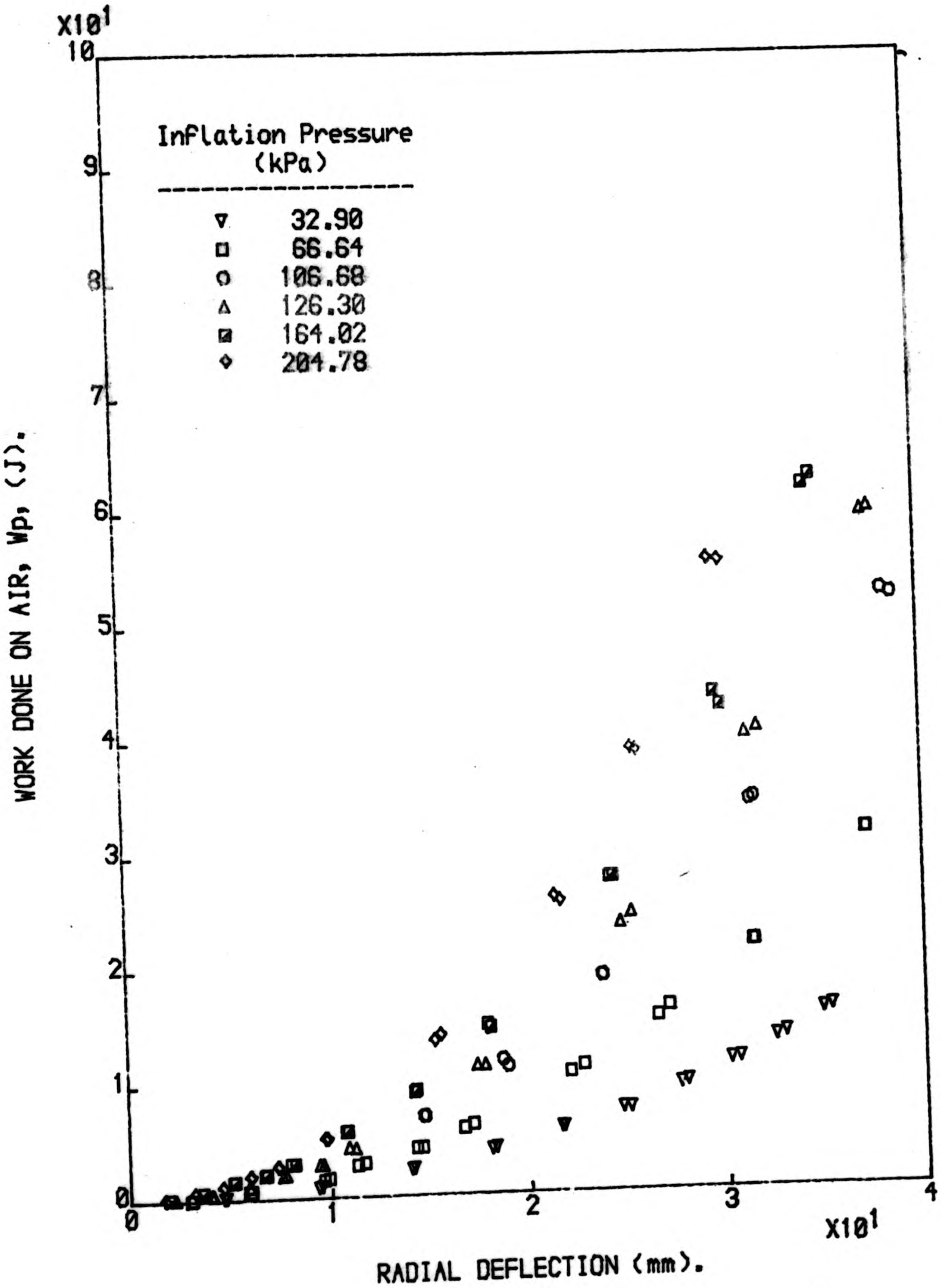

Fig. 6.17. Plot of work done on air against radial deflection for rayon-belted radial tyre.

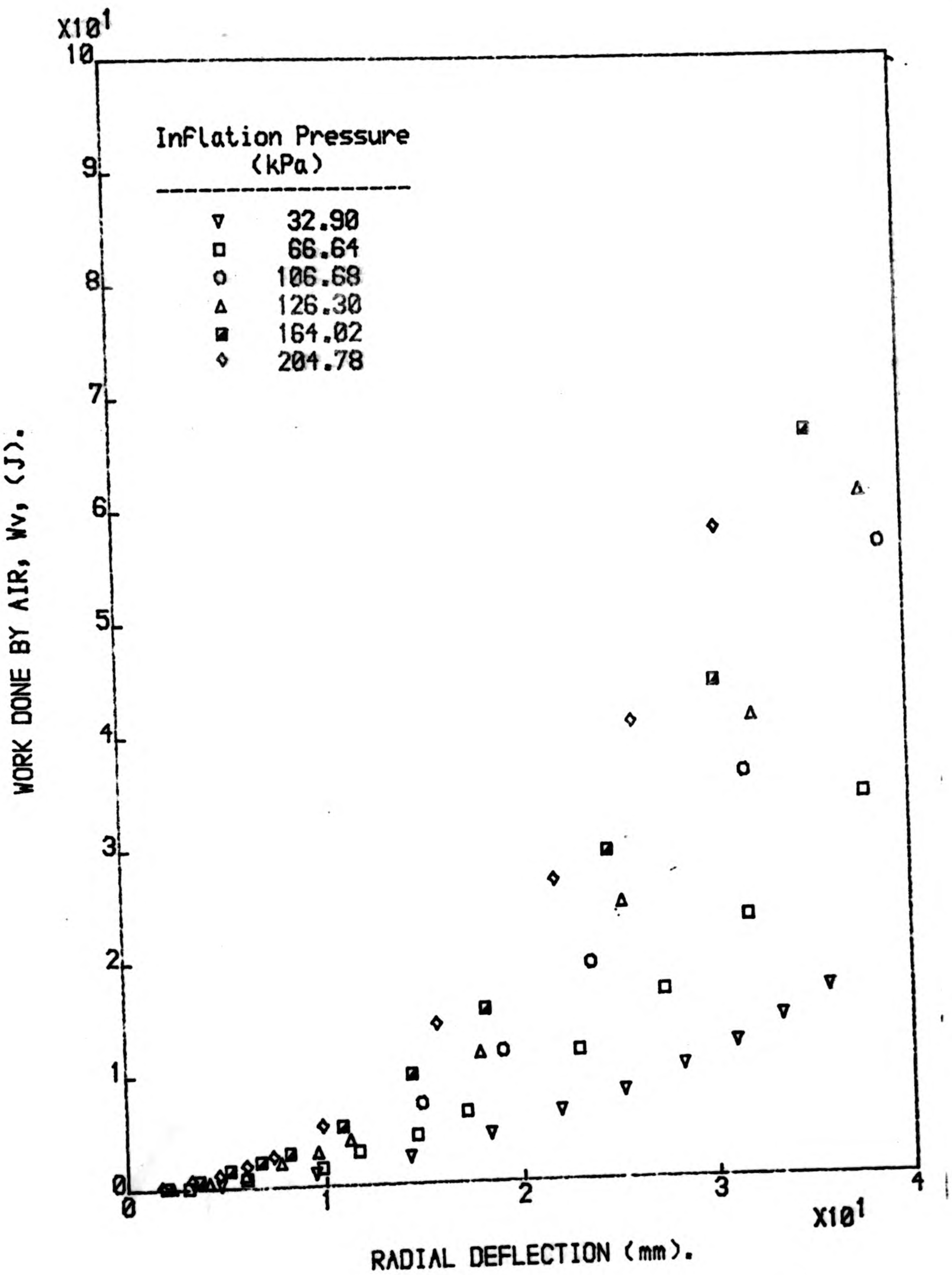

Fig. 6.18. Plot of work done by air against radial deflection for rayon-belted radial tyre.

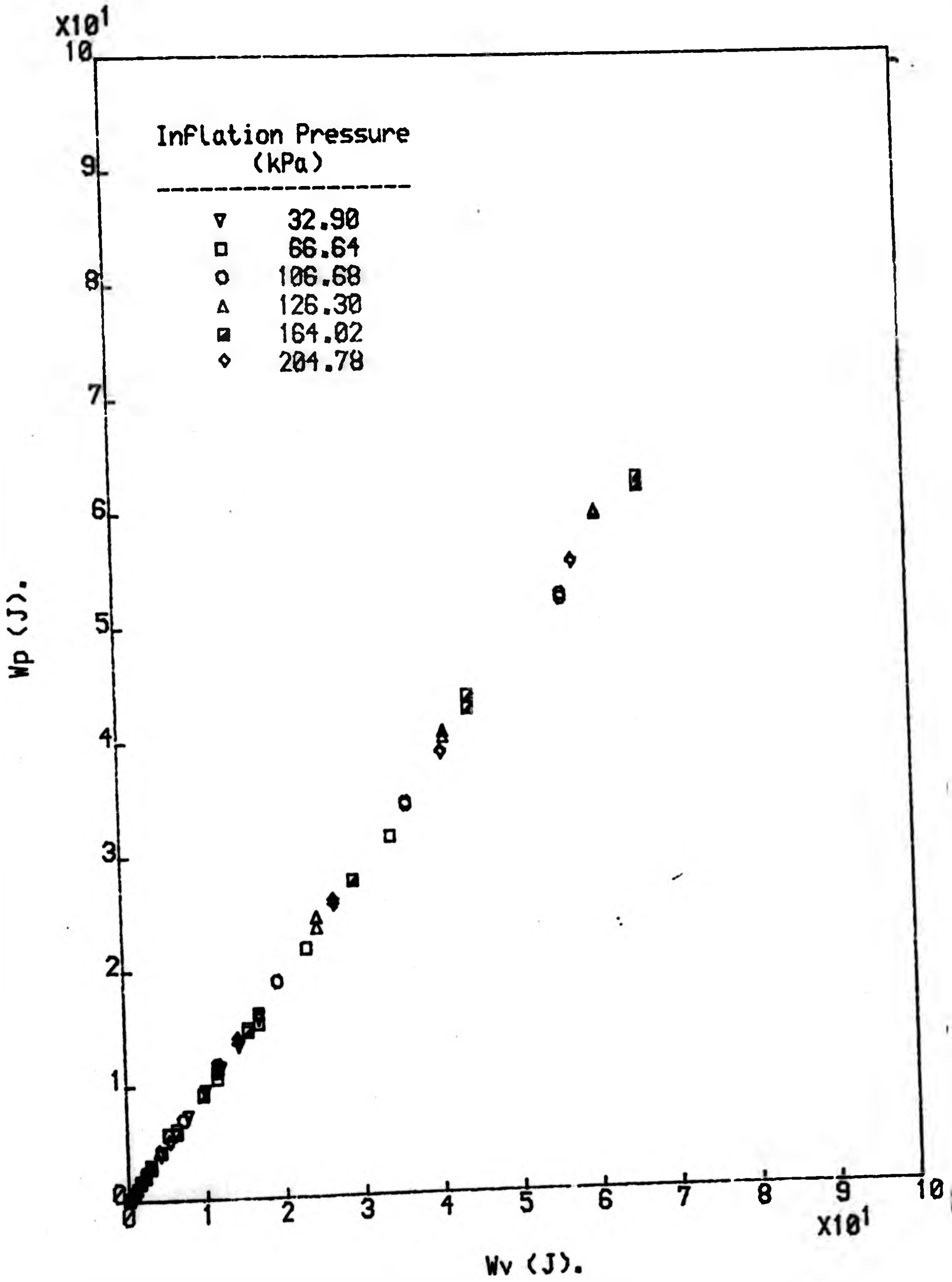

Fig. 6.19. Plot of work done on air against work done by air for a rayon-belted radial tyre.

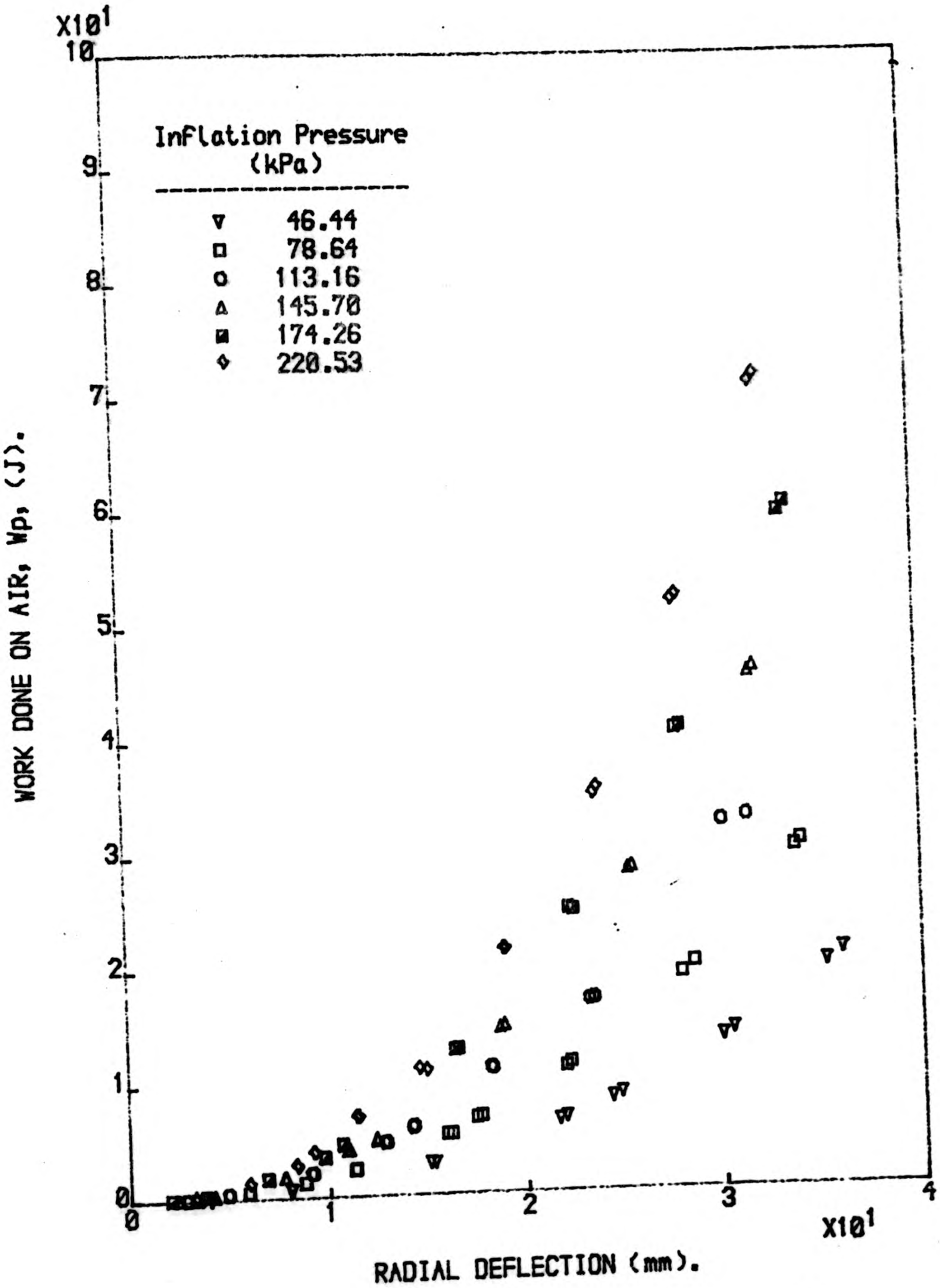

Fig. 6.20. Plot of work done on air against radial deflection for steel-belted radial tyre.

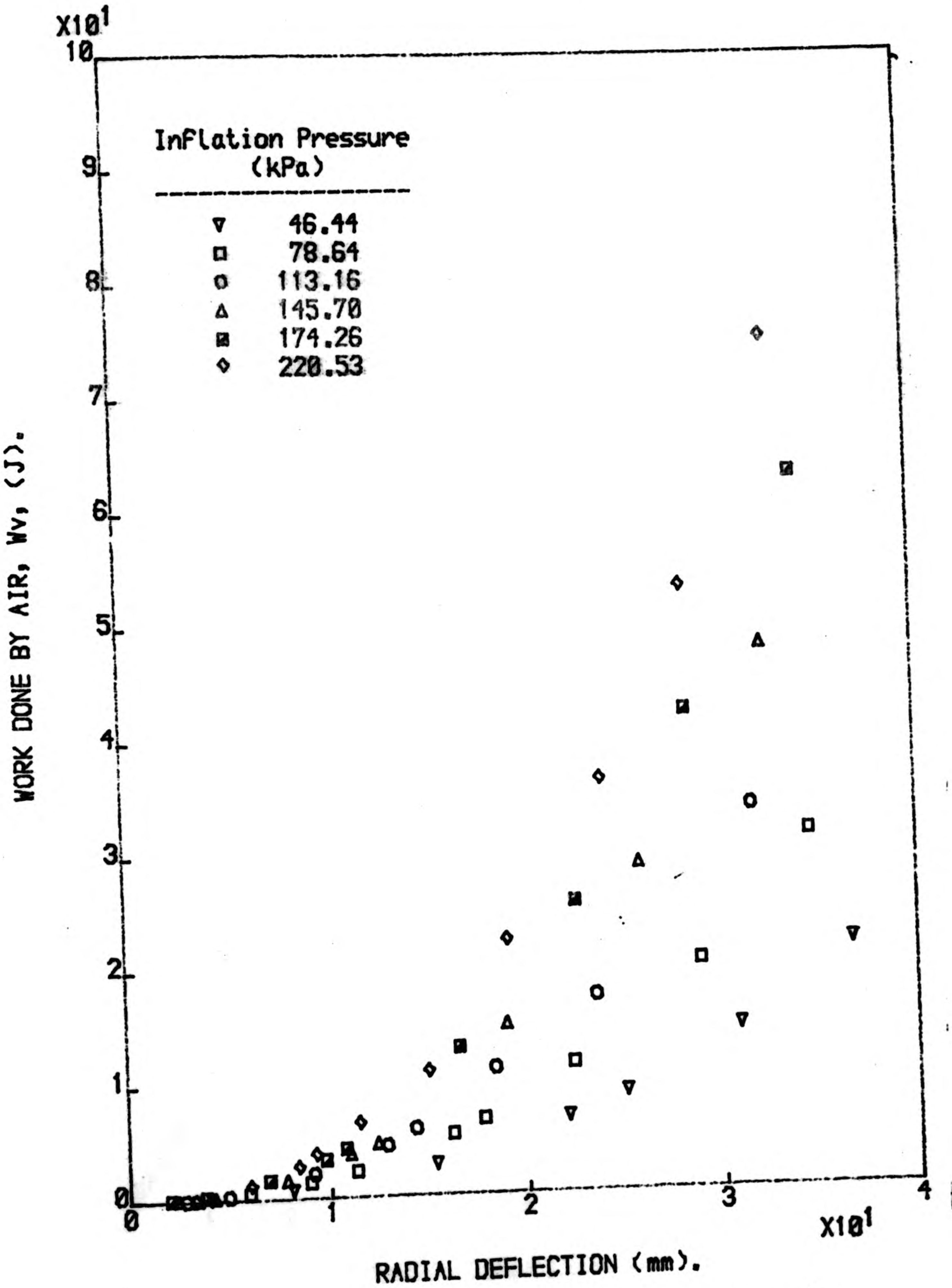

Fig.6.21. Plot of work done by air against radial deflection for steel-belted radial tyre.

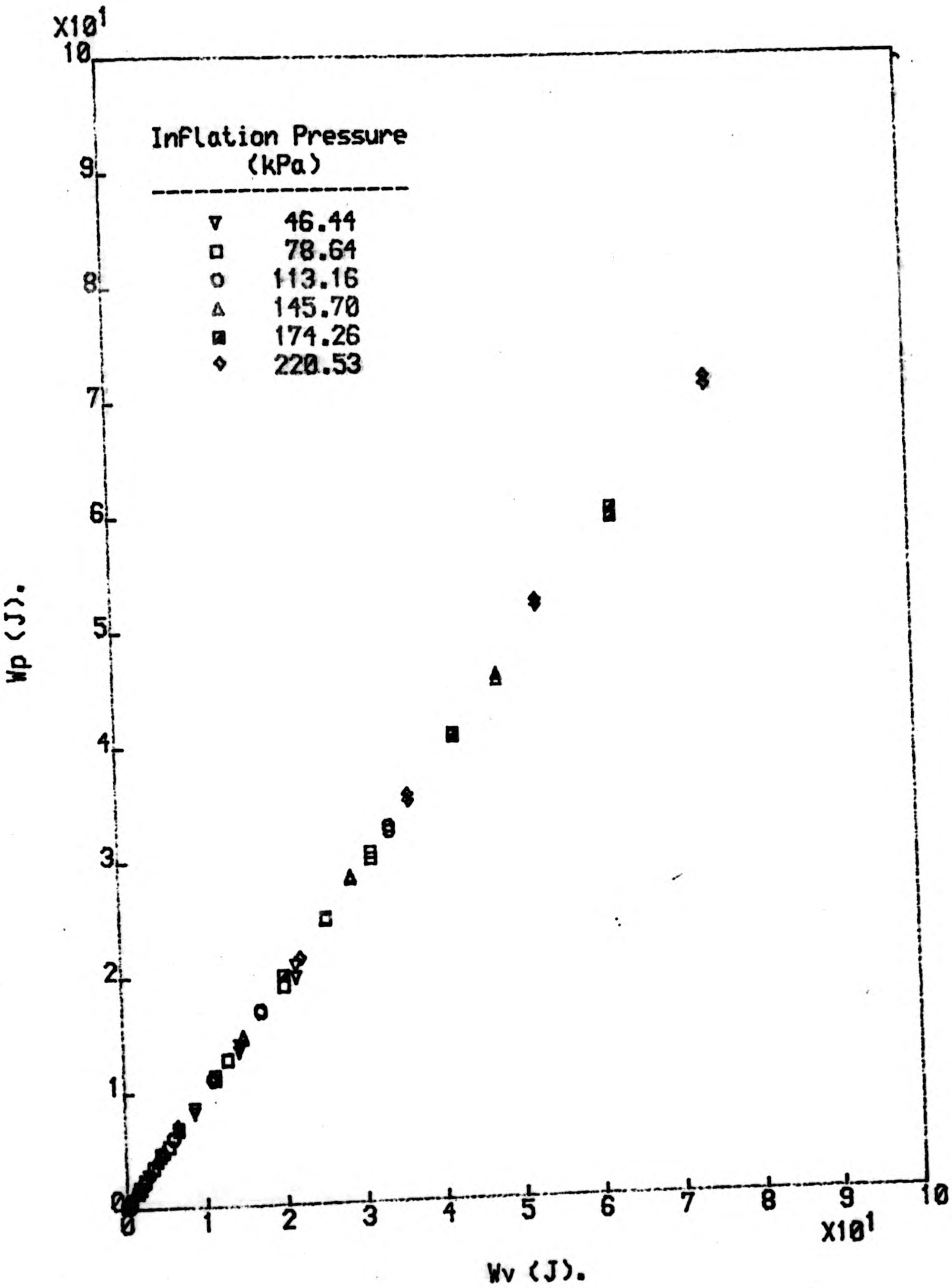

Fig. 6.22. Plot of work done on air against work done by air for a steel-belted radial tyre.

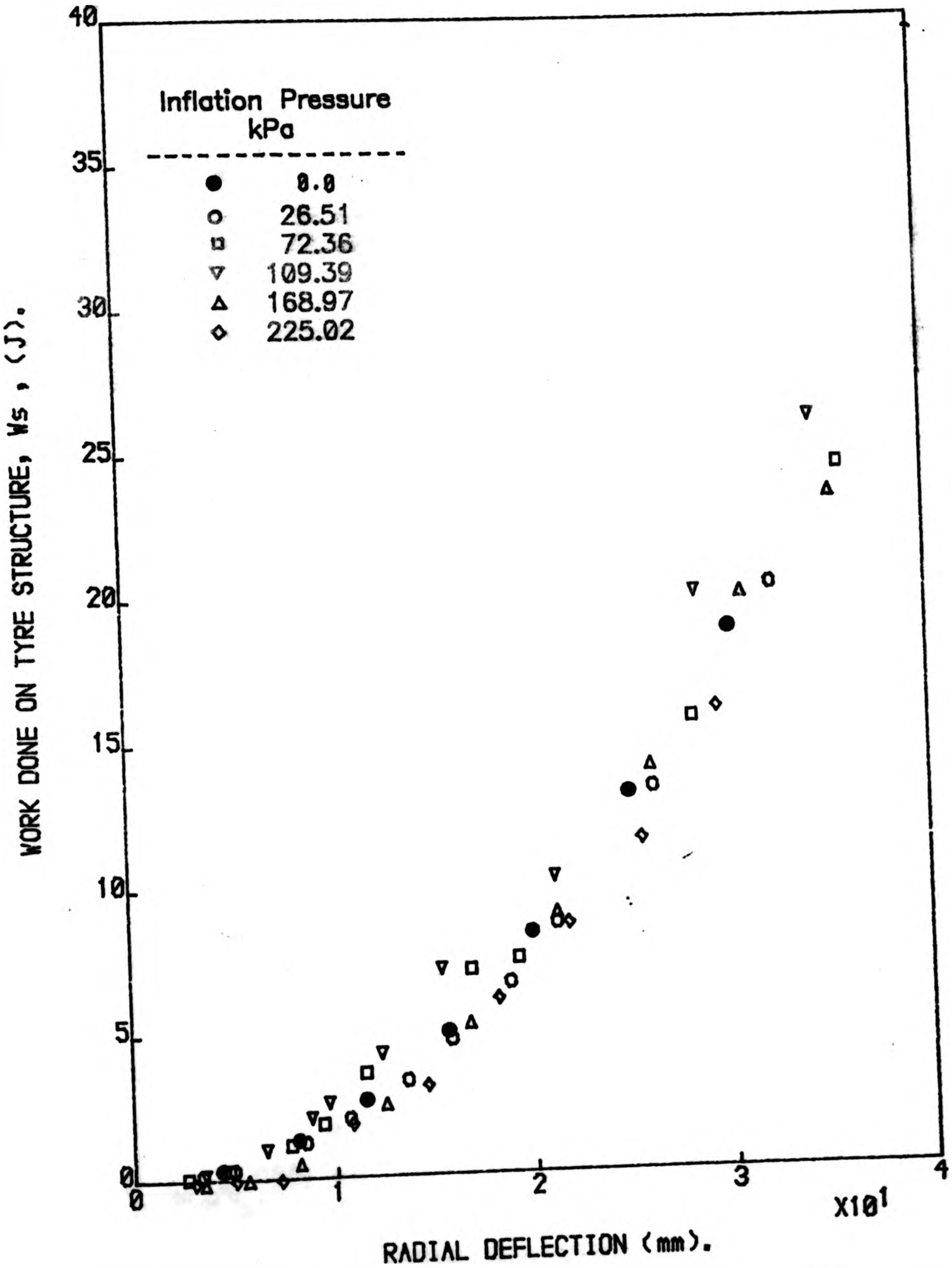

Fig. 6.23a. Plot of work done on tyre structure against radial deflection for cross-ply tyre.

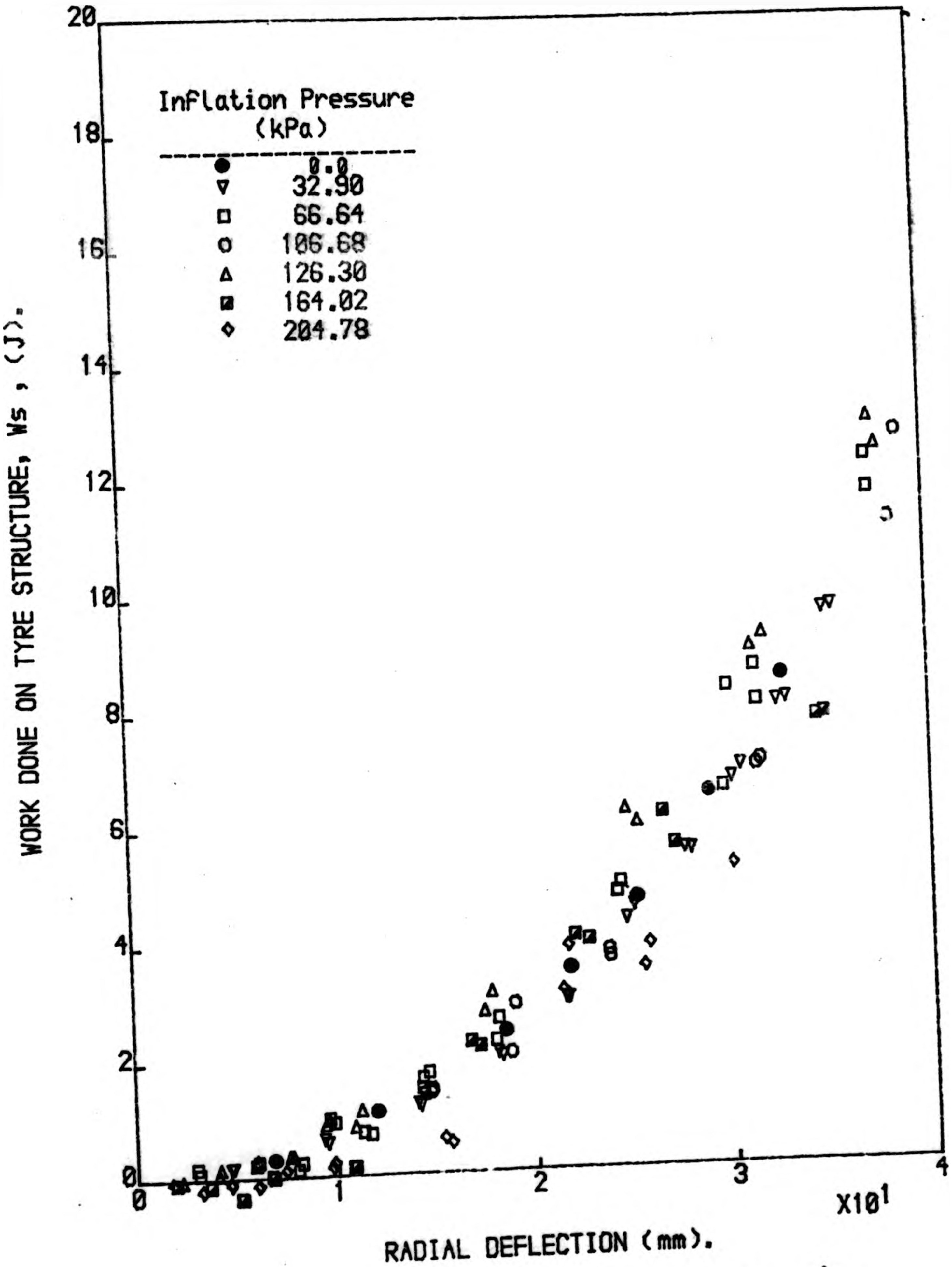

Fig. 6.23b. Plot of work done on tyre structure against radial deflection for rayon-belted radial tyre.

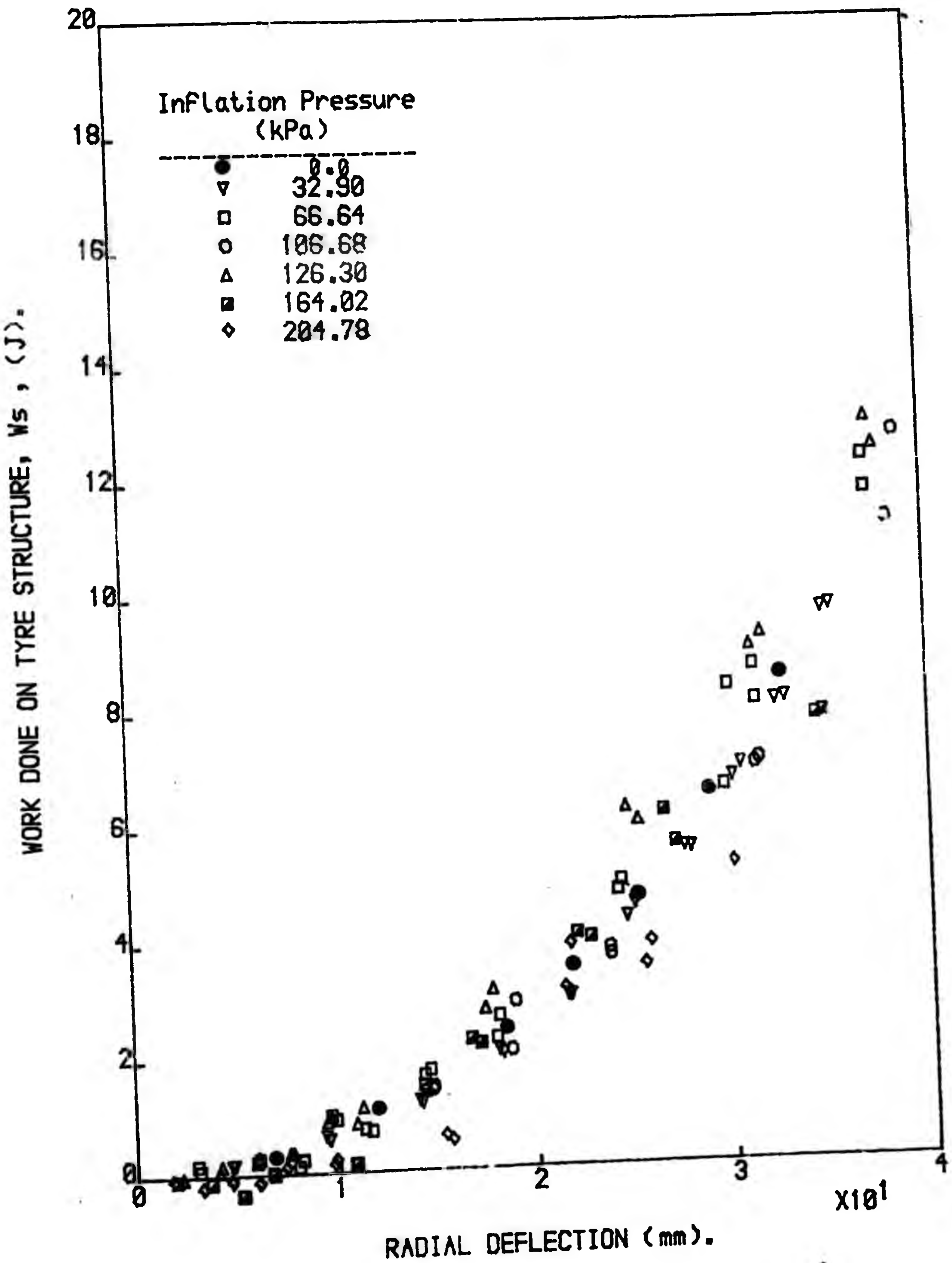

Fig. 6.23b. Plot of work done on tyre structure against radial deflection for rayon-belted radial tyre.

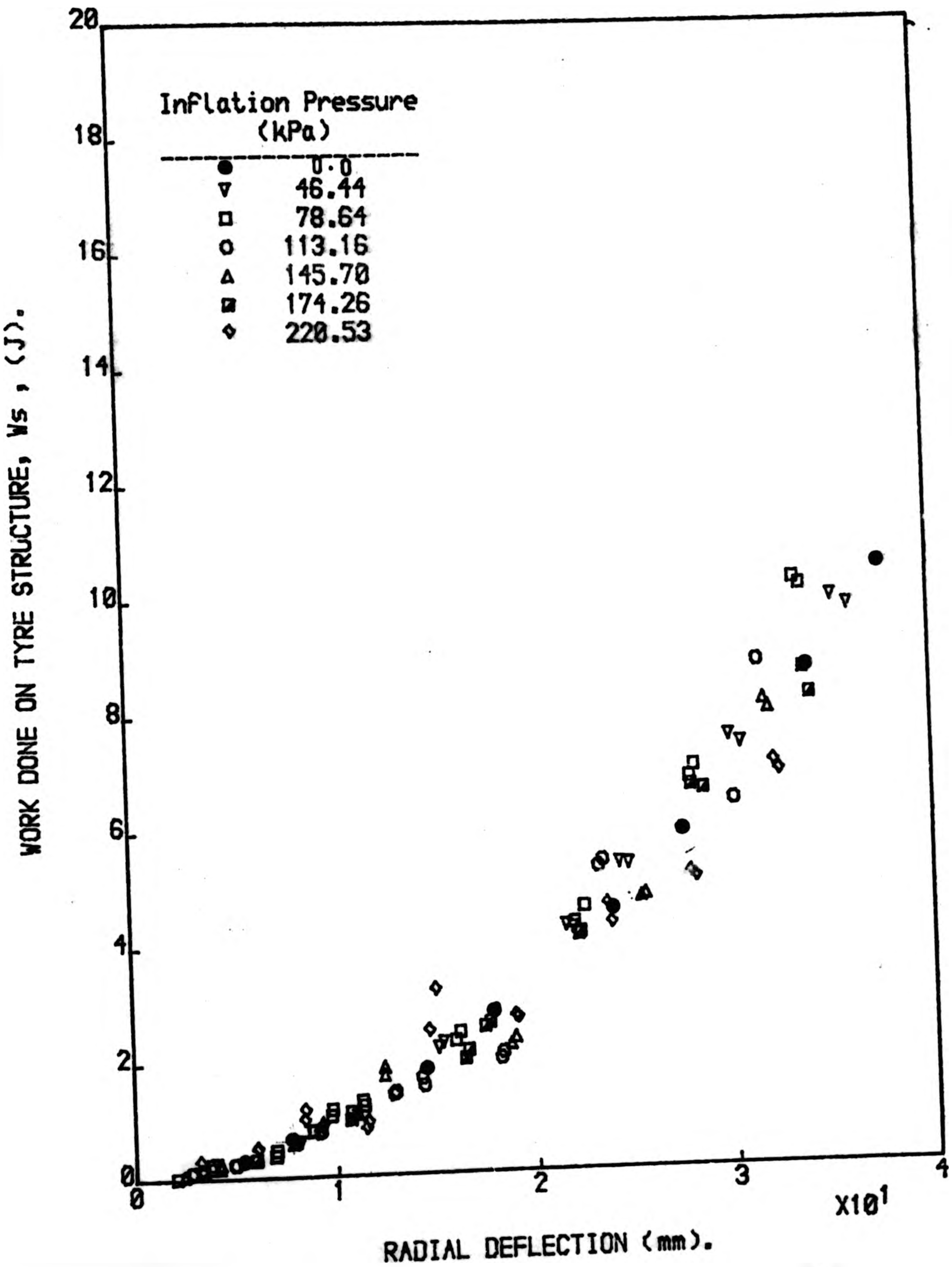

Fig. 6.23c. Plot of work done on tyre structure against radial deflection for steel-belted radial tyre.

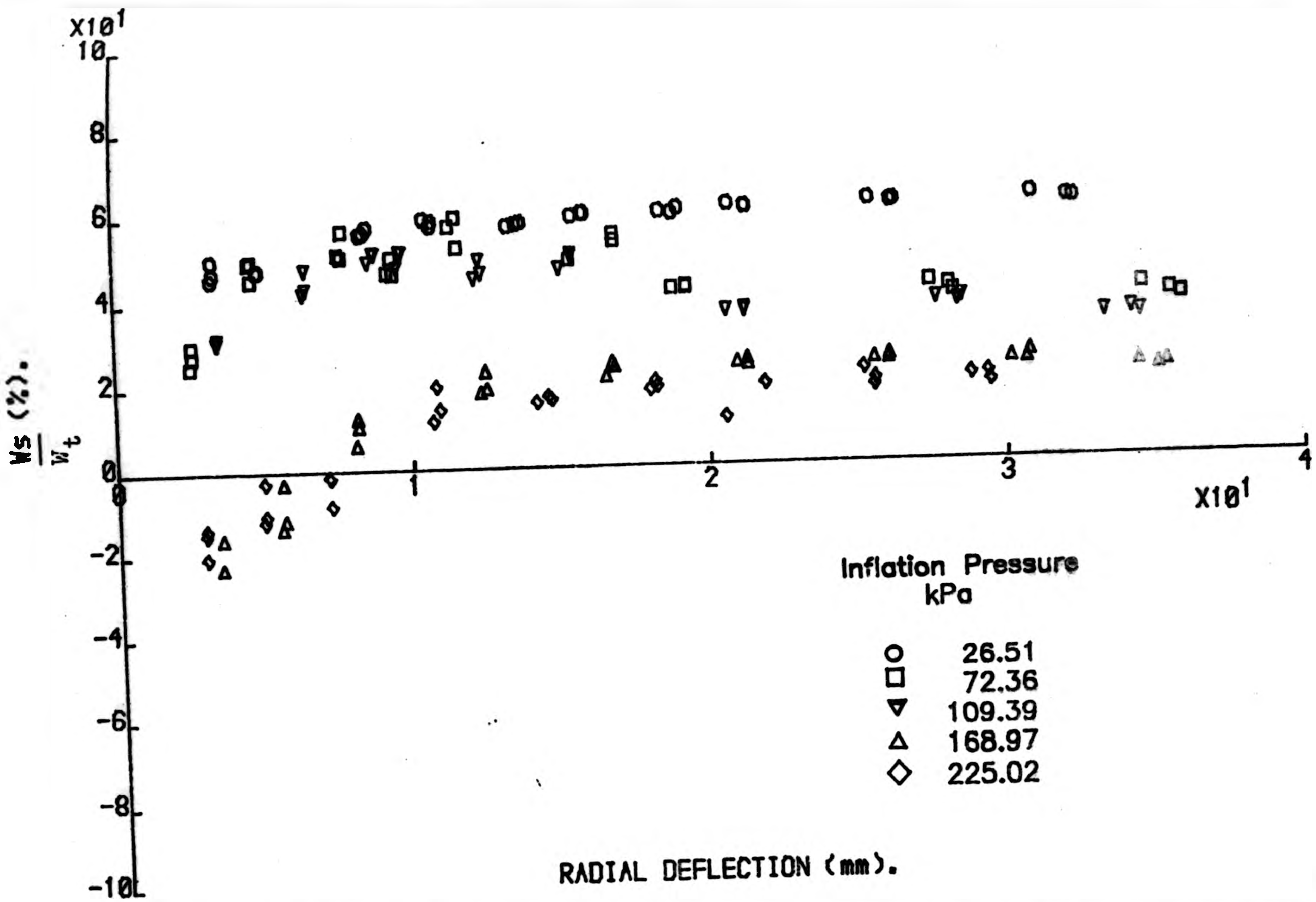

Fig. 6.24a. Plot of ratio of work done on structure to total work done against radial deflection for cross-ply tyre.

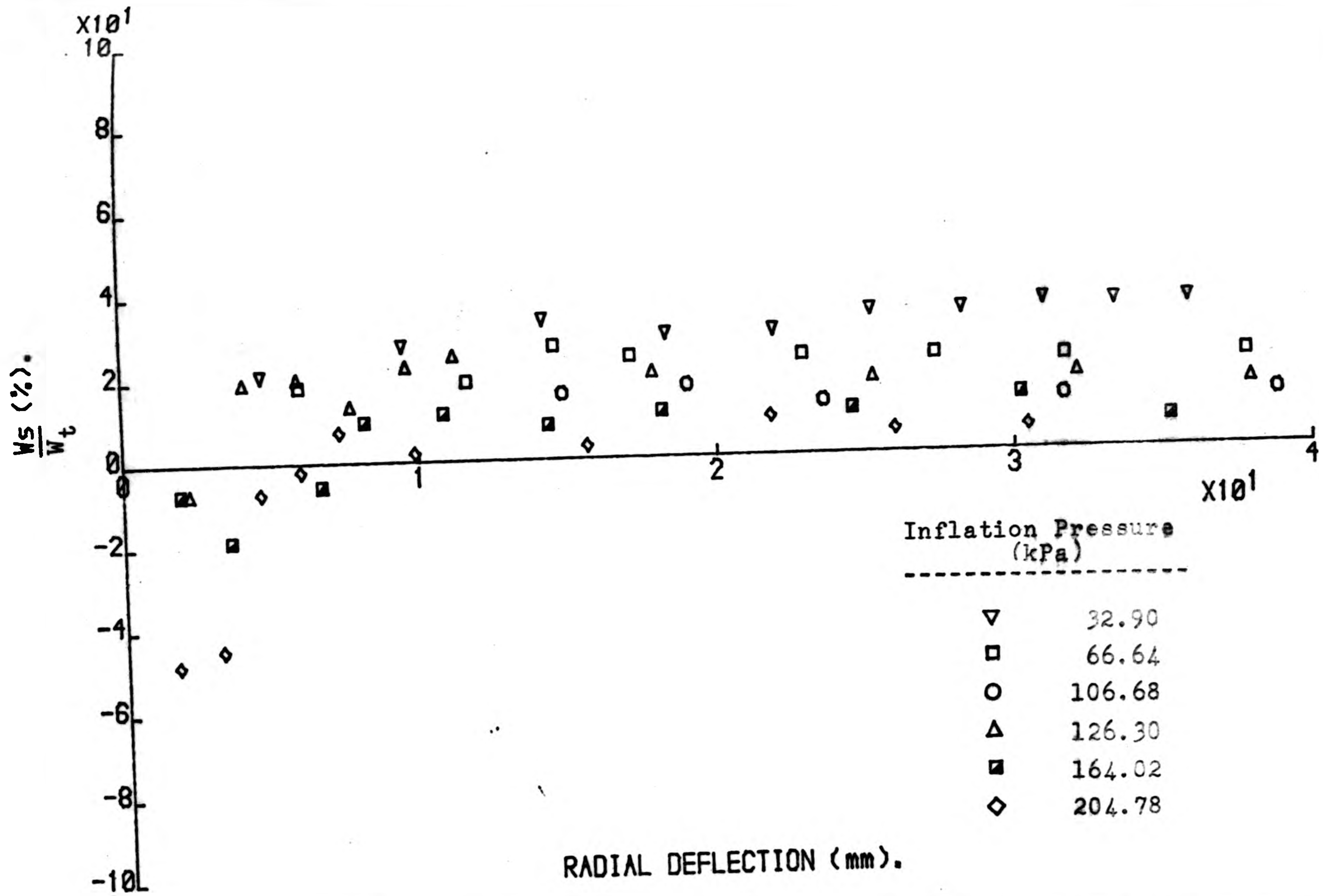

Fig. 6.24b. Plot of ratio of work done on structure to total work done against radial deflection for rayon-belted radial tyre.

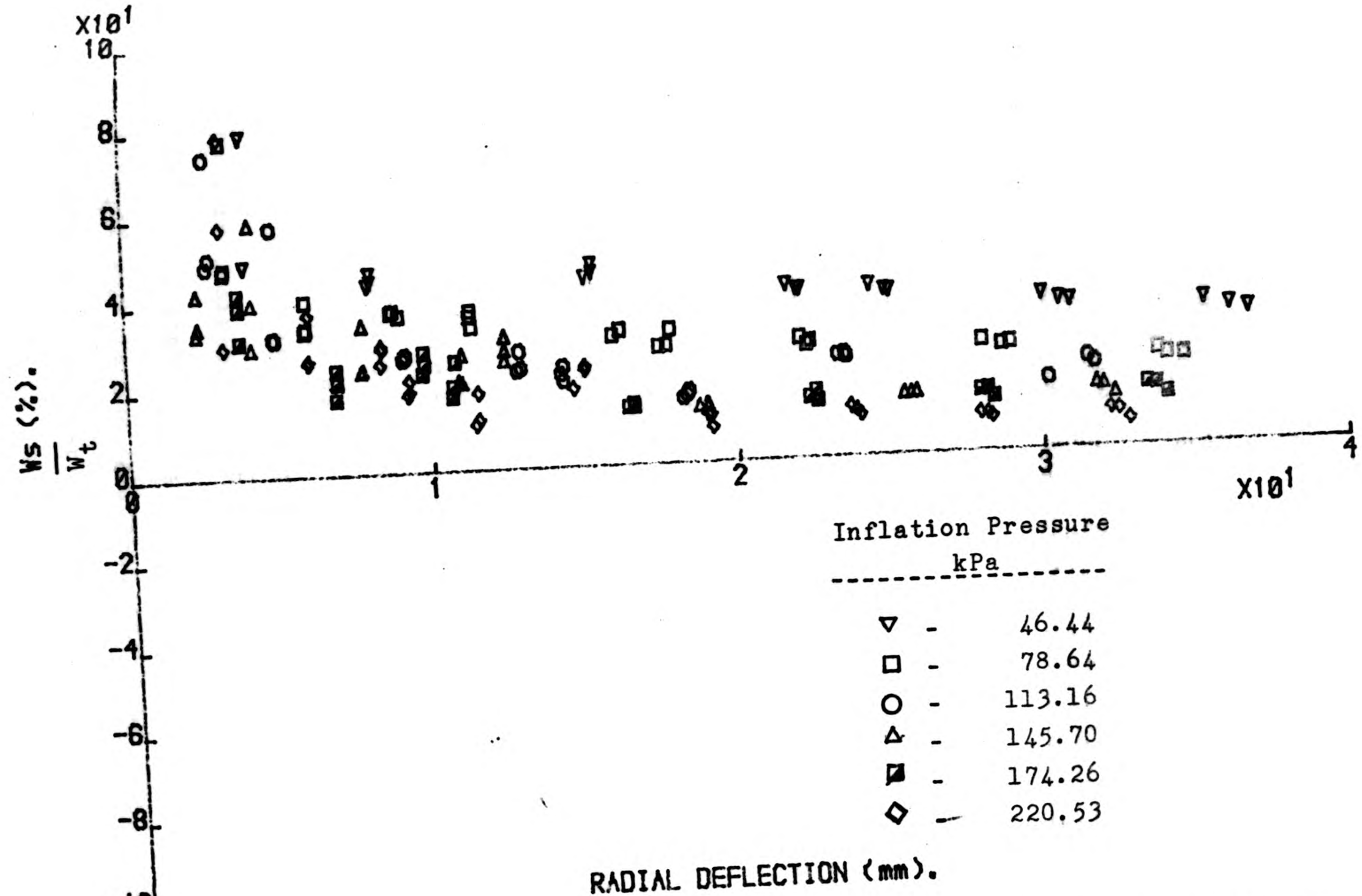

Fig. 6.24c. Plot of ratio of work done on structure to total work done against radial deflection for steel-belted radial tyre.

6.7. Discussions.

6.7.1. Apparatus and experimental techniques.

From the results obtained it can be said that the load-deflection and pressure-volume measuring apparatus performed very satisfatorily considering its simplicity. The accuracy in the measurement of the load on the tyre is estimated to be in the order of less than 1 percent and in the case of pressure-volume measurement the accuracy is in the order of 2 percent.

In the case of the load-deflection measuring apparatus, the accuracy in the calculation of the load-deflection characteristics of the tyre depends on the measured dimensional and calculated parameters and to some extent on the conditon in which the flat surface is applied onto the tyre.

One of the parameters involved is the coefficient of friction of the pivot bearing. The value of this parameter, μ_{pb}, as shown in Table 6.1. is relatively high. Reduction of this coefficient of friction will undoubtly be more desirable especially in the case of small loadins. One system that is thought to be most appropriate for this type of work is the 'knife-edge' fulcrum, commonly used in balances. However, changing from the present pivot bearing system would require significant rebuilding of the apparatus. To avoid this, the simple expedient of applying low frequency vibration to the pivot bearing was employed. This was achieved by placing a rather noisy vacuum pump directly on the apparatus frame under the pivot bearing. It was found that a significant improvement is obtained by the use of this method.

The manner in which the flat loading plate is applied onto the tyre is important because of the possibility of friction between the tyre and the flat plate. During the course of the loading process care must be taken to ensure that the flat plate is applied horizontally at all times to minimise the shearing effect in the tyre. The friction between the flat surface and the tyre has an effect on the load-deflection behaviour of the tyre. Charrier (1) reported that load-deflection behaviour of a membrane loaded between two plates is dependent upon the restraints in the contact surfaces. Increase in the friction between the membrane and the flat plates surfaces will cause an increase in the stiffness of the membrane. Similar observation was reported by Walter(2) on actual tyres.

The performance of the pressure-volume measuring equipment is dependent upon the sensitivity and accuracy of the temperature control($\pm$ 0.1 C). In the present arrangement, the changes in the volume of the air is measured by a single expansion/compression column. Even though it has performed satisfactorily by the consistency of the result obtained, it would enhance the performance of this system if two volume measuring columns, one for measuring small changes in volume and the other for measuring large changes in volume, are used.

However, the major disadvantage or handicap with the present arrangement is that the amount of manual operations that have to be performed is rather laborious. It would be interesting if the operations could be carried out automatically, partially or full. This could be carried out by using pressure, load and displacement transducers and interfacing them with a microcomputer. Apart from reducing the number of manual operations in carrying out the procedures as detailed in Chapter 5 and the recording of the experimental data, it will also reduce the time consumed in analysing the data.

6.7.2. Effect of radial deflection on pressure rise and change in volume of the tyre.

The curves for the pressure rise ratio(i.e., the ratio of $\Delta p/P_{abs}$ against radial deflection) are depicted in Figs. 6.9a, 6.9b and 6.9c for the cross-ply tyre, rayon-belted radial and steel-belted radial tyres respectively. It is interesting to note that all the points on these graphs are coincident with the exception of the cross-ply tyre at very low inflation pressures. Hence, the points can be fitted to a single master curve. This implies that the pressure rise ratio is only dependent upon the radial deflection of the tyre. Another interesting feature of the curves is that there are differences in the amount of scatter of points shown by the radial and the cross-ply tyres. There is less scatter in the radial tyres especially in the steel-belted radial tyre. Since the scatter of points in the cross-ply tyre and the rayon-belted tyre is not at random and have a definite trend, it indicates that some form of physical change to the tyre structure is taking place. One of the plausible reason is the increase in the volume of tyre with increase in the internal pressure. Assuming that the volume of these tyres at low inflation pressure is comparatively smaller than when it is highly inflated, then for the same deflection the percentage decrease in volume is larger at low inflation pressure. Correspondingly the increase in pressure will be bigger. The experimental points in Figs. 6.10a and 6.10b support the above argument.

6.7.3. Load-deflection characteristics of tyre.

As mentioned in Chapter 2, the mechanism of load transmission from the contact patch to the tyre axle is very complex. However, it is of particular interest to study the amount of force transmitted through the contact patch by the tyre structure. This can be achieved by the determination of the inflation pressure at which zero tyre to ground contact pressure occurs, i.e., when there is no external load to the tyre. There are two methods whereby this can be determined, graphical and analytical. In the analytical method, the load-deflection characteristics are analysed by regression analysis according to the relationship(3),

$$L = (A + B.P)\,Z^{n} \qquad \text{...........(6.1)}$$

where L = radial load, N

P = inflation pressure, kPa

Z = radial deflection, mm

n = exponent depending on tyre construction

From the analysis of the experimental load-deflection data, the following relationship are obtained:

For the cross-ply tyre:

$$L = (26.49 + 0.3144\,P)\,Z^{1.25} \qquad \text{........(6.1a)}$$

For the rayon-belted radial tyre:

$$L = (15.95 + 0.3741\,P)\,Z^{1.1375} \qquad \text{.........(6.1b)}$$

For the steel-belted radial tyre:

$$L = (13.21 + 0.3321\ P)\ Z^{1.175} \qquad ....(6.1c)$$

By setting L=0 in Equations 6.1a, 6.1b and 6.1c, the zero tyre to ground contact pressure occurs at hypothetical inflation pressures of -82.26, -42.64 and -39.78 kPa for the cross-ply, rayon-belted radial and steel-belted radial tyres respectively. Thus, the casing stiffness of the cross-ply , rayon-belted radial and steel-belted radial tyres transmit a force through the contact patch an equivalent to an inflation pressures of 82.26, 42.64 and 39.78 kPa respectively. It is interesting to note that, within the limits of experimental error, there is no significant difference in the casing stiffness between the radial tyres having different belt materials.

6.7.4. Work done on the tyre structure.

The work done on the tyre structure is dependent upon the design of the tyre and on the stiffness of the tread band and sidewalls. At low deflection bending of the tread is dominant and at high deflection bending of the sidewalls is dominant.

Normally, when a tyre is inflated there is a tendency for the tyre to conform to a more circular cross-

For the steel-belted radial tyre:

$$L = (13.21 + 0.3321 P)\, Z^{1.175} \qquad ....(6.1c)$$

By setting L=0 in Equations 6.1a, 6.1b and 6.1c, the zero tyre to ground contact pressure occurs at hypothetical inflation pressures of -82.26, -42.64 and -39.78 kPa for the cross-ply, rayon-belted radial and steel-belted radial tyres respectively. Thus, the casing stiffness of the cross-ply , rayon-belted radial and steel-belted radial tyres transmit a force through the contact patch an equivalent to an inflation pressures of 82.26, 42.64 and 39.78 kPa respectively. It is interesting to note that, within the limits of experimental error, there is no significant difference in the casing stiffness between the radial tyres having different belt materials.

6.7.4. Work done on the tyre structure.

The work done on the tyre structure is dependent upon the design of the tyre and on the stiffness of the tread band and sidewalls. At low deflection bending of the tread is dominant and at high deflection bending of the sidewalls is dominant.

Normally, when a tyre is inflated there is a tendency for the tyre to conform to a more circular cross-sectional shape. This is because the increased sidewall tension tends to pull the edges of the breaker or belt assembly inwards toward the tyre beads while the inflation pressure pushes the centre of the breaker or belt assembly outwards. This tendency to change shape is dependent upon the restraint of the breaker or belt assembly to bending moment about the circumferential centre line.

In the case of the cross-ply tyre and rayon-belted radial tyre, there is an increase in the width of the tyre and also in the height of the tyre at the centre of the tread band along the circumferential line with increase in inflation pressure. In other words, there is an increase in the curvature of the tread and also in the sidewalls. Hence, at low deflection most of the work done on the tyre will corresponds to flattening or straightening of the tread surface. Thus as a consequence of this , most of the work done in the early stages of loading will be that of compressing the air in the tyre. Also in flattening the tread, some of the energy is being released. This phenomena is depicted in Figs. 6.24a and 6.24b.

However, in the case of steel-belted radial tyre because of its stiff tread band due to the presence of the steel belt, there is little change in the curvature of the tread curvature as a result of increase in inflation pressure. Thus in the early stages of deflection, most of the work done on the tyre will be that of a combination of the work done in compressing the tread band and that of work done in deflecting the sidewalls. De Eskinazi et.al. (4) in his analysis of the stress resultants in the steel-belted tyre by the Finite Element Method, reported that reduction of the tyre bending stiffness has great influence in the magnitude of the meridian and circumferential stress resultant. This account for the difference in behaviour of the steel-belted radial tyre compared to the cross-ply tyre.

CHAPTER 7

AN ANALYSIS OF THE LOAD-DEFLECTION BEHAVIOUR OF A STATICALLY DEFLECTED PNEUMATIC TYRE.

As a first step towards an understanding of the behaviour of a pneumatic tyre under load, the tyre is modelled as consisting of a fexible and inextensible membrane with a stiff band around it circumference. The theory of air-spring developed by Gent and Thomas (1) will be used in this analysis. Similar treatment have been carried out by Yamagishi and Jenkins (2) in their analysis of the contact pressures of tyre. However, the approach taken here is slightly different and the treatment is further simplified.

Basically, the model is developed based on the assumption that the flexible and inextensible membrane takes up a circular arch of radius, r, and support a tension, t = pr, per unit length. Further the air contained is assumed to obey Boyle's Law and that the process of deformation takes place isothermally.

The compressive load, F, on a thin segment as shown in Fig. 7.1 is given by the relationship (1),

$$\frac{F}{2pw} = \left(1 - \frac{s \cos\phi}{w\,\phi}\right) \qquad \ldots\ldots\ldots\ldots\ldots\ldots (7.1)$$

and $\frac{h}{s} = \frac{\sin \phi}{\phi}$ .... (7.2)

where p = the inflation pressure

s = contour length between plate edge and horizontal normal to the membrane.

h = the height between the plate and the horizontal normal to the membrane.

w = plate half-width

ϕ = angle substended by the membrane contour distance s.

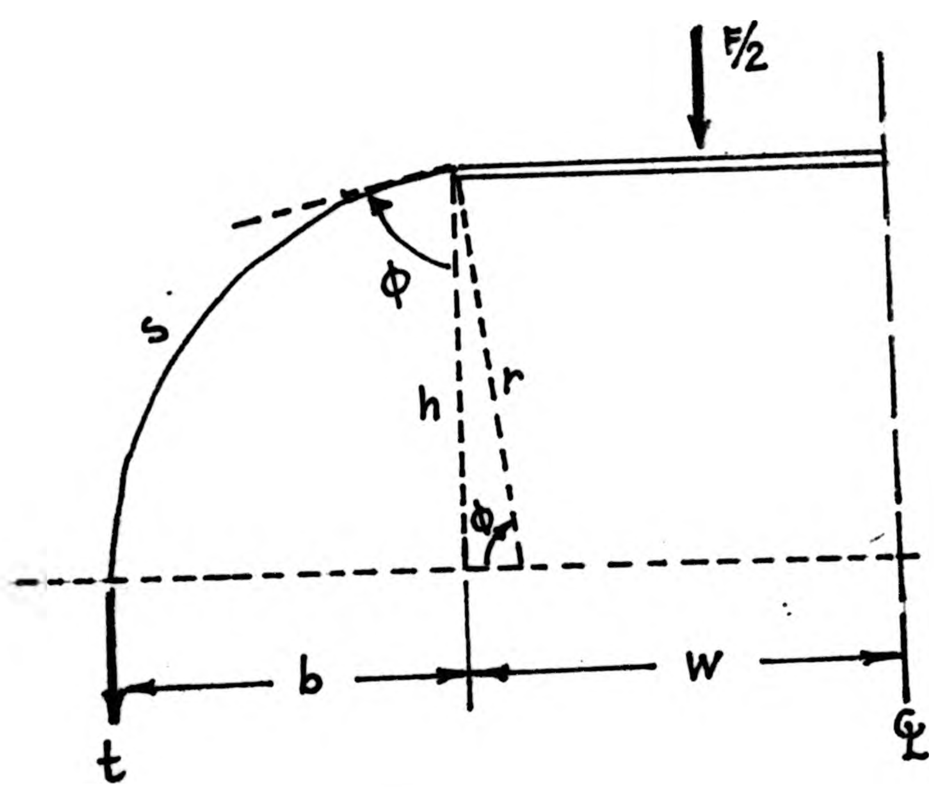

Fig. 7.1. Geometry of the thin segment under the action of compressive load.

From Fig.(7.1), it can be easily derived that the volume per unit length, V, of the segment at arbitrary deflection is ,

$$\frac{V}{4ws} = \{2 \sin \phi + \frac{s}{w}(2\phi - \sin 2\phi)\} / 2\phi \quad \ldots(7.3)$$

and the initial volume of the segment, V_o, corresponding to F = 0 in Equation (7.1) is given by the relationship,

$$\frac{V_o}{4ws} = (\sin\phi_o + \frac{s}{w})/2\phi_o \quad \ldots\ldots\ldots\ldots\ldots\ldots(7.4)$$

where $\phi_o = \arccos \frac{w\phi_o}{s}$

Since the air contained in this segment is assumed to obey Boyle's law and that the compression takes place isothermally, the pressure of the air at arbitrary deflection is given by the relationship,

$$\frac{P}{P_o} = \frac{V_o}{V} = \frac{(\sin\phi_o + \frac{s}{w})/\phi_o}{\{2\sin\phi + \frac{s}{w}(2\phi - \sin 2\phi)\}/\phi} \quad \ldots\ldots\ldots\ldots\ldots\ldots(7.5)$$

Subtituting the value of P in Equation (7.5) into Equation (7.1) and rearranging, gives

$$F = 2P_o w\left(1 - \frac{s}{w}\frac{\cos \phi}{\phi}\right) \frac{(\sin \phi_o + \frac{s}{w})/\phi_o}{\{2\sin\phi + \frac{s}{w}(2\phi - \sin 2\phi)\} / \phi}$$

.........(7.6)

Equation (7.6) constitutes the load supported by a single segment and this is governed by the parametric angle ϕ, which itself is a function of the deflection.

If the tyre contact length is 2a and the deflection at the centre of the contact patch is z_o, then the relationship between a and z_o is given by the Equation (2.3) in p.28 is,

$$a = \sqrt{z_o(D_t - z_o)}$$

From Fig. 7.2. the deflection experience by the segment at a distance, x, from the centre of the contact patch is

$$z = \frac{(a-x)(a+x)}{\left\{\sqrt{\left(R_t\right)^2 - x^2} + R_t - z_o\right\}} \qquad \text{..........(7.7)}$$

If z_o is small compared to R_t, Equation (7.7) can be simplified to give z explicitly a function of x,

$$z = \frac{a^2 - x^2}{2\sqrt{R_t^2 - x^2}} \qquad \text{...........(7.8)}$$

If the contact length a is divided in N segments of thickness Δx, then the distance of the nth segment from the centre of the contact patch is,

$$x = (n-1)\,\Delta x + \frac{\Delta x}{2}$$

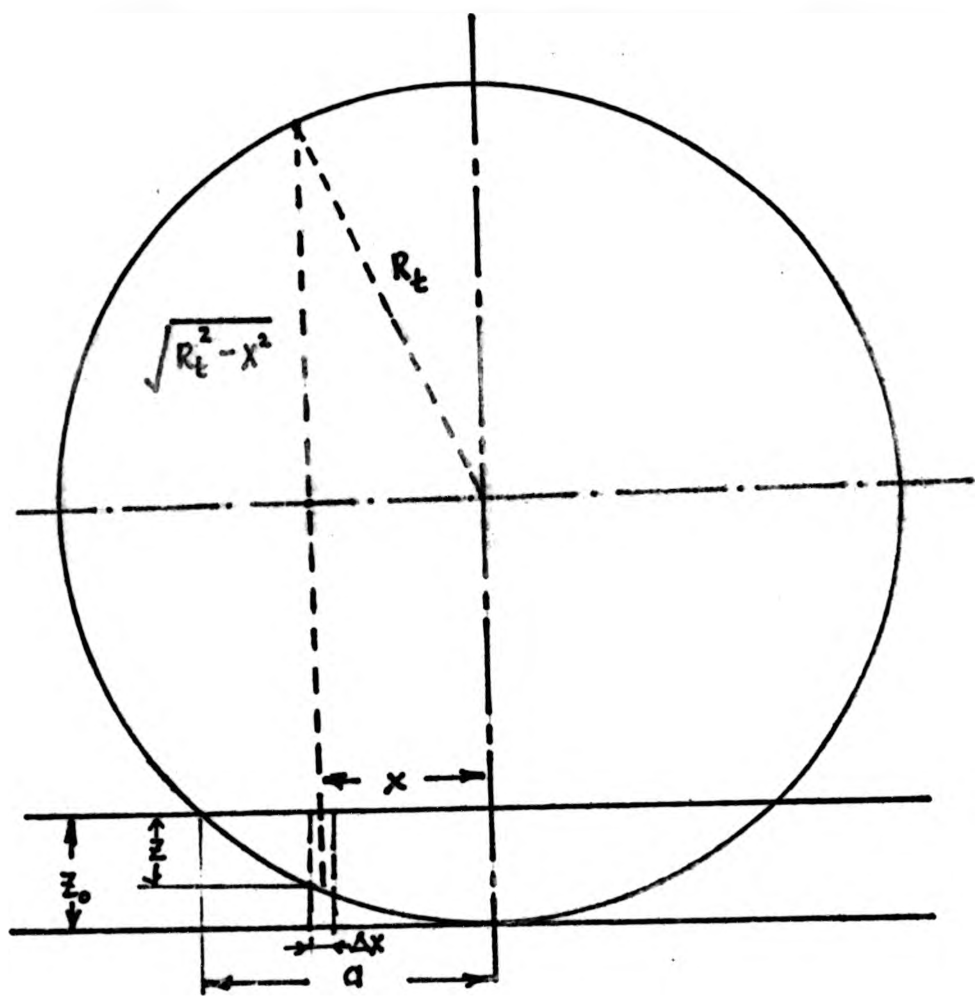

Fig. 7.2. Relationship between deflection and contact length.

$$x = (n - \tfrac{1}{2})\,\Delta x$$

and,

$$x^2 = (n - \tfrac{1}{2})^2\,\Delta x^2$$

$$\simeq n(n - 1)\,\Delta x^2$$

$$x^2 \simeq n(n - 1)\left\{\frac{a}{N}\right\}^2 \qquad \text{................(7.9)}$$

Substituting Equation (7.9) into Equation (7.8) will give the value of z in term of the contact length of the patch.

$$z = \frac{a^2 - n(n-1)\{\frac{a}{N}\}^2}{2.\sqrt{R_t^2 - n(n-1)\{\frac{a}{N}\}^2}}$$

$$z = \frac{a\,(1 - n(n-1)\frac{1}{N^2})}{2.\sqrt{\left[\frac{R_t}{a}\right]^2 - n(n-1)\frac{1}{N^2}}} \qquad \ldots\ldots(7.10)$$

Accordingly the new ratio of the height to length of the membrane is,.

$$\frac{h}{s} = \frac{h_o}{s} - \frac{z}{2s} \qquad \ldots\ldots(7.11)$$

From Equations (7.2),(7.10) and (7.11), the new angle subtended by the membrane for that particular segment can be expressed as,

$$\frac{\sin\phi}{\phi} = \frac{h_o}{s} - \frac{a\,(1 - n(n-1)/N^2)}{4s\sqrt{\left(\frac{R_t}{a}\right)^2 - n(n-1)/N^2}} \qquad \ldots\ldots(7.12)$$

Hence, the value of ϕ for every segment can be determined from Equation (7.12). By substituting this value of ϕ into Equation(7.6) , the load supported by that segment can be evaluated. Therefore, the total load supported by the tyre will be equal to the sum of the load supported by each segment.

$$F_{total} = 2 \sum_{n=1}^{N} F_n \left\{\frac{a}{N}\right\} \qquad \text{........(7.13)}$$

From the above equations the load supported by the tyre at any deflection, z_o, can be predicted if the values of the initial parameters P_o, h, s, w and R_t are known.

A comparison between the predicted values and the experimental values based on the measured parameters (Table 7.1) for the cross-ply tyre, rayon-belted and steel-belted radial tyres are shown in Figs. 7.3a, 7.3b and 7.3c respectively.

Table.7.1: Measured tyre construction variables

Parameters (mm)	Cross-ply	Radial	
		Rayon	Steel
2h	104 ± 1	90 ± 1	96 ± 1
2w	115 ± 1	106 ± 1	120 ± 1
2s	120 ± 1	100 ± 1	105 ± 1
Rim diameter	360 ± 1	360 ± 1	360 ± 1

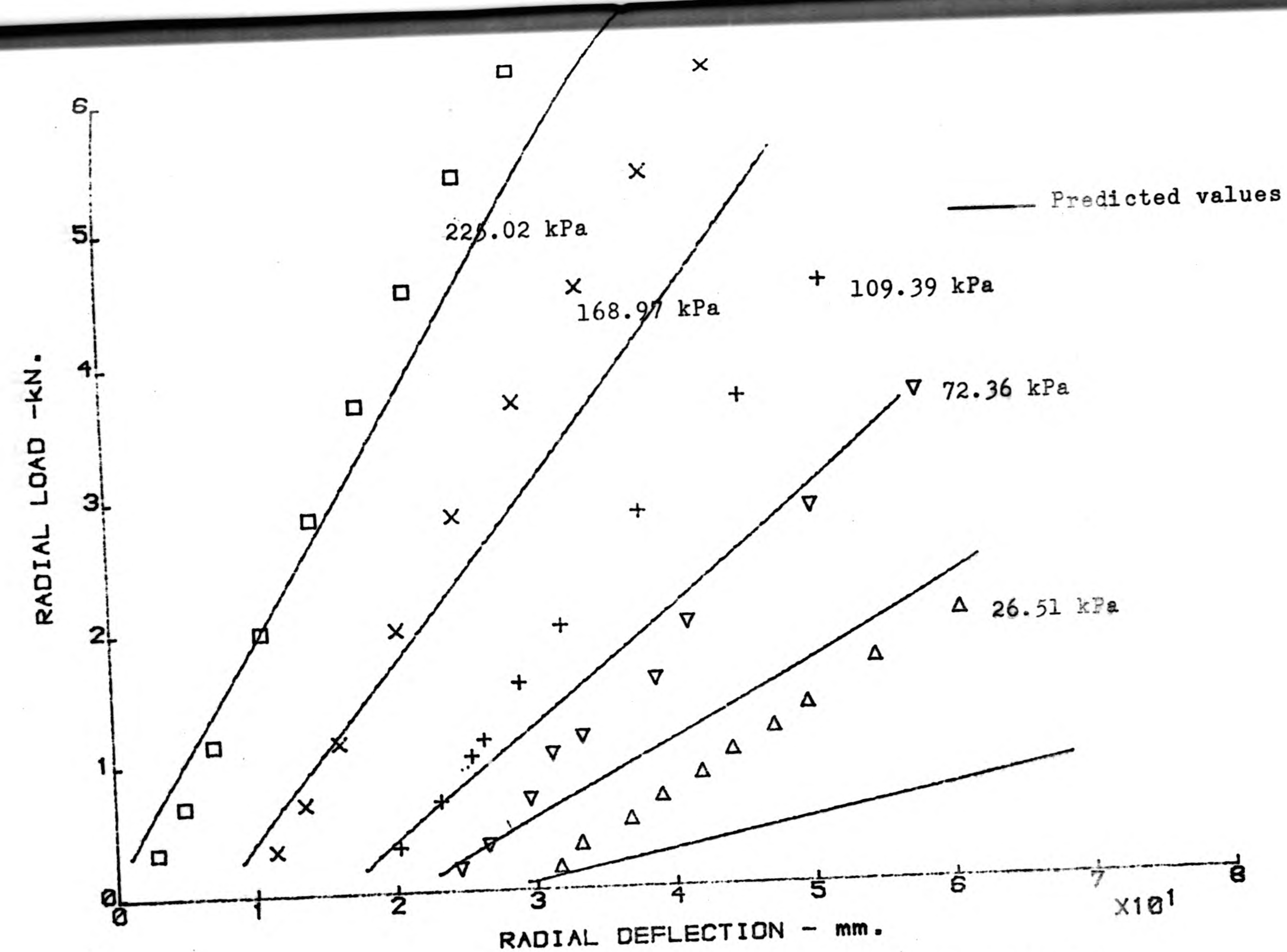

Fig. 7.3a. Load-deflection characteristics of a cross-ply tyre.

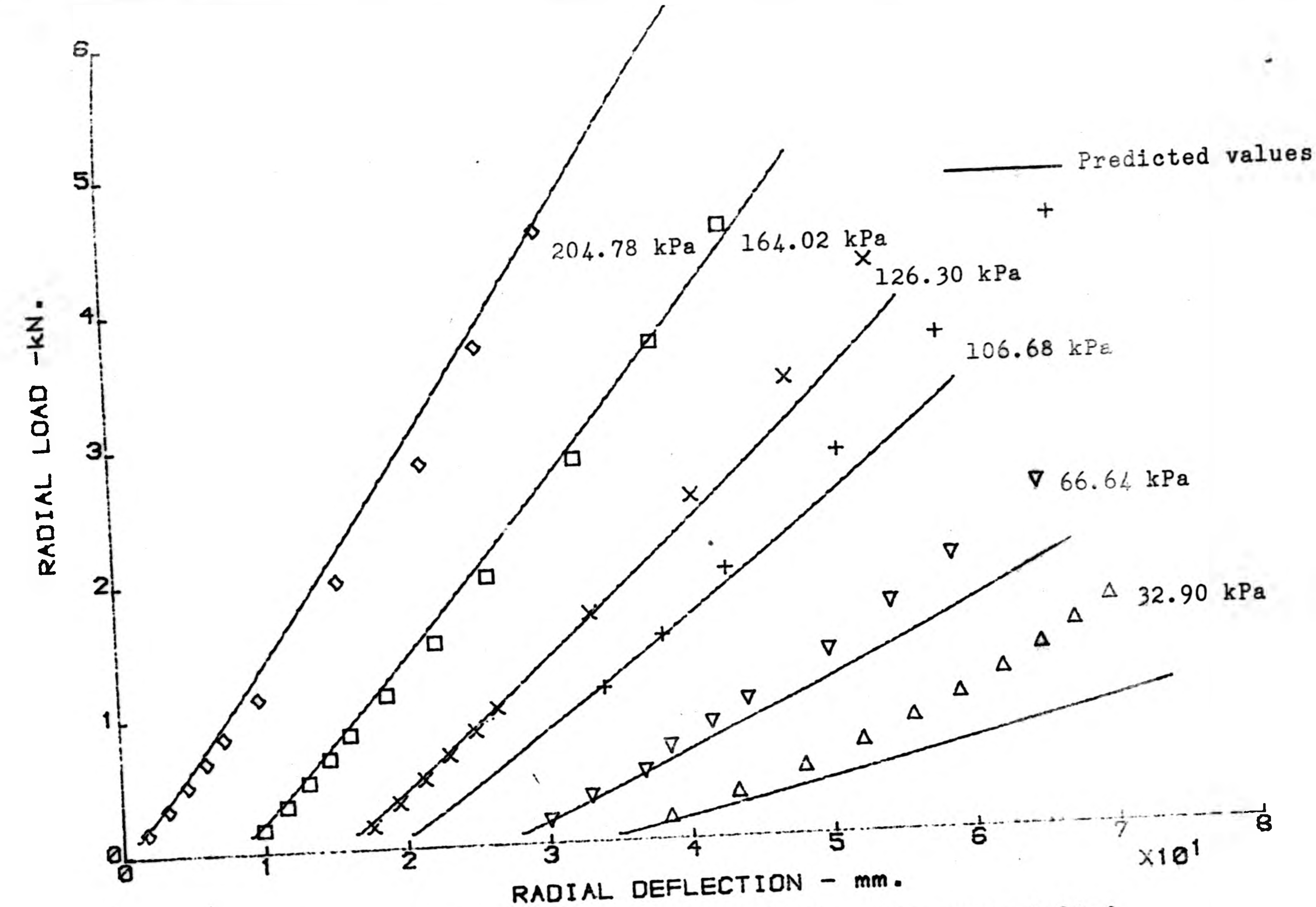

Fig. 7.3b. Load-deflection characteristics of a rayon-belted radial tyre.

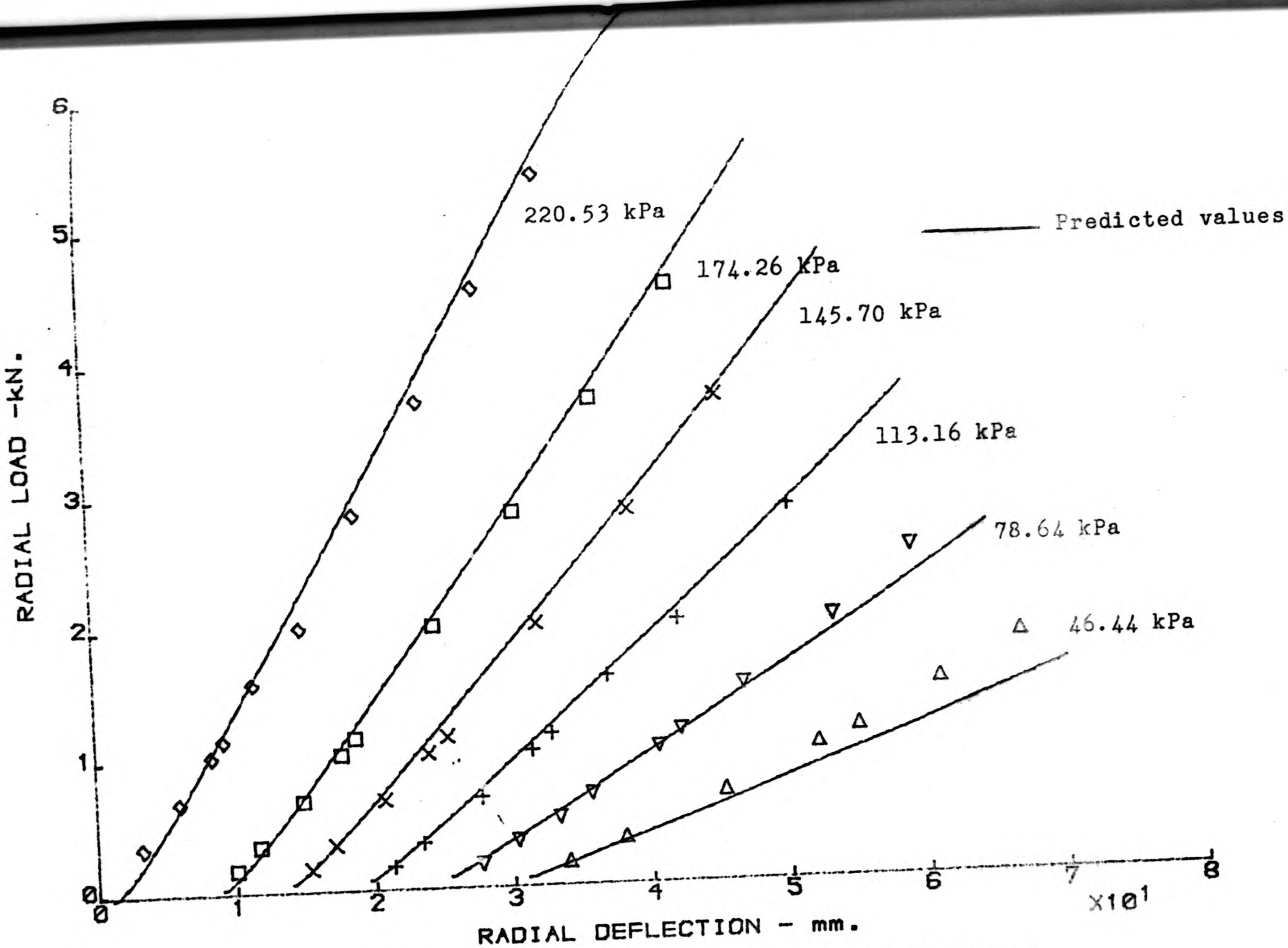

Fig. 7.3c. Load-deflection characteristics of a steel-belted radial tyre.

From the graphs it can be seen that the predicted values for the radial tyres agree satisfactorily with the experimental results whereas in the case of the cross-ply tyre it predicted reasonably well at higher inflation pressures. This is as expected because the model was developed based on the assumption that the sidewalls behave like a flexible membrane with no stiffness. Hence, from the difference between the theoretical and experimental values, especially at low inflation pressures, one can infer that the bigger the difference the stiffer will be the sidewalls. Base on this criteria, it is not too difficult to qualify that the cross-ply tyre has the most rigid sidewall followed by the rayon-belted radial tyre. The steel-belted radial having the least stiff sidewalls. This is in accordance with the experimental results obtained as reported in chapter 6.

In conclusion, the fact that this model has successfully predicted the load-deflection behaviour of tyres from the knowledge of its construction parameters means that this model will be a valuable tool in the study of the effect of the construction parameters upon the load deflection characteristics of tyres.

CHAPTER 8

CONCLUSIONS AND SUGGESTIONS FOR FURTHER WORK.

8.1. Conclusions

From the results of the experiment it can be concluded that a reasonable amount of accuracy can be obtained from the system used. The calculated load was found to accurate in the region of 1 percent.

Within the limits of experimental error the volume of the tyre determined by the air expansion/compression method is in close agreement with the value obtained by the method of filling the tyre with water. However, there is one distinct advantage of using the air expansion/compression method in that it eliminates the problem of dismantling the system.

The change in the pressure rise ratio $\frac{\Delta P}{P_{abs}}$ and the change in the volume of the tyre, ΔV, are dependent upon the tyre deflection and independent of the inflation pressure. The relationship between ΔV and $\frac{\Delta P}{P_{abs}}$ was found to be linear, thereby, confirming the assumption that the process of deformation of the tyre took place isothermally.

Comparison of the work done on the air determined by the method of pressure measurement and that determined by volume measurements were found to lie within $\pm$ 2 percent of each other. The major contributory factor for the difference between the values of the work done on air by the two methods is the effect of temperature changes in the air during the compression and expansion processes. This is especially so in the case at large deformation of tyre.

The load required to deform the tyre depends upon the inflation pressure and the tyre construction. At rated inflation pressure, 80-90 percent of the load supported by the tyre is due to its pneumatic contribution and 10-20 percent due to its structural contribution. Further, it was found that the structural contribution of the tyre is independent of the inflation pressure. The equation used to characterise the load-deflection behaviour of the tyre in the form of $L=(A + B.P)z^n$ agrees satisfactorily with the experimental results especially in the case of radial tyres. The percentage proportion of the work done on the tyre structure decreases with increase in inflation pressure. A difference in behaviour between the steel-belted radial and the other tyres was observed.

A simplified treatment of the load -deflection behaviour of the tyres based on Gent and Thomas theory of air spring has been developed. The predicted result agrees satisfactorily with the experimental values.

8.2. Suggestions for further work.

One of the most intriguing aspect of the results gathered from the experiment is the releasing of part of the energy stored in the structure of the tyre and the applicability of the Gent and Thomas theory to predict the load-deflection behaviour of the pneumatic tyre. In view of this, the following suggestions for further work are proposed.

1. Further development in the construction of the apparatus and experimental techniques.

2. Study the effect of tread curvature and stiffness on the energy release.

3. Extend the study to include the effect of adiabatic process.

4. Study the effect of tilting and twisting on tyre.

8.2.1 Further development in the construction of the apparatus and experimental techniques.

Though the present apparatus performed satisfactorily, it is only for development system. One of its shortcomings is the tremendous amount of manual work involved in carrying out the procedures and also the time consumed in collecting and analysing the data. This system can be enhanced through the use of sensitive load, pressure and displacement transducers and interfacing them to a computer. This will undoubtedly reduce the manual operations and time. Furthermore, with increase sensitivity of the system, improvement in the system performance could be achieved.

8.2.2. <u>Study the effect of tread curvature and stiffness on the energy release behaviour of tyre</u>.

When a tyre cord which is in tension undergoes compression, part of its stored energy is being released. The tranferance of this energy to the other part of the tyre effect the performance of the tyre. Study in this field will give a better understanding into the behaviour of tyre.

8.2.3. <u>Study the effect of adiabatic process of air upon the load-deflection behaviour of tyre</u>.

The work that has been carried out involves mainly with the isothermal type of deformation. In real world, however, this is not the case. As a result of rolling and thumping, the air contained in the tyre is undergoing an adiabatic type of process. As a consequence of this there will an increase in the temperature. The effect of temperature rise upon the stiffness of the tyre has been studied by Nicholson(1) on model tyre. Amongst other things, he reported that an increase in the temperature of the air in the tyre has a significant effect on tyre stiffness. It would therefore broaden our understanding of the behaviour of the tyre if the study of the effect of adiabatic process be enlarged to cover a wider aspect of tyre constructions and materials.

8.2.4. Study the effect of tilting and twisting.

The investigations that has been carried out in this project covers mainly one aspect of tyre behaviour. Other aspect of tyre behaviour such as tilting and twisting, in which the tyre has to endure in service have not been investigated. It would therefore be most appropriate to include this aspect of tyre behaviour into future studies.

REFERENCES

Chapter I

1. Tompkins, E., The history of the pneumatic tyre, 1981
2. Gardner,E.R.,Progress of Rubber Technology,40,1977,p50.
3. Davisson,J.A.,SAE Paper No. 69001,1969
4. Ridha,R.A.,Rubber Chemistry and Technology,53,1980,p849
5. Young,M.A.,Progress of Rubber Technology,37,1973/4,p127
6. Gardner,E.R.,Progress of Rubber Technology,38,1975,p35
7. Givens,L.,Automotive Engineering,84,1,1976,p38
8. Clark,S.K,Kautschuk und Gummi Kunstoffe,8,1969,p433
9. Walter,J.D. and Conant,F.S.,Tire Science and Technology, 2,4,1974,p235
10. Collins,J.M.et. al.,Trans IRI,40,6,1964,p239
11. Kainradl,P. and Kaufmann,G.,Rubber Chemistry and Technology,49,1979,p823
12. Willet,P.R.,Rubber Chemistry and Technology,46,1973, p425.
13. Prevorsek,D.C.,et. al,ASTM STP-694,1979,p263
14. Okazaki,T. et. al,US Patents 4 385 653,1983
15. Stanley,P.M.,US Patents 4 362 200,1982
16. Plastics and Rubber Weekly No.904,Sept 12,1981,p76
17. Chang,L.Y., and Shackleton,J.S.,Elastomerics,March 1983, p18
18. Glemming,D.A. and Bowers,P.A.,Tire Science and Technology,2,4,1974,p286
19. Clark,S.K.,Ed. NBS Monograph 122,1970,p553
20. Schuring,D.J.,Rubber Chemistry and Technology,53,1980, p600
21. Lippmann,S.A.,et. al,SAE Paper 780258,1978

22. Klingbell, W. W., SAE Paper 800088, 1980

Chapter 2

1. Schippel, H.F., Industrial and Engineering Chemistry, 15, 1923, p.1121-1131

2. Frank, F. and Hofferberth, W., Rubber Chemistry and Technology, 40, 1967, p.271

3. Yoshimura, N., International Polymer Science and Technology, 4, 8, 1977, p.T/21

4. Hofferberth, W., Kautschuk und Gummi, 8, 1955, pWT.124

5. Purdy, J. F., Mathematics Underlying the Design of Pneumatic tires, Edward Bros., Ann Arbor, Michigan, 1963

6. Biderman, V.L., NASA-TT-F-12382, Sept. 1969.

7. Biderman, V. L. et. al, Soviet Rubber Technology, 25, 5, 1966

8. Bukhin, B. L., Soviet Rubber Technology, 22, 10, 1963, p.38

9. Lauterbach, H. G. and Ames, W.F., Proceedings of International Rubber Conference, Washington, 1959, p. 50

10. Ellis, J. R. and Frank, F., A.S.A.E. Report No. 1, Cranfield, 1966.

11. Walston, W. H. and Ames, W. F., Textile Research Journal, 35, 1965, p.1078

12. Robecci, E. and Amici, L., Tire Science and Technology, 1, 3, 1973, p.290

13. Brewer, H. K., Tire Science and Technology, 1, 1, 1973, p.47

14. Clark, S. K., Budd, Ch.B. and Tielking, J. T., Kautschuk und Gummi Kunststoff, 25, 12, 1972, p.587

15. Koutny, F., International Polymer Science and Technology, 5, 8, 1978, p.T/100

16. Zorowski, C. F., Tire Science and Technology 1, 1, 1973, p.99

17. Biderman, V. L., RABRM Translation No. 798, 1960

18. Jackson, W. L., BP 1 576 409

19. Monzini, R., French Patent Applications No. 7 637 352

20. Markow, E. G., U.S. Patent 4 111 249

21. Nadezdin, G. V., Soviet Rubber Technology, 25, 5, 1966, p.20

22. Slyudikov, L. D., Soviet Rubber Technology, 21, 8, 1962, p.24

23. Gough, V., NBS Monograph 122, 1970, p.355

24. Rotta, J., Ing-Archiv, 17, 1949, p.129

25. Rekitar, M. I., Soviet Rubber Technology, 29, 6, 1970, pg. 41

26. Hadekel, R.S., S & T. Memo No. 10/52 (British Ministry of Supply TPA 3/TIB), 1952

27. Smiley, R. F. and Horne, W. B., NACA TN 4010, 1958

28. Prashikin, N., Soviet Rubber Technology, 23, 3, 1964 p. 11

29. Cooper, D. H., Trans. IRI, 40, 1, 1964, p. T58

30. Micheal, F., NACA TM 689, 1932

31. Tiemann, R., A.T.Z., 65, 4, 1963, p.97

32. Seitz, N. and Hussman, A.W., SAE Preprint No. 710626, 1971

32. Givens, L., Automative Engineering, 84, 1, 1976, p.38

33. Clark, S. K., NBS Monograph 122, 1970, p.447

34. Charrier, J. M., Int. J. Mech. Sci., 15, 1973, p.435

35. Nicholson, D. W., Tire Science and Technology, 2, 1, 1974, p.3

36. Martin, F., Jahrbuch der Deutschen Luftfahrtforschung Part 1, 1939

37. Nicholson, D. W., Tire Science and Technology, 3, 1, 1975, p.29

38. Yamagishi, K., Ph.D. Dissertation, Cornell University, 1978

39. Yamagishi, K. and Jenkins, J. T., Journal of Applied Mechanics, 47, 1980, p. 513

Chapter 3

1. Holman, T., Thermodynamics,

2. Frank, T. et.al., Physical Chemistry, 1967

3. Shah, K. K. and Thodos, G., Industrial and Engineering Chemistry, 57, 3, March 1965, p. 30

4. Goff, J.A. and Gratch, S., Heating, Piping & Air Conditioning, ASHVE, June, 1945

Chapter 4

1. Koutny, F., Tire Science and Technology, 4, 3, 1976, p. 190
2. Poulter, K.F., Journal of Physics, E., 10, 1977, p. 112
3. Rutherford, W.M., Review of Scientific Instruments, 49, 10, 1978, p. 1415
4. Hadekel, R., S & T. Memo No. 10/52 (British Ministry of Supply TPA 3/TIB), 1952
5. Biderman, V.L., NASA-TT-F-12382, Sept. 1969

Chapter 6

1. Charrier, J.M., Rubber Chemistry and Technology, 43, 1970, p. 382
2. Walter, J.D., Textile Research Journal, Feb. 1969, p. 191
3. Jackson, W.L., BP 1 576 409
4. De Eskinazi, J. et.al., Tire Science and Technology, 3, 1, 1975, p. 43

Chapter 7

1. Gent, A.N. and Thomas, A.G., Rubber Chemistry and Technology, 47, 2, 1974, p. 384
2. Yamagishi and Jenkins, Journal of Applied Mechanics, 47, 1980, p. 513.

Chapter 8

1. Nicholson, D.W., Tire Science and Tech., 2, 1, 1974, p3

Selected Readings

1. Wark, K., Thermodynamics, McGrawHill Kogakusha Ltd., 1977
2. Bronson, S.H., Applied Thermodynamics, D. Van Nostrand Co. Ltd. London, 1961
3. Van Vylen, G. J. and Sonntag, R.E., Fundamentals of Classical Thermodynamics, Wiley, New York 1976
4. Schenck, H., Theories of Engineering Experimentation, 3rd. Ed. McGrawHill Book Co. 1961
5. Brombacher, W. G., et.al., NBS Monograph 8, 1960.

APPENDIX

CALCULATIONS AND ANALYSIS OF EXPERIMENTAL ERRORS.

The error in the calculated values presented in this work have been determined by means of a simple propagation of error analysis. This method says that for a calculated value, f, which is a function of measured quantities x_i and which is determined by the relationship

$$f = f(x_i) \quad \ldots\ldots\ldots\ldots\ldots\ldots\ldots\ldots \quad (1.i)$$

the most probable error or the uncertainty, Δf, propagated in the calculation of f is approximately

$$\Delta f = \left\{ \sum_{i=1}^{n} \left[\left(\frac{\partial f}{\partial x_i} \right)^2 \Delta x_i^2 \right] \right\}^{\frac{1}{2}} \quad \ldots\ldots\ldots\ldots\ldots\ldots \quad (1.ii)$$

where Δx_i = error in the measured quantity x_i

APPENDIX I

Determination of the coefficient of friction of the pulley bearing.

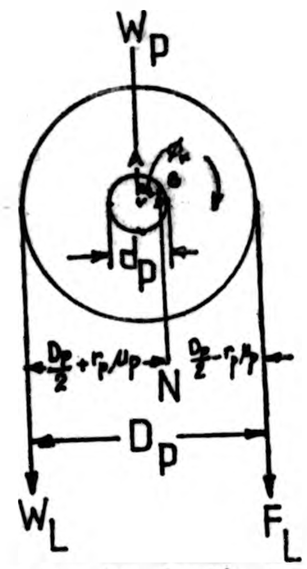

When the forces in both parts of the wire cable are equal contact between the pulley and the shaft takes place at A. The force F is then increased until the pulley just slide around the shaft.

The perpendicular distance from the centre of the pulley to the line of action of N is r_f where r_f = r sin $\phi_k \approx r_p \mu_p$ and ϕ_k = the limiting angle

Summing the moment of forces about B and equating it to zero,

$$M_B + \curvearrowright = 0$$

$$(D_p/2 + r_p\mu_p)W_L + W_p\, r_p\mu_p - (D_p/2 - r_p\mu_p)F_L = 0$$

$$\mu_p r_p(W_L + W_p + F_L) = D_p/2(F_L - W_L)$$

$$\mu_p = \frac{D_p(F_L - W_L)}{d_p(W_L + W_p + F_L)} \qquad \text{..................(I1)}$$

Analysis of experimental error in the determination of the coefficient of friction of the pulley bearing.

The coefficient of friction of the pulley bearing, μ_p, is determined from equation (I.1)

$$\mu_p = \frac{(F_L - W_L)D_p}{(W_L + W_p + F_L)d_p}$$

The most probable value of the experimental error in the determination of the coefficient of friction of the pulley bearing $\Delta\mu_p$ is given by the relationship.

$$\Delta\mu_p = \pm\left\{\left(\frac{\partial\mu_p}{\partial F_L}\Delta F_L\right)^2 + \left(\frac{\partial\mu_p}{\partial W_L}\Delta W_L\right)^2 + \left(\frac{\partial\mu_p}{\partial W_p}\Delta W_p\right)^2 + \left(\frac{\partial\mu_p}{\partial D_p}\Delta D_p\right)^2 + \left(\frac{\partial\mu_p}{\partial d_p}\Delta d_p\right)^2\right\}^{\frac{1}{2}} \quad \text{.... (I.2)}$$

where

$$\frac{\partial\mu_p}{\partial F_L} = \frac{D_p}{d_p}\left[\frac{(W_L + W_p + F_L) - (F_L - W_L)}{(W_L + W_p + F_L)^2}\right]$$

$$= \frac{D_p}{d_p}\left[\frac{2W_L + W_p}{(W_L + W_p + F_L)^2}\right]$$

$$\frac{\partial\mu_p}{\partial W_L} = \frac{D_p}{d_p}\left[\frac{-(W_L + W_p + F_L) - (F_L - W_L)}{(W_L + W_p + F_L)^2}\right]$$

$$= -\frac{D_p}{d_p}\left[\frac{2F_L + W_p}{(W_L + W_p + F_L)^2}\right]$$

$$\frac{\partial \mu_p}{\partial W_p} = \frac{-D_p}{d_p}\left[\frac{F_L - W_L}{(W_L + W_p + F_L)^2}\right]$$

$$\frac{\partial \mu_p}{\partial D_p} = \frac{1}{d_p}\left[\frac{F_L - W_L}{W_L + W_p + F_L}\right]$$

$$\frac{\partial \mu_p}{\partial d_p} = \frac{D_p}{d_p^2}\left[\frac{F_L - W_L}{W_L + W_p + F_L}\right]$$

APPENDIX II <u>Analysis of experimental error in the determination of the centre of gravity of the beam assembly.</u>

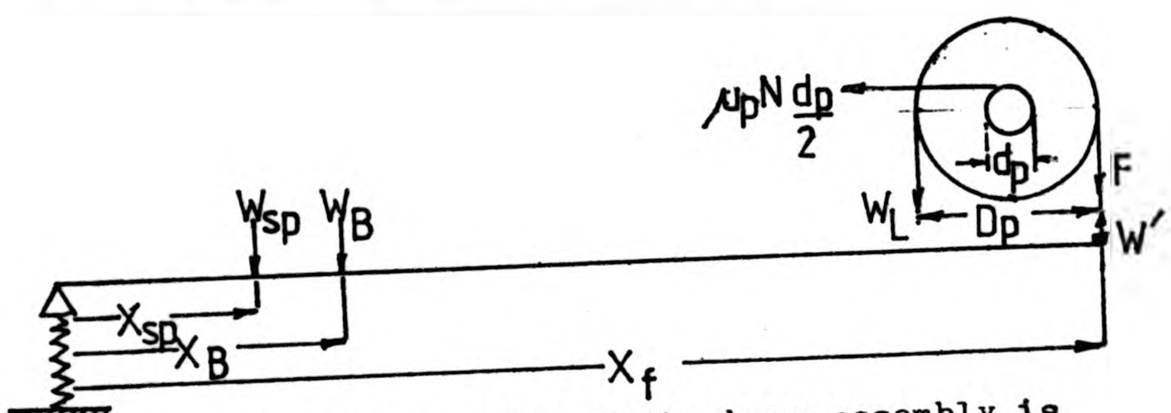

The centre of gravity of the beam assembly is calculated according to the relationship

$$X_B = \frac{F^1 . X_F - Wsp.Xsp}{W_B} \quad \ldots\ldots\ldots\ldots\ldots\ldots \text{(II.1)}$$

and the true force F^1 is calculated according to the relationship

$$F^1 = \frac{W_L\,(D_p + \mu_p d_p) + \mu_p d_p W_p}{D_p - \mu_p d_p} - W^1 \quad \ldots\ldots\ldots \text{(II.2)}$$

and W' is the weight of the hook.

Let $D = \mu_p d_p$

The uncertainty in D is calculated from the relationship.

$$\Delta D = \left\{ \left(\frac{\partial D}{\partial \mu_p} \Delta \mu_p \right)^2 + \left(\frac{\partial D}{\partial d_p} . \Delta d_p \right)^2 \right\}^{1/2} \quad \ldots\ldots\ldots \text{(II.3)}$$

where

$$\frac{\partial D}{\partial \mu_p} = d_p$$

$$\frac{\partial D}{\partial d_p} = \mu_p$$

substituting D into equation (II.2)., gives

$$F^1 = \frac{W_L(D_p + D) + D.W_p}{(D_p - D)} - W^1$$

In other form,

$$F^1 = f(W_L, D_p, D, W_p, W^1)$$

Therefore the uncertainty in the calculation of F^1 can be represented by the relationship.

$$\Delta F^1 = \left\{ \left(\frac{\partial F^1}{\partial W_L} \Delta W_L \right)^2 + \left(\frac{\partial F^1}{\partial D_p} \Delta D_p \right)^2 + \left(\frac{\partial F^1}{\partial D} \Delta D \right)^2 + \left(\frac{\partial F^1}{\partial W_p} \Delta W_p \right)^2 + \left(\frac{\partial F^1}{\partial W^1} \Delta W^1 \right)^2 \right\}^{\frac{1}{2}} \quad \ldots\ldots\ldots \text{(II.4)}$$

where

$$\frac{\partial F^1}{\partial W_L} = \frac{D_p + D}{D_p - D}$$

$$\frac{\partial F^1}{\partial D_p} = - \frac{D.W_L}{(D_p - D)^2}$$

$$\frac{\partial F^1}{\partial D} = \frac{W_p D_p - 2D(W_L + W_p)}{(D_p - D)^2}$$

$$\frac{\partial F^1}{\partial W_p} = \frac{D}{D_p - D}$$

$$\frac{\partial F^1}{\partial W^1} = 1$$

Since $X_B = f(F^1, X_F, W_{sp}, X_{sp}, W_B)$

The uncertainty in x_B is calculated according to the relationship

$$\Delta X_B = \left\{ \left(\frac{\partial X_B}{\partial F^1} \Delta F^1 \right)^2 + \left(\frac{\partial X_B}{\partial X_F} \Delta X_F \right)^2 + \left(\frac{\partial X_B}{\partial W_{sp}} . \Delta W_{sp} \right)^2 + \left(\frac{\partial W_B}{\partial X_{sp}} . \Delta X_{sp} \right)^2 + \left(\frac{\partial X_B}{\partial W_B} . \Delta W_B \right)^2 \right\}^{\frac{1}{2}} \quad \ldots\ldots\ldots \text{II}.5$$

where

$$\frac{\partial X_B}{\partial F^1} = \frac{X_F}{W_B}$$

$$\frac{\partial X_B}{\partial X_F} = \frac{F^1}{W_B}$$

$$\frac{\partial X_B}{\partial W_{sp}} = \frac{-X_{sp}}{W_B}$$

$$\frac{\partial X_B}{\partial X_{sp}} = - \frac{W_{sp}}{W_B}$$

$$\frac{\partial X_B}{\partial W_B} = - \frac{(F^1.X_F - W_{sp}.X_{sp})}{X_B^2}$$

APPENDIX III. <u>Calculation for the determination of the coefficient of friction of pivot bearing.</u>

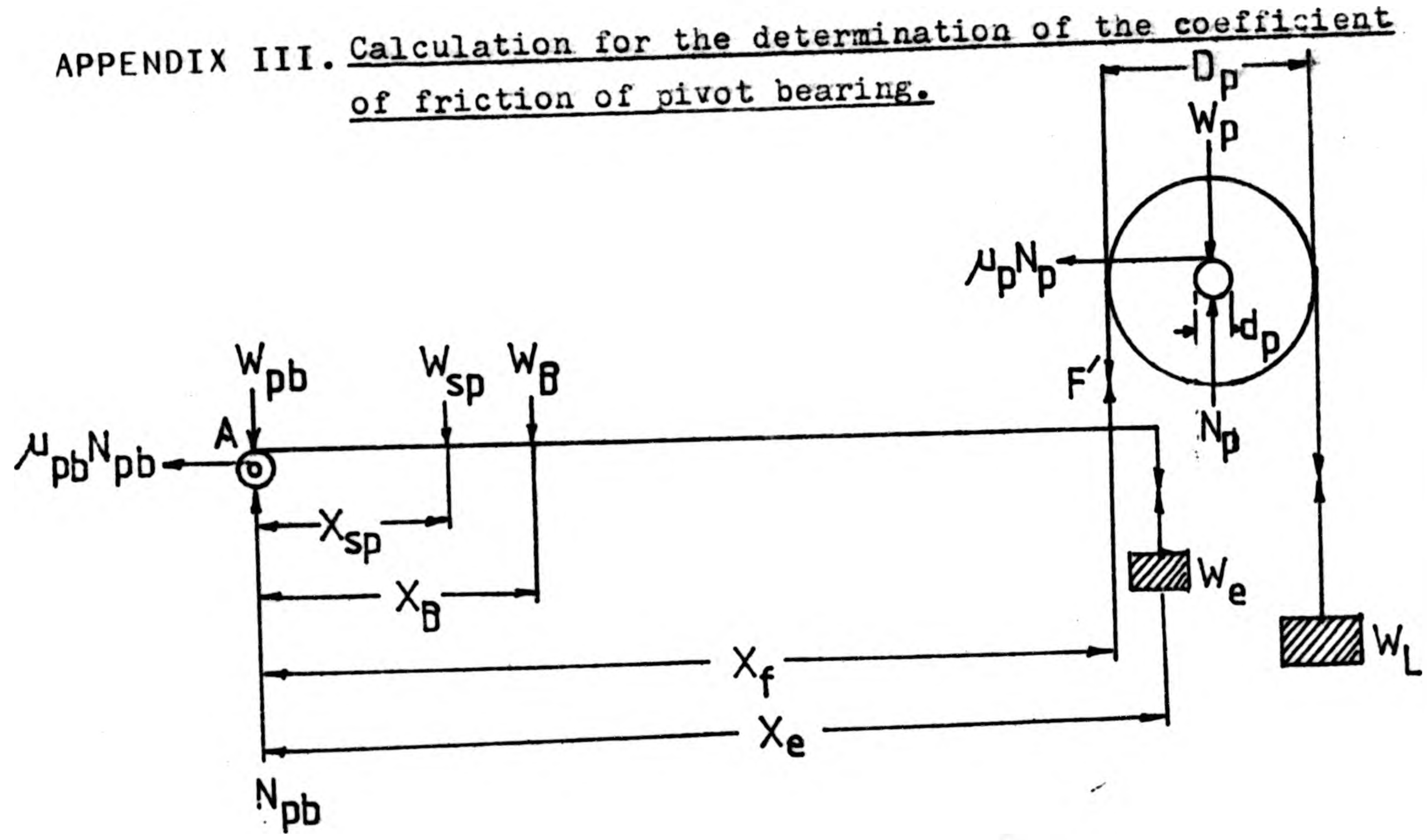

The coefficient of friction of the pivot bearing can be calculated from the following relationship. Taking the moment of all forces about A .i.e., the centre of the pivot bearing.

$$\sum M_A = 0 : - \mu_{pb} . N_{pb} . d_{pb}/2 + W_{sp}.X_{sp} + W_B.X_B - F^1.X_p + W_e.X_e = 0$$

on rearranging the above equation,

$$\mu_{pB} = \frac{W_{sp}.X_{sp} + W_B X_B + W_E X_E - F^1 X_F}{N_{pb}.d_{pb}/2} \quad \ldots\ldots\ldots \quad (\text{III}.1)$$

where F^1 the true limiting force required to prevent the beam assembly from turning and N_{pB} is the normal reaction acting at the pivot bearing. F^1 can be calculated according to the relationship given in the equation (II.2).

$$F^1 = \frac{W_L(D_p + u_p d_p) + u_p d_p W_p}{D_p - u_p d_p} - W^1$$

and N_{pB} is calculated by taking the summation of all the vertical forces and equating it to zero i.e.,

$$\sum FY = 0 : W_{pb} + W_{sp} + W_B - F^1 + W_E - N_{pb} = 0$$

$$\text{therefore } N_{pb} = W_{pb} + W_{sp} + W_B + W_E - F^1 \quad \ldots\ldots\ldots\ldots\ldots \quad (\text{III}.2)$$

<u>Analysis of the experimental error in the determination of the coefficient of friction of the pivot bearing.</u>

From equation (III.1), the coefficient of friction of the pivot bearing is,

$$\mu_{pb} = \frac{W_{sp}.X_{sp} + W_p X_B + W_E X_E - F^1.X_F}{(W_{sp} + W_B + W_{pb} + W_E - F^1) d_{pb}/2}$$

$$\text{therefore } \mu_{pb} = f(W_{sp}, X_{sp}, X_B, W_E, X_E, F^1, X_F, d_{pb})$$

The uncertainty in the determination of μ_{pb} can be calculted according to the relationship.

$$\Delta\mu_{pb} = \left\{ \left[\frac{\partial\mu_{pb}}{\partial W_{sp}}\cdot\Delta W_{sp}\right]^2 + \left[\frac{\partial\mu_{pb}}{\partial x_{sp}}\cdot\Delta x_{sp}\right]^2 + \left[\frac{\partial\mu_{pb}}{\partial W_B}\cdot\Delta W_B\right]^2 + \left[\frac{\partial\mu_{pb}}{\partial x_B}\cdot\Delta x_B\right]^2 + \left[\frac{\partial\mu_{pb}}{\partial W_E}\cdot\Delta W_E\right]^2 + \left[\frac{\partial\mu_{pb}}{\partial x_E}\cdot\Delta x_E\right]^2 + \left[\frac{\partial\mu_{pb}}{\partial F^1}\cdot\Delta F^1\right]^2 + \left[\frac{\partial\mu_{pb}}{\partial x_F}\cdot\Delta x_F\right]^2 + \left[\frac{\partial\mu_{pb}}{\partial d_{pb}}\cdot\Delta d_{pb}\right]^2 \right\}^{\frac{1}{2}} \quad \text{III.3}$$

where

$$\frac{\partial\mu_{pb}}{\partial W_{sp}} = \frac{(W_{sp}+W_B+W_{pb}+W_E-F')\frac{d_{pb}}{2}x_{sp}-(W_{sp}x_{sp}+W_Bx_B+W_Ex_E-F'x_F)\frac{d_{pb}}{2}}{\left[(W_{sp}+W_B+W_{pb}+W_E-F')\frac{d_{pb}}{2}\right]^2}$$

$$= \frac{W_B(x_{sp}-x_B)+W_{pb}x_{sp}+W_E(x_{sp}-x_E)+F'(x_F-x_{sp})}{\frac{d_{pb}}{2}(W_{sp}+W_B+W_{pb}+W_E-F')^2}$$

$$\frac{\partial\mu_{pb}}{\partial x_{sp}} = \frac{W_{sp}}{(W_{sp}+W_B+W_{pb}+W_E-F')\frac{d_{pb}}{2}}$$

$$\frac{\partial\mu_{pb}}{\partial W_B} = \frac{(W_{sp}+W_B+W_{pb}+W_E-F')\frac{d_{pb}}{2}\cdot x_B-(W_{sp}x_{sp}+W_Bx_B+W_Ex_E-F'\cdot x_F)\frac{d_{pb}}{2}}{\left[(W_{sp}+W_B+W_{pb}+W_E-F')\frac{d_{pb}}{2}\right]^2}$$

$$\frac{\partial \mu_{pb}}{\partial W_{\mathcal{B}}} = \frac{W_{sp}(x_{\mathcal{B}}-x_{sp})+W_{pb}x_{\mathcal{B}}+W_{E}(x_{\mathcal{B}}-x_{\mathcal{E}})+F'(x_{\mathcal{F}}-x_{\mathcal{B}})}{\frac{d_{pb}}{2}(W_{sp}+W_{\mathcal{B}}+W_{pb}+W_{\mathcal{E}}-F')^2}$$

$$\frac{\partial \mu_{pb}}{\partial x_{\mathcal{B}}} = \frac{W_{\mathcal{B}}}{(W_{sp}+W_{\mathcal{B}}+W_{pb}+W_{\mathcal{E}}-F')\ \frac{d_{pb}}{2}}$$

$$\frac{\partial \mu_{pb}}{\partial W_{\mathcal{E}}} = \frac{(W_{sp}+W_{\mathcal{B}}+W_{pb}+W_{\mathcal{E}}-F')\cdot\frac{d_{pb}}{2}x_{\mathcal{E}}-(W_{sp}\cdot x_{sp}+W_{\mathcal{B}}+W_{\mathcal{E}}x_{\mathcal{E}}-F'x_{\mathcal{F}})\frac{d_{pb}}{2}}{\left((W_{sp}+W_{\mathcal{B}}+W_{pb}+W_{\mathcal{E}}-F')\frac{d_{pb}}{2}\right)^2}$$

$$= \frac{W_{sp}(x_{\mathcal{E}}-x_{sp})+W_{\mathcal{B}}(x_{\mathcal{E}}-x_{\mathcal{B}})+W_{pb}+F'(x_{\mathcal{F}}-x_{\mathcal{E}})}{\frac{d_{pb}}{2}\ (W_{sp}+W_{\mathcal{B}}+W_{pb}+W_{\mathcal{E}}-F')^2}$$

$$\frac{\partial \mu_{pb}}{\partial x_{\mathcal{E}}} = \frac{W_{\mathcal{E}}}{(W_{sp}+W_{\mathcal{B}}+W_{pb}+W_{\mathcal{E}}-F')\frac{d_{pb}}{2}}$$

$$\frac{\partial \mu_{pb}}{\partial F'} = \frac{(W_{sp}+W_{\mathcal{B}}+W_{pb}+W_{\mathcal{E}}-F')\frac{d_{pb}}{2}\cdot x_{\mathcal{F}}+(W_{sp}\cdot x_{sp}+W_{\mathcal{B}}\cdot x_{\mathcal{B}}+W_{\mathcal{E}}\cdot x_{\mathcal{E}}-F'\cdot x_{\mathcal{F}})\frac{d_{pb}}{2}}{\left((W_{sp}+W_{\mathcal{B}}+W_{pb}+W_{\mathcal{E}}-F')\frac{d_{pb}}{2}\right)^2}$$

$$= \frac{W_{sp}(x_{\mathcal{F}}+x_{sp})+W_{\mathcal{B}}(x_{\mathcal{F}}+x_{\mathcal{B}})+W_{pb}x_{\mathcal{F}}+W_{\mathcal{E}}(x_{\mathcal{F}}+x_{\mathcal{E}})-2F'\cdot x_{\mathcal{F}}}{\frac{d_{pb}}{2}(W_{sp}+W_{\mathcal{B}}+W_{pb}+W_{\mathcal{E}}-F')^2}$$

$$\frac{\partial \mu_{pb}}{\partial x_{\mathcal{F}}} = \frac{F'}{\frac{d_{pb}}{2}\ (W_{sp}+W_{\mathcal{B}}+W_{pb}+W_{\mathcal{E}}-F')}$$

$$\frac{\partial \mu_{pb}}{\partial d_{pb}} = \frac{2(W_{sp}\cdot x_{sp}+W_{\mathcal{B}}x_{\mathcal{B}}+W_{\mathcal{E}}\cdot x_{\mathcal{E}}-F'\cdot x_{\mathcal{F}})}{d_{pb}^2(W_{sp}+W_{\mathcal{B}}+W_{pb}+W_{\mathcal{E}}-F')}$$

APPENDIX IV. Calculation of the load acting on the tyre

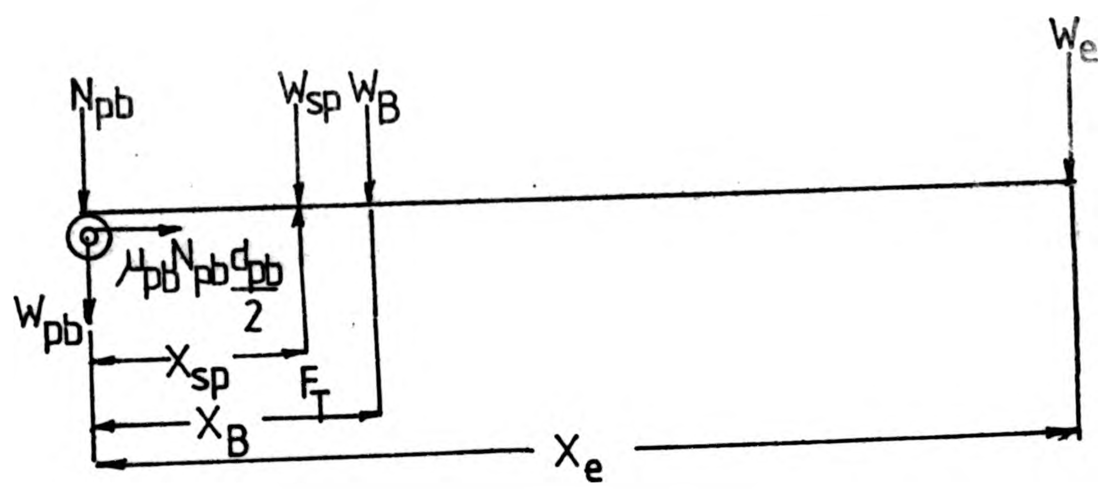

$$\sum F_y = 0 : \quad N_{pb}+W_{pb}+W_{sp}+W_B+W_E-F_T = 0$$

$$\therefore N_{pb} = F_T-(W_{pb}+W_{sp}+W_B+W_E) \quad \ldots\ldots\ldots\ldots\ldots\ldots \text{(IV.1)}$$

$$\sum M_o = 0 \circlearrowright + : \quad -\mu_{pb}\cdot\frac{d_{pb}}{2}\cdot N_{pb}+W_{sp}\cdot x_{sp}+W_E\cdot x_E-F_T\cdot x_{sp} = 0 \quad \ldots\ldots \text{(IV.2)}$$

Substitute (IV.1) into (IV.2):

$$-\mu_{pb}\cdot\frac{d_{pb}}{2}\left[F_T-(W_{pb}+W_{sp}+W_B+W_E)\right]+W_{sp}\cdot x_{sp}+W_B+W_E\cdot x_E-F_T\cdot x_{sp} = 0$$

$$-F_T\left(x_{sp}+\mu_{sp}\cdot\frac{d_{pb}}{2}\right)+\mu_{pb}\cdot\frac{d_{pb}}{2}(W_{pb}+W_{sp}+W_B)+\mu_{pb}\cdot\frac{d_{pb}}{2}\cdot W_E+W_{sp}\cdot x_{sp}+W_B x_B+W_E\cdot x_E = 0$$

$$-F_T\left(x_{sp}+\mu_{pb}\cdot\frac{d_{pb}}{2}\right)+\mu_{pb}\cdot\frac{d_{pb}}{2}(W_{pb}+W_{sp}+W_B)+W_E\left(x_E+\mu_{pb}\cdot\frac{d_{pb}}{2}\right)+W_{sp}\cdot x_{sp}+W_B x_B = 0$$

$$\therefore F_T = \frac{W_{sp}x_{sp}+W_Bx_B+\mu_{pb}\cdot\frac{d_{pb}}{2}(W_{pb}+W_{sp}+W_B)+W_E\left(x_E+\mu_{pb}\cdot\frac{d_{pb}}{2}\right)}{\left(x_{sp}+\mu_{pb}\cdot\frac{d_{pb}}{2}\right)} \quad \ldots\ldots \text{(IV.3)}$$

since W_E is the only variable parameter, equation (IV.3) can be written as

$$F_T = A + B.W_E \quad \ldots\ldots\ldots\ldots\ldots\ldots \text{(IV.4)}$$

where :

$$A = \frac{W_{sp}.x_{sp}+W_B.x_B+\mu_{pb}.\frac{d_{pb}}{2}(W_{pb}+W_{sp}+W_B)}{(x_{sp}+\mu_{pb}.\frac{d_{pb}}{2})} \text{ and } B = \frac{(x_E+\mu_{pb}.\frac{d_{pb}}{2})}{(x_{sp}+\mu_{pb}.\frac{d_{pb}}{2})}$$

<u>Calculation of experimental error of the load applied on the tyre.</u>

The load applied on the tyre is calculated from equation (IV.4).

$$F_T = (A+B.W_E)\, g_l \quad \ldots\ldots\ldots\ldots\ldots\ldots \text{(IV.5)}$$

where g_l = Local acceleration due to gravity

$$A = \frac{(W_{sp}.x_{sp})+(W_B.x_B)+(\mu_{pb}.\frac{d_{pb}}{2}.(W_{pb}+W_{sp}+W_B))}{x_{sp}+\mu_{pb}.\frac{d_{pb}}{2}} \ldots. \text{(IV.6)}$$

$$B = \frac{x_E+\mu_{pb}.\frac{d_{pb}}{2}}{x_{sp}+\mu_{pb}.\frac{d_{pb}}{2}} \quad \ldots\ldots\ldots\ldots\ldots\ldots \text{(IV.7)}$$

Let $C = \mu_{pb}.\frac{d_{pb}}{2}$, and substituting this value into equation (IV.6) and (IV.7) and rearranging, gives

$$A = \frac{W_{sp}(x_{sp}+C)+W_B(x_B+C)+W_{pb}.C}{(x_{sp}+C)} \quad \ldots\ldots\ldots\ldots \text{(IV.8)}$$

$$B = \frac{x_{\ell}+C}{x_{sp}+C} \quad \ldots\ldots\ldots\ldots\ldots\ldots\ldots\ldots \quad (IV.9)$$

From the above, $C = f(\mu_{pb}, d_{pb})$.

The uncertainty in C is represented by ΔC in the form of ,

$$\Delta C = \left\{ \left(\frac{\partial C}{\partial \mu_{pb}} \Delta \mu_{pb}\right)^2 + \left(\frac{C}{d_{pb}} \Delta d_{pb}\right)^2 \right\}^{\frac{1}{2}} \quad \ldots\ldots\ldots\ldots \quad (IV.10)$$

where,

$$\frac{\partial C}{\partial \mu_{pb}} = d_{pb}/2$$

$$\frac{\partial C}{\partial d_{pb}} = \mu_{pb}/2$$

Substituting these values of the derivations of C into equation. (IV.10) gives

$$\Delta C = (d_{pb} \cdot u_{pb})^2 + (u_{pb} \cdot d_{pb})^2 \ \frac{1}{2} \quad \ldots\ldots\ldots\ldots \quad (IV.11)$$

From equation (IV.8)

$$A = f(W_{sp}, x_{sp}, W_B, x_B, W_{pb}, C)$$

The uncertainty in the value of A, represented by ΔA is calculated in accordance with the relationship.

$$\Delta A = \left\{ \left(\frac{\partial A}{\partial W_{sp}} \Delta W_{sp}\right)^2 + \left(\frac{\partial A}{\partial X_{sp}} \Delta x_{sp}\right)^2 + \left(\frac{\partial A}{\partial W_B} \Delta W_B\right)^2 + \left(\frac{\partial A}{\partial x_B} \Delta x_B\right)^2 + \left(\frac{\partial A}{\partial W_{pb}} \Delta W_{pb}\right)^2 + \left(\frac{\partial A}{\partial C} \Delta C\right)^2 \right\}^{\frac{1}{2}} \quad \ldots\ldots\ldots\ldots \quad (IV.12)$$

where $\frac{\partial A}{\partial W_{sp}} = 1$

$$\frac{\partial A}{\partial W_B} = \frac{x_B+C}{x_{sp}+C}$$

$$\frac{\partial A}{\partial W_{sp}} = \frac{C}{x_{sp}+C}$$

$$\frac{\partial A}{\partial x_{sp}} = \frac{-(W_B.(x_B+C)+W_{pb}.C)}{(x_{sp}+C)^2}$$

$$\frac{\partial A}{\partial x_b} = \frac{W_B}{x_{sp}+C}$$

$$\frac{\partial A}{\partial C} = \frac{W_B(x_{sp}-x_B)W_{pb}.x_{sp}}{(x_{sp}+C)^2}$$

From equation (IV.9), $B = f(x_B, x_{sp}, C)$

The uncertainty in B is calculated according to the relationship.

$$\Delta B = \left\{\left(\frac{\partial B}{\partial x_B}.\Delta x_B\right)^2+\left(\frac{\partial B}{\partial x_{sp}}.\Delta x_{sp}\right)^2+\left(\frac{\partial B}{\partial C}.\Delta C\right)^2\right\}^{\frac{1}{2}} \quad \ldots\ldots\ldots\ldots \text{(IV.13)}$$

where

$$\frac{\partial B}{\partial x_B} = \frac{1}{x_{sp}+C}$$

$$\frac{\partial B}{\partial x_{sp}} = \frac{-(x_B+C)}{(x_{sp}+C)}2$$

$$\frac{\partial B}{\partial C} = \frac{x_{sp}-x_B}{(x_{sp}+C)^2}$$

From equation (IV.5),

$$F_T = f(A, b, W_E)$$

therefore the uncertainty in the calculation of F_T, ΔF_T, is calculated according to the relationship.

$$\Delta F_T = \left\{ \left(\frac{\partial F}{\partial A} . \Delta A\right)^2 + \left(\frac{\partial F}{\partial B} . \Delta B\right)^2 + \left(\frac{\partial F}{\partial W_E} . \Delta W_E\right)^2 \right\}^{\frac{1}{2}} \quad \text{.......... (IV.14)}$$

where $\frac{\partial F_T}{\partial A} = 1$

$$\frac{\partial F_T}{\partial B} = W_E .$$

$$\frac{\partial F_T}{\partial W_E} = B$$

APPENDIX V. Analysis of the experimental error in the determination of the volume of the tyre.

The volume of the tyre is calculated from the relationship:

$$V_T = \frac{d . \rho_2 . A}{\rho_1 . S} \quad \text{.......................... (V.1)}$$

where d = the absolute pressure in mm Hg

ρ_2 = density of mercury

ρ_1 = density of water

A = cross-sectional area of the expansion column,

S = slope of the graph of h against H.

The most probable value of the experimental error in V_T is calculated from the relationship.

$$\Delta V_T = \pm \left\{ \left(\frac{\partial V_T}{\partial d} \Delta d\right)^2 + \left(\frac{\partial V_T}{\partial \rho_2/\rho_1} . \Delta \rho_2/\rho_1\right)^2 + \left(\frac{\partial V_T}{\partial A} . \Delta A\right)^2 + \left(\frac{\partial V_T}{\partial S} . \Delta S\right)^2 \right\}^{\frac{1}{2}} \quad \text{(V.2)}$$

$$\frac{\partial V_T}{\partial d} = (p_2/p_1)\cdot\frac{A}{S}$$

$$\frac{\partial V_T}{\partial (p_2/p_1)} = \frac{d.A}{S}$$

$$\frac{\partial V_T}{\partial A} = p_2/p_1\cdot\frac{d}{S}$$

$$\frac{\partial V_T}{\partial S} = \frac{d.p_2 A}{p_1 . S^2}$$

If the volume of the tyre is calculated from the relationship,

$$V_T = d.\frac{p_2}{p_1}.\left(\frac{A}{S}-a\right) \qquad \text{......(V.3)}$$

where a is the cross-sectional area of the water differential manometer, the most probable value of the experimental error is calculated from the relationship

$$\Delta V_T = \pm\left\{\left(\frac{\partial V_T}{\partial d}.\Delta d\right)^2+\left(\frac{V_T\cdot\Delta(p_2/p_1)}{\partial(p_2/p_1)}\right)^2+\left(\frac{\partial V_T}{\partial A}.\Delta A\right)^2+\left(\frac{\partial V_T}{\partial S}\Delta S\right)^2+\left(\frac{\partial V_T}{\partial a}\Delta a\right)^2\right\}^{\frac{1}{2}} \qquad \text{.......(V.4)}$$

where

$$\frac{\partial V_T}{\partial d} = \frac{p_2}{p_1}\left(\frac{A}{S}\ \ a\right)$$

$$\frac{\partial V_T}{\partial (p_2/p_1)} = d\left(\frac{A}{S}\ \ a\right)$$

$$\frac{\partial V_T}{\partial A} = \frac{p_2 . d}{p_1 . S}$$

$$\frac{\partial V_T}{\partial S} = \frac{d.p_2 A}{p_1 . S^2}$$

$$\frac{\partial V_T}{\partial a} = \frac{d.p_2}{p_1}$$

APPENDIX VI. Work done by air

The work done by air culculated by measuring the change in pressure is represented by the equation (4.16) of chapter (4).

$$W_p = (p_i + p_a)V_T \, \text{In.}\left\{\frac{p_f + p_a}{p_i + p_a}\right\} + p_a V_T\left\{\left(\frac{p_i + p_a}{p_f + p_a}\right) - 1\right\}$$

where

$$p_a = \rho_w g_1 \, hc_b$$

$$p_i = \rho_w g_1 \, hcm$$

$$p_f = \rho_w g_1 (hcm + h'_{cw})$$

substituting the above values in the above equation and rearranging,

$$W_p = \rho_w g_1 V_T \left[(hcm + hc_b) \ln\left(\frac{hcm + h'cw + hc_b}{hcm + hc_b}\right) + hc_b\left(\frac{hcm + hc_b}{hcm + h'cw + hc_b} - 1\right)\right]$$

Assuming that the percentage uncertainty in p and g are negligible.

$$W_p = f(V_T, h_{cb}, h_{cm}, h'_{cw})$$

therefore,

$$\frac{\partial W_p}{\partial V_T} = \rho_w g_1 \left[(h_{cm} + h_{cb}) \text{In}\left\{\frac{h_{cm} + h'_{cw} + h_{cb}}{h_{cm} + h_{cb}}\right\} + h_{cb}\left\{\frac{h_{cm} + h_{cb}}{h_{cm} + h'_{cw} + h_{cb}} - 1\right\}\right]$$

$$= \frac{W_p}{V_T}$$

$$\frac{\partial W_p}{\partial h_{cb}} = P_w \cdot g_t V_T \quad \frac{\ln(h_{cm}+h'_{cw}+h_{cb})}{h_{cm}+h_{cb}} - \frac{h'_{cw}(h_{cb}+2(h_{cm}+h'_{cw})}{(h_{cm}+h'_{cw}+h_{cb})^2}$$

$$\frac{\partial W_p}{\partial h_{cm}} = P_w \cdot g_t V_T \quad \frac{\ln(h_{cm}+h'_{cw}+h_{cb})}{(h_{cm}+h_{cb})} - \frac{h'_{cw}(h_{cm}+h'_{cw})}{(h_{cm}+h'_{cw}+h_{cb})^2}$$

$$\frac{\partial W_p}{\partial h'_{cw}} = P_w \, g_t V_T \quad \frac{(h_{cm}+h_{cb})}{(h_{cm}+h'_{cw}+h_{cb})} - \frac{h_{cb}(h_{cm}+h_{cb})}{(h_{cm}+h'_{cw}+h_{cb})^2}$$

The uncertainty in the work done by air is calculated in accordance with the equation,

$$\Delta W_p = \left\{ \left(\frac{W_p}{V}\Delta V_T\right)^2 + \left(\frac{W_p}{h_{cb}} \cdot \Delta h_{cb}\right)^2 + \left(\frac{W_p}{h_{cm}}\Delta h_{cm}\right)^2 + \left(\frac{W_p}{h'_{cw}} \cdot \Delta h'_{cw}\right)^2 \right\}^{\frac{1}{2}} \quad \text{.. (VI.1)}$$

where

ΔV_T = uncertainty in the volume measurement of tyre

Δh_{cb} = uncertainty in the barometric

Δh_{cm} = uncertainty in the mercury height in the mercury manometer.

$\Delta h'_{cw}$ = uncertainty in the equivalent mercury height in the water manometer.

Volume of expanded air

The volume of the expanded air is calculated according to the relationship.

$$V_c = \frac{\pi}{4} \cdot d_c^2 \cdot h_c \quad \text{........................} \quad \text{(VI.2)}$$

The uncertainty in the calculation of the volume of expanded air, V_c, is represented by the relationship

$$\Delta V_c = \left\{ \left(\frac{\partial V_c}{\partial d_c} \cdot \Delta d_c\right)^2 + \left(\frac{\partial V_c}{\partial h_c} \cdot \Delta h_c\right)^2 \right\}^2 \quad \ldots\ldots\ldots\ldots\ldots \text{(VI.3)}$$

where

$$\frac{\partial V_c}{\partial d_c} = \frac{\pi}{2} \cdot d_c \cdot h_c$$

$$\frac{\partial V_c}{\partial h_c} = \frac{\pi}{4} \cdot d_c^2$$

Δd_c = uncertainty in the measurement of diameter of expansion/compression column.

Δh_c = uncertainty in the measurement of the height of expansion/compression column.

<u>Work done by air by measurement of change in volume.</u>

From equation (4.18) of chapter (4), the work done by air is represented by

$$W_v = (p_i + p_a) V_T \, \text{In} \frac{1}{1 - \frac{V_c}{V_T}} - p_a V_c$$

where

p_a = atmospheric pressure $= \rho_L \cdot g_L h_{cb}$

p_i = intial pressure $= \rho_L g_L h_{cm}$

substituting the values in the above equation and rearranging, gives

$$W_v = \rho_L g_L (h_{cm} + h_{cb}) V_T \, \text{In}\left(\frac{1}{1 - V_c/V_T}\right) - h_{cb} \cdot V_c \quad \ldots\ldots\ldots \text{(VI.4)}$$

Assuming that the percentage of uncertainty in ρ_m and g_l are negligble,

$$W_v = f(V_T, h_{cm}, h_{cb}, V_c)$$

the derivatives of W_v are,

$$\frac{\partial W_v}{\partial V_T} = \rho_m g_1 (h_{cm} + h_{cb}) \; \mathrm{In}\left(\frac{1}{1 - V_c/V_T}\right) - \left(\frac{(V_c/V_T}{1 - V_c/V_T}\right)$$

$$\frac{\partial W_v}{\partial h_{cm}} = \rho . g_1 V_T \; \mathrm{In}\left(\frac{1}{1 - V_c/V}\right)$$

$$\frac{\partial W_v}{\partial h_{cb}} = \rho_m g_1 \; V_T \; \mathrm{In}\left(\frac{1}{1 - V_c/V_o}\right) - V_c$$

$$\frac{\partial W_v}{\partial V_c} = \rho_m g_1 \; (h_{cm} + h_{cb})\left(\frac{1}{1 - V_c/V_T}\right) - h_{cb}$$

therefore the uncertainty in the calculation of work done by the measurement of change in volume is,

$$\Delta W_v = \left\{ \left(\frac{\partial W_v}{\partial V_T} \, \Delta V_T\right)^2 + \left(\frac{\partial W_v}{\partial h_{cm}} . \Delta h_{cm}\right)^2 + \left(\frac{\partial W_v}{\partial h_{cb}} . \Delta h_{cb}\right)^2 + \left(\frac{\partial W_v}{\partial V_c} . \Delta V_c\right)^2 \right\}^{\frac{1}{2}}$$

.... (VI.5)

APPENDIX VII <u>Computation of corrections for the barometer and the manometer.</u>

<u>Fortin Barometer</u>

The following readings are taken:

Reading of mercury height	:	h_b	mm
Barometer temperature	:	t	^oC

The corrected height of the mercury column is calculated according to the following equation. (42)

$$h_{cb} = (h_b + C_s) \cdot \frac{g_1}{g_s} \left\{ 1 - \frac{(\beta_m - \alpha_b) t}{1 + \beta_m t} \right\} \ldots\ldots\ldots\ldots \text{(VII.1)}$$

where

g_s = standard acceleration of gravity = 9.806 65 ms^{-2}

β_m = coefficient of expansion of mercury = 0.000 181 8 $^oC^{-1}$

α_b = coeffient of linear expansion of brass = 0.000 018 4 $^oc^{-1}$

Local acceleration of gravity ( ) g_1 = 9.811 818 6 ms^{-2}

Scale corrections (includes correction for zero, capillary and vacuum errors)( )C_s = 0.15 mm H_g

Brass scale calibrated to be accurate at 0^oC.

Analysis of experimental error

The corrected height of the barometer reading is according to equation (VII.1)

$$h_{cb} = (h_b + C_s) \cdot \frac{g_1}{g_s} \left\{ 1 - \frac{(\beta m - \alpha_b) \cdot t}{(1 + \beta m \cdot t)} \right\}$$

Assuming that the percentage uncertainty in C_s, g_l, g_s, βm, α_b are small,

$$h_{cb} = f(h_b, t)$$

therefore

$$\Delta h_{cb} = \left\{ \left(\frac{\partial h_{cb}}{\partial h_b} \cdot \Delta h_b\right)^2 + \left(\frac{\partial h_{cb}}{\partial t} \cdot \Delta t\right)^2 \right\}^{\frac{1}{2}}$$

where

$$\frac{\partial h_{cb}}{\partial h_b} = g_1/g_s . \left\{ 1 - \frac{(\beta m - \alpha_o) t}{1 + \beta m . t} \right\}$$

$$\frac{\partial h_{cb}}{\partial t} = -(h_b + C_s) . g_1/g_s . \frac{(\beta m - \alpha_b)}{(1 + \beta mt)^2}$$

Thus the uncertainty in the height of the barometer reading is

$$\Delta h_{cb} = \frac{g_1}{g_s} . \left[\left\{ (1 - \frac{(\beta m - \alpha_b) t}{1 + \beta mt} . \Delta h_o \right\}^2 + \left\{ -(h_o + C_s) \frac{(\beta m - \alpha_b)}{(1 + \beta mt)^2} . \Delta t \right\}^2 \right]^{\frac{1}{2}} \quad \text{(VII.2)}$$

Mercury U-tube manometer

The following readings are taken :

Reading on scale : Left-hand arm : h_{1m} mm.

Right-hand arm: h_{rm} mm.

Manometer temperature : t ^oC

The corrected height of the mercury column is calculated according to the following relationship.

$$h_{cm} = (h_{1m} + h_{rm} + C_s) \frac{g_1}{g_s} \frac{\rho_{20}}{\rho_s} \frac{(1 - (\beta m - \alpha_g)(t - 20)}{1 + \beta m(+-20)} \quad \ldots\ldots \quad \text{(VII.3)}$$

where ρ_{20} = density of mercury at 20^oC = 13.545 884 g cm^{-3}

ρ_s = density of mercury at 0^oC = 13.595 1 g cm^{-3}

α_g = coefficient of linear expansion of glass = 0.000 009 6^oC

Bore of manometer tube d_m = 5.75 mm.

Paper scale attached to the glass-tube are assumed to be accurate at 20^oC

Scale corrections ( ) C_s = 0.025 mm. Hg

Analysis of experimental error

The corrected height of the mercury manometer reading is given by the equation (VI.3).

$$h_{cm} = (h_{1m}+h_{rm}+C_s) \cdot \frac{g_1}{g_s} \cdot \frac{\rho_{20}}{\rho_s} \cdot \left[1 - \frac{(\beta_m - \alpha_g)(t-20)}{1+\beta_m(t-20)} \right]$$

Assuming that the uncertainties in g_1, g_s, β_m, α_g, C_s are negligible.

$$h_{cm} = f(h_{1m}, h_{rm}, t)$$

therefore

$$\Delta h_{cm} = \left\{ \left(\frac{\partial h_{cm}}{\partial h_{1m}} \cdot \Delta h_{1m} \right)^2 + \left(\frac{\partial h_{cm}}{\partial h_{rm}} \Delta h_{rm} \right)^2 + \left(\frac{\partial h_{cm}}{\partial t} \Delta t \right)^2 \right\}^{\frac{1}{2}}$$

where

$$\frac{\partial h_{cm}}{\partial h_{1m}} = \frac{g_1}{g_s} \cdot \frac{\rho_{20}}{\rho_s} \quad 1 - \frac{(\beta_m - \alpha_g)(t-20)}{1+\beta_m\,(t-20)}$$

$$\frac{\partial h_{cm}}{\partial h_{rm}} = \frac{g_1}{g_s} \cdot \frac{\rho_{20}}{\rho_s} \quad 1 - \frac{(\beta_m - \alpha_g)(t-20)}{1+\beta_m(t-20)}$$

$$\frac{\partial h_{cm}}{\partial t} = \frac{g_1}{g_s} \cdot \frac{\rho_{20}}{\rho_s} \cdot (h_{1m}+h_{rm}+C_s) \cdot \frac{(\beta_m - \alpha_g)}{1+\beta_m(t-20)^{\;2}}$$

Thus the uncertainty in the height of the mercury manometer reading is

$$\Delta h_{cm} = \frac{g_1}{g_s} \cdot \frac{\rho_{20}}{\rho_s} \cdot \left\{ \left(1 - \frac{(\beta_m - \alpha_g)(t-20)}{1+\beta_m(t-20)}\right)^2 \left(h_{1m}^2 + h_{rm}^2\right) + \left(\frac{-(h_{1m}+h_{rm}+C_s)(\beta_m - \alpha_g) \cdot t}{(1+\beta_m(t-20))^2} \right)^2 \right\}^{1/2} \qquad \text{(VI.4)}$$

Water differential manometer

The following readings are taken

Reading on scale: Left-hand arm : h_{lw} mm.

Right-hand arm: h_{rw} mm.

Manometer temperature : t ^{o}C

The corrected height of the water column in mm H_g is calculated according to the relationship:

$$h_{cw} = \frac{(h_{lw} + h_{rw} + C_s) x g_1}{S} \frac{}{g_s} \times \frac{\rho_{20}}{\rho_s} \times \left(1 - \frac{(\beta_w - \alpha_g)(t-20)}{1 + \beta_w(t - 20)}\right) \quad \ldots \text{(VII.5)}$$

where :

S = relative density of mercury, $\frac{(\rho_m)}{\rho_w}$ = 13.595 43

β_w = coefficient of expansion of water = 0.000 195 9 $^{o}C^{-1}$

Bore of manometer tube, dw = 5.32 mm.

Paper scales attached to the glass-tubes are assummed to be accurate at 20^{o}C

Scale accuracy of paper C_s = 0.025 mm.

Analysis of experimental error

The corrected height of the water differential manometer in mm Hg is given by the equation (VII.5).

$$h_{cw} = \frac{(h_{lw}+h_{rw}+C_s) \cdot g_1 \cdot}{S} \frac{}{g_s} \frac{\rho_{20}}{\rho_s} \cdot \left(1 - \frac{(\beta_w - \alpha_g)(t-20)}{1 + \beta_w(t-20)}\right)$$

Assuming that the percentage uncertainties in g_1, g_s, β_w, α_g, C_s, S are negligible.

$$h_{cw} = f(h_{lw}, h_{rw}, t)$$

therefore,

$$\Delta h_{cw} = \left\{ \left(\frac{\partial h_{cw}}{\partial h_{lw}} \cdot \Delta h_{lw} \right)^2 + \left(\frac{\partial h_{cw}}{\partial h_{rw}} \cdot \Delta h_{rw} \right)^2 + \left(\frac{\partial h_{cw}}{\partial t} \cdot \Delta t \right)^2 \right\}^{\frac{1}{2}}$$

where

$$\frac{\partial h_{cw}}{\partial h_{lw}} = \frac{g_1 \cdot \rho_{20}}{s \cdot g_s \cdot \rho_s} \left[1 - \frac{(\beta_w - \alpha_g)(t - 20)}{1 + \beta_w (t - 20)} \right]$$

$$\frac{\partial h_{cw}}{\partial h_{rw}} = \frac{g_1 \cdot \rho_{20} \cdot}{s \cdot g_s \cdot \rho_s} \left[1 - \frac{(\beta_w - \alpha_g)(t - 20)}{1 + \beta_w (t - 20)} \right]$$

$$\frac{\partial h_{cw}}{\partial t} = \frac{g_1 \cdot \rho_{20} . (h_{lw} + h_{rw} + C_s)}{s \cdot g_s \cdot \rho_s} \quad \frac{(\beta_w - \alpha_g)}{\left(1 + \beta_w (t - 20)\right)^2}$$

Thus the uncertainty in the height of the water manometer reading is

$$\Delta h_{cw} = \frac{g_1 \cdot \rho_{20}}{s \cdot g_s \cdot \rho_s} \left\{ \left[1 - \frac{(\beta_w - \alpha_g)(t - 20)}{1 + \beta_w (t - 20)} \right]^2 (\Delta h_{lw}^2 + \Delta h_{rw}^2) + \left[- \frac{(h_{lw} + h_{rw} + C_s)(\beta_w - \alpha_g)\, \Delta t}{(1 + \beta_w (t - 20))^2} \right]^2 \right\}^{\frac{1}{2}} \qquad \text{(VII.6)}$$

```
00001'*******************************************************************
00002'*                                                                  *
00003'*     This program calculates the following quantities:           *
00004'*                                                                  *
00005'*            1.  The corrected barometer and manometer height     *
00006'*            2.  Volume and pressure changes of air               *
00007'*            3.  Work done on/by air                              *
00008'*            4.  Linear regression                                *
00009'*            5.  Volume of tyre                                   *
00010'*            6.  External work done on tyre                       *
00011'*            7.  Work done on tyre structure                      *
00012'*                                                                  *
00013'*******************************************************************
00014'
00015'
00020   Rem  Open the input and output file
00030'
00040   Open "WSPROG.DAT" for output as file #1
00050   Open "INPUT3 .DAT" for input as file #2
00060   Open "PLDDAT.DAT" for output as file #3
00062   Open "PREDEF.DAT" for output as file #4
00064   Open "WOKDEF.DAT" for output as file #5
00066   Open "STRDEF.DAT" for output as file #6
00068   Open "FORDEF.DAT" for output as file #7
00070'
00075   MARGIN ALL 132
00080   Rem enter the dimensions of the variables
00100   DIM T(30), T1(30), A(21)
00110   DIM X(30), Y(30)
00120   DIM H1(30), V1(30), V2(30), V3(30)
00130   DIM P (30), P1(30), P2(30), R1(30), R2(30), R3(30), R4(30)
00140   DIM F1(30), Z(30), Z1(30), Z2(30), Z3(30)
00150   DIM W1(30), W2(30), W3(30), W4(30), W5(30), W6(30)
00160   DIM S1(30), S2(30), S3(30),S4(30),S5(30),S6(30)
00170'
00180'
00200   Rem read the t-value at 95% level of significance
00210'
00220   MAT READ T(30)
00230   DATA 12.706,4.303,3.182,2.776,2.571,2.447,2.365,2.306,2.262,2.228
00240   DATA 2.201,2.179,2.160,2.145,2.131,2.120,2.110,2.101,2.093,2.086
00250   DATA 2.080,2.074,2.069,2.064,2.060,2.056,2.052,2.048,2.045,2.042
00260'
00270   Rem read the t-value at 99% level of significance
00280'
00290   MAT READ T1(30)
00300   DATA 63.657,9.925,5.841,4.604,4.032,3.707,3.499,3.355,3.250,3.169
00310   DATA 3.106,3.055,3.012,2.997,2.947,2.921,2.898,2.878,2.861,2.845
00320   DATA 2.831,2.819,2.807,2.797,2.787,2.779,2.771,2.763,2.756,2.750
```

```
00330'
00340'
00350   Rem read the values of the constants
00360'
00370   MAT READ A(21)
00380   DATA 0.15,0.025,9.8118186,9.80665,1.816E-4,1.959E-4,1.84E-5,9.6E-6
00390   DATA 13.5951,13.545884,13.59543,0.05,0.5,0.5,1.005271,0.99637987
00400   DATA 133.3224,0.02606,0.00532,0.00002,0.00005
00410'
00420'
00440 A$="++++++++++++++++++++++++++++++++++++++++++++++++++++++++++++++++++++++++++++"
00450'
00500   Rem Defined Functions
00510   DEF FNA(D1,D2)=A(15)*A(16)*(D1+A(2))*D2
00520   DEF FNC(D3,D4,D5)=A(13)*A(15)*A(16)*SQR((2*D4*D4)+((D5+A(2))*D3)**2)
00530   DEF FND(D)=PI*D*D/4
00540   DEF FNP(D6)=D6*A(3)*A(10)*1E-3
00550   DEF FNV(D7,D8,D9)=D7*1E-3*A(11)*(FND(A(18)))*(1/D8-((A(19)/A(18))**2)*(1+1/D9)/2)
00560   DEF FNW(U1,U2,U3)=A(17)*A2 *(((LN(U3))*U1)+(U2*(1/U3-1)))
00600   GOTO 2750
00610'
00620'
01000   REM SUBROUTINE PROGRAMS
01010'
01020   Rem subroutine for the linear regression analysis
01030'
01040   Rem calculation of the sums and sums of squares
01050   X1=X2=Y1=Y2=Z=0
01060   FOR I=1 TO N
01070           X1=X1+X(I)
01080           X2=X2+X(I)*X(I)
01090           Y1=Y1+Y(I)
01100           Y2=Y2+Y(I)*Y(I)
01110           Z =Z +X(I)*Y(I)
01120   NEXT I
01130'
01140   Rem calculation of the means
01150   M1=X1/N
01160   M2=Y1/N
01170'
01180   Rem calculation of the sum of squares of deviations
01190   S1=X2-N*M1*M1
01200   S2=Y2-N*M2*M2
01210   S3=Z -N*M1*M2
01220'
01230   Rem calculation of slope and intercept
01240   B=S3/S1
01250   A=M2-B*M1
01260'
01270   Rem calculation of analysis of variance
01280   S4=S2-(B*B*S1)
```

```
01290  F =B*B*S1*(N-2)/S4
01300'
01310  Rem print the calculated values
01330  PRINT #1
01340  PRINT #1,A$
01350  PRINT #1
01360  PRINT #1,"Number of pairs of data: N = ";N
01370  PRINT #1
01380  PRINT #1,"Variables","Mean","Std.Deviation"
01390  PRINT #1,"    X    ",M1    ,SQR (S1/(N-1))
01400  PRINT #1,"    Y    ",M2    ,SQR (S2/(N-1))
01410  PRINT #1
01420  PRINT #1,"For the least square line"
01430  PRINT #1,"Intercept","Slope"
01440  PRINT #1,    A      ,B
01450  PRINT #1
01460  PRINT #1,"Analysis of variance"
01470  PRINT #1,"Source","S.S","D.O.F","M.S","M.S.R"
01480  PRINT #1,"Regression",B*B*S1,N-(N-1),B*B*S1,F
01490  PRINT #1,"Residual",S4,N-2,S4/(N-2)
01500  PRINT #1,"Total",S2,N-1
01510  PRINT #1
01520  PRINT #1,"Std.Err.B","Std.Err.A","Corr.Coef"
01525  B2=SQR (S4/(S1*(N-2)))
01530  PRINT #1,B2,SQR((S4*(S1+(N*M1*M1)))/(N*S1*(N-2))),B*SQR(S1/S2)
01540'
01545  PRINT #1
01550  Rem test the significance of the regression coefficient
01560  Rem (Null hypothesis)
01570  T=(B-0)/SQR (S4/(S1*(N-2)))
01580  PRINT #1,,"t-cal = ";T,
01590  IF T<T1(N-2) THEN PRINT #1,"***"
01600  IF T>T1(N-2) AND T<T(N-2) THEN PRINT #1,"**"
01610  PRINT #1
01615  PRINT #1
01620'
01630  PRINT #1,,"X(expt)","Y(expt)","Y(cal)"
01640  FOR I=1 TO N
01650          PRINT #1,,X(I),Y(I),A+B*X(I)
01660  NEXT I
01670  PRINT #1
01680  PRINT #1,A$
01690  PRINT #1,<PA>
01700  RETURN
01710'
02000  Rem Subroutine for temperature corrections
02010  C1=(B1-L)/(1+B1*T)**2
02020  C2=1-C1*T
02030  RETURN
02040'
02050'
```

```
02500   Rem Subroutine for the calculation of external work done
02510'      on the tyre by the trapezoidal method
02520   W=W + (F1(I+1)+F1(I))*(Z(I+1)-Z(I))/2
02530   RETURN
02540'
02550'
02560   Rem subroutine for printing the labels of the table
02570'
02580:     'LLLLLL   'LLLLL      'LLLLLLLL     'LLLLLLLL     'LLLLLLLL   'LLLLL
02600'
02610   PRINT #1,A$
02620   PRINT #1 USING 2580,"F(kN)","Z(mm)","Wt(J)","Wa(J)","Ws(J)","Ws(%)"
02625   PRINT #1,A$
02630   PRINT #1
02640   RETURN
02650'
02660'
02670'
02680   REM MAIN PROGRAM
02690'
02700'
02750   Rem Date of experiment or END
02760   READ #2, B$
02765   IF LEFT$(B$,1) = "E" THEN 10195
02770   PRINT'#1,"Date of experiment : ";B$
02775   PRINT B$
02780   PRINT #1
02785'
02790   Rem Inflation pressure <NEW> or <SAME>
02795   READ #2, C$
02800   IF LEFT$ (C$,1)= "S" THEN GOTO 4250
02810'
02820'
03000   Rem Barometer Readings
03010   Rem read data in the order of T,H
03040   READ #2,T, H
03050   B1=A(5)
03060   L =A(7)
03070   GOSUB 2000
03080'
03090   Rem correction of barometer reading
03100   P1=A(15)*C2*(H+A(1))
03110   P2=A(15)*SQR((C2*A(12))**2+((H+A(1))*C1*A(14))**2)
03120'
03130'
04000   Rem Mercury Manometer Reading
04010   Rem read data in the order of T,H(left),H(right)
04025   READ #2,T, H1, H2
04030   T=T-20
04040   B1=A(5)
04050   L =A(8)
```

```
04060   GOSUB 2000
04070'
04080   Rem correction of the mercury manometer readings
04090   P3=FNA(H1+H2,C2)
04100   P4=FNC(C1,C2,H1+H2)
04110'
04120   Rem calculation of the absolute initial pressure
04130   P5=P1+P3
04140   P6=SQR(P2*P2+P4*P4)
04150'
04160'
04170   Rem volume of tyre in m↑3
04180   READ #2, A2
04210'
04215   Rem ratio of Vr/Vt
04220   READ #2 , A1
04223
04250   Rem print the calculated pressures
04255   PRINT #1
04260:  'LLLLLLLLLLL pressure (kPa) :  ####.####  +/-  ####.####
04270   PRINT #1 USING 4260,"Atmospheric",FNP(P1),FNP(P2)
04280   PRINT #1 USING 4260,"Inflation",FNP(P3),FNP(P4)
04290   PRINT #1 USING 4260,"Absolute",FNP(P5),FNP(P6)
04295   PRINT #3, FNP(P3)
04305   PRINT #1
04310'
04320   Rem set counter to zero
04330   k=0
04340'
04350'
05000   Rem calculation of the volume of the air expanded/compressed
05010   H1(1)=V1(1)=0
05020'
05030'
05040   Rem read the number of data N
05050   READ #2 , N
05060'
05070'
05075   Rem read the Nth. values of Hc(mm)
05080   FOR I = 1 TO N
05090           Rem read the height of the expanded/compressed air
05105           READ #2, H1
05110           H1(I+1) = H1
05120'
05130           Rem calculate the volume of the expanded/compressed air(M↑3)
05140           V1(I+1) = FND (A(18))*H1*1E-3
05150           V2(I+1) = FND (A(18))*SQR ((2*H1*1E-3*A(20)/A(18))**2+A(21)**2)
05160           V3(I+1) = V1(I+1)/A2
05170'
05180   NEXT I
05190'
```

```
04060   GOSUB 2000
04070'
04080   Rem correction of the mercury manometer readings
04090   P3=FNA(H1+H2,C2)
04100   P4=FNC(C1,C2,H1+H2)
04110'
04120   Rem calculation of the absolute initial pressure
04130   P5=P1+P3
04140   P6=SQR(P2*P2+P4*P4)
04150'
04160'
04170   Rem volume of tyre in m↑3
04180   READ #2, A2
04210'
04215   Rem ratio of Vr/Vt
04220   READ #2 , A1
04223
04250   Rem print the calculated pressures
04255   PRINT #1
04260:  'LLLLLLLLLLL pressure (kPa) :  ####.####  +/-  ####.####
04270   PRINT #1 USING 4260,"Atmospheric",FNP(P1),FNP(P2)
04280   PRINT #1 USING 4260,"Inflation",FNP(P3),FNP(P4)
04290   PRINT #1 USING 4260,"Absolute".FNP(P5),FNP(P6)
04295   PRINT #3, FNP(P3)
04305   PRINT #1
04310'
04320   Rem set counter to zero
04330   k=0
04340'
04350'
05000   Rem calculation of the volume of the air expanded/compressed
05010   H1(1)=V1(1)=0
05020'
05030'
05040   Rem read the number of data N
05050   READ #2 , N
05060'
05070'
05075   Rem read the Nth. values of Hc(mm)
05080   FOR I = 1 TO N
05090           Rem read the height of the expanded/compressed air
05105           READ #2, H1
05110           H1(I+1) = H1
05120'
05130           Rem calculate the volume of the expanded/compressed air(M↑3)
05140           V1(I+1) = FND (A(18))*H1*1E-3
05150           V2(I+1) = FND (A(18))*SQR ((2*H1*1E-3*A(20)/A(18))**2+A(21)**2)
05160           V3(I+1) = V1(I+1)/A2
05170'
05180   NEXT I
05190'
```

```
05200'
05500  Rem calculation of the rise in pressure pressure rise ratio
05510  P1(1)= R1(1) = 0
05520'
05522  PRINT #1,A$
05525  PRINT #1 USING 9020,"P(mmH2O)","P1(mmHg)","P1/P5","Pf/P5","P1c/P5","Pfc/P5"
05527  PRINT #1,A$
05530'
05532  PRINT #1
05537'
05538  Rem read the Nth. values of Tw, Hwl, Hwr
05540  FOR I= 1 TO N
05550         Rem read data in the order of T, H(left), H(right)
05565         READ #2, T, H1, H2
05570         T=T-20
05580         B1=A(6)
05590         L =A(8)
05600         GOSUB 2000
05610'
05620         Rem correction of the water manometer readings (mm)
05625         P (I+1)=FNA(H1+H2,C2)
05630         P1(I+1)=(FNA(H1+H2,C2))/A(11)
05640         P2(I+1)=(FNC(C1,C2,H1+H2))/A(11)
05650'
05660         Rem calculation of pressure rise ratio
05670         R1(I+1)=P1(I+1)/P5
05680         R2(I+1)=1 + R1(I+1)
05690'
05700         Rem calculation of the corrected pressure rise ratio
05710         R3(I+1)=R1(I+1)+FND(A(19))*(H1+H2)*1E-3*(1+1/A1)/(2*A2)
05720         R4(I+1)=1 + R3(I+1)
05730'
05732  PRINT #1 USING 9010,P(I+1),P1(I+1),R1(I+1),R2(I+1),R3(I+1),R4(I+1)
05740  NEXT I
05750'
05755  PRINT #1,<PA>
05770'
05780'
06000  Rem linear regression analysis of P(I+1) vs H1(I+1)
06010  FOR I= 1 TO N
06020         X(I)=H1(I+1)
06030         Y(I)=P (I+1)
06040  NEXT I
06050'
06060  PRINT #1,"Linear regression analysis of P(I+1) vs H1(I+1)"
06070  GOSUB 1000
06080'
06085  PRINT #1,,"Volume of tyre at different volume ratios"
06087  PRINT #1
06079: Vr/Vt =  ##.###        Vt =  ##.########       m^3
06100'
```

```
06110  FOR R = 1 TO 0.8 STEP -0.025
06120         PRINT #1 USING 6090,R,FNV(P5,B,R)
06130  NEXT R
06140'
06150'
06160  PRINT #1,<PA>
06170'
06250  Rem linear regression analysis of V1(I+1) vs R1(I+1)
06260  FOR I=1 TO N
06270         X(I)=R1(I+1)
06280         Y(I)=V1(I+1)
06290  NEXT I
06300'
06310  PRINT #1,"Linear regression analysis of Del.V vs Del.P/P(initial)"
06320  GOSUB 1000
06330'
06500  Rem linear regression analysis of V1(I+1) vs R3(I+1)
06510  FOR I=1 TO N
06520         X(I)=R3(I+1)
06530         Y(I)=V1(I+1)
06540  NEXT I
06550'
06560  PRINT #1,"Linear regression analysis of Del.V vs corr.Del.P/P(initial)"
06570  GOSUB 1000
06580'
06590'
06600  Rem add one to the counter
06610  k=k + 1
06615  PRINT , k
06620'
06630'
06640  Rem set flag
06650  ON k GOTO 7000,8000
06660'
06670'
07000  Rem read the load and deflections datas
07010  F1(1)=Z1(1)=Z2(1)=Z3(1)=0
07020'
07025  Rem read the Nth. values of Fi, Ze, Zc1, Zc2
07027  PRINT #7, N
07030  FOR I=1 TO N
07047         READ #2, F1(I+1), Z1(I+1), Z2(I+1), Z3(I+1)
07048         PRINT #3 F1(I+1)*1E3,(Z1(I+1)+Z2(I+1)+Z3(I+1))/3
07049         PRINT #7, F1(I+1), Z1(I+1), Z2(I+1), Z3(I+1)
07050  NEXT I
07060  PRINT #3,"-1.0","-1.0"
07065  PRINT #3\PRINT #7
07080'
07090'
07100  REM CALCULATE THE EXTERNAL WORK DONE ON THE TYRE
07110'
```

```
07120   Rem external work done w.r.t. expansion process
07130   W=Z(1)=0
07140   FOR I=1 TO N
07150           Z(I+1)=Z1(I+1)
07160           GOSUB 2500
07170           W1(I+1)=W
07180   NEXT I
07190'
07200'
07250   Rem external work done w.r.t. 1st. compression process
07260   W=Z(1)=0
07270   FOR I= 1 TO N
07280           Z(I+1)=Z2(I+1)
07290           GOSUB 2500
07300           W2(I+1)=W
07310    NEXT I
07320'
07330'
07500   Rem external work done w.r.t. 2nd. compression process
07510   W=Z(1)=0
07520   FOR I= 1 TO N
07530           Z(I+1)=Z3(I+1)
07540           GOSUB 2500
07550           W3(I+1)=W
07560    NEXT I
07570'
07580'
08500   REM CALCULATION OF THE WORK DONE ON THE STRUCTURE
08510   W4(1)=W5(1)=W6(1)=0
08520'
08530   Rem calculation for the expansion process
08535   PRINT #1,"EXPANSION PROCESS"
08540   FOR I=1 TO N
08550           Rem work done by air
08560           G4= A2/(A2-V1(I+1))
08570           W4(I+1)= FNW (P5,P1,G4)
08580'
08590           Rem work done on the structure of the tyre
08600           S1(I+1)= W1(I+1) - W4(I+1)
08605           S4(I+1)=S1(I+1)/W1(I+1)*100
08610    NEXT I
08620'
08630'
08650   Rem print the calculated values
08660   GOSUB 2560
08670'
08700'
08710   FOR I = 1 TO N
08720           PRINT #1 USING 9000,F1(I+1),Z1(I+1),W1(I+1),W4(I+1),S1(I+1),S4(I+1)
08730    NEXT I
08740'
```

```
08750   PRINT #1,A$
08760   PRINT #1,<PA>
08770'
08780   GOTO 9000
08800   Rem work done on the air w.r.t. 2nd. compression process
08810   FOR I= 1 TO N
08820           Z2(I+1)=Z3(I+1)
08830           W2(I+1)=W3(I+1)
08840   NEXT I
08850'
08860'
08870   Rem format for printing the calculated result
09000: ##.####    ###.##    ####.####    ####.####    ####.####    ###.###
09010: ##.###^^^^  ##.###^^^^  ##.###^^^^  ##.####^^^^  ##.###^^^^ ##.####^^^^
09020:   'LLLLLLLL   'LLLLLLLL   'LLLLLLLL    'LLLLLLL   'LLLLLLL    'LLLLLL
09030'
09040'
09500   Rem compression process (uncorrected pressure)
09510   PRINT #1,"COMPRESSION PROCESS (Uncorrected pressure)"
09520   PRINT #1
09530   GOSUB 2560
09540'
09550   FOR I = 1 TO N
09560           Rem work done on tne air
09570           G1=R2(I+1)
09580           W5(I+1)= FNW (P5,P1,G1)
09590'
09600           Rem work done on the structure of the tyre
09610           S2(I+1)=W2(I+1) - W5(I+1)
09615           S5(I+1)=S2(I+1)/W2(I+1)*100
09620'
09630           Rem print the calculated values
09640           PRINT #1 USING 9000,F1(I+1),Z2(I+1),W2(I+1),W5(I+1),S2(I+1),S5(I+1)
09650'
09660   NEXT I
09670   PRINT #1,A$
09680   PRINT #1,<PA>
09690'
09700'
09750   Rem compression process (corrected pressure)
09760   PRINT #1,"COMPRESSION PROCESS (Corrected pressure)"
09770   PRINT #1
09780'
09790   GOSUB 2560
09800'
09810   FOR I= 1 TO N
09820           Rem work done on the air
09830           G2= R4(I+1)
09840           W6(I+1)= FNW (P5,P1,G2)
09850'
09860           Rem work done on the structure
```

```
09870          S3(I+1)=W2(I+1) - W6(I+1)
09875          S6(I+1)=S3(I+1)/W2(I+1)*100
09880'
09890          Rem print the calculated values
09900          PRINT #1 USING 9000,F1(I+1),Z2(I+1),W2(I+1),W6(I+1),S3(I+1),S6(I+1)
09910'
09920   NEXT I
09930'
09940   PRINT #1,A$
09950   PRINT #1,<PA>
09960'
09970'
09980   Rem linear regression analysis of Wa(exp) vs Wa(comp)
09990   FOR I = 1 TO N
10000          X(I)=W5(I+1)
10010          Y(I)=W4(I+1)
10020   NEXT I
10030'
10040   PRINT #1,"Linear regression analysis of Wa(exp) vs Wa(comp)"
10050   GOSUB 1000
10060'
10070   Rem linear regression analysis of Wa(exp)/Wa(comp) vs Wa(comp)"
10080   FOR I = 1 TO N
10090          X(I)=W5(I+1)
10100          Y(I)=W4(I+1)/W5(I+1)
10110   NEXT I
10120'
10130   PRINT #1,"Linear regression analysis of Wa(exp)/Wa(comp) vs Wa(comp)"
10140   GOSUB 1000
10142   PRINT #4\PRINT #5\PRINT #6
10143   PRINT #4,N\PRINT #5,N\PRINT #6,N
10144   FOR I= 1 TO N
10146          PRINT #4 Z1(I+1),Z2(I+1),P1(I+1),R3(I+1),R4(I+1),V1(I+1)*1E6
10148          PRINT #5 Z1(I+1),Z2(I+1),W1(I+1),W2(I+1),W4(I+1),W6(I+1),S1(I+1),S3(I+1)
10155          PRINT #6 Z1(I+1),Z2(I+1),W4(I+1)/W1(I+1),W6(I+1)/W2(I+1),S4(I+1),S6(I+1)
10158   NEXT I
10160'
10170   Rem set flag
10180   ON k GOTO 5500, 2750
10190'
10195   PRINT " End of data in file #2 "
10196   PRINT #3,"-1.0"
10197'
10200   Rem close file
10210   CLOSE 1,2,3,4,5,6
10220'
10230'
99999   END
```

```
C     ANALYSIS OF TYRE LOAD-PRESSURE-DEFLECTION DATA
C
C
            PROGRAM TWPD
            REAL *8 H1,H2
            DIMENSION W(1000),D(1000),P(1000),WD(1000),SD(3),AA(3),BB(3)
C
C           SPECIFY THE INPUT AND OUTPUT FILE
C
            OPEN(UNIT=20,DEVICE='DSK',FILE='PLDDAT.DAT',ACCESS='SEQIN')
            OPEN(UNIT=1,DEVICE='DSK',FILE='LODEPE.DAT',ACCESS='SEQOUT')
C
C           READ THE TITLE OF THE PROGRAM
C
            TYPE 100
 100        FORMAT (1H ,'TITLE, MAX OF 16 CHRS.')
            READ (5,1) H1,H2
 1          FORMAT (2A8)
C
C
C           READ THE INFLATION PRESSURE
            K=0
 2          READ(20,*)PP
            IF (PP) 6,3,3
C
C           READ THE LOAD AND DEFLECTION
C
 3          READ(20,4)WW,DD
 4          FORMAT (5F)
            IF (DD) 2,5,5
 5          K=K+1
            W(K)=WW
            D(K)=DD
            P(K)=PP
            GO TO 3
 6          CDN=1.0
            DDN=0.1
C
C
C           3 VALUES FOR POWER INDEX
C
            DO 9 J=1,3
 7          DN=CDN+(J-2)*DDN
C
C           TRANSFORM LOAD/DEFLECTION TO GIVE LINEAR EQUATION
C
            DO 8 I=1,K
 8          WD(I)=W(I)/D(I)**DN
 9          CALL REG (P,WD,K,AA(J),BB(J),SD(J))
```

```
C
C      TERMINATE ANALYSIS IF POWER INDEX INCREMENT = 0.0125
C
       IF (DDN.LT.0.013) GO TO 16
       IF (SD(2)-SD(3))11,13,10
C
C      INCREASE POWER INDEX
C
10     CDN=CDN+DDN
       GO TO 7
11     IF (SD(2)-SD(1))15,14,12
C
C      DECREASE POWER INDEX
C
12     CDN=CDN-DDN
       GO TO 7
C
C      HALVE POWER INDEX INCREMENT AND INCREASE INDEX
C
13     DDN=DDN/2.0
       CDN=CDN+DDN
       GO TO 7
C
C      HALVE POWER INDEX AND DECREASE INDEX
C
14     DDN=DDN/2.0
       CDN=CDN-DDN
       GO TO 7
C
C      HALVE POWER INDEX INCREMENT BUT MAINTAIN INDEX
C
15     DDN=DDN/2.0
       GO TO 7
C
C      CHOOSE BEST FIT ON BASIS OF RMS
C
16     IF (SD(2)-SD(3))18,20,17
17     DN=CDN+DDN
       SDN=SD(3)
       A=AA(3)
       B=BB(3)
       GO TO 21
18     IF (SD(2)-SD(1))20,20,19
19     DN=CDN-DDN
       SDN=SD(1)
       A=AA(1)
       B=BB(1)
       GO TO 21
20     DN=CDN
       SDN=SD(2)
       A=AA(2)
```

```
      B=BB(2)
C
C     CALCULATE SUM OF SQUARES ABOUT FITTED EQUATION
C
21    SDA=0.0
      DO 22 I=1,K
22    SDA=SDA+(W(I)-(A+B*P(I))*D(I)**DN)**2.0
C
C     ROOT MEAN SQUARE
C
      SDA=SQRT(SDA/(K-3))
      TYPE 104
      READ(5,*)KP
      TYPE 105
      READ(5,4)(P(J),J=1,KP)
      TYPE 106
      READ(5,*)KD
      TYPE 107
      READ(5,4)(D(J),J=1,KD)
104   FORMAT(1H ,'NUM. OF PRESSURES FOR FITTED VALUES')
105   FORMAT(1H ,'PRESSURES (KPA) - TAB. 5 ')
106   FORMAT(1H ,'NUM. OF DEFLECTIONS FOR FITTED VALUES')
107   FORMAT(1H ,'DEFLECTIONS (MM) -TAB. 5 ')
C
C     CALCULATE FITTED VALUES
C
      I=0
      DO 23 K=1,KP
      DO 23 J=1,KD
      I=I+1
23    WD(I)=(A+B*P(K))*D(J)**DN
      WRITE(1,27)
27    FORMAT(1H ,'ANALYSIS OF LOAD-PRESSURE-DEFLECTION DATA')
      WRITE(1,24)H1,H2,A,B,DN,SDM,SDA
24    FORMAT(///1H ,15X,'W = (A + B*P) * D**N'///1H ,2A8/'1H ,5X,
     1'A =',E11.4,5X,'B =',E11.4,5X,'N =',F7.4//1H ,10X,
     2'REG.N.RMS =',E11.4/1H ,10X,'EQN.N.RMS =',E11.4///1H ,
     3'FITTED VALUES'/1H ,7X,'P' ,9X,'D' ,12X,'W')
C
C     PRINT THE FITTED VALUES
C
      I=0
      DO 25 K=1,KP
      DO 25 J=1,KD
      I=I+1
25    WRITE(1,26)P(K),D(J),WD(I)
26    FORMAT(1H ,F10.1,F10.2,E15.4)
      WRITE(1,28)
28    FORMAT(1H ,5X,'(KPA)',5X,'(MM)',10X,'(N)')
      STOP
      END
```

```
C
      SUBROUTINE REG(X,Y,N,A,B,SD)
C
C     SUBROUTINE FOR LINEAR REGRESSION
C
      DIMENSION X(1000),Y(1000)
      SX=0.0
      SY=0.0
      SXY=0.0
      SXSQ=0.0
      SYSQ=0.0
C
      DO 1 J=1,N
      SX=SX+X(J)
      SY=SY+Y(J)
      SXY=SXY+X(J)*Y(J)
      SXSQ=SXSQ+X(J)*X(J)
    1 SYSQ=SYSQ+Y(J)*Y(J)
      AN=FLOAT(N)
C
C     SLOPE OF LINE
C
      B=(SXY-SX*SY/AN)/(SXSQ-SX*SX/AN)
C
C     INTERCEPT OF THE LINE
C
      A=SY/AN-B*SX/AN
      E=(SYSQ-SY*SY/AN)-B*B*(SXSQ-SX*SX/AN)
C
C     ROOT MEAN SQUARE
C
      SD=SQRT(E/(AN-2.0))
      RETURN
C
C
C
      CLOSE(UNIT=1)
      END
```

```
C         PROGRAM TO CALCULATE THE LOAD DEFLECTION BEHAVIOUR OF A
C         TYRE BY GENT AND THOMAS THEORY OF AIR SPRING.


C         OPEN THE OUTPUT FILE
          OPEN(UNIT=1,DEVICE='DSK',ACCESS='SEQOUT',FILE='WSTIFF.DAT')


C         INITIATE THE PROGRAM
1         PAUSE' THIS IS THE START OF THE PROGRAM '
          TYPE 1000
1000      FORMAT('  ENTER TYPE OF TYRE   ',/)
          READ(5,2000)TITLE1
          WRITE(1,2000)TITLE1
2000      FORMAT( ' TEST TYRE:',2X,A6)


C         ENTER THE INPUT DATA
5         TYPE 3000
3000      FORMAT('  ENTER CHORD(MM),WIDTH(MM),DRIM(MM),NUM. OF ITER')
          READ(5,*)CHORD,WIDTH,DRIM,NUM
3500      FORMAT(//)


C         CONVERT THE DATA INPUT INTO METRES
          METRE=1000
          CHORD=CHORD/(2.0*FLOAT(METRE))
          WIDTH=WIDTH/(2.0*FLOAT(METRE))
          ROWS=WIDTH/CHORD
          CHWID=1.0/ROWS
          DRIM=DRIM/FLOAT(METRE)


C         ENTER THE INFLATION PRESSURE
30        TYPE 4000
4000      FORMAT( ' ENTER THE INFLATION PRESSURE IN KPA (-1.0 TO END)')
          READ(5,*)PRESS
          IF(PRESS.LT.0.0)GOTO 1


C         ENTER THE HEIGHT OF THE TYRE IN MILLIMETRES
          TYPE 4500
4500      FORMAT('  ENTER THE INITIAL AND FINAL HEIGHT IN MM ')
          READ(5,*)HFIRST,HLAST
          DO 750 THEIGH=HFIRST,HLAST,1.0
          HEIGHT=THEIGH/(2.0*FLOAT(METRE))
          WRITE(5,*)THEIGH
          RATIO=HEIGHT/CHORD
```

```
C         PROGRAM TO CALCULATE THE LOAD DEFLECTION BEHAVIOUR OF A
C         TYRE BY GENT AND THOMAS THEORY OF AIR SPRING.


C         OPEN THE OUTPUT FILE
          OPEN(UNIT=1,DEVICE='DSK',ACCESS='SEQOUT',FILE='WSTIFF.DAT')


C         INITIATE THE PROGRAM
1         PAUSE' THIS IS THE START OF THE PROGRAM '
          TYPE 1000
1000      FORMAT('  ENTER TYPE OF TYRE  ',/)
          READ(5,2000)TITLE1
          WRITE(1,2000)TITLE1
2000      FORMAT( ' TEST TYRE:',2X,A6)


C         ENTER THE INPUT DATA
5         TYPE 3000
3000      FORMAT('  ENTER CHORD(MM),WIDTH(MM),DRIM(MM),NUM. OF ITER')
          READ(5,*)CHORD,WIDTH,DRIM,NUM
3500      FORMAT(//)


C         CONVERT THE DATA INPUT INTO METRES
          METRE=1000
          CHORD=CHORD/(2.0*FLOAT(METRE))
          WIDTH=WIDTH/(2.0*FLOAT(METRE))
          ROWS=WIDTH/CHORD
          CHWID=1.0/ROWS
          DRIM=DRIM/FLOAT(METRE)


C         ENTER THE INFLATION PRESSURE
30        TYPE 4000
4000      FORMAT( ' ENTER THE INFLATION PRESSURE IN KPA (-1.0 TO END)')
          READ(5,*)PRESS
          IF(PRESS.LT.0.0)GOTO 1


C         ENTER THE HEIGHT OF THE TYRE IN MILLIMETRES
          TYPE 4500
4500      FORMAT('  ENTER THE INITIAL AND FINAL HEIGHT IN MM ')
          READ(5,*)HFIRST,HLAST
          DO 750 THEIGH=HFIRST,HLAST,1.0
          HEIGHT=THEIGH/(2.0*FLOAT(METRE))
          WRITE(5,*)THEIGH
          RATIO=HEIGHT/CHORD
```

```
      DTYRE=DRIM+(2.0*HEIGHT)

C     ESTIMATE THE CURVATURE ANGLE BY NEWTON RAPHSON METHOD
      CALL NEWTON(RATIO,BETA,DEG)
10    TYPE 5000,RATIO,CHWID,DTYRE,DEG
      WRITE(1,5000)RATIO,CHWID,DTYRE,DEG
5000  FORMAT(2X,'RATIO OF HEIGHT/CHORD      :',F12.6,/,
     12X,'RATIO OF CHORD/WIDTH        :',F12.6,/,
     22X,'DIAMETER OF TYRE (METRES) :',F12.6,/,
     32X,'THETA (DEGREES-SIN)         :',3X,F6.3)

C     COMPUTE THE INITIAL ANGLE FOR PRESSURE CALCULATION
      CALL NEWOWS(ROWS,ALPHA,DEG)
      WRITE(5,5575)DEG
      WRITE(1,5575)DEG
5575  FORMAT(2X,'ALPHA (DEGREES-COS)          :',3X,F5.3)

      WRITE(1,5580)PRESS
5580  FORMAT(2X,'INITIAL PRESSURE(KPA)       :',2X,F8.4,/)

C     PRINT THE HEADING OF THE TABLE
      WRITE(1,6000)
6000  FORMAT(5X,'  PF(KPA)    ',3X,'    PF/PI    ',5X,'DEF(MM)',
     15X,'  LOAD(KN)   ',//)



C     COMPUTE THE LENGTH OF CONTACT
      DO 70 DEFI=1.0,40.0,1.0
      DEF=DEFI/FLOAT(METRE)
50    SEGLEN=2.0*SQRT((DTYRE*DEF)-(DEF*DEF))

60    FORCE=0.0
      P=0.0
      DELTAP=0.0

C     COMPUTE THE RADIAL DEFLECTION OF SEGMENT
      DO 500 N=1,NUM
      VAR=FLOAT(N)*(FLOAT(N)-1.0)/(FLOAT(NUM)*FLOAT(NUM))
      H=(SEGLEN/(8.0*CHORD))*(1.0-VAR)/SQRT((DTYRE/SEGLEN)*
     1(DTYRE/SEGLEN)-VAR)
      DIFFER=RATIO-H
C
C
```

```
C       COMPUTE THE NEW CURVATURE ANGLE
        CALL NEWTON(DIFFER,GAMMA,DEG)
        THETA=GAMMA

C       COMPUTE THE NEW PRESSURE
        VFIRST=(SIN(ALPHA)+CHORD/WIDTH)/ALPHA
        VLAST=(2.0*SIN(THETA)+(CHORD/(2.0*WIDTH*THETA))*(2.0*THETA-
       1SIN(2.0*THETA)))/THETA

        P=PRESS*VFIRST/VLAST

C       COMPUTE THE RATIO OF FINAL PRESSURE/INITIAL PRESSURE
        DELTAP=DELTAP+PRESS*(P/PRESS-1.0)/FLOAT(NUM)

C       COMPUTE THE LOAD SUPPORTED BY THE SEGMENT
        FORCE=FORCE+P*2.0*WIDTH*(1.0-(CHORD*COS(THETA))/(WIDTH*
       1THETA))*SEGLEN/FLOAT(NUM)
C
C
C
  500   CONTINUE
        PRATIO=(PRESS+DELTAP)/PRESS

C       PRINT THE PRESSURE(KPA),DEFLECTION(MM) AND FORCE(KN)
C       WRITE(5,7000)P,PRATIO,DEFI,FORCE
        WRITE(1,7000)P,PRATIO,DEFI,FORCE
 7000   FORMAT(2X,E12.6,5X,E12.6,5X,F6.2,5X,E12.6)

   70   CONTINUE
        WRITE(1,6500)
 6500   FORMAT(1H1)
  750   CONTINUE
        GOTO 30

C       CLOSE THE OUTPUT FILE
        CLOSE(UNIT=1)
        STOP
        END



        SUBROUTINE NEWTON(A,DELTA,ANGLE)
        DELTA=1.57
```

```
            F=0.0
            IF (A-0.475)1,4,4
1           TYPE 1000
1000        FORMAT( 'COEFFICIENT TOO SMALL')
            GOTO 100
3           DELTA=DELTA-F/(COS(DELTA)-A)
4           F=SIN(DELTA)-A*DELTA
            ANGLE=DELTA*180.0/3.142
            IF (ABS(F)-0.000001)5,5,3
5           A=A
            DELTA=DELTA
            ANGLE=ANGLE
100         CONTINUE
C
C
            RETURN
            END




            SUBROUTINE NEWOWS(A,DELTA,ANGLE)
            DELTA=1.57
            F=0.0
            IF (A-0.475)1,4,4
1           TYPE 1000
1000        FORMAT( 'COEFFICIENT TOO SMALL')
            GOTO 100
3           DELTA=DELTA+F/(SIN(DELTA)+A)
4           F=COS(DELTA)-A*DELTA
            ANGLE=DELTA*180.0/3.142
            IF (ABS(F)-0.000001)5,5,3
5           A=A
            DELTA=DELTA
            ANGLE=ANGLE
100         CONTINUE
C
C
            RETURN
            END
```

VI